

JUNE 1975

**AUTOMOTIVE  
ENERGY EFFICIENCY PROGRAM**



Presented Papers at the  
**CONTRACTORS COORDINATION MEETING**  
January 15-17, 1975

Sponsored by

U.S. DEPARTMENT OF TRANSPORTATION  
OFFICE OF THE ASSISTANT SECRETARY  
FOR SYSTEMS DEVELOPMENT & TECHNOLOGY



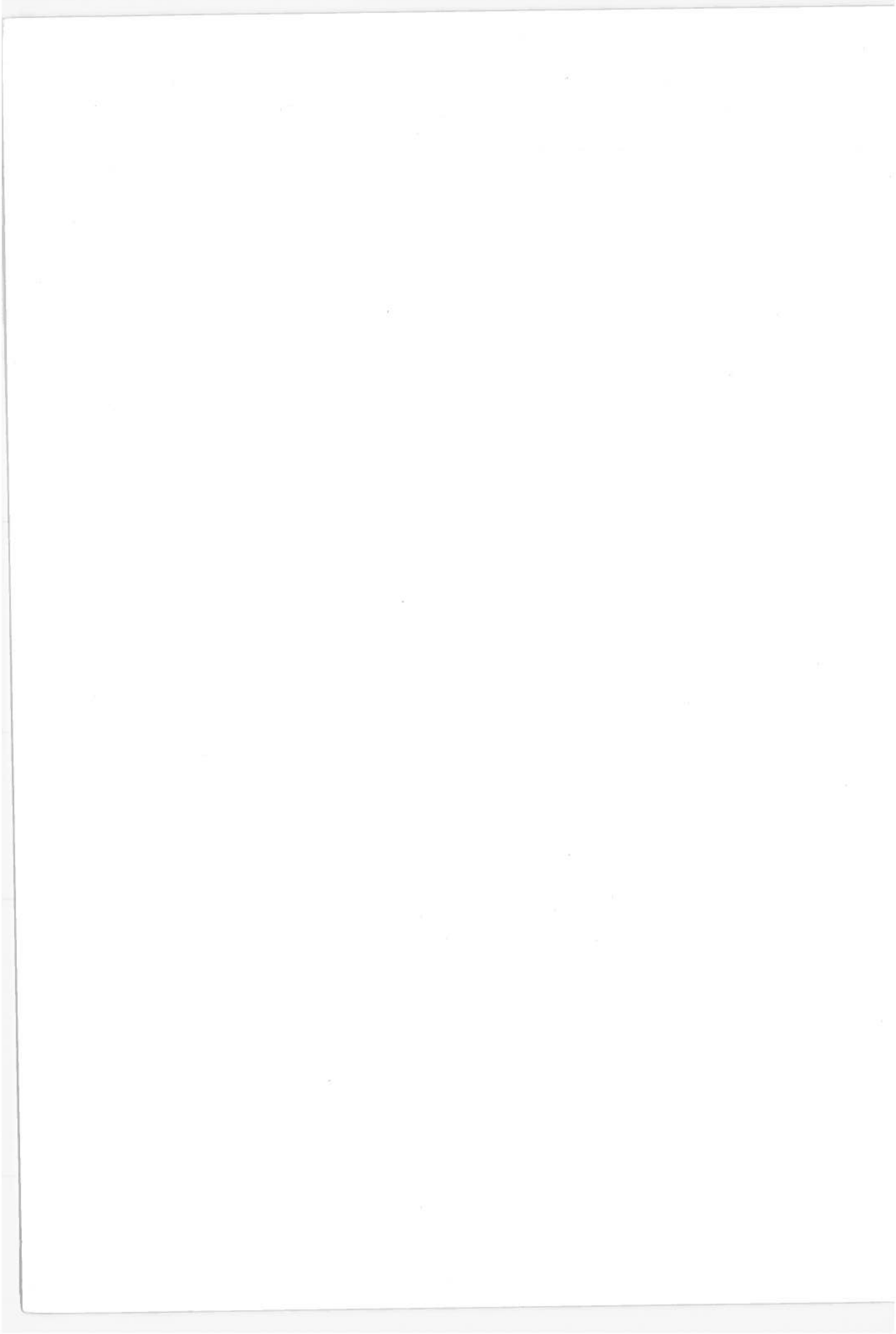
at

U.S. Department of Transportation  
Transportation Systems Center  
Cambridge, MA

DOCUMENT IS AVAILABLE TO THE PUBLIC  
THROUGH THE NATIONAL TECHNICAL  
INFORMATION SERVICE, SPRINGFIELD,  
VIRGINIA 22161

TECHNICAL REPORT STANDARD TITLE PAGE

1. Report No. DOT-TSC-OST-75-31		2. Government Accession No.		3. Recipient's Catalog No.	
4. Title and Subtitle AUTOMOTIVE ENERGY EFFICIENCY PROGRAM - PRE-SENTED PAPERS AT THE CONTRACTORS COORDINATION MEETING, JANUARY 15-17, 1975				5. Report Date June 1975	
				6. Performing Organization Code	
7. Author(s) Harold G. Miller, Chairman				8. Performing Organization Report No. DOT-TSC-OST-75-31	
9. Performing Organization Name and Address U.S. Department of Transportation Transportation Systems Center Kendall Square Cambridge, Mass. 02142				10. Work Unit No. OS514/R5515	
				11. Contract or Grant No.	
12. Sponsoring Agency Name and Address U.S. Department of Transportation Office of the Assistant Secretary for Systems Development and Technology				13. Type of Report and Period Covered CONFERENCE PAPERS January 15-17, 1975	
				14. Sponsoring Agency Code	
15. Supplementary Notes					
16. Abstract <p>This volume contains working papers presented at the Contractors Coordination Meeting of the Automotive Energy Efficiency Program held at the DOT Transportation Systems Center, January 15-17, 1975. This program is the Federal Government's major effort to assess the capability of the automotive industry to significantly improve the fuel economy of production vehicles and assess the related socio-economic effects.</p> <p>The primary objective of the conference was to report on progress to date and future plans of the Automotive Energy Efficiency Program and to promote the exchange of information between government, industry and university investigators.</p> <p>Twenty-two papers and illustrated lectures were presented at the conference, 20 of which are included in this volume. Some are copies of visual material and others are more formal technical papers.</p>					
17. Key Words Engines, Fuel, Aerodynamics, Tires, Emissions, Safety, Manufacturing				18. Distribution Statement  DOCUMENT IS AVAILABLE TO THE PUBLIC THROUGH THE NATIONAL TECHNICAL INFORMATION SERVICE, SPRINGFIELD, VIRGINIA 22161	
19. Security Classif. (of this report) Unclassified		20. Security Classif. (of this page) Unclassified		21. No. of Pages 280	22. Price



# AGENDA

15 January 1975

9:30-10:15 AM

## INTRODUCTORY SESSION

Welcome

**ROBERT K. WHITFORD**  
Acting Director, Transportation Systems Center

Briefing Introduction

**WILLIAM E. STONEY**  
Assistant Secretary for Systems Development and  
Technology (Acting), U.S. Department of  
Transportation

Automotive Energy Efficiency Program Overview

**RICHARD L. STROMBOTNE**  
Chief, Energy & Environment Division  
Office of the Secretary of Transportation

10:15-10:45 AM - BREAK

10:45-11:00 AM

Automotive Component Evaluation Subproject  
**HERBERT H. GOULD** - Transportation Systems  
Center

11:00-11:40 AM

Truck Fuel Economy State-of-the-Art Assessment  
**DONALD HURTER** - Arthur D. Little, Inc.

11:40-12:10 PM

Highway Vehicle Retrofit Evaluation  
**JOSEPH MELTZER** - The Aerospace Corporation

12:10-12:50 PM

Automotive Power Plant Evaluation  
**WILLIAM F. MARSHALL** - Bureau of Mines

12:50-1:50 PM - LUNCH

1:50-2:30 PM

Lean Mixture Engine Testing and Evaluation  
**M.W. DOWDY** - Jet Propulsion Laboratory

2:30-3:10 PM

Evaluation of Lithium Sulfur Batteries for Automobiles  
**PAUL A. NELSON** - Argonne National Laboratory

3:10-3:30 PM - BREAK

3:30-4:10 PM

Study of Truck Aerodynamics  
**LAWRENCE MONTOYA** - NASA/Flight Research  
Center

4:10-4:50 PM

Study of Automotive Aerodynamic Drag  
**BAIN DAYMAN, JR.** - Jet Propulsion Laboratory

4:50-5:30 PM

Rolling Resistance of Tires  
**S.K. CLARK** - University of Michigan

## AGENDA

16 January 1975

- 9:30-9:45 AM  
Test and Evaluation Subproject  
**PHILIP W. DAVIS** - Transportation Systems Center
- 9:45-10:25 AM  
Automotive Fuel Economy Evaluation  
**CARLOS W. COON, JR.** - Southwest Research Institute
- 10:25-10:50 AM - BREAK
- 10:50-11:30 AM  
Evaluation of Automotive Fuel Flow Meters  
**BALDWIN ROBERTSON** - National Bureau of Standards
- 11:30-11:45 AM  
Automotive Manufacturing Assessment Subproject  
**SAMUEL F. POWEL** - Transportation Systems Center
- 11:45-12:25 PM  
Automotive Manufacturing Data  
**L.H. LINDGREN** - Rath & Strong, Inc.
- 12:25-1:05 PM  
Assessment of Impacts on Automotive Manufacturing  
**MERRILL L. EBNER** - Boston University
- 1:05-1:50 PM - LUNCH
- 1:50-2:30 PM  
Alternative Engine Cost Data Base  
Presented by **ALAN E. AUSTIN**, Transportation Systems Center for **T.A. BARBER**, Jet Propulsion Laboratory
- 2:30-3:10 PM  
Automotive Manufacturing Assessment Support for Congressional Fuel Economy Study  
**ROBERT MENCHEN** - Hittman Associates
- 3:10-3:30 PM - BREAK
- 3:30-3:45 PM  
Vehicles/Highway Systems Analysis Subproject  
**ERNEST T. KENDALL** - Transportation Systems Center
- 3:45-4:25 PM  
Safety Implication of Increased Small Car Usage  
**HANS C. JOKSCH** - Center for the Environment and Man, Inc.
- 4:25-4:40 PM  
Requirements Analysis Subproject  
**RONALD A. MAURI** - Transportation Systems Center
- 4:40-4:55 PM  
Vehicle Systems Integration Subproject  
**KARL M. HERGENROTHER** - Transportation Systems Center

17 January 1975

- 9:30-9:45 AM  
Opening Remarks  
**SHEILA WIDNAL**  
Director, Office of University Research  
U.S. Department of Transportation
- 9:45-10:10 AM  
Fuel Economy By Energy Management  
**N. BEACHLEY** - University of Wisconsin
- 10:10-10:35 AM  
Loop Control for I.C. Engine Emissions  
**J.D. POWELL** - Stanford University
- 10:35-10:55 AM - BREAK
- 10:55-11:20 AM  
Development of Valved Hot-Gas Engine  
**JOSEPH SMITH** - Massachusetts Institute of Technology
- 11:20-11:45 AM  
Alcohols as Fuel Extenders  
**R.T. JOHNSON** - University of Missouri
- 11:45-12:10 AM  
Alternative Fuel Research with a CFR Engine  
**P.C.T. de BOER** - Cornell University
- 12:10-12:35 PM  
Performance and Emission Modeling for H<sub>2</sub> Fueled I.C. Engines  
**WILLIAM J. McLEAN** - Cornell University
- 11:35-1:00 PM  
Hydrogen Car Development  
**W. VAN VORST** - University of California, Los Angeles
- 1:00-1:45 PM - LUNCH
- 1:45-3:45 PM - DISCUSSION
- 3:45-  
Summary of Implications of DOT Automotive Research Programs  
**RAYMOND E. GOODSON**  
Chief Scientist  
U.S. Department of Transportation

## PREFACE

This volume contains working papers presented at the Contractors Coordination Meeting of the Automotive Energy Efficiency Program held at the DOT Transportation Systems Center, January 15-17, 1975 and chaired by Harold Miller of TSC. This program is the Federal Government's major effort to assess the capability of the automotive industry to significantly improve the fuel economy of production vehicles and assess the related socio-economic effects.

The primary objective of the conference was to report on progress to date and future plans of the Automotive Energy Efficiency Program and to promote the exchange of information between government, industry and university investigators. The studies reported in the last seven papers in this volume were supported by the DOT's Office of University Research.

Twenty-two papers and illustrated lectures were presented at the conference, 19 of which are included in this volume. Some are copies of visual material while others are more formal technical papers.

The Program Office appreciates the cooperation of the various authors and contractors who helped make this conference a success and acknowledges with special thanks the efforts of Paul Phaneuf and James Kelly of Raytheon Service Company.



## TABLE OF CONTENTS

	<u>Page</u>
TRUCK FUEL ECONOMY STATE-OF-THE-ART ASSESSMENT Donald A. Hurter.....	1
HIGHWAY VEHICLE RETROFIT EVALUATION Joseph Meltzer.....	19
AUTOMOTIVE POWER PLANT EVALUATION William F. Marshall.....	35
LEAN MIXTURE ENGINE TESTING AND EVALUATION M.W. Dowdy.....	39
EVALUATION OF LITHIUM/SULFUR BATTERIES FOR AUTOMOBILES Paul A. Nelson.....	51
AERODYNAMIC DRAG REDUCTION TESTS ON TRACTOR-TRAILER COMBINATIONS Lawrence C. Montoya and Louis L. Steers .....	75
STUDY OF AUTOMOTIVE AERODYNAMIC DRAG Jack E. Marte and Bain Dayman, Jr.....	95
ROLLING RESISTANCE OF PNEUMATIC TIRES S.K. Clark.....	107
AUTOMOTIVE FUEL ECONOMY EVALUATION Carlos W. Coon, Jr.....	117
EVALUATION OF AUTOMOTIVE FUEL FLOW METERS Baldwin Robertson.....	121
AUTOMOTIVE DATA BASE AND IMPACT ASSESSMENT L.H. Lindgren and Merrill L. Ebner.....	135
SAFETY IMPLICATIONS OF SMALL CAR USAGE H.C. Joksch.....	147
INCREASED FUEL ECONOMY IN TRANSPORTATION SYSTEMS BY USE OF ENERGY MANAGEMENT N.H. Beachly and A.A. Frank.....	153
CLOSED LOOP CONTROL OF SPARK TIMING J. David Powell and Mont Hubbard.....	173
DEVELOPMENT OF THE VALVED HOT-GAS ENGINE Joseph L. Smith.....	187
ALCOHOLS AS VEHICLE FUEL EXTENDERS R.T. Johnson.....	197



TABLE OF CONTENTS (cont'd)

	<u>Page</u>
PERFORMANCE AND EMISSIONS OF HYDROGEN FUELED INTERNAL COMBUSTION ENGINES	
P.C.T. de Boer, W.J. McLean and H.S. Homan .....	207
PERFORMANCE AND EMISSION MODELING FOR H <sub>2</sub> FUELED I.C. ENGINES	
William J. McLean and Jean-Jacques Fagelson.....	233
HYDROGEN CAR DEVELOPMENT	
William D. Van Vorst.....	255
CONFERENCE ATTENDEES LIST.....	267

# TRUCK FUEL ECONOMY STATE-OF-THE-ART ASSESSMENT

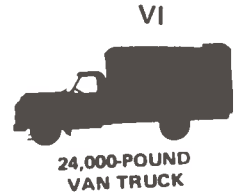
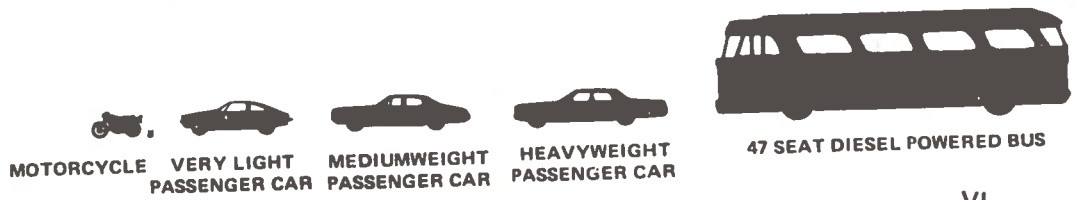
Donald A. Hurter  
Arthur D. Little, Inc.  
Cambridge, Massachusetts

## ABSTRACT

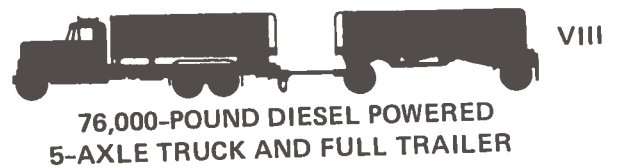
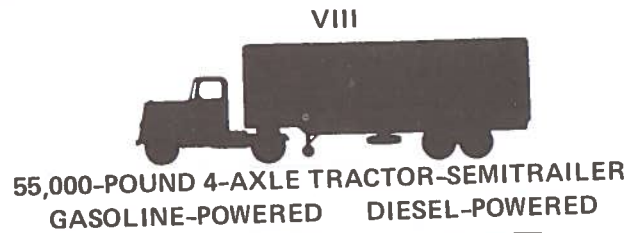
A study was conducted to determine the potential reduction in truck fuel consumption based on the use of innovative systems and improved components. Technological areas investigated were: spark ignited engines with and without turbocharging, electronic feedback controlled fuel injection with dual bed catalytic converters, stratified charge combustion, lightweight diesels, lock-up torque converters, continuously variable ratio transmission, tires aerodynamic drag, vehicle weight, engine accessories and optional equipment.

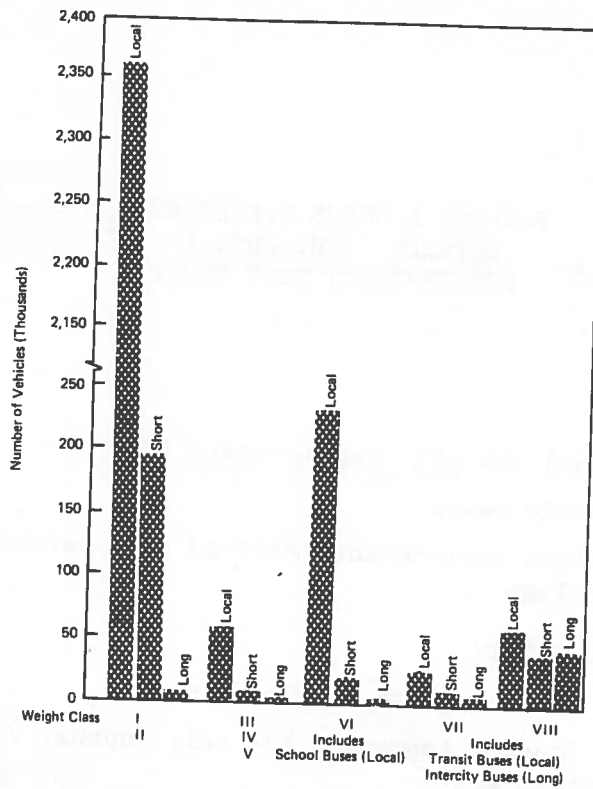
1973 model year trucks from various weight and duty classes were selected for analysis using a computer-simulation program to predict fuel usage and performance with and without incorporation of the improvements. In addition, estimates were made as to whether modified vehicles compiled with study constraints such as emission, safety, noise and user requirements. Cost effectiveness, manufacturing adaptability and probable time frame for introduction of improvements were also estimated.

The study, while not yet complete, indicates that material improvement in fuel economy (mpg) of 1973 model year trucks can be attained on a mass produced scale by the early 1980's.

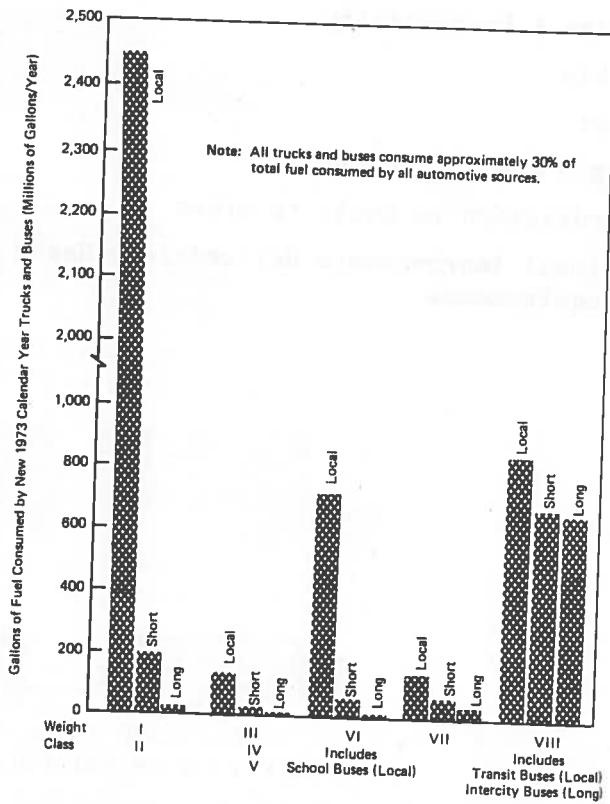


TYPICAL TYPES OF TRUCKS BY WEIGHT CLASS





**NEW TRUCK AND BUS REGISTRATIONS, 1973  
CALENDAR YEAR BY WEIGHT CLASS AND DRIVING MODE**



**FUEL CONSUMPTION BY WEIGHT CLASS AND DRIVING MODE  
FOR NEW 1973 CALENDAR YEAR, TRUCKS AND BUSES**

PURPOSE & USAGE DIFFERENCE  
BETWEEN LIGHT DUTY &  
MEDIUM/HEAVY DUTY TRUCKS

LIGHT DUTY

- Personal use 45% Agriculture 24%
- Privately owned
- Potential improvements derived from automobile technology

MEDIUM/HEAVY DUTY

- Cost Effectiveness vs Fuel Economy
- Fuel Economy important but only Approx. 2 - 3% of Operating costs
- Reliability & Durability Paramount
- Downtime & Revenue Loss
- Trip time & Productivity
- Ownership
  - Fleet
  - Single Operator/Owner
- Standardization vs built to order
- Potential Improvements derived from Heavy Duty Requirements

INTERCITY CARRIERS

FUEL & OIL COST COMPARED TO  
OTHER OPERATING EXPENSES  
(ADL Estimate)

	Percent
Fuel and Oil	2.4
Maintenance	9.3
Drivers and Helpers	28.4
Terminal Expenses	22.0
Traffic Expenses	2.9
Insurance & Safety	2.6
Cargo Loss and Damage Insurance	1.5
Administrative and General	6.7
Other Transportation	14.1
Other Expenses (Depreciation, operating Taxes and Licenses)	10.1
	<hr/> 100.0
Fuel and Oil Expenses	4.5¢/mile
Tires and Tubes	2.0¢/mile
Servicing	7.8¢/mile
Other Maintenance	1.9¢/mile
	<hr/>
Total	16.2¢/mile

TRUCK EMISSION REQUIREMENTS

VEHICLES ≤ 6000 lbs		VEHICLES > 6000 lbs		VEHICLES ≤ 10,000 lbs		VEHICLES > 10,000 lbs	
gms/mi.		gms/BHP-hr		gms/mi.		gms/BHP-hr	
HC	2.6	HC+NO <sub>x</sub>	16	HC	.41	HC+NO <sub>x</sub>	16
NO <sub>x</sub>	3.1	CO	20	NO <sub>x</sub>	2.0 (.4 in 1978)	CO	40
CO	20			CO	3.4		
	1975		1975		1977		1977

TRUCK LOAD FACTORS & FUEL ECONOMY

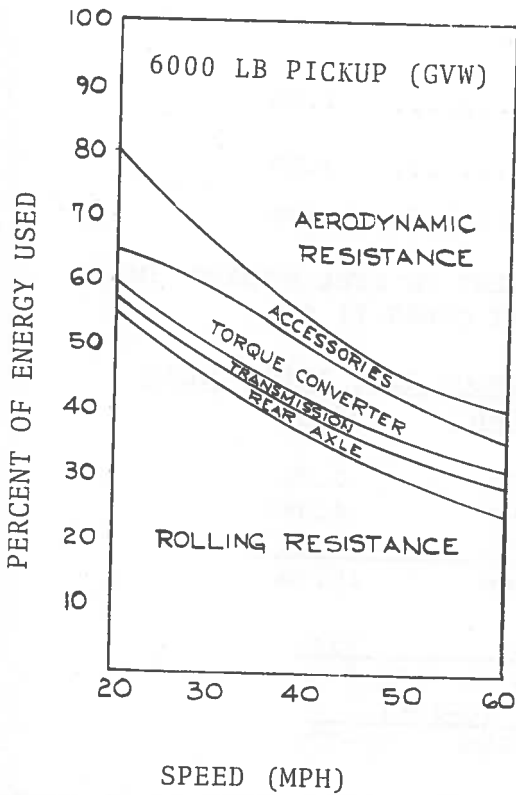
Class	Gross Vehicle Weight (lbs)	Duty	% Load to Cargo Capacity	Type of Fuel Used	Fuel Economy	
					Miles/Gal	Ton-Miles/Gal
I	6,000 & less	Light	20%	Gasoline-100%	11.7	1.2
II	6,001-10,000	Light			11.0	1.6
III	10,001-14,000	Medium			8.5	17.0
IV	14,001-16,000	Medium	40-55%	Gasoline-100%	7.0	16
V	16,001-19,500	Medium			6.0	18
VI	19,500-26,000	Light/ Heavy	50-60%	Gasoline-98% Diesel - 2%	5.8 6.9	41 48
VII	26,001-33,000	Heavy	50-60%	Gasoline-50% Diesel -50%	5.3 6.0	59 60
VIII	33,000 and over	Heavy	60-85%	Diesel -80% Gasoline-20%	5.7 4.9	86 74

SELECTED REFERENCE TRUCKS

Class	Driving Mode	Mfg	Model	Engine	Transmission	Gross Vehicle Wgt
I	Mixture of local, short and long	Chevrolet	C-10 Pickup	Chev. 350 CID	3-Speed Auto	6,000
II	Mixture of local, short and long	Ford	F-250 Camper Special Pick-up and Camper	Ford 361-CID	3-Speed Heavy Duty Auto	10,000
VI	Local	Interna. Harvester	1800 Van 1850 Van	IH DV 392 Cummins 8VE 170 HT	5-Speed T-35 5-Speed T-36	22,500 24,500
VIII	Local and Short	Mack	DM-600	Mack End-673E	10-Speed TRD-722	62,000
VIII	Short	Interna. Harvester	Fleetstar F-2070	Cummins NTC 290	10-Speed RT-910	48,860
VIII	Long	Interna. Harvester	Transtar F-4379	Cummins NTC 290	10-Speed RT-910 Manual	73,000

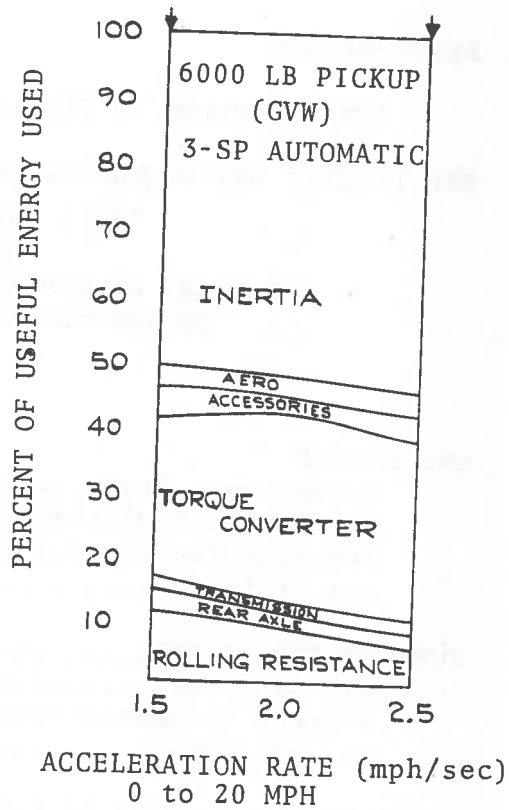
These vehicles account for 88% of truck fleet fuel consumption

ENERGY PARTITIONING DURING STEADY CRUISE



ENERGY PARTITIONING DURING ACCELERATION

AVERAGE ACCELERATION RANGE IN FTP





SUMMARY OF PERCENT IMPROVEMENT IN FUEL ECONOMY (MPG)  
 BY INNOVATION FOR LIGHT DUTY TRUCKS  
 (WEIGHT CLASS 1 and 2)

<u>INNOVATION</u>	<u>LIGHT DUTY ANNUAL MIX</u>
<b>ENGINE</b>	
Substitute Diesel.....	20-35%
Lean Burn*.....	10-15%
Closed Loop Stoichiometric*.....	10-15%
Turbocharge.....	5-10%
Stratified Charge.....	15-25%
<b>COOLING SYSTEM</b> .....	3%
<b>POWER TRAIN</b>	
Transmission	
4-speed and lockup.....	7-15%
CVT.....	12-30%
Radial Tires.....	2.5%
<b>AERODYNAMICS</b>	
10% Reduction in Drag.....	1.3%
<b>TEN PERCENT WEIGHT REDUCTION</b> .....	2.7%
*Both carbureted & Fuel Injection	

SUMMARY OF PERCENT IMPROVEMENT IN FUEL ECONOMY (MPG)  
 BY INNOVATION FOR WEIGHT CLASS VI \*\*

	<u>VAN TRUCK TYPE DUTY CYCLE</u>	
	<u>LOCAL</u>	<u>SHORT</u>
<b>GAS ENGINE</b>		
Reduce Aero Drag.....	1.5%	2.2%
Substitute Radial Tires.....	3.0%	4.3%
Modulate Fan Control.....	3.0%	4.0%
All of Above.....	7.5%	10.5%
<b>SUBSTITUTED DIESEL</b> .....	<u>67%</u>	<u>55%</u>
All of Above.....	75%	65%
4-speed Automatic Transm.....	(0-10%)	
All of Above.....	75-85%	65-75%

\*\* Ninety percent of the fuel consumed by this class is in local service

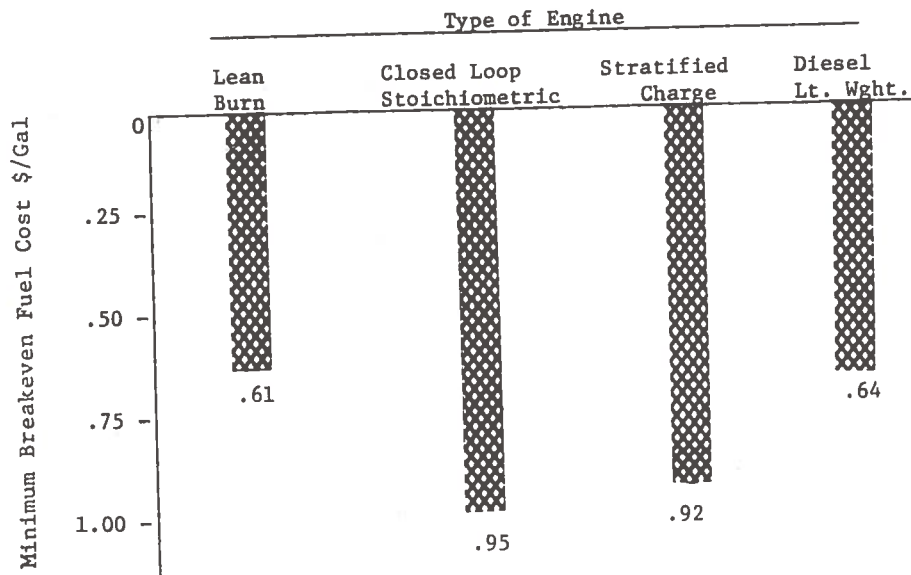
SUMMARY OF PERCENT IMPROVEMENT IN FUEL ECONOMY (MPG) BY INNOVATION

FOR HEAVY DUTY TRUCKS OF WEIGHT CLASS VIII

	Truck Type					
	Dump Truck Duty Cycle		Tractor-Trailer 50,000 # GVW Duty Cycle		Tractor-Trailer 70,000 # GVW Duty Cycle	
	<u>Local</u> (%)	<u>Short</u> (%)	<u>Short</u> (%)	<u>Long</u> (%)	<u>Short</u> (%)	<u>Long</u> (%)
Reduce Aero Drag	1.2	1.0	3	3	1.2	2.2
Substitute Radial Tires	4.3	3.0	3	3	4.4	4.2
Derate Engine Speed	-0-	1	.8	2.4	.4	4.4
Modulated Fan	3.4	3.5	4.8	4.5	5.2	4
All of Above	9	7.7	10.0	12.5	--	--
Tag Axle	2.3	2.3	2.2	2.3	2.2	2.4
Turbocharge	(1)	(2.5)	(2.5)	( 4)	2.5	4.2
All of Above	11(12)	9(11.5)	12(14)	14(18)	12.8	23
C.V.T.	(10-15)		(10-15)	--	(10-15)	--
All of Above	(20-27)	(20-25)	(24-29)	14(18)	(23-28)	23

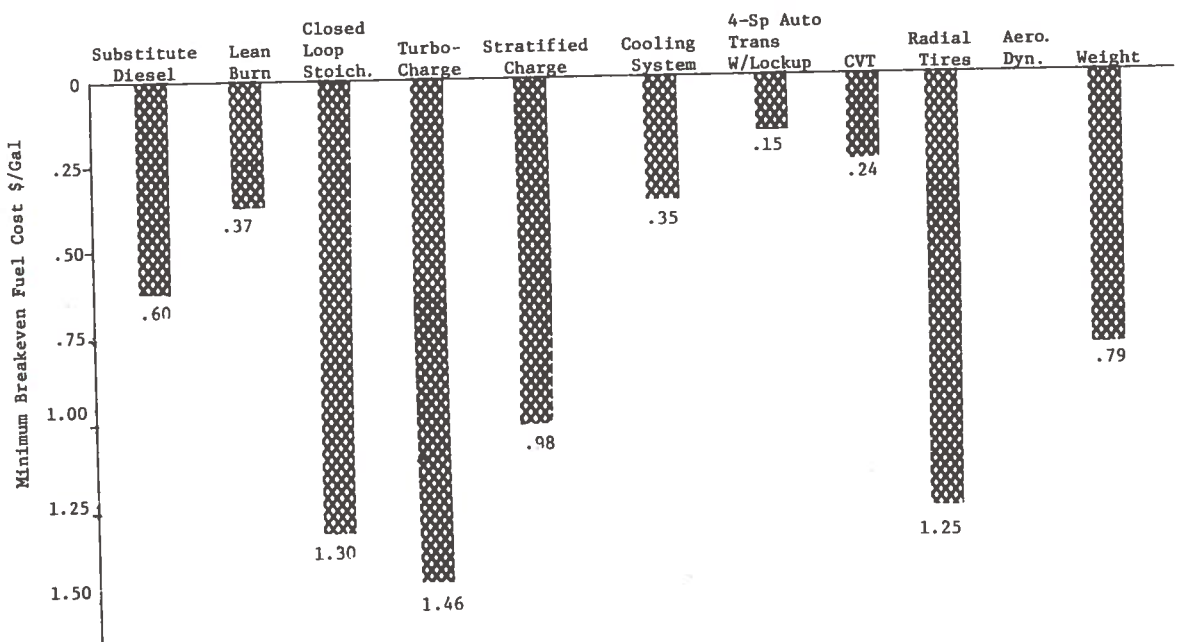
( ) denotes ADL estimate since computer simulations could not be made.

WEIGHT CLASS I AND II PICKUP TRUCK  
 LIGHT DUTY ANNUAL TRUCK - SYNTHESIZED VEHICLES

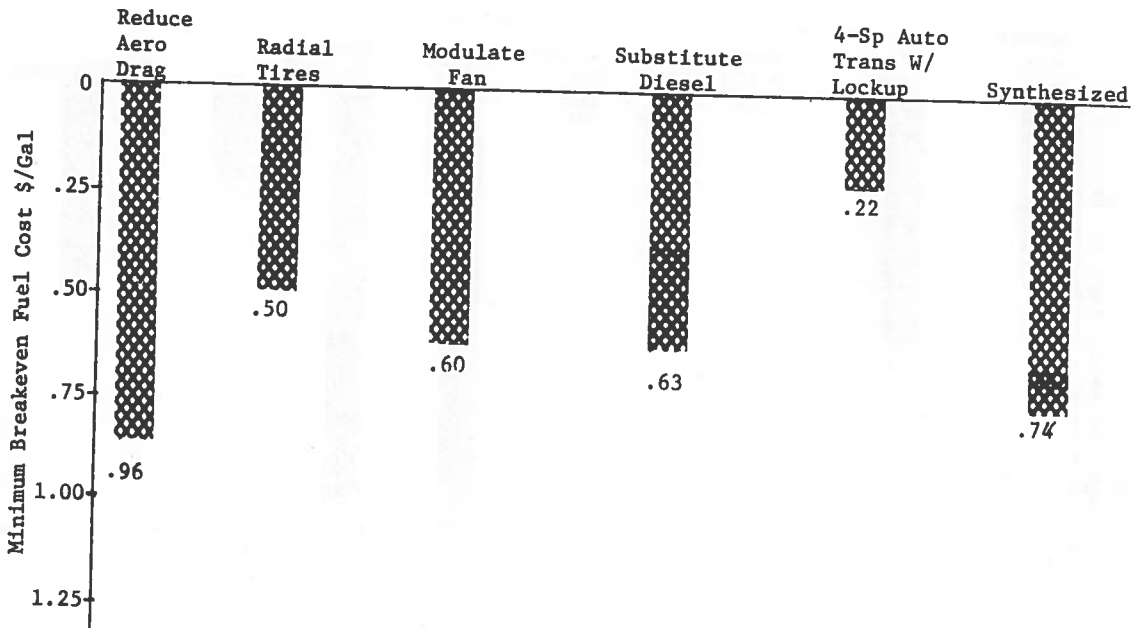


Includes: Cooling System  
 4-Speed Auto Trans.  
 Radial Tires  
 Aerodynamic Drag Reduction  
 Weight Reduction

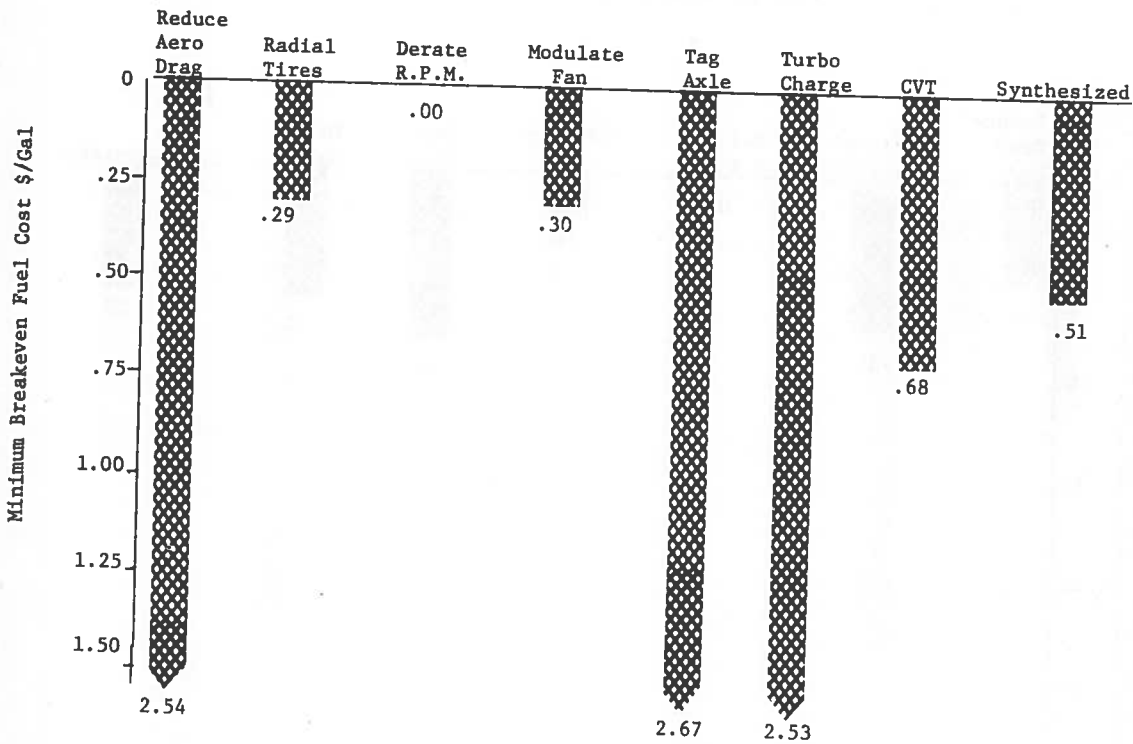
WEIGHT CLASS I AND II PICKUP TRUCK  
 LIGHT DUTY ANNUAL MIX



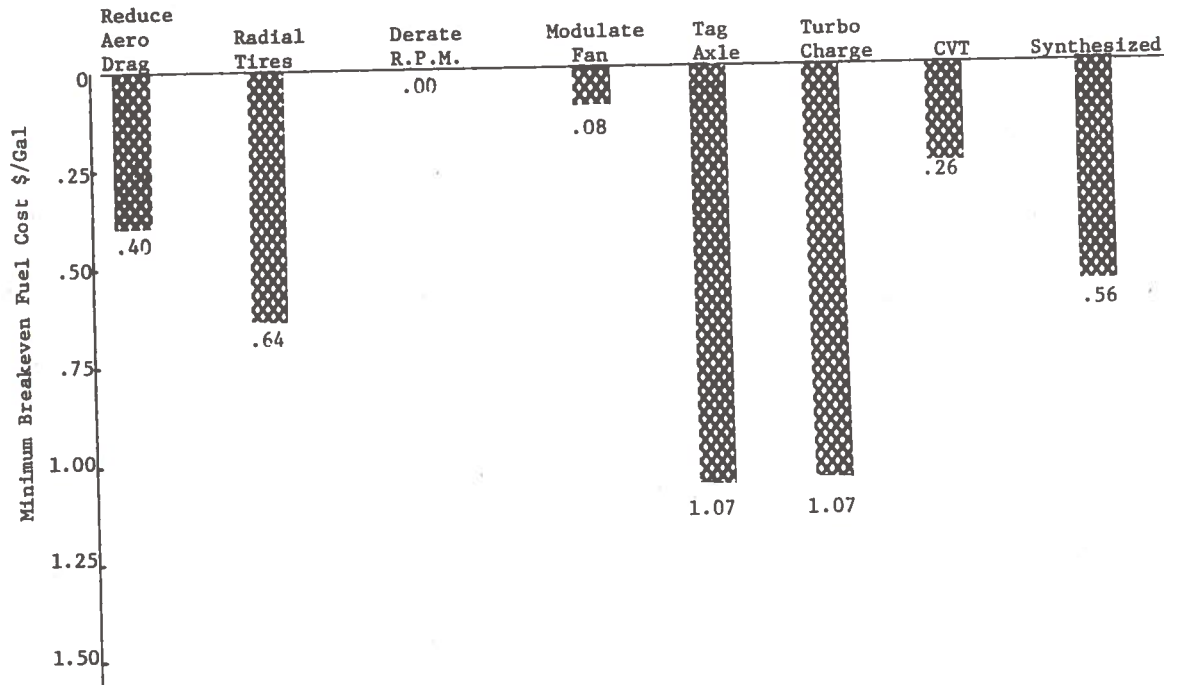
WEIGHT CLASS VI - VAN TYPE (LOCAL DUTY CYCLE)



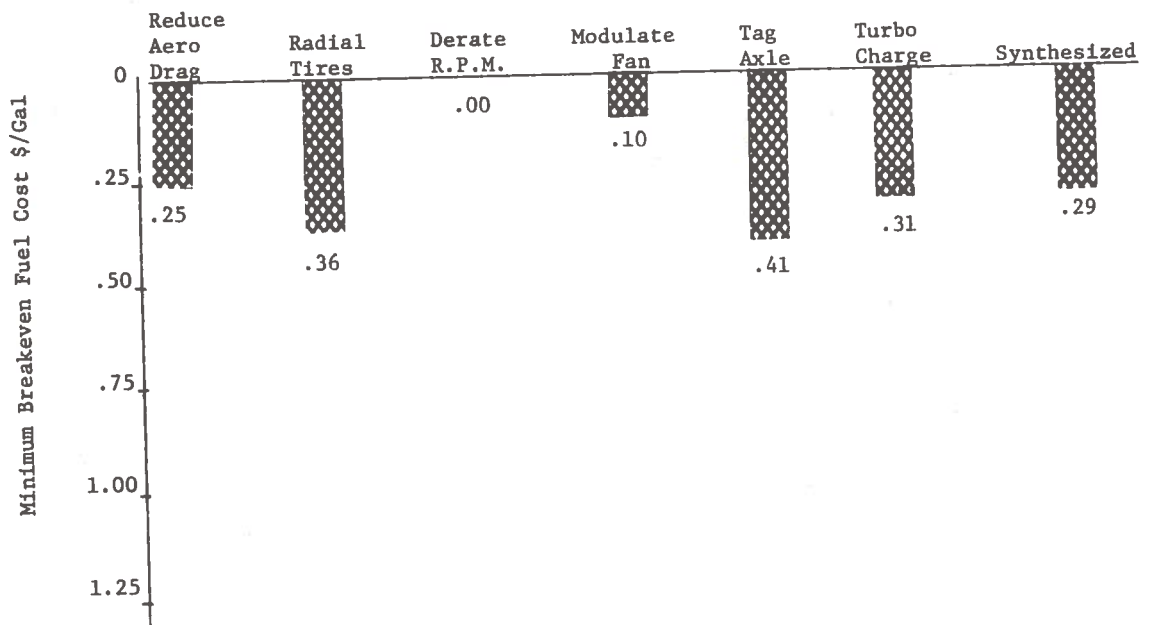
WEIGHT CLASS VIII - DUMP TRUCK (LOCAL DUTY CYCLE)



WEIGHT CLASS VIII - 50,000 LBS TRACTOR TRAILER  
( SHORT DUTY CYCLE )






WEIGHT CLASS VIII - 70,000 LBS TRACTOR TRAILER  
( LONG DUTY CYCLE )



Percent Improvement in Fuel Economy with  
Optimum Combination of Options

CLASS	DRIVING CYCLE	SPECIFIC OPTIONS	% GAIN IN FUEL ECONOMY (MPG)
I & II	Annual	<ul style="list-style-type: none"> <li>● Improved S.I. Engine</li> <li style="text-align: center;">or</li> <li>● Diesel Substitution</li> </ul>	
	Mix	<ul style="list-style-type: none"> <li>● 4-sp Auto Trans</li> <li>● Radial Tires</li> <li>● Modulated Fan</li> <li>● Reduced Weight</li> </ul>	25 - 40
VI	Local	<ul style="list-style-type: none"> <li>● Diesel Engine Substitution</li> <li>● Modulated Fan</li> <li>● 4-sp Auto Trans</li> <li>● Radial Tires</li> </ul>	70-80
VIII	Local	<ul style="list-style-type: none"> <li>● Derated RPM</li> <li>● Modulated Fan</li> <li>● C.V.T.</li> </ul>	15 - 20
VIII	Short	<ul style="list-style-type: none"> <li>● Radial Tires</li> <li>● Derated RPM</li> <li>● Modulated Fan</li> <li>● Tag Axle</li> <li>● C.V.T.</li> <li>● Reduced Aero Drag</li> </ul>	20 - 30
VIII	Long	<ul style="list-style-type: none"> <li>● Radial Tires</li> <li>● Derated RPM</li> <li>● Modulated Fan</li> <li>● Tag Axle</li> <li>● C.V.T.</li> <li>● Reduced Aero Drag</li> <li>● Turbocharged</li> </ul>	18 - 23

# TRUCK FUEL CONSUMPTION DATA

Industry - Duty Class Category - Weight Class	Light Duty	
	I	II
Gross Vehicle Weight #	6,000 & less	6,001-10,000
Most Popular Model		Pickup
		Van
		Van
Principal Use	Personal Transportation	Personal Transportation
Principal Type of Fuel Currently Being Used	Gas	Gas
New Truck Registrations 1973 Calendar Year*(1)(5)		
By Weight Class	1,842,891	716,534
By Duty Class	2,559,425	
Total Light Duty Trucks (2)		
By Weight Class	11,168,000	4,200,000
By Duty Class	15,368,000	
Gallons of Fuel Consumed by New 1973 Calendar Year Trucks (Million Gals/Year)(3)		
By Weight Class	1,890	782
By Duty Class	2,672	
Gallons of Fuel Consumed By Total In-Service Fleet (Million of Gals/Year)(3)		
By Weight Class	10,100	4,052
By Duty Class	14,152	
% of Fuel Consumed(Based on Total Fuel Used by all Automotive Sources)(3)		
By Weight Class	9.3%	3.6%
By Duty Class	13.1%	
Truck Miles Traveled Per Year (Miles/Year) For New Trucks By Weight (3) Class	12,000	12,000
% of Total Trucks For Each Duty Class By Primary Use (3)		
Local-Urban	92.3%	
Short Range	7.5%	
Long Range	.2%	
Average Miles/Per Year Traveled (4) for Each Duty Class by Specific Driving Mode		
Local-Urban***	10,000	
Short Range	17,400	
Long Range	13,000	
Weighted Average	10,600	
Average Truck Fuel Economy For Each Weight Class By Specific Driving Mode.(MPG)(4)	Gas	Gas
Local-Urban	12.2	11.7
Short Range	11.0	9.8
Long Range	11.9	11.5
Weighted Average	11.7	11.0
Vehicle Ton Miles Per Gal for Each Duty Class By Specific Driving Mode (Ton-Miles/ (3)		
Local-Urban	1.2	1.8
Short Range	1.1	1.5
Long Range	1.2	1.7
Weighted Average	1.2	1.6

\* Calendar Year from 1/1/73 to 12/31/73

\*\*\* Local-Urban - Similar to Federal Testing Procedure (F.T.P.)  
Short Range - Under 200 Miles Round Trip-Returning to Base Each Night  
Long Range - Over 200 Miles - in Line Hauling Across Country

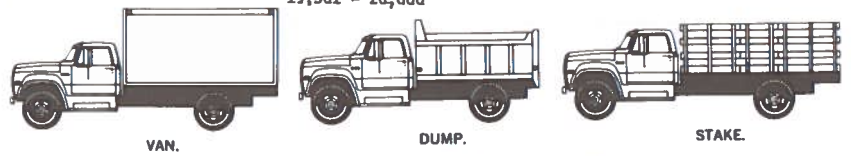




# TRUCK FUEL CONSUMPTION DATA

Industry - Duty Class  
 Category - Weight Class  
 Gross Vehicle Weight (Pounds)  
 Most Popular Model

Light Heavy Duty  
 VI  
 19,501 - 26,000



Principal Use WHOLESALE & RETAIL - BEVERAGE DELIVERY - DUMP TRUCK - AGRICULTURE

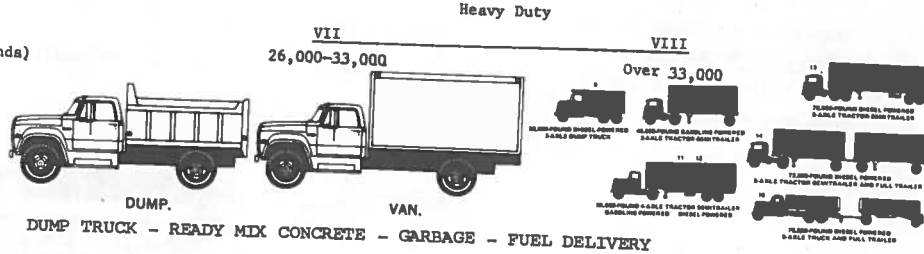
	Gas	Diesel
Principal Type of Fuel Currently Being Used		
New Truck Registrations 1973 Calendar Year* (1)		
By Weight Class	213,569	4,270
By Duty Class		217,839
Total Light Heavy Duty Trucks(2)		
By Weight Class	2,070,000	73,000
By Duty Class		2,143,000
Gallons of Fuel Consumed by New 1973 Calendar Year Trucks (3) (Million Gals/Year)		
By Weight Class	736	17
By Duty Class		753
Gallons of Fuel Consumed By Total In-Service Fleet (Million of Gals/Year) (4)		
By Weight Class	3,340	240
By Duty Class		3,580
% of Fuel Consumed (Based on Total Fuel Used by all Automotive Sources) (5)		
By Weight Class	3.1%	0.2%
By Duty Class		3.30%
Truck Miles Traveled Per Year (Miles/Year) For New Trucks By Weight Class (6)		
By Weight Class	20,000	28,000
% of Total Trucks For Each Duty Class By Primary Use (6)		
Local-Urban	88%	74%
Short Range	10%	23%
Long Range	2%	3%
Average Miles/Per Year Traveled for Each Duty Class by Specific Driving Mode (6)		
Local-Urban***	8,700	15,400
Short Range	20,400	28,400
Long Range	29,500	53,000
Weighted Average	10,500	20,000
Average Truck Fuel Economy For Each Weight Class By Specific Driving Mode (MPG) (6)	Gas	Diesel
Local-Urban	5.7	6.8
Short Range	5.7	7.0
Long Range	6.0	7.0
Weighted Average	5.8	6.9
Vehicle Ton Miles Per Year for Each Duty Class By Specific Driving Mode (Ton-Miles/Gal.) (6)		
Local-Urban	39.9	47.6
Short Range	39.9	49.0
Long Range	42.0	49.0
Weighted Average	40.6	48.3

\* Calendar Year from 1/1/73 to 12/31/73

\*\*\* Local-Urban - Pickup and Delivery Service within the City  
 Short Range - Under 200 Mile Round Trip-Returning to Base Each Night  
 Long Range - Over 200 Mile - in Line Hauling Across Country

# TRUCK FUEL CONSUMPTION DATA

Industry - Duty Class  
 Category - Weight Class  
 Gross Vehicle Weight (Pounds)  
 Most Popular Model





	VII 26,000-33,000		VIII Over 33,000	
	Gas	Diesel	Gas	Diesel
Principal Use				
Principal Type of Fuel Currently Being Used				
New Truck Registrations 1973 Calendar Year* (1)(5)				
By Weight Class	27,000	14,000	15,000	127,000
By Duty Class	41,000		142,000	
Total Heavy Duty Trucks (2)				
By Weight Class	324,000	100,000	434,000	700,000
By Duty Class	424,000		1,134,000	
Gallons of Fuel Consumed by New 1973 Calendar Year Trucks (3) (Million Gals/Year) (3)				
By Weight Class	137	124	131	2,000
By Duty Class	261		2,131	
Gallons of Fuel Consumed By Total In-Service Fleet (Million of Gals/Year) (3)				
By Weight Class	773	807	2,344	8,627
By Duty Class	1,580		10,971	
% of Fuel Consumed (Based on Total Fuel Used by all Automotive Sources) (3)				
By Weight Class	.7%	.7%	2.2%	8.0%
By Duty Class	1.4%		10.2%	
Truck Miles Traveled Per Year (Miles/Year) For New Trucks By Weight (3) Class	27,000	53,000	43,000	90,000
% of Total Trucks For Each Duty Class By Primary Use (3)				
Local-Urban	Gas		Diesel	
Short Range	76%		35%	
Long Range	20%		33%	
Weighted Average	4%		32%	
Average Miles/Per Year Traveled for Each Duty Class by Specific Driving Mode (4)				
Local-Urban***	Gas		Diesel	
Short Range	12,700		22,500	
Long Range	26,800		53,000	
Weighted Average	42,900		90,000	
Weighted Average	16,800		54,000	
Average Truck Fuel Economy For Each Weight Class By Specific Driving Mode (MPG) (4)				
Local-Urban	Gas		Diesel	
Short Range	5.3		4.9	
Long Range	5.3		5.7	
Weighted Average	5.3		5.7	
Weighted Average	5.3		5.7	
Vehicle Ton Miles Per Year for Each Duty Class By Specific Driving Mode (Ton-Miles/Gal.) (3)				
Average	58.7	66	73.5	85.5

\* Calendar Year from 1/1/73 to 12/31/73

\*\*\* Local-Urban - Pickup and Delivery (Service within the city)  
 Short Range - Under 200 Mile Round Trip-Returning to Base Each Night  
 Long Range - Over 200 Mile - in Line Hauling Across Country

## BUS FUEL CONSUMPTION DATA

Industry - Duty Class Category - Weight Class Gross Vehicle Weight (Pounds) Most Popular Model	SCHOOL	INTERCITY	TRANSIT
			
Principal Type of Fuel Currently Being Used	Gas	Diesel	Diesel
New Bus Registrations 1973 Calendar Year*(1)	44,488	4,184	3,200
Total Buses (1)	323,000	30,367	48,286
Gallons of Fuel Consumed by New 1973 Calendar Year Buses (Million Gals/Year (2))	45	26	31
Gallons of Fuel Consumed By Total In-Service Fleet (Million of Gals/Year) (2)	328	191	295
% of Fuel Consumed (Based on Total Fuel Used by all Automotive Sources) (2)	.3	.35	.14
Bus Miles Traveled Per Year (Miles/Year) For New Buses By Weight (2) Class	7,500	52,700	45,000
Average Miles/Per Year Traveled (2)	7,500	52,700	28,500
Average Bus Fuel Economy For Each Class (MPG) (2)	7.4	6.0	4.6
Passenger Miles Per Year for Each Class (Thousands of Passenger-Miles/ Year) (3)	144	195	342

\* Calendar Year from 1/1/73 to 12/31/73

## HIGHWAY VEHICLE RETROFIT EVALUATION

Joseph Meltzer  
The Aerospace Corporation  
El Segundo, California

### ABSTRACT

The current status of the Highway Vehicle Retrofit Evaluation program is presented. The objective of this effort is to evaluate the potential of used car and truck fuel economy retrofit devices for reducing fuel consumption in a timely, economic, and effective manner; to provide the information necessary for the Federal government to determine if it should encourage the use of such retrofit concepts, as well as a plan for DOT to develop any needed additional information, if appropriate.

Over twenty representative classes of retrofit devices/concepts/techniques, including over 130 specific items, were examined in the Phase I portion of the study. A major portion of the analysis effort was directed to the evaluation of 16 advanced, novel, or new carburetors which had been brought to the attention of the Department of Transportation as having the potential to improve automotive fuel economy. In addition to carburetors, the spectrum of devices examined included: acoustic and mechanical atomizers; lean-bleed devices; vapor injectors; fuel modifications (additives, blends of water, alcohol, and gasoline); inlet manifolds; ignition systems; drivetrain components (radial tires, transmissions, overdrives); drag reduction techniques; driver aids; cooling fans; valve timing modifications; tune-ups; compression ratio increases; exhaust-related systems (tuned exhaust systems, turbochargers, etc.); and engine oils, oil additives, and filters. A number of the more promising devices are being experimentally evaluated in a Phase II test program. Testing will begin in the very near future.

## INTRODUCTION

This presentation, prepared by The Aerospace Corporation for the U.S. Department of Transportation, Transportation Systems Center, presents an analysis and preliminary evaluation of the potential of selected used car and truck fuel economy retrofit devices for reducing fuel consumption. A number of the more promising devices are recommended for experimental evaluation in a Phase II test program.

The preliminary evaluation results presented herein are necessarily based on and restricted to the results of the best comparative test data available for a given device or class of devices. In general, such comparative test data (before and after installation of a device in a vehicle), when available, is based on at most a few vehicles. Thus, it is not possible to extrapolate such test data to the general vehicle population. Therefore, wherever possible, an analysis was made of the general operational principles of a given device and its possible effects on spark-ignition engine operation in order to substantiate or explain test data results.

The following charts and headings describe the basic findings of the preliminary evaluation phase and the elements of the phase II test program currently in progress.

### OBJECTIVES

- Evaluate The Potential Of Used Car And Truck Fuel Economy Retrofit Devices For Reducing Fuel Consumption In A Timely, Economic, And Effective Manner
- Provide a Plan for D.O.T. to Develop any Needed Additional Information if Appropriate
- Provide Information Necessary for the Federal Government to Determine if it Should Encourage the use of Such Retrofitting

### METHOD OF APPROACH

- Identify and Characterize Retrofit Devices, Ideas, Concepts, And/Or Fuel Modifications Postulated to Reduce Automotive Fuel Consumption

- Analyze Each Such Promising Device/Concept With Regard To Fuel Economy Gains, Degree Of Availability, And Side Effects
- Conduct Initial Comparative Evaluation Of Contending Retrofit Concepts
- Define Test Program For Experimental Verification Of Selected Retrofit Devices
- Conduct Verification Test Program
- Evaluate Relative Merit Of Selected Devices With Regard To Fuel Economy Based On Test Results

FACTORS CONSIDERED IN  
EVALUATION OF FUEL ECONOMY RETROFIT DEVICES

- Degree Of Fuel Economy Improvement
- Effect On Exhaust Emissions
- Type Of Data Available
- Source And Reliability Of Data Base
- Retrofit Device or "Kit" Content And Physical Characteristics
- Compatibility With Mass Production
- Potential Availability In Near Future
- Applicable Vehicle Or Engine Models
- Installation Requirements (Including Necessary Facilities)
- Installation Time
- Cost To Consumer For Installation
- Maintenance Requirements
- Effect On Vehicle Power And Acceleration Performance

BASIC RETROFIT TYPES

<u>FUEL/AIR METERING</u>	<u>EMISSION CONTROL</u>
Carburetors And Carburetor-Related	Spark-Control Related
Atomizers	EGR-Related

FUEL/AIR METERING (CONT.)

Lean-Bleed Systems  
Vapor Injectors  
Fuel Modifications  
Inlet Manifolds  
Fuel Pressure Regulators  
Fuel Pre-Agitator

IGNITION

Capacitive Discharge  
Electronic Inductive  
Spark Plug  
Ignition Bridges

AUXILIARIES AND ACCESSORIES

Driver Aids  
Cooling System

EXHAUST SYSTEMS

Tuned Exhaust Headers  
Dual Exhaust Systems  
Exhaust Cut-Out  
Turbochargers

DATA SOURCES

- Dot-Supplied Documents, Inventors, Developers, Congressmen
- EPA Test Reports
- California Air Resources Board Test Reports
- Prof. D.E. Cole -- Univ. Of Michigan
- Technical Publications
- Sales Brochures
- Adertisements

EMISSION CONTROL (CONT.)

Carburetor Plus Distributor  
Retrofit

Catalyst Systems

DRIVETRAIN

Tires  
Transmissions  
Overdrive Units  
Rear Axle And/Or Gear Ratio  
Changes

VEHICLE STRUCTURE

Drag Reduction

OPERATIONAL ADJUSTMENT TECHNIQUES

Valve Timing  
Compression Ratio  
Tune-Ups

MISCELLANEOUS

Engine Clean-Up  
Engine Oil And/Or Additive  
Removal Of ECSs (Emission  
Control Systems)

- Catalogs
- Newspaper Articles/Magazine Articles
- Contacts With Retrofit Device Manufacturers

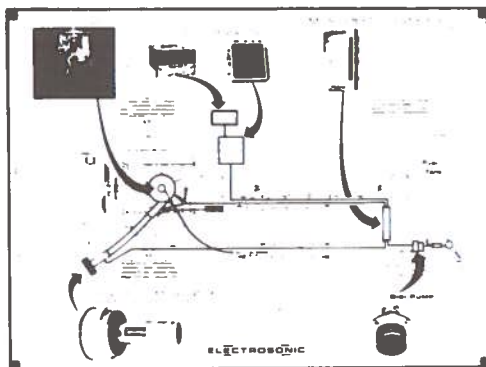
OTHER PUBLICIZED CARBURETORS

- Electrosonic Fuel Induction System
- Ultrasonic Fuel System
- Cal Tech Super Carburetor
- Kendig Carburetor
- Woodworth Carburetor
- Arpaia Fuel Injection
- Dresserator System
- Fish Carburetor
- Gelb Digital-Controlled Carburetor
- Pogue Carburetor
- Vaporator
- Fessenden Carburetor System
- Vapipe
- Graybill VMM Injector
- Ethyl Carburetor



## ELECTROSONIC FUEL INDUCTION SYSTEM

AUTOTRONICS CONTROL CORPORATION



### ● COST FACTORS

- HARDWARE COST -- \$50 OVER CONVENTIONAL SYSTEM
- INSTALLATION TIME -- NOT SPECIFIED

### ● TYPE

- COMPUTER-CONTROLLED ACOUSTIC ATOMIZER

### ● COMPONENTS

- ATOMIZER
- COMPUTER
- AIR FLOW TRANSDUCER
- FUEL METERING PUMP

### ● APPROACH

- DELIVER A PRE-SET, LEAN AIR-FUEL MIXTURE OVER A RANGE OF OPERATING CONDITIONS

### ● CLAIMS

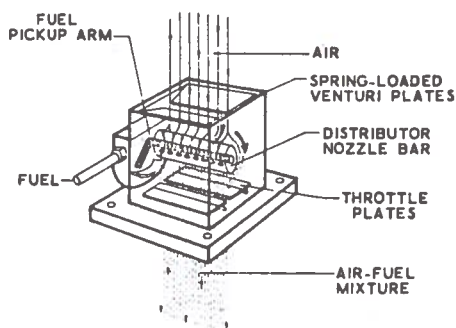
- 20-25% FUEL ECONOMY IMPROVEMENT
- MEET 1975 EMISSION STANDARDS
- NO PERFORMANCE DEGRADATION

### ● DEVELOPMENT STATUS

- RESEARCH PROTOTYPE UNITS
- 120 PRODUCED

## KENDIG CARBURETOR

POLLUTION CONTROL INDUSTRIES



### ● TYPE

- AIR-VALVE CARBURETOR

### ● COMPONENTS

- DUAL THROTTLE PLATES
- DUAL SPRING-LOADED VENTURI PLATES
- FUEL SPRAY BAR
- FUEL METERING ORIFICE (linked mechanically with venturi plates)
- CONVENTIONAL FUEL FLOAT CHAMBER

### ● AIR-FUEL RATIO -- NOMINALLY 16 TO 18

### ● CLAIMS

- PRINCIPAL CLAIM IS FOR REDUCED EMISSIONS
- IMPROVED FUEL ECONOMY ALSO

### ● DEVELOPMENT STATUS

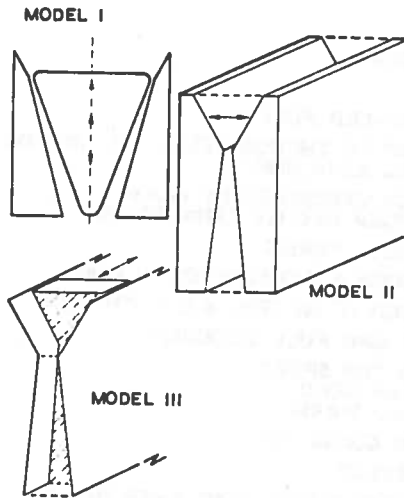
- DEVELOPMENT PROTOTYPE

### ● COST FACTORS

- \$65 TO 70 HARDWARE COST
- 3/4 hr INSTALLATION TIME

## DRESSERATOR SYSTEM

DRESSER INDUSTRIES, INC



Dresserator Models

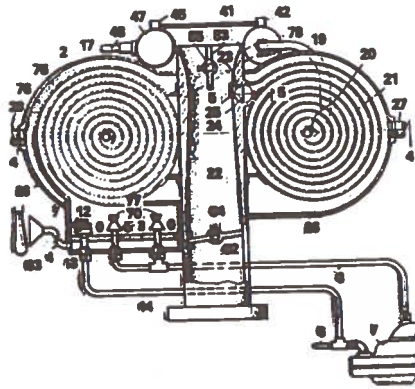
- TYPE
  - SONIC VARIABLE-VENTURI SYSTEM
- COMPONENTS
  - ATOMIZING CORE (variable-venturi)
  - PRESSURE FUEL SYSTEM
  - FUEL METERING APPARATUS
  - FUEL SPRAY BAR
    - UPSTREAM OF VENTURI
- AIR-FUEL RATIO -- 18 TO 19
- CLAIMS
  - REDUCED EMISSIONS
  - VERY CLOSE CONTROL OF A/F RATIO
    - SONIC FLOW FEATURE
  - FUEL ECONOMY IMPROVEMENT
- DEVELOPMENT STATUS
  - DEVELOPMENT PROTOTYPE
- COST FACTORS
  - NONE AVAILABLE

### AVAILABLE DATA

Dresserator System 1972 Federal CVS Test Results

	Emissions, g/mi			Fuel Economy (mi/gal)
	HC	CO	NO <sub>x</sub>	
<u>1971 Ford Galaxie, 351 CID</u>				
1. Dresserator	0.3 - 0.5	4.5 - 7.5	1.2 - 1.7	10.5 - 11.0
2. Dresserator	0.32	4.68	1.58	10.8
3. Dresserator with Conventional Exhaust	0.8 - 1.0	6 - 7	1 - 1.3	11 - 13
4. Baseline	1.5 - 2.5	30 - 40	4.0 - 4.2	10.4 - 10.6
<u>1973 Chevrolet Monte Carlo, 350 CID</u>				
5. Dresserator	0.65 - 0.95	4.9 - 6.2	1.16 - 1.60	11.2 - 12.0
6. Baseline	1.71	24.0	2.42	11.6
7. Dresserator with Vac. Advance	1.07	5.84	2.00	13.0
1975 California Standards	0.9	9.0	2.0	

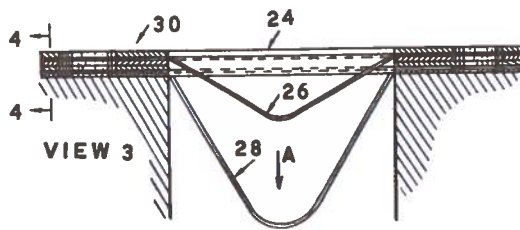
**POGUE CARBURETOR**  
 BASED ON 3 PATENTS ISSUED TO CHARLES N. POGUE  
 IN 1931, 1935, AND 1936



Representation of Pogue Carburetor (from patent)

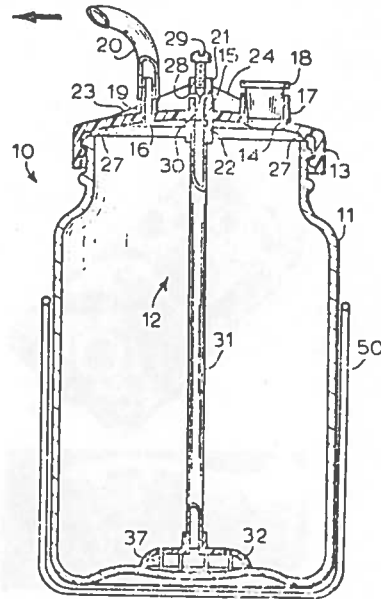
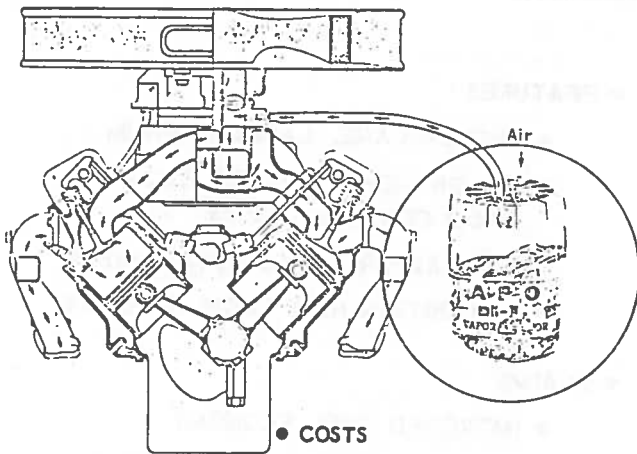
- TYPE
  - VAPORIZER
- FEATURES
  - PRESSURE-FED FUEL
  - AIR BUBBLED THROUGH FUEL TO PROVIDE AIR-FUEL EMULSION
  - EMULSION VAPORIZED BY HEAT EXCHANGER FED BY EXHAUST GAS
- CLAIMS BY C. A. FERRIS
  - BUILT SUCH A CARBURETOR IN 1940s
  - INSTALLED IT ON 1936, 6 CYL CHEV
  - HAD 150 MPG FUEL ECONOMY
  - LIMITED TOP SPEED
    - 38 mph COLD
    - 28 mph WARM
- EVALUATION COMMENTS
  - NO INTEREST
  - NOT IN EXISTENCE: NONE EVER BUILT
  - INVOLVES COMPLEX, HIGH PRESSURE LOSS HEAT EXCHANGER
  - FUEL ECONOMY CLAIMS TECHNICALLY UNSUPPORTABLE FOR CONVENTIONAL AUTOS

**HYDRO-CATALYST SYSTEM**



- TYPE
  - MECHANICAL SCREEN
- COMPONENTS
  - PLATE WITH CONICAL SCREEN CUPS
  - EACH CUP HAS 2 WIRE SCREENS SEPARATED BY GASKET
    - TREATED TO ACT AS CATALYSTS
- OPERATION CLAIMS
  - PRECOMBUSTION CATALYTIC EFFECT
    - SUPPRESSES KNOCK
  - ELECTROSTATIC ACTION
    - CHARGES FUEL DROPLETS
    - ATTRACTED TO HOT MANIFOLD WALL
- EPA TESTS (1972 Cadillac)
  - NO BASELINE (compared to cert. data)
  - 25% BETTER FUEL ECONOMY
  - CO IMPROVED
  - HC INCREASED 50%
  - NO<sub>x</sub> DOUBLED
- SCOTT TESTS (1973 Mustang)
  - IGNITION TIMING ADVANCED 7 deg
  - 34% BETTER FUEL ECONOMY
  - CO REDUCED ~50%
  - HC AND NO<sub>x</sub> INCREASED TO 6 TO 11%
- UNIV OF MICHIGAN TESTS (350 CID Chev. engine)
  - STANDARD TIMING (4 deg BTDC)
    - DECREASED FUEL ECONOMY (3 to 23%)
  - ADVANCED TIMING (11 deg BTDC)
    - INSIGNIFICANT CHANGE TO 5% DECREASE
- ESSO RESEARCH TESTS
  - 1971 CHEV AND 1965 DODGE
  - SLIGHT INCREASE IN FUEL CONSUMPTION
- COST -- \$28

## TYPICAL VAPOR INJECTOR CONFIGURATIONS



- COSTS
  - \$30-\$50 HARDWARE
  - 1 TO 1.5 hr INSTALLATION TIME
- FLUID REPLACEMENT
  - APPROXIMATELY EVERY 2000 mi

### INLET MANIFOLDS

#### EDELBRICK TEST DATA

- Edelbrock And Motor Trend Tests
  - 1974 Monte Carlo, 400 CID
    - Chassis Dynamometer, Seven-Mode Cycle
    - 18 Percent Fuel Economy Improvement
    - Street Driving
    - 16 Percent Fuel Economy Improvement
    - No Emissions Data
- Edelbrock CVS Test
  - 1973 Chevrolet 150 CID
  - Test Procedure
    - Federal CVS (Do Not Know if Hot Or Cold)
  - Results (Percent Changes)
    - Fuel Economy, +9.2 %
    - HC, -6%
    - CO, -17.8%
    - NO<sub>x</sub>, -30.8%

## INLET MANIFOLDS

### EDELBROCK



VIEW OF THE EDELBROCK  
STREETMASTER INLET  
MANIFOLD

#### ● FEATURES

- SINGLE-PLANE, LARGE PLENUM
- ALL BRANCHES EMERGE RADIALLY FROM CENTRAL CAVITY
- REDUCED CROSS-SECTIONAL AREAS
  - OBTAIN HIGH FLOW VELOCITY

#### ● CLAIMS

- IMPROVED FUEL ECONOMY
  - UP TO 20% IN RECREATIONAL VEHICLES
  - REDUCED EMISSIONS

#### ● COST FACTORS

- HARDWARE, \$135 TO \$165
- INSTALLATION TIME, 2 TO 6 hr

## OTHER IGNITION SYSTEMS

### "Improved Design" Category

- Replace Existing Components of System
- Magna Flash, Uhland, Azure Blue, Gas Energizer
- Generally Provide a Small Increase in Voltage Level or Extension of Spark Duration
- Fuel Economy Improvement Potential Very Limited

### "Unconventional" Category

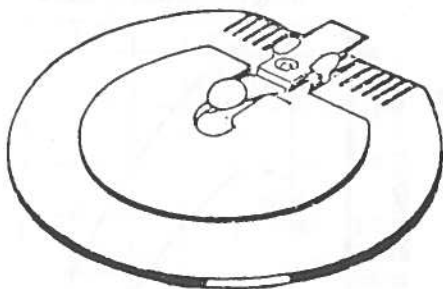
- Are Added to System
- Allude to Some Basic Principle to Explain Advantages They Claim. Avoid Details Necessary to Understand How They Might Alter Performance
- Magic Ionizer, Electronic Super Charger, Auto Saver
- Not Possible to Make Analytical Judgement of Effects on Fuel Economy

## ELECTRONIC SUPERCHARGER

### ● CLAIMS

"SUPERCHARGE YOUR CAR. GET MORE POWER ON LESS GAS THAN YOU EVER DREAMED POSSIBLE - IN LESS THAN 2 MINUTES. "

"14% - 36% INCREASE IN GAS MILEAGE REPORTED "



ELECTRONIC SUPERCHARGER  
REPLACES ROTOR IN DISTRIBUTOR

### ● HOW IT WORKS (manufacturer's quote)

"ELECTRONIC SUPERCHARGING SENDS HOT ELECTRICITY (amperage) TO ONE CYLINDER AT A TIME, BUT SIMULTANEOUSLY SENDS POWER FROM COLD ELECTRICITY (voltage) TO EVERY OTHER CYLINDER --- THIS SUPERCHARGES GAS-AIR MIXTURE --- ADDS EXTRA POWER "

### ● UNIV OF MICHIGAN TEST RESULTS (350 CID engine dyno tests)

4% INCREASE IN FUEL ECONOMY AT 25 mph  
4% DECREASE IN FUEL ECONOMY AT 35 mph  
NO OTHER CHANGES NOTED

## IGNITION SYSTEM SUMMARY

- Unlikely That Significant Fuel Economy Improvements Would Result From Retrofitting Ignition Systems

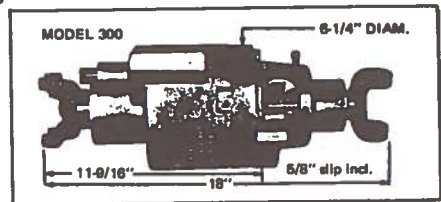
As Long As Conventional System is Properly Maintained

- Capacitative Discharge Systems Have Greatest Potential If Retrofit Were To Be Made
- Multiple-Spark-Discharge (MSD) System May Be Most Attractive
  - Up To 15 High Energy Discharges Per Firing Can Be Delivered Over 20° Of Crankshaft Rotation
  - Improves Statistical Probability Of Igniting Very Lean Mixtures
  - Might Provide Most Benefit To Late-Model Emission-Controlled Vehicles

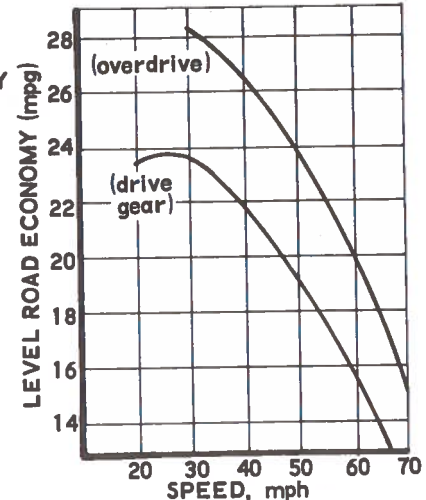
## DRIVETRAIN COMPONENTS

### ● OVERDRIVE UNITS

- REDUCES ENGINE TO DRIVE WHEEL SPEED RATIO BY ~30%
- PERMIT DOWN-SHIFTING TO NORMAL GEAR RATIOS FOR BETTER ACCELERATION IN CITY TRAFFIC DRIVING
- GENERALLY CAN IMPROVE FUEL ECONOMY > 20% AT STEADY STATE DRIVING CONDITIONS
- AVAILABLE ON RETROFIT BASIS
- FURTHER TESTING NOT REQUIRED
- COST FACTORS
  - HARDWARE, \$200 TO \$400
  - INSTALLATION, \$100 TO \$150
  - HEAVY DUTY COOLING SYSTEM (\$100) FOR VEHICLES >7500 lb GVW



**HONE OVERDRIVE ASSEMBLY  
FOR PASSENGER CARS**

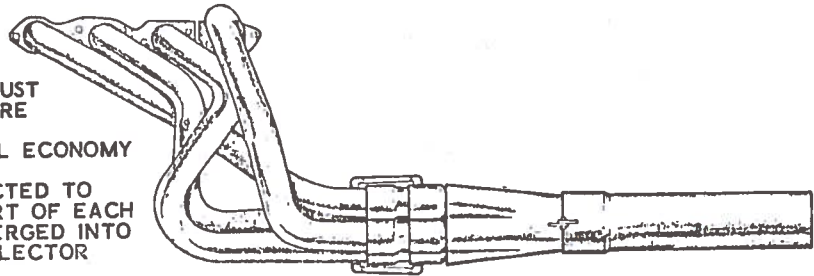


**EFFECT OF 30% OVERDRIVE ON FUEL ECONOMY OF A PASSENGER CAR**

## EXHAUST-RELATED SYSTEMS

### ● TUNED EXHAUST SYSTEMS

- REDUCE EXHAUST BACK-PRESSURE
- IMPROVE FUEL ECONOMY
- PIPES CONNECTED TO EXHAUST PORT OF EACH CYLINDER MERGED INTO COMMON COLLECTOR
- OPERATION
  - PRESSURE WAVE CREATED IN EXHAUST PIPE AT BEGINNING OF OPENING OF EXHAUST VALVE AND DISCHARGE OF EXHAUST GASES
  - WAVE PROPAGATES THROUGH PIPE WITH SONIC VELOCITY
  - REFLECTED BACK AS A SUCTION WAVE TOWARDS STILL-OPEN EXHAUST VALVE
  - AT VALVE, SUCTION WAVE EXERTS EVACUATING EFFECT ON GASES STILL IN CYLINDER
    - IF PIPE IS TUNED (has correct length)
- HIGH ENGINE SPEEDS
  - POWER OUTPUT INCREASED DUE TO CYLINDER SCAVENGING (volumetric efficiency)
- LOW AND MEDIUM ENGINE SPEEDS
  - REDUCED PUMPING LOSSES AND IMPROVED FUEL ECONOMY
- MULTI-CYLINDER EFFECTS
  - INTERFERENCE EFFECTS AT COMMON COLLECTOR CAN STRONGLY INFLUENCE BASIC CHARACTERISTICS



EXHAUST-RELATED SYSTEMS

Tuned Exhaust Systems

Fuel Economy Test Data

Aesi Tests Of Hooker Headers

	Fuel Economy Improvement -- %		
	Federal Driving Cycle	Steady 50 MPH	Steady 60 MPH
1973 Vega	+5.7	+14.4	+4.5
1974 Chevrolet Pickup	+6.2	+5.1	+6.8

Edelbrock Tests Of Hooker Header Plus Edelerbock Inlet  
Manifold (7-Mode Tests Of 1974 Chevelle, 454 CID)

	Fuel Economy Improvement -- %		
	Dyno	Town	Highway
Hooker Headers Only	+5.2	+4.8	+3.5
Headers Plus Manifold	+10.5	+17.7	+17.2



**COMPARISON OF CONCEPTS/DEVICES  
FUEL ECONOMY POTENTIAL**

CLASS/DEVICE	FUEL ECONOMY IMPROVEMENT POTENTIAL*			
	NEGATIVE - TO 0%	NEGLECTIBLE 0 TO 4%	MODEST 5 TO 14%	SUBSTANTIAL 15 AND ABOVE
CARBURETORS (selected ones)			X	
ATOMIZERS		SCREENS	ACOUSTIC (PCA)	
LEAN-BLEED SYSTEMS		X	SOME PRE-CONTROLLED CARS COULD HAVE MODEST INCREASE	
VAPOR INJECTORS		X		
FUEL MODIFICATIONS				
FUEL ADDITIVES		X		
FUEL MIXTURES		X		
INLET MANIFOLDS		OFFENHAUSER DATA	EDELBROCK DATA	
PRESSURE REGULATORS		X		
FUEL PRE-AGITATOR	X			
IGNITION SYSTEMS				
CAPACITIVE DISCHARGE		ON MAINTAINED VEHICLES	ON CARS WITH LEAN AIR- FUEL RATIOS	
ELECTRONIC INDUCTIVE		ON MAINTAINED VEHICLES	ON CARS WITH LEAN AIR- FUEL RATIOS	
OTHERS		X		

\* Based on present State-of-Art and available data

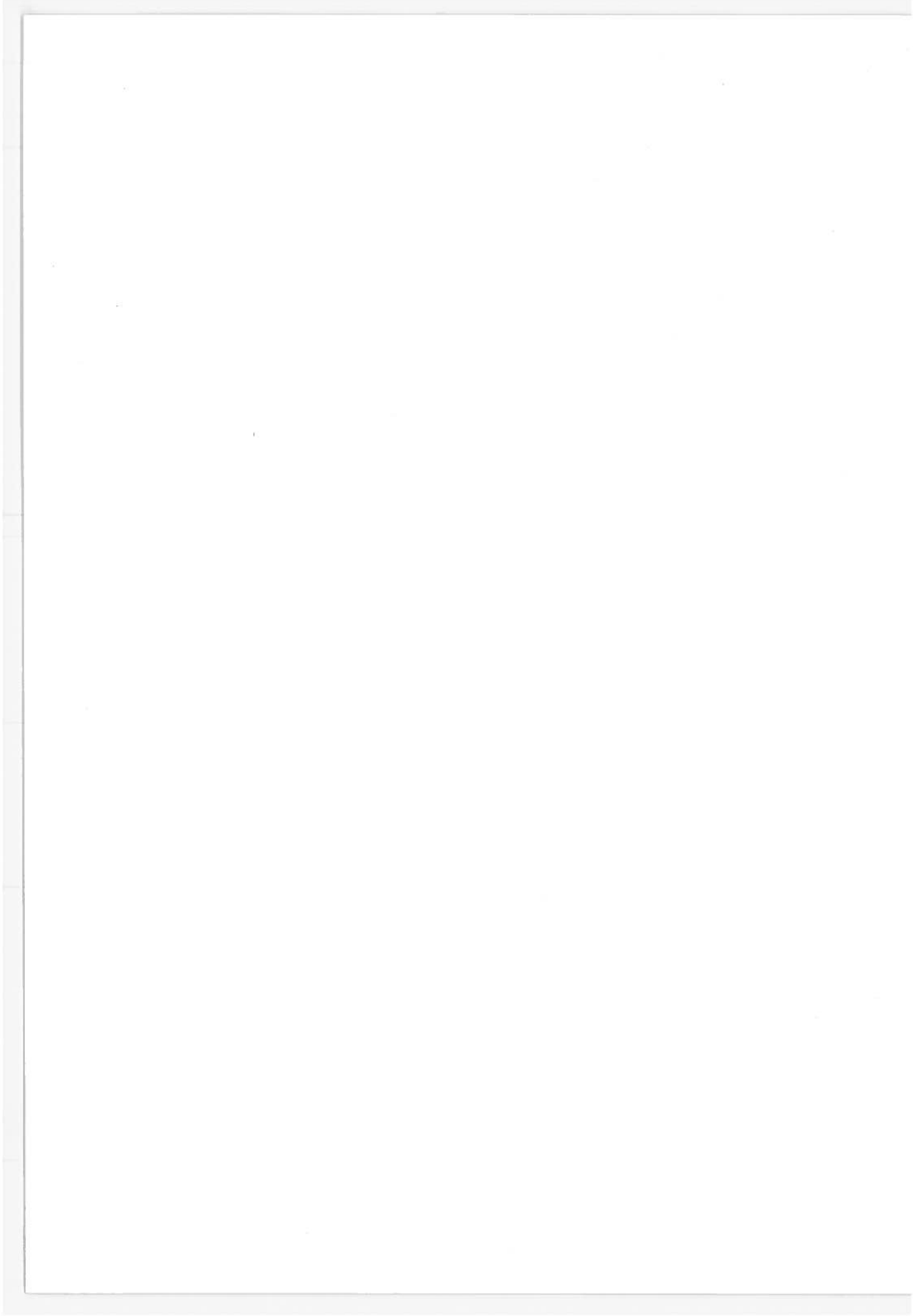
CLASS/DEVICE	FUEL ECONOMY IMPROVEMENT POTENTIAL*			
	NETATIVE - TO 0%	NEGLECTIBLE 0 TO 4%	MODEST 5 TO 14%	SUBSTANTIAL 15 AND ABOVE
EMISSION CONTROL RETROFITS	X			
DRIVETRAIN				
TIRES			RADIAL TIRES	
TRANSMISSIONS			TRUCK AUTOMATIC TRANSMISSIONS	
REAR AXLE GEAR RATIOS			X	HIGHWAY DRIVING
OVERDRIVE UNITS			X	HIGHWAY DRIVING
DRAG REDUCTION DEVICES		X	HIGHWAY DRIVING	
DRIVER AIDS		←	INDETERMINATE	→
FLEXIBLE COOLING FANS		X		
VALVE TIMING		X		
TUNEUPS			X	
COMPRESSION RATIO INCREASE			X - NOT RECOMMENDED	

COMPARISON OF CONCEPTS/DEVICES (Cont'd)

FUEL ECONOMY POTENTIAL

	FUEL ECONOMY IMPROVEMENT POTENTIAL*			
	NEGATIVE - TO 0%	NEGLIGIBLE 0 TO 4%	MODEST 5 TO 14%	SUBSTANTIAL 15 AND ABOVE
TUNED EXHAUST SYSTEMS			X	
DUAL EXHAUST SYSTEMS		X		
EXHAUST CUT-OUT			X - NOT RECOMMENDED ILLEGAL IN SOME STATES	
TURBO CHARGERS	X - WITH SAME ENG			WITH REDUCED ENG CID
ENGINE OIL			MAY BE POSSIBLE	
ENGINE OIL ADDITIVES			MAY BE POSSIBLE	
ENGINE OIL FILTER		X (1)		
TAMPERING WITH ECSs	← X →			
SUGGESTED COMBINATIONS				
INLET MANIFOLD AND TUNED EXHAUST			X	POSSIBLE
CARBURETOR PLUS CD IGNITION - MSD, IN PARTICULAR			X - LEAN AIR FUEL RATIOS	

(1) Prevents Performance Degradation Over Lifetime



AUTOMOTIVE POWER PLANT EVALUATION  
William F. Marshall  
U.S. Department of Interior/Bureau of Mines  
Bartlesville Energy Research Center  
Bartlesville, Oklahoma  
ABSTRACT

The objective of this program is to obtain automotive engine performance data for use in estimating vehicle emissions and fuel economy in varied service and duty.

An experimental test procedure for generating fuel consumption and emissions data adequate to describe an engine's characteristics over its full operating range, including transient modes, will be developed and validated. These data, referred to as "engine maps" will be obtained for 23 different engines, including:

- 15 current production spark ignition engines,
- 4 pre-production or prototype advanced design spark ignition engines (lean-burn),
- 4 diesel engines which are, or might be, used in passenger car applications.

To date, several engines have been installed and coupled to dynamometers. Although the program is yet in its initial stages, some data have been collected and is reported below.

This program has just been initiated and it is too early to report on definitive conclusions as yet. The objective of this program is to obtain automotive engine performance data for use in estimating emissions and fuel economy in varied service and duty. The intent of this work is to provide the basic engine characteristic data which are required as input for engineering calculations in systems and analysis involving ground transportation. Specifically, our objectives are to develop a procedure for generating fuel consumption and emissions data adequate to describe an engine's characteristics over its full operating range. These data, referred as an "engine maps", will include information collected from engines operated over transients as well as steady-state modes. The procedure for mapping will then be applied to 23 different engines to obtain their emissions and fuel consumption characteristics.

The experiments will be done with engines on test stands. The engines will be coupled to eddy current dynamometers and variable inertia loading systems. In addition, capability for motoring is available for several of the engines to be tested. Fuel consumption will be determined by direct metering and by carbon balance in conjunction with constant-volume-sampling (CVS). The carbon balance/CVS method is particularly useful for engines operated over transients for both fuel consumption and emission rates.

Emission levels will be determined with commonly accepted analytical equipment. These analyses include:

- CO and CO<sub>2</sub> by nondispersive infrared absorption
- Unburned hydrocarbons by heated flame ionization detector
- NO<sub>x</sub> by chemiluminescence detector and,
- O<sub>2</sub> by a polarographic technique

Mass emission rates will be determined from CVS samples or computed from fuel rate and raw exhaust composition.

The program elements include:

1. Development and Validation of test procedure;
2. Generating data for engine maps for three classes of engines;
3. Developments toward an Alternative Fuel Technology.

The first of these elements, procedures development, will include work with three spark ignition engines. The engines will be operated over their entire speed/load range encountered in normal use. The steady-state test will include approximately 100 speed/load points. This matrix pattern is to be developed in sufficient detail targeted to define the engine's performance characteristics within +5% at any point within the engine's operating envelope. Estimative or predictive accuracy will be verified by reiterated estimations from generated data followed by tests at the operating points for which the estimations were made.

Transient mode data will be obtained by continuous measurements made during discrete accelerations, decelerations, and engine warm-up periods. Inertial and power absorber loadings will be varied as appropriate to the duty of the engines. The basis for the engine's duty cycle will be obtained from measurements made on engines in vehicles operated over three different driving cycles: the LA-4, EPA and SAE highway fuel economy cycles.

From these data, a procedure will be developed to call out the minimal testing required to define an engine's operating characteristics adequate for prediction or estimation of fuel economy and emission during steady-state and appropriately varied cyclic-mode tests. The need for including transient tests in the engine maps will be based on the ability to predict cyclic data from steady-state data.

In addition to the engine maps obtained under procedures development, 12 current production 1975 model year engines will be mapped. These maps will be obtained using the procedures developed in the first program element.

Maps will be obtained for four prototype engines. Included is at least one Honda-type engine/combustion system. Maps will also be obtained for four light duty diesel engines which either are or appear suitable for use in passenger car application.

The final program element deals with developments toward an alternative fuel technology. This does not include any experimental work within this specific program, but is directed toward surveillance of developments toward the use of alternative fuels in transport applications. Information on engine performance with alternative fuels will be summarized and updated periodically. The source of this information is industry and results of experimental work done at the BERL in its in-house research and in cooperation with other governmental agencies.

Nearly all of the engines to be used in the program are on order or have been received. Negotiations are underway for the remainder. The test facilities are complete with the exception of installation of the inertia load and CVS systems.

Engine mapping was initiated with a Honda CVCC engine. This map consists of data from steady-state modes, including motored operation. Results show that, although there were variations in air-fuel ratio over the test period, emissions and fuel consumption were fairly stable.

Work planned for the immediate future includes:

1. Continuation of engine mapping-steady state modes;
2. Obtaining engine data in vehicle test (defining engine transients);
3. Mapping engines-transient modes;
4. Testing ability of steady state data for estimating emissions and fuel consumption over transients.

# LEAN MIXTURE ENGINE TESTING AND EVALUATION

M. W. Dowdy

Jet Propulsion Laboratory  
California Institute of Technology  
Pasadena, California

## ABSTRACT

The present JPL work is aimed at defining analytically and demonstrating experimentally the potential of the "lean burn concept". Fuel consumption and emissions data were obtained on the engine dynamometer for the baseline engine and two lean burn configurations of the same engine. Data comparisons were then made. Individual cylinder equivalence ratios were measured to evaluate the cylinder-to-cylinder distribution. Pressure-time traces from individual cylinders were used to get information about ignition delay, combustion duration and cycle-to-cycle pressure variations. Fuel consumption and emissions data for one lean burn configuration were obtained over the Federal Driving Cycle using a chassis dynamometer and the results were compared with the stock baseline results. Using experimental results and information from the existing literature, the potential of the "lean burn concept" was assessed using the Blumberg-Kummer cycle analysis program.

## 1. INTRODUCTION

In this evaluation only the concepts which are practical for near term application have been considered. The emissions standards which have been used are 2 gm/mi NO<sub>x</sub>, 3.4 gm/mi CO and 0.41 gm/mi HC. A literature review was made to identify any significant achievements and the most promising methods for good lean burn operation. Considerable lean burn engine analysis was performed to help in assessing the potential of the lean burn concept. In conjunction with this analysis, the Blumberg-Kummer cycle analysis program was used and a computer simulation model of the urban driving cycle was used to calculate the performance of the lean burn engine over the Federal Driving cycle using engine mapping data. A series of stock baseline tests were made to provide fuel consumption and emissions data to be used in comparisons with the lean burn engine. Lean burn engine tests were performed on two configurations. Both engine and chassis dynamometer tests were performed with emissions.



## 2. ENGINE CONFIGURATIONS

The stock baseline engine was a 1973 Chevrolet V-8 having 350 cu. inch displacement (c.i.d.), 8.5 compression ratio, and a 4 barrel carburetor. It had an air injection reactor to reduce hydrocarbons and CO emissions by the addition of air into the exhaust. It also had exhaust gas recirculation to dilute the incoming charge to reduce the peak temperatures for  $\text{NO}_x$  control and also provided for positive crank case ventilation to return blow-by gases to the engine. In addition it had a modified spark characteristic to aid in the reduction on  $\text{NO}_x$ .

The lean burn configuration removed the stock carburetor and replaced it with an Autotronics induction system which allows additional flexibility in fuel/air ratio control for testing purposes. The intake manifold was replaced with a single-plane manifold and in addition a fuel atomizer was used to promote better atomization and mixing for improved mixture control of the charge. Turbulator intake valves and slant plug heads were used to increase the turbulence in the combustion chamber and increase the compression ratio to 9.5. The General Motors high energy ignition system was also added to provide higher energy discharge for the ignition of lean mixtures. All of the emissions control devices were removed from the stock engine except for the positive crankcase ventilation control.

## 3. TEST FINDINGS

Lean burn operation offers the potential for improved fuel economy as shown in Figure 1, a plot of indicated thermal efficiency versus equivalence ratio. The curves were generated based on the Blumberg-Kummer cycle analysis program. Shown in this plot are three curves for three different combustion durations. Note that the higher thermal efficiency is achieved with the shorter combustion interval. The thermal efficiency increases as the equivalence ratio is decreased. Also shown in this figures is a line representing the gasoline lean flammability limit. This represents the leanest equivalence ratio at which gasoline will burn. If it were possible to maintain a constant combustion interval while

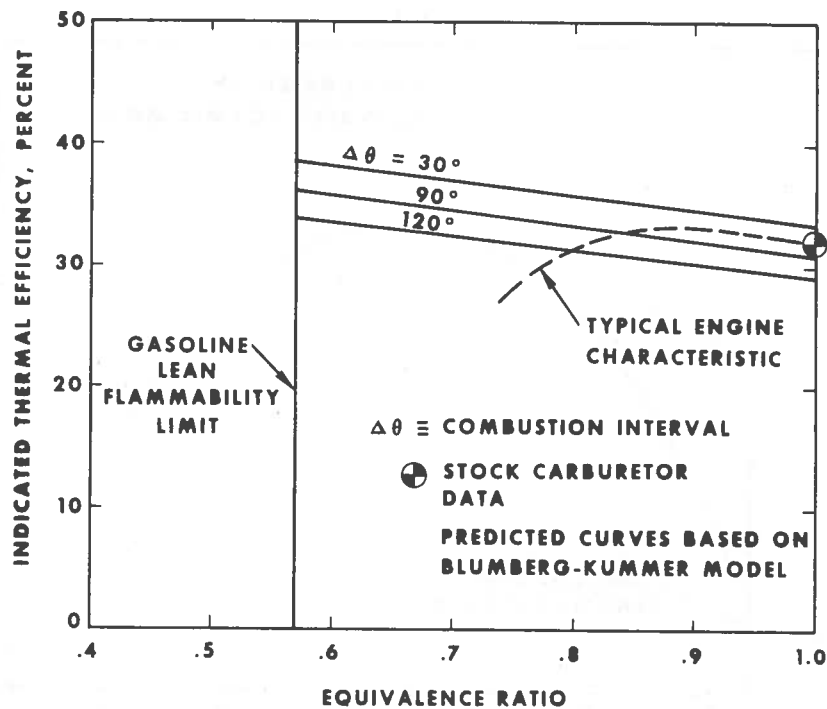


Figure 1. Predicted Thermal Efficiency

lowering the equivalence ratio, significant improvements in engine thermal efficiency could be achieved; however, in most practical engine systems the engine performance is represented by the dashed line. As the engine is leaned-out the flame speed decreases, leading to a longer combustion interval, which results in a decrease in thermal efficiency. To achieve the potential fuel economy benefits of lean operation it is necessary that the lean burn engine maintain a fast burning charge in lean mixtures.

In addition to its fuel economy benefits the lean burn concept offers the potential for controlling  $\text{NO}_x$  emissions as shown in Figure 2. This figure shows  $\text{NO}_x$  emissions versus equivalence ratio as predicted by the Blumberg-Klumner model. Also shown is a line representing the lean flammability limit of gasoline. The curve indicates that  $\text{NO}_x$  emissions reach a peak for an equivalence ratio of 0.85. Significant reductions in  $\text{NO}_x$  emissions can be achieved for leaner equivalence ratios.

The fuel consumption characteristics of the lean burn engine are given in Figure 3 showing the effects of equivalence ratio and

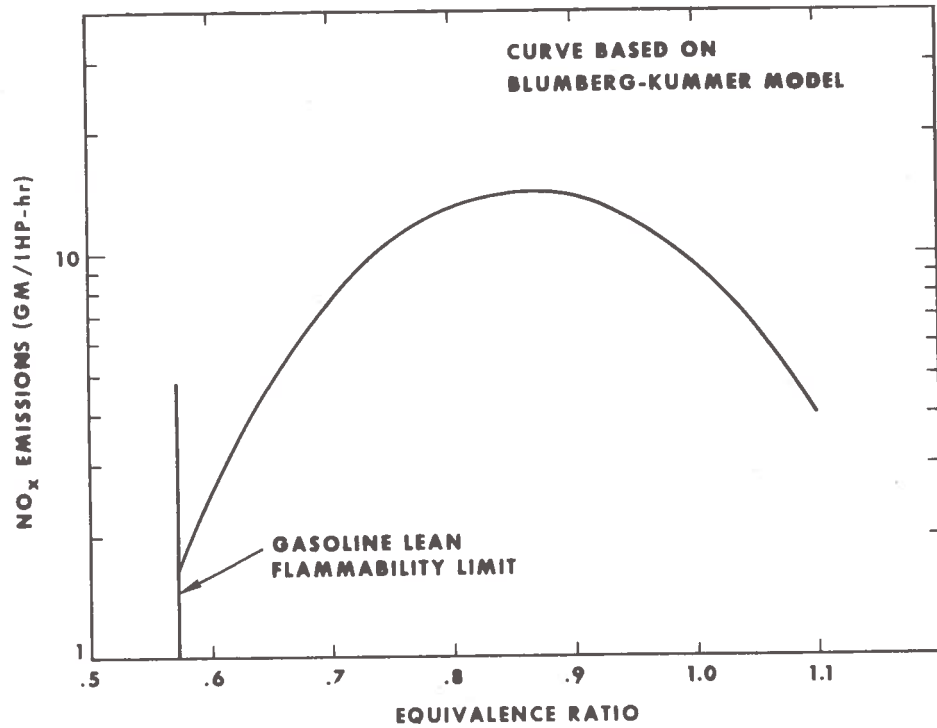


Figure 2. Predicted NO<sub>x</sub> Emissions

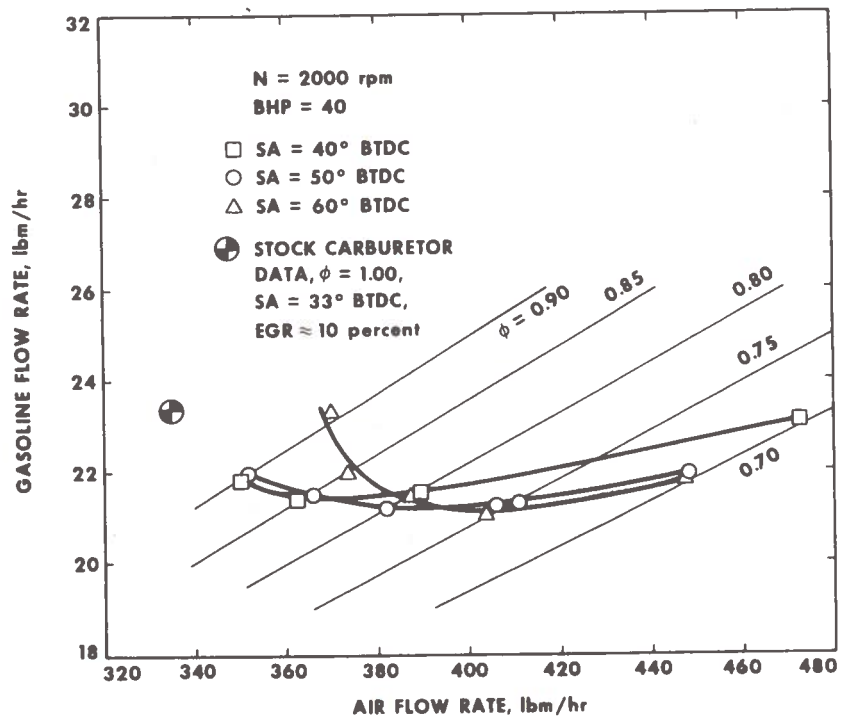


Figure 3. Fuel Consumption Characteristics

spark timing on fuel consumption. A data point for the stock engine is included for comparison. The minimum fuel consumption occurs at an equivalence ratio of 0.75 with a spark advance (SA) of 60° BTDC. To achieve minimum fuel consumption, more spark advance is required as the equivalence ratio is decreased. The minimum fuel consumptions for equivalence ratios of 0.75 and 0.80 are almost equal with emissions performance becoming important in choosing an operating point.

Figure 4 illustrates the tradeoff between brake specific fuel consumption (BSFC) and brake specific NO<sub>x</sub> (BSNO<sub>x</sub>) emissions. The minimum brake specific fuel consumption for the lean engine is about 10 percent less than the stock value; however, the brake specific NO<sub>x</sub> emissions at this condition are twice that of the stock engine with emission control devices. The stock brake specific NO<sub>x</sub> emissions level can be met by the lean burn engine while maintaining a brake specific fuel consumption 6 percent less than the stock value.

The relationship between brake specific hydrocarbon (BSHC) emissions and brake specific NO<sub>x</sub> emissions is shown in Figure 5. A dashed line is drawn through the data points with MBT spark timing for each equivalence ratio. When the lean burn engine is tuned to produce NO<sub>x</sub> emissions equal to the stock values, then it is seen that the hydrocarbons are much higher than those of the stock engine. For MBT spark timing and reductions in brake specific NO<sub>x</sub> emissions are accompanied by significant increases in brake specific hydrocarbons for the lean burn engine. Another interesting trend which this figure illustrates is that although retarding the spark timing from MBT timing does reduce brake specific NO<sub>x</sub> emissions, it does not reduce brake specific hydrocarbon emissions, and in fact causes a slight increase in hydrocarbon emissions for the leaner equivalence ratios. This effect is different from that of engines running rich where retarding the spark timing decreases the hydrocarbon emissions by increasing the exhaust temperatures to promote further hydrocarbon reactions in the exhaust system. At leaner equivalence ratios, retarding the spark timing leads to an increase in unburned hydrocarbons in the

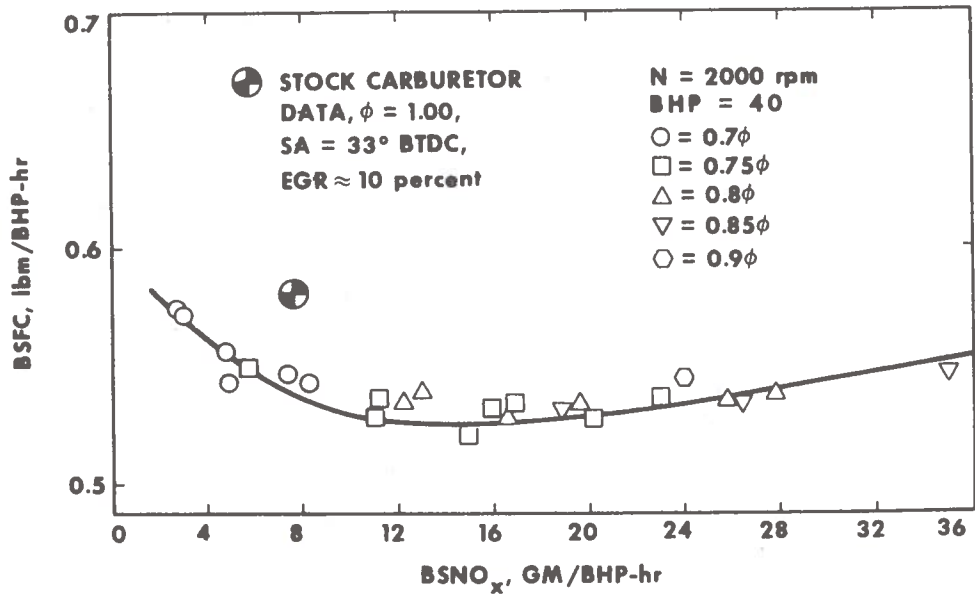


Figure 4. BSFC versus BSNO<sub>x</sub> Emissions

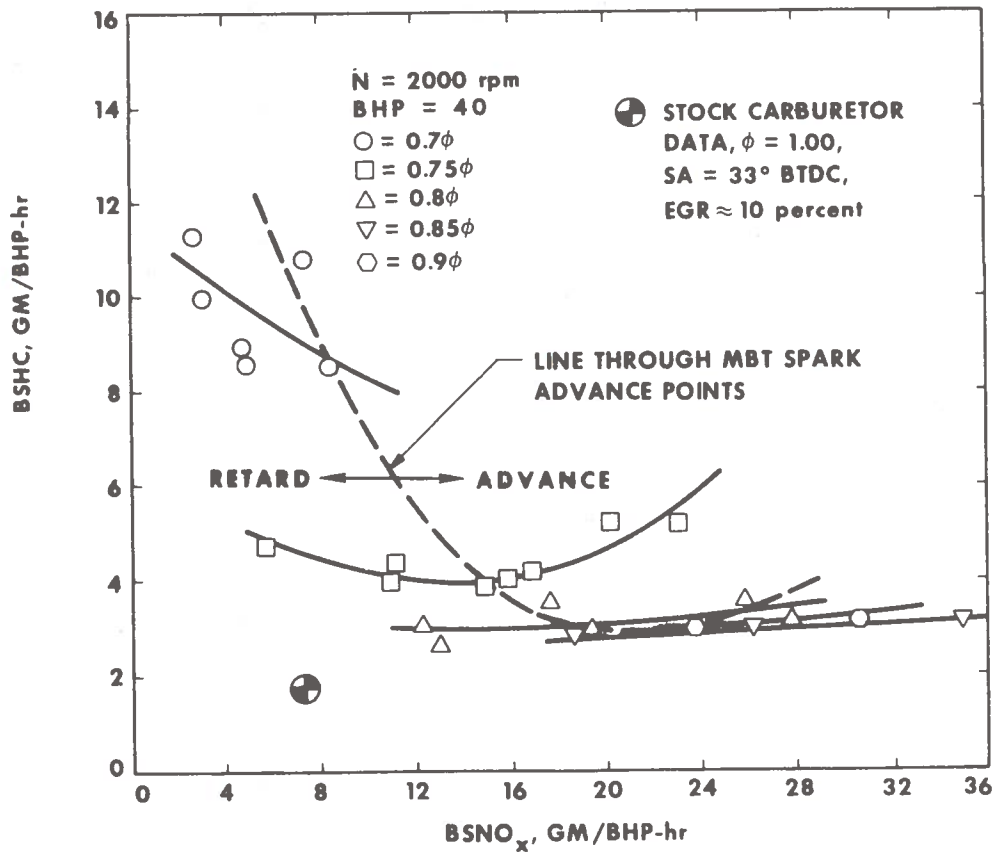


Figure 5. BSHC versus BSNO<sub>x</sub> Emissions

combustion chamber because of the lowered peak temperatures and apparently does not increase the exhaust temperatures sufficiently to promote further hydrocarbon reaction in the exhaust system. Although it is apparent that the lean burn configuration tested does not control hydrocarbon emissions, tests of a similar lean burn engine at JPL have shown that exhaust temperatures are still high enough to permit control of hydrocarbon emissions with the use of a catalytic converter.

#### 4. PRESSURE-TIME DATA

To help in understanding the performance of the lean burn engine, one cylinder of the V-8 was instrumented with a high-response pressure transducer to record pressure-time data. These measurements yielded information about ignition delay, combustion interval and cycle-to-cycle pressure variations. Figure 6 shows a plot of the pressure difference between a firing pressure trace plotted versus crank angle. The pressure difference is normalized with respect to the peak pressure difference. Also indicated is the point at which the spark is initiated. Two parameters are defined. An ignition delay parameter is defined to be the interval from spark initiation until the pressure difference reaches 10% of the peak pressure difference. The flame speed parameter is defined to be the interval from the attainment of 10% of the peak pressure difference until 95% of the peak pressure difference is attained.

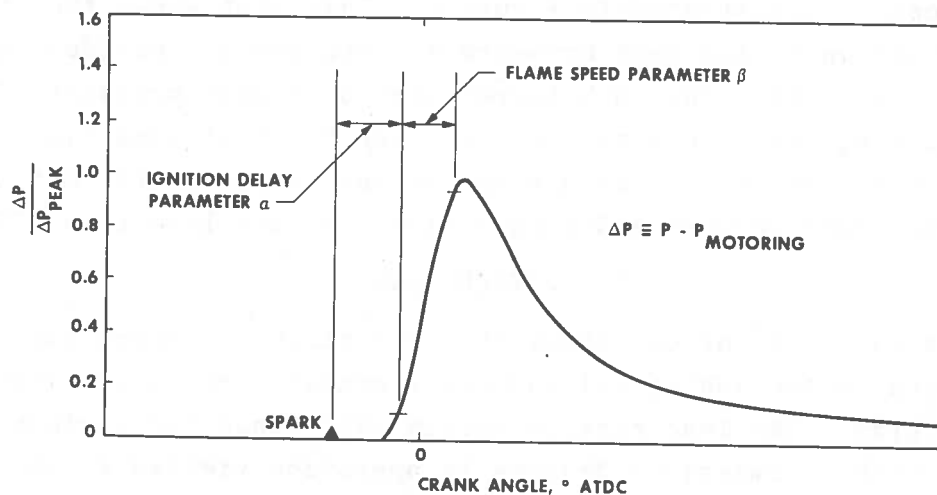


Figure 6. Definition of Ignition Delay and Flame Speed Parameters

The ignition delay parameter versus the cylinder equivalence ratio is shown in Figure 7. The individual cylinder equivalence ratio was derived from an exhaust gas analysis of that cylinder. Note that all data shown for the four operating conditions are at MBT spark timing. The ignition delay parameter is seen to increase significantly as the equivalence ratio is decreased. This indicates that lean mixtures require a much longer time than stoichiometric mixtures for establishing a flame front. No significant dependence of ignition delay on engine RPM and engine load can be established from the test data with all of the data being adequately correlated with a single curve.

Figure 8 shows the flame speed parameter versus the cylinder equivalence ratio. Flame speed is seen to decrease only slightly as the equivalence ratio is decreased. This indicates that once a flame front is established, the lean mixture is being burned almost as fast as a stoichiometric mixture in this lean burn configuration. This flat characteristic could explain the reason why the lean burn engine maintained high efficiency at an equivalence ratio of .75 even though a large spark advance was required. From this test data no significant dependence of flame speed on engine RPM and load can be established, with all data being adequately correlated by a single curve.

The influence of equivalence ratio on cycle-to-cycle pressure variations is illustrated in Figure 9. This plot shows the standard deviation of the peak pressure plotted versus cylinder equivalence ratio. Note the much larger spread in peak pressures for the leaner equivalence ratio points. For the test conditions examined, cycle-to-cycle pressure variations remain fairly constant until the sharp increases for equivalence ratios less than .75.

## 5. CONCLUSIONS

Certain conclusions about the lean mixture concept can be made based on the analytical and experimental work accomplished in this program. The lean mixture engine when tuned for maximum fuel economy with no emissions devices in operation yielded a 12% decrease in brake specific fuel consumption when compared to the

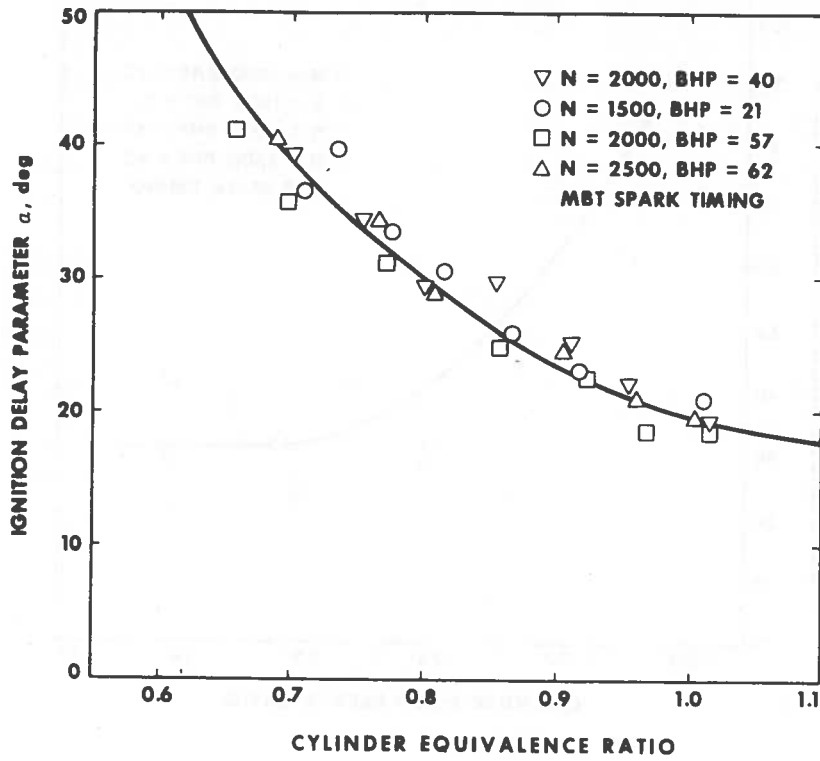


Figure 7. Ignition Delay Parameter versus Equivalence Ratio

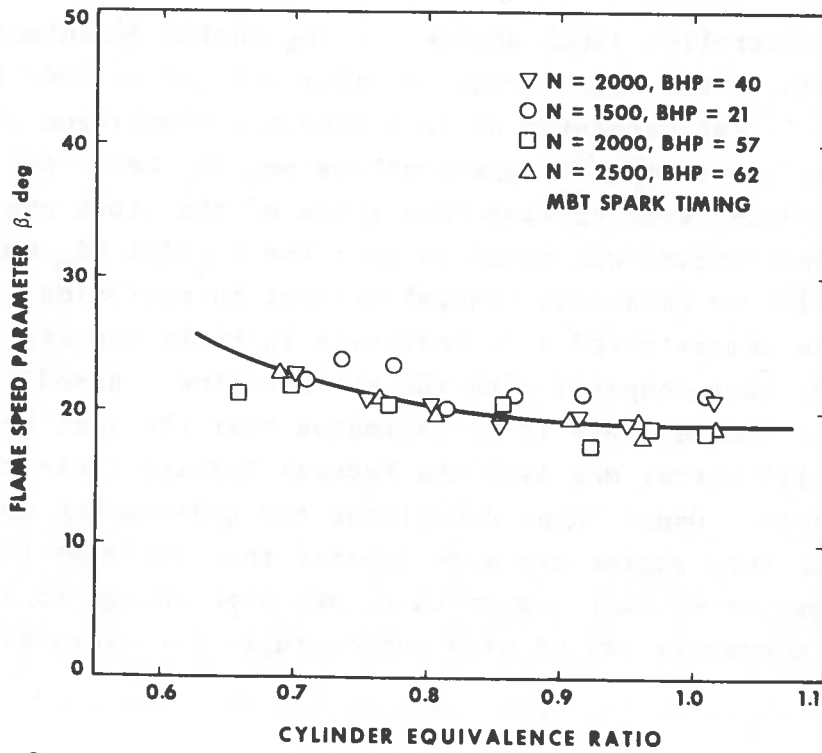


Figure 8. Flame Speed Parameter versus Equivalence Ratio



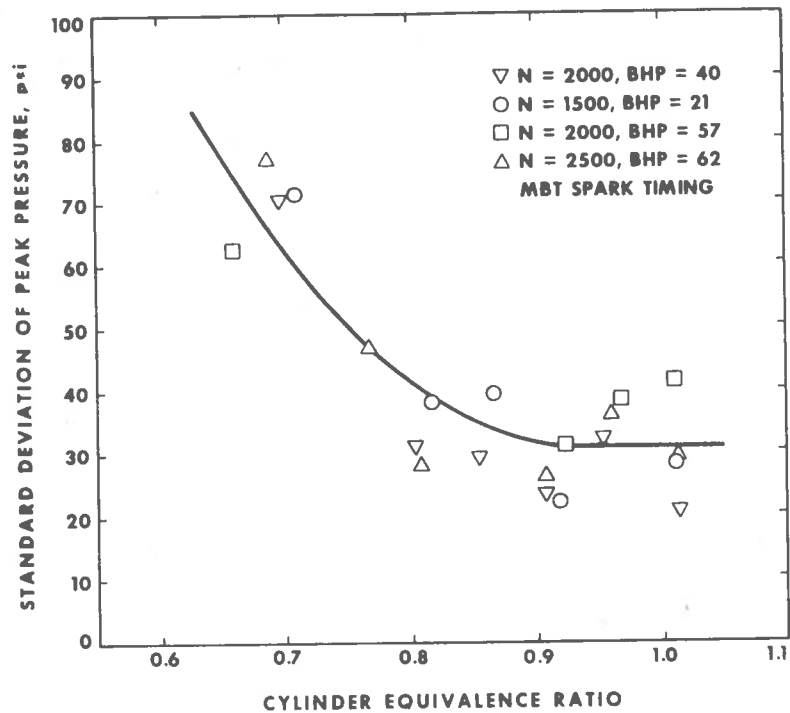
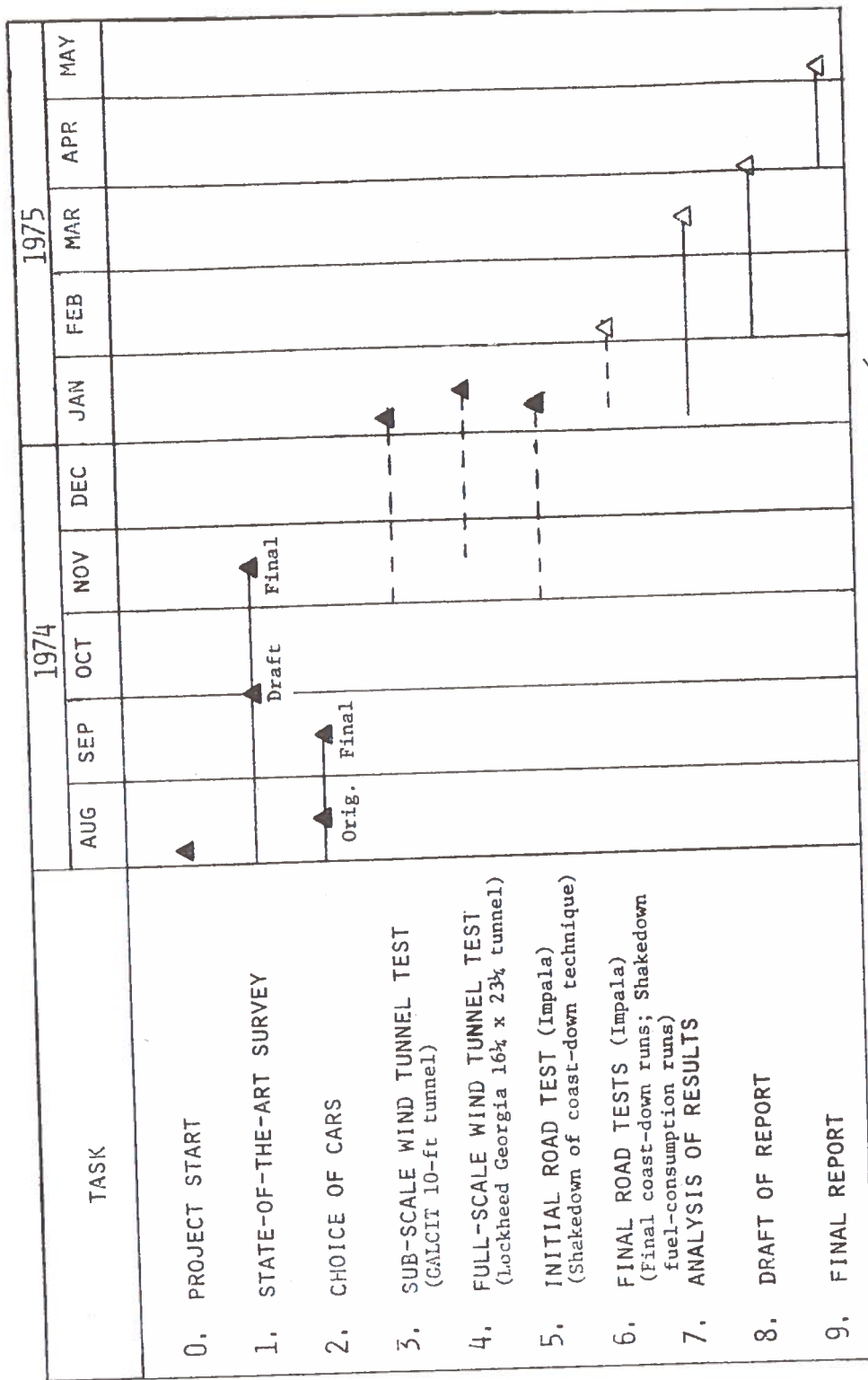


Figure 9. Peak Pressure Standard Deviation vs. Equivalence Ratio

emissions controlled stock engine. Using engine dynamometer mapping data, a 22% improvement in miles per gallon over the Federal Driving Cycle was estimated using a computer simulation program. Under these conditions the hydrocarbons and  $\text{NO}_x$  emissions of the lean burn engine were greater than those of the stock engine. When the lean burn engine was tuned to meet the 2 gm/mi  $\text{NO}_x$  emission standard with no emissions control devices in operation, the lean burn engine demonstrated a 7% reduction in brake specific fuel consumption when compared with the stock engine. Based on engine dynamometer mapping data it is estimated that the lean burn engine will show 12% better mpg over the Federal Driving Cycle than the stock vehicle. Under these conditions the hydrocarbon emissions of the lean burn engine are much greater than those of the stock engine, however exhaust temperatures are high enough so that a catalytic converter can be used successfully for hydrocarbon control.

It is felt that further improvement over the performance demonstrated with the lean burn engine tested in this program can be achieved with further engine modifications. With improvements in the ignition system and in cylinder-to-cylinder distribution the lean burn concept should be able to meet the 2 gm/mi NO<sub>x</sub> emissions standard while achieving a 25% improvement in mpg over the Federal Driving Cycle.

# SCHEDULE



Testing period has been shifted (→) about 6 weeks from original plans.

- - - - - TEST PREPARATION

## EVALUATION OF LITHIUM/SULFUR BATTERIES FOR AUTOMOBILES

Paul A. Nelson  
Argonne National Laboratory  
Argonne Illinois

A lithium-aluminum/metal sulfide (Li-Al/FeS) battery (60 kw, 42 kw-hr, 350 kg) was designed for installation under the hood of a compact car (3400 lbs) having a range of about 100 miles. Calculations showed that this battery could be recharged at home in about five hours and recharged at a recharging station in 1 to 2 hours. A Li-Al/FeS<sub>2</sub> cell having a capacity of about 100 amp-hr and weighing 1.8 kg is being tested on a computer controlled cycling system that simulates the power requirements for automobile driving conditions. On the SAE-J227 driving profile and a maximum power draw of 45 watts, the cell completed 275 driving cycles in a single discharge of 67.5 amp-hr. The performance projected for improvements in the cells which are now underway indicates that the calculated performance required for the automobile battery are obtainable with the lithium-aluminum/metal-sulfide system.

### 1. INTRODUCTION

#### Objectives of Program

This program is divided into two tasks. The objective of the first task is to study the design of high-specific-energy lithium/metal sulfide batteries for electric automobile propulsion, and to determine the effect of recharging rates upon the overall design requirements. The second task is directed toward testing and evaluation of full-scale prototype lithium/metal sulfide battery cells (developed in an AEC program) under the variable power conditions typical of automobile driving, and to determine how well they meet the design criteria set in the first task.

### Background Information on Lithium/Metal Sulfide Batteries

In a program at ANL funded by the U.S. Atomic Energy Commission (AEC), lithium/metal sulfide batteries are being developed for use as (1) energy storage devices for load leveling on electric utilities and (2) power sources for electric automobiles. This is a large program involving a total of about 50 personnel for both applications. The part of the program for development of the energy storage battery has a broad scope and includes cell chemistry studies, material studies, electrode development, cell development, battery development, and systems studies. The AEC program on development of the car battery consists of systems design studies and a limited amount of work on cell and battery development.

Because the DOT program deals with the assessment of lithium/metal sulfide battery designs for electric cars and the testing of cells developed in the AEC program, it is appropriate to review the status of the AEC Battery Program at ANL.

In early work in the ANL program, cells having molten lithium and molten sulfur electrodes were developed. These cells had limited life and could not be constructed in a compact configuration because of attack on ceramic separators and insulators in contact with the molten lithium electrodes. In the past 18 months, however, we have been developing cells with electrodes of solid lithium-aluminum alloys and solid metal sulfides. These solid-electrode cells have stable capacity and can be constructed in a compact configuration with a specific energy of 120 to 150 w-hr/kg (about four to six times that of lead-acid batteries). These cells have a molten electrolyte of LiCl-KCl eutectic (mp, 352°C), which fills the pores in the electrode and the separator. The use of this salt requires operation of the cell at about 400-450°C. Boron nitride fabric has been a satisfactory separator material and has permitted the development of compact cells in which the separator is compressed between the electrodes.

In the past year, emphasis has been given to improvement of electrodes and the techniques for constructing compact cells. Lithium-aluminum negative electrodes prepared by various methods have been tested. Results of these tests have indicated that the performance goals for the program can probably be met with several types of electrodes and that the choice may depend upon fabrication costs and the ease of battery startup. Recently, testing of lithium-aluminum electrodes containing various additives and of other lithium-alloy electrodes has been initiated, and these promise further improvements.

Various metal sulfide electrodes have been tested; however,  $\text{FeS}_2$  and  $\text{FeS}$  electrodes have shown the most promise. These two types of electrodes provide cells having considerably different performance characteristics, materials problems, and perhaps cost potential. Cells having  $\text{FeS}_2$  electrodes have achieved high specific energy (150 w-hr/kg) and have high power capabilities with  $\text{FeS}_2$  electrodes up to 2 cm thick. These electrodes are corrosive to most metallic current collectors, but molybdenum current collectors have given satisfactory service. The  $\text{FeS}$  electrode can achieve high sulfur utilization (greater than 70%) only at low current densities (less than 50 mA/cm<sup>2</sup>) and, therefore, the usable thickness of these electrodes is limited to about 0.5-1.0 cm for the applications of interest. A problem that is now being given special attention is swelling of the  $\text{FeS}$  electrode, which requires the use of a high volume fraction of the electrolyte and, consequently, results in a lower specific energy than is calculated for a more compact electrode. When this problem is solved, the specific energy of Li-Al/ $\text{FeS}$  cells should be 120 to 140 w-hr/kg. The  $\text{FeS}$  electrode has a promising feature of being compatible with iron current collectors as demonstrated in cell tests of several thousand hours.

It is apparent that the problems of developing FeS electrodes are quite different from those of developing FeS<sub>2</sub> electrodes; FeS electrodes require improved performance and the development of compact cells with thin electrodes, whereas the FeS<sub>2</sub> electrodes require development of a low cost current collector. Both approaches appear promising and are being pursued.

Ten lithium-aluminum/iron sulfide cells, approximately 13 cm in diameter and 4 cm high, most of which had theoretical capacities of approximately 150 A-hr, have been constructed and tested. One of the Li-Al/FeS<sub>2</sub> cells attained 248 cycles in 3300 hours of operating time and had a maximum specific energy of 150 w-hr/kg. A Li-Al/FeS cell that is now in operation has attained 88 cycles in 2400 hours of operation and a maximum specific energy of about 80 w-hr/kg. Considerable improvement in both types of cells is expected on the basis of recent results in electrode development work.

## 2. REPORT OF PROGRESS

### Task A. Assessment Studies for Electric Automobile Batteries

In the initial effort to determine appropriate design criteria for lithium/metal sulfide batteries for electric cars, the available literature was reviewed to determine power and energy requirements for cars of various sizes and types. Also, experimental data on lithium/metal sulfide cells were reviewed to determine specific power and specific energy restrictions for full size batteries. As a result of this study, criteria were set for lithium/metal sulfide batteries for three types of cars: a subcompact weighing 800 kg (1760 lb), a compact weighing 1136 kg (2500 lb), and a family car weighing 1818 kg (4000 lb). The battery requirements for these cars and the resulting driving ranges are shown in Table 1.

As part of the AEC program on development of batteries for electric vehicles, a design study was undertaken to determine whether a lithium/metal sulfide battery could be installed under the hood of a compact American car

TABLE 1. ELECTRIC VEHICLE PERFORMANCE CHARACTERISTICS

(Basis: Specific Energy 140 w-hr/kg)

		SUB-COMPACT	COMPACT	FAMILY
<u>CAR AND BATTERY SPECS</u>				
LOADED CAR WEIGHT	kg	800	1136	1818
BATTERY WEIGHT	kg	143	250	500
RATIO OF BATTERY TO TOTAL CAR WEIGHT		0.179	0.220	0.275
BATTERY ENERGY OUTPUT	kw-hr	20	35	70
<u>ACCELERATION AND MAX. SPEED</u>				
ACCELERATION				
0-40 MPH, SECONDS		20	-	-
0-60 MPH, SECONDS		-	15	15
MAX. SPEED, MPH		60	88	95
<u>POWER AND ENERGY REQUIREMENTS<sup>a</sup></u>				
PEAK POWER	kw <sup>b</sup>	16	49	78
PEAK SPECIFIC POWER	w/kg <sup>b</sup>	112	196	156
ENERGY DURING ACCL.				
0-40 MPH		0.075	-	-
0-60 MPH		-	0.183	0.285
<u>DRIVING RANGE</u>				
URBAN/SUBURBAN PROFILE, miles		100	120	170
CONSTANT SPEED, miles				
25 MPH		166	218	250
40 MPH		114	155	215
60 MPH		75	110	145

<sup>a</sup>Partly based upon equations for power requirements in "Prospects for Electric Vehicles," J. N. B. George *et al.*, A. D. Little, Inc., May 15, 1968.

<sup>b</sup>Power delivered at the battery terminals.



to achieve the desired performance goals. The selection and redesign of the car for electric propulsion, selection of the electrical components, and calculation of the performance characteristics of the car and its total weight, were subcontracted to Linear Alpha Corporation. It was decided that this opportunity should be taken to design a battery under the DOT contract specifically for the car selected by the Linear Alpha Corporation in the AEC study. This has been done and a report on the battery design and its characteristics and of the resulting performance calculated for the car are given below.

The car which was selected for this design study was a 1975 Ford Mustang II. Trial and error calculations resulted in a loaded car weight (two passengers) of 1540 kg (3400 lb) including a 360 kg battery. This was an iterative process involving estimation of the car weight, calculation of the required battery power and energy capacity, design of the battery cells, and calculation of the battery weight. It was decided that the car should have an acceleration of 0 to 50 miles per hour in 15 seconds, and a driving range of about 100 miles at 50 mph. The calculated battery characteristics that are required for these specifications are shown on Table 2. A specific energy of 120 W-hr/kg for the insulated battery was determined and this is believed to be consistent with the projected capabilities for Li-Al/FeS batteries.

A multiple electrode cell was designed to meet these battery requirements; the cell is expected to meet the specifications of Table 2 on the basis of electrode tests and cell demonstrations that have been carried out at ANL. The cell design is shown in Figure 1. Details on the parameters for this cell and for Li-Al/FeS<sub>2</sub> cells that would also meet the requirements of Table 2 (but at even lower battery weight) are shown in Table 3. It is expected that the cells with FeS<sub>2</sub> positive electrodes would meet the power requirements more easily, but such cells would require molybdenum current collectors, or current collectors with equivalent corrosion resistance.

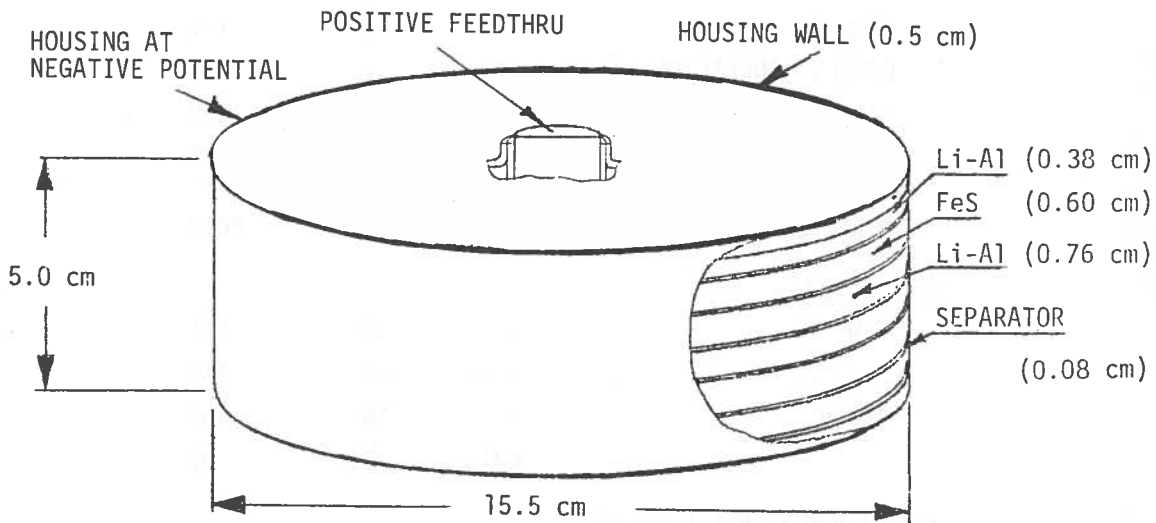
The design of a module containing 13 cells is shown in Figure 2. In this module, the cell housings are insulated from each other and from the module jacket. The module jacket, which is a hermetically sealed

TABLE 2. Li-Al/FeS BATTERY SPECIFICATIONS FOR ELECTRIC CAR

Basis: Converted 1975 Ford Mustang II, loaded weight 1540 kg (3400 lb)

POWER	
PEAK.....	60 kw <sup>a</sup>
SUSTAINED POWER AT 55 MPH.....	25 kw
SPECIFIC ENERGY.....	120 w-hr/kg
ENERGY OUTPUT.....	42 kw-hr
BATTERY WEIGHT.....	360 kg
DISCHARGE TIME.....	2 hr
CHARGE TIME.....	5 hr <sup>b</sup>
WATT-HR EFFICIENCY (URBAN DRIVING)...	70%
BATTERY LIFE	
NUMBER OF CYCLES.....	1000
YEARS.....	4
COST OF CAPACITY	
\$/kw-hr.....	20-30
\$/BATTERY.....	840-1260
HEAT LOSS THROUGH INSULATION.....	150-200 w

- a Provides acceleration of 0-50 mph in 15 sec.
- b The 5 hour value has been chosen for overnight charge. Quick-charge capability covering the range of 5 to 120 minutes is also under study.



CELL SPECIFICATIONS

WEIGHT.....	2.34 kg	ENERGY OUTPUT.....	334 w-hr
THEORETICAL CAPACITY..	405 A-hr	SPECIFIC ENERGY...	142 w-hr/kg

Figure 1. Conceptual Design of a Multiplate Cell for an EVP Battery (Li-Al/FeS)

TABLE 3. DESIGN SPECIFICATIONS FOR EVP MULTI-PLATE CELLS  
(42 kw-hr Battery Output)

DESIGN SPECIFICATION		Li-Al/FeS	Li-Al/FeS <sub>2</sub>
<u>CELL</u>			
NUMBER OF CELLS/BATTERY		126	106
CELL DIAMETER	cm	15.5	15.5
HEIGHT	cm	5.0	4.5
AVERAGE VOLTAGE		1.10	1.30
THEORETICAL CAPACITY	A-hr	405	405
% UTILIZATION		75	75
ENERGY OUTPUT	w-hr	334	396
SPECIFIC ENERGY	w-hr/kg	142	196
<u>CELL COMPONENT WEIGHTS,</u> grams			
Li-Al		513	513
FeS or FeS <sub>2</sub>		665	453
SEPARATOR		13	13
LiCl/KCl		574	495
HOUSING		186	170
CURRENT COLLECTOR		47	47
PLATE HARDWARE		271	250
FEEDTHROUGH		75	75
TOTAL WEIGHT		2344	2016
<u>CELL POWER</u>			
PEAK	w	476	566
	w/kg	203	280
NORMAL	w	166	198
	w/kg	71	98
<u>CELL CURRENT AND CURRENT</u> <u>DENSITY</u>			
PEAK	A	434	
	A/cm <sup>2</sup>	0.397	
NORMAL	A	152	
	A/cm <sup>2</sup>	0.139	

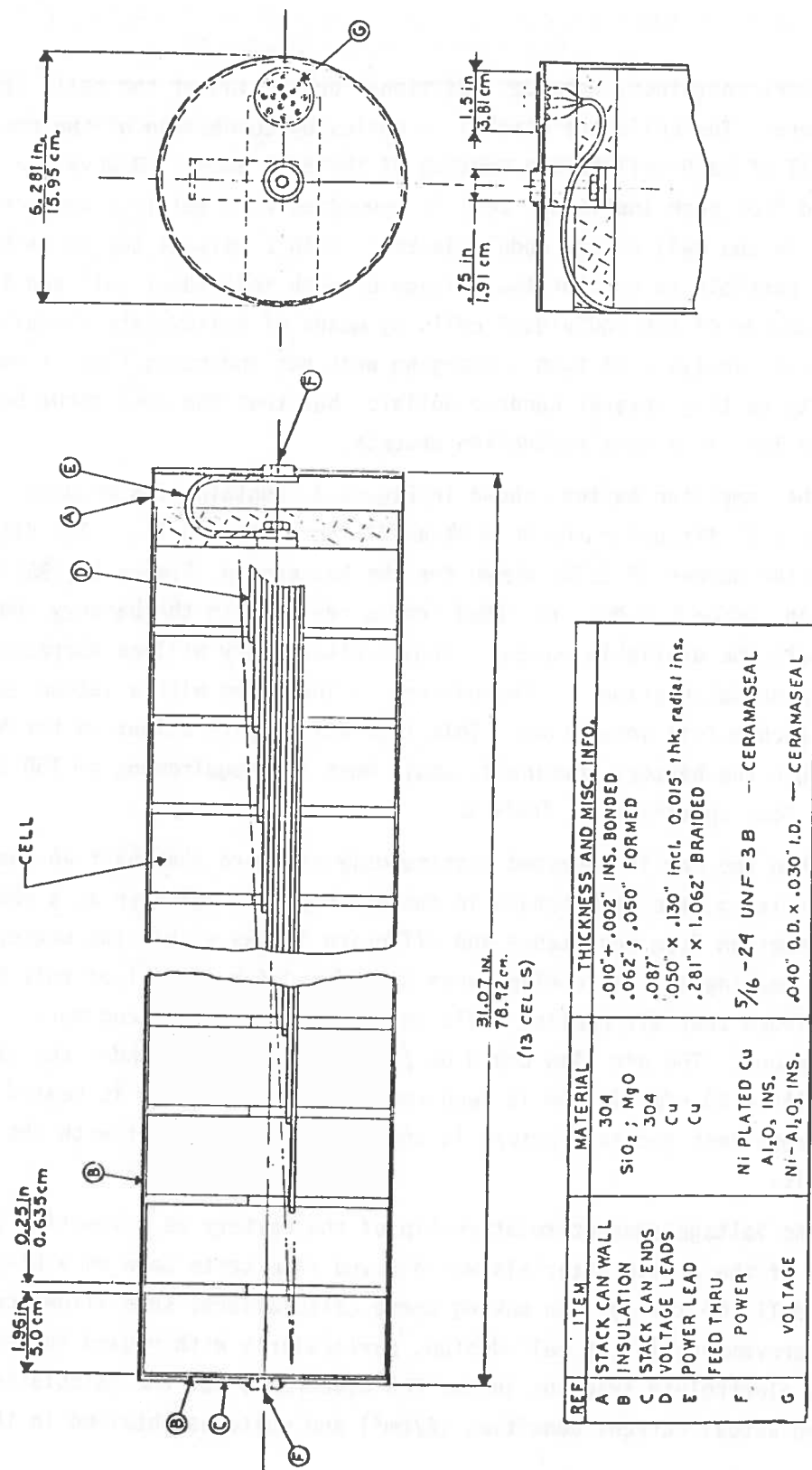


Figure 2. Cell Stack for EVP Battery (13 cells)

stainless steel container, provides additional protection of the cells from the atmosphere. The cells are stacked in series by connection of the positive terminal of each cell to the housing of the cell above. However, a voltage lead from each individual cell is connected to a multiple conductor feedthrough in the wall of the module jacket. With a voltage tap to each cell, it is possible to monitor the voltage of each individual cell and to adjust the charge of the individual cells by means of solid state circuitry. The preliminary analysis of such a charging unit has indicated that it would contain parts costing several hundred dollars, but that the cost might be considerably less in a mass-production process.

The completed battery shown in Figure 3, contains ten modules. This battery will fit under the hood of a 1975 Ford Mustang II. The discrepancy in the number of cells shown for the battery in Figure 3 (130) and that shown in Table 3 (126) resulted from a revision in the battery shape to accommodate the available space. This discrepancy will be corrected in final design calculations. The battery is insulated with a vacuum jacket containing vacuum foil insulation. This insulation, with allowance for heat losses through the battery terminals, would meet the requirement of 150 to 200 W heat loss specified in Table 2.

When the car is operated continuously for more than half an hour of highway driving, the temperature in the battery will build up as a result of heat generation from resistance and diffusion losses within the battery. Both liquid cooling and air cooling were considered for removal of this heat. It was concluded that air cooling would be the less expensive and more efficient method. The air flow could be provided by a scoop under the car, since only 15 to 20 cfm airflow is required. The incoming air is heated by counter-current heat exchange before it comes in direct contact with the battery cells.

The voltage-current relationship of the battery as a function of utilization of the active materials was derived from tests made on a Li-Al/FeS laboratory cell (Cell Y-2). In making these calculations, some allowance was made for improvements in the cell design, particularly with regard to reduction in the electrolyte fraction in the FeS electrode, but the calculations are based on actual current densities ( $A/cm^2$ ) and voltages obtained in that

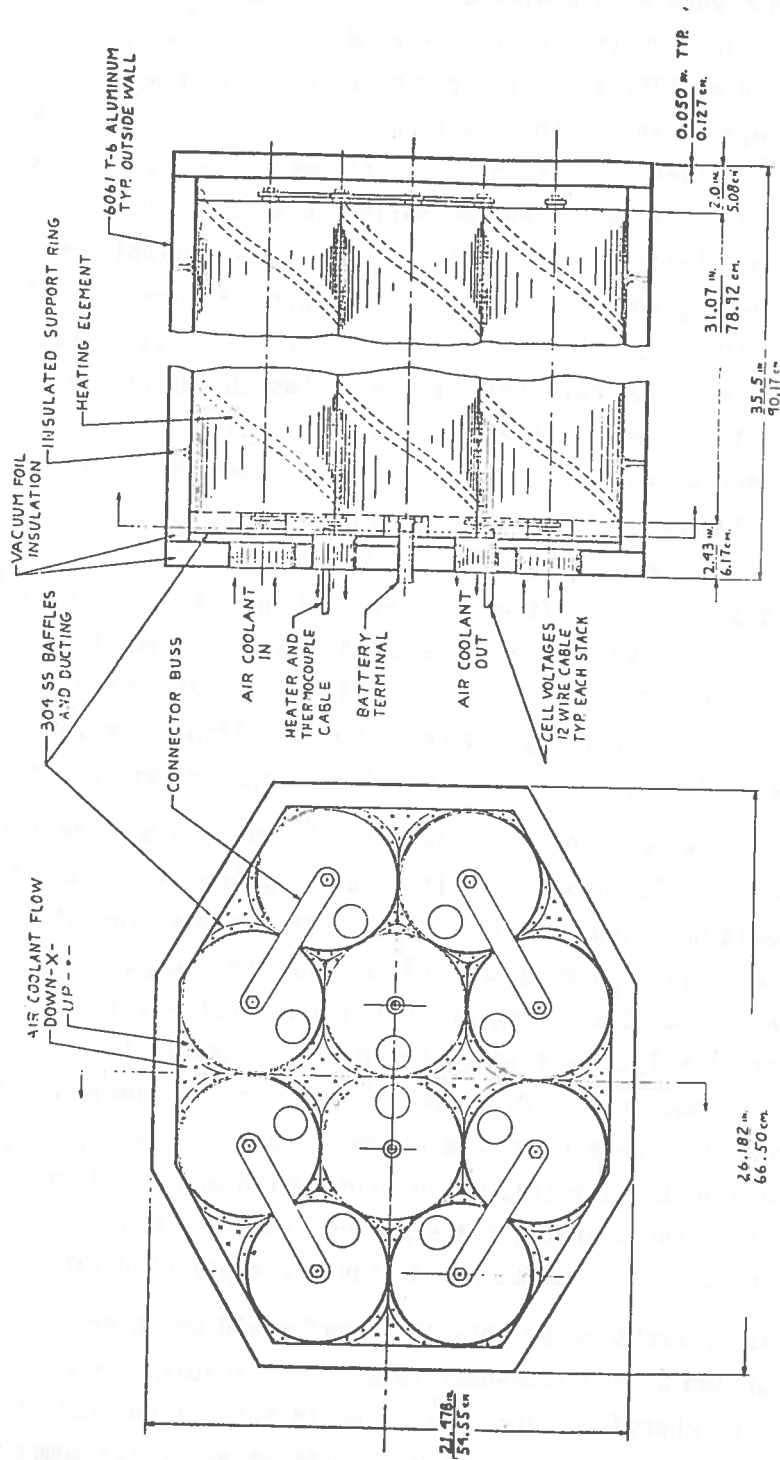


Figure 3. EVP Battery 42 kW (130 cells)

cell. Shown in Figure 4 is a plot of the calculated voltage-current relationship for various stages of battery discharge in terms of active material utilization (75% is considered to be full discharge). Lines of constant power are shown for the power ranges of interest for constant speed driving conditions. A second plot, Figure 5, was derived from Figure 4 to show the effect of the extent of battery discharge upon the power capability of this battery. As is shown for a 500 A current, which should be readily handled by the solid-state motor control system, the peak design power output of 60 kW is available until the battery is discharged to 50% utilization of the active materials, which is two-thirds of a full discharge, based on 75% utilization of active materials at full discharge. At the end of discharge about 48 kW is still available. Because 30 kW are required to maintain a 60 mph speed, as is shown in Figure 6, the car would still be capable of a speed in excess of 60 mph and would have adequate acceleration at the end of discharge. As is also shown in Figure 6, the expected range at a constant speed of 50 mph would be about 100 miles, and the range at 20 mph would be about 225 miles. An initial attempt at battery design that was based on a 35-kw-hr battery was shown to have inadequate power and energy storage by this analysis and the size of the battery was increased.

A study was made of the effect of charging rate on selected battery parameters. The results of these calculations is shown on Table 4. The battery could be charged in five hours with a power draw of about 11 kW. This could be accomplished on a home circuit having a capacity of 230 V AC and 50 A, using an AC-DC converter charging unit that would be mounted in the car. Alternatively, the battery could be charged at a charging station at the two or one-hour rate. At higher charging rates, however, the power requirement and heat generation rate become excessive. Also, the battery bus bars would have to be increased in size, which would add somewhat to the battery weight for charging times of less than one hour. Further consideration is being given to battery design for these high rates.

It is interesting to note that heat would be absorbed by the battery on charging at the five-hour rate. This results from a positive entropy change on charging. This factor would make it possible to charge Li-Al/FeS batteries at a fairly high rate without excessive temperature

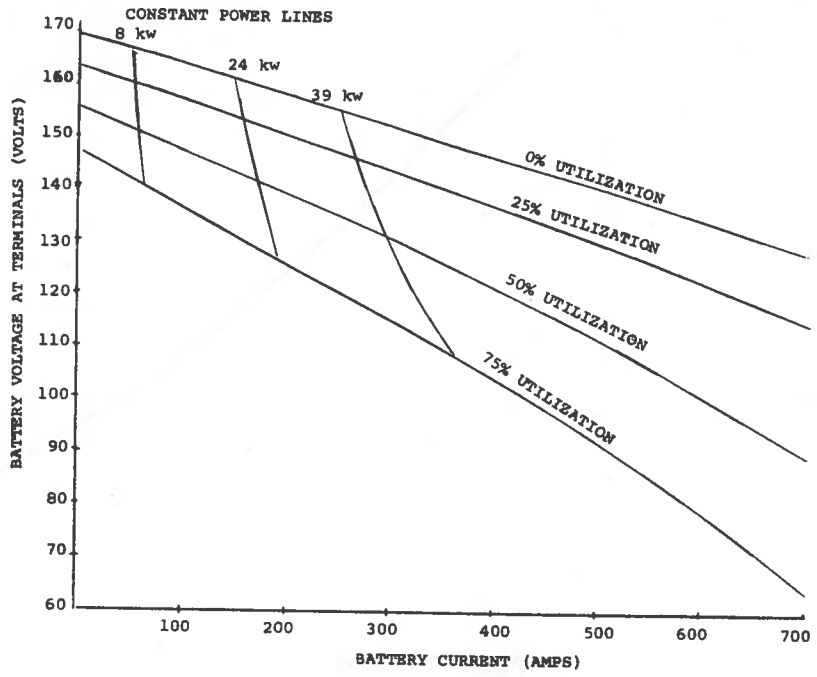


Figure 4. Current-Voltage Relationship for a 42 kw-hr EVP Battery

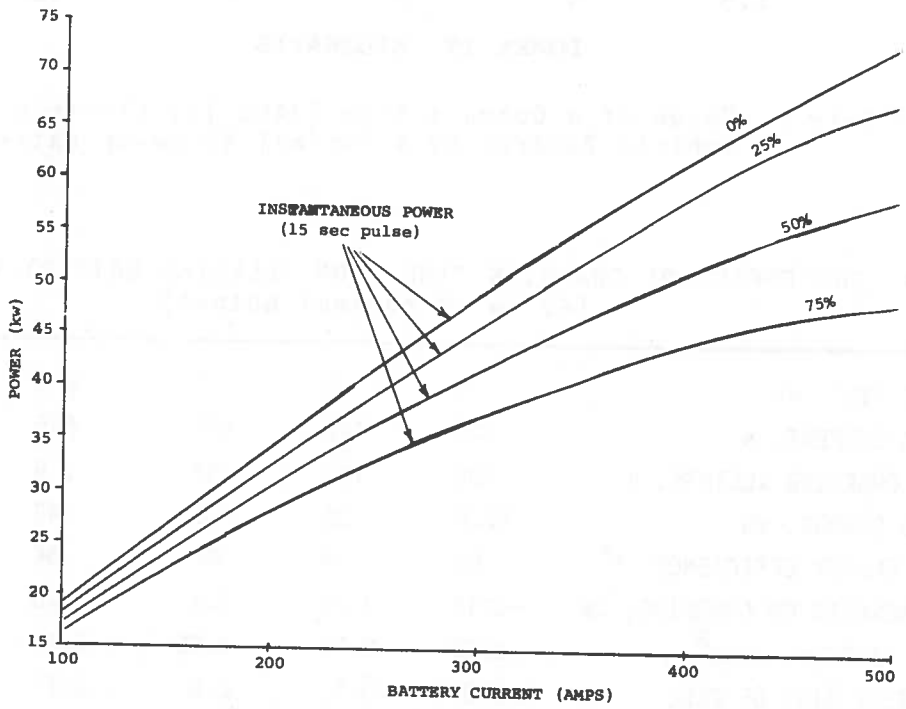


Figure 5. Power Delivered by a 42 kw-hr EVP Battery as a Function of Battery Discharge



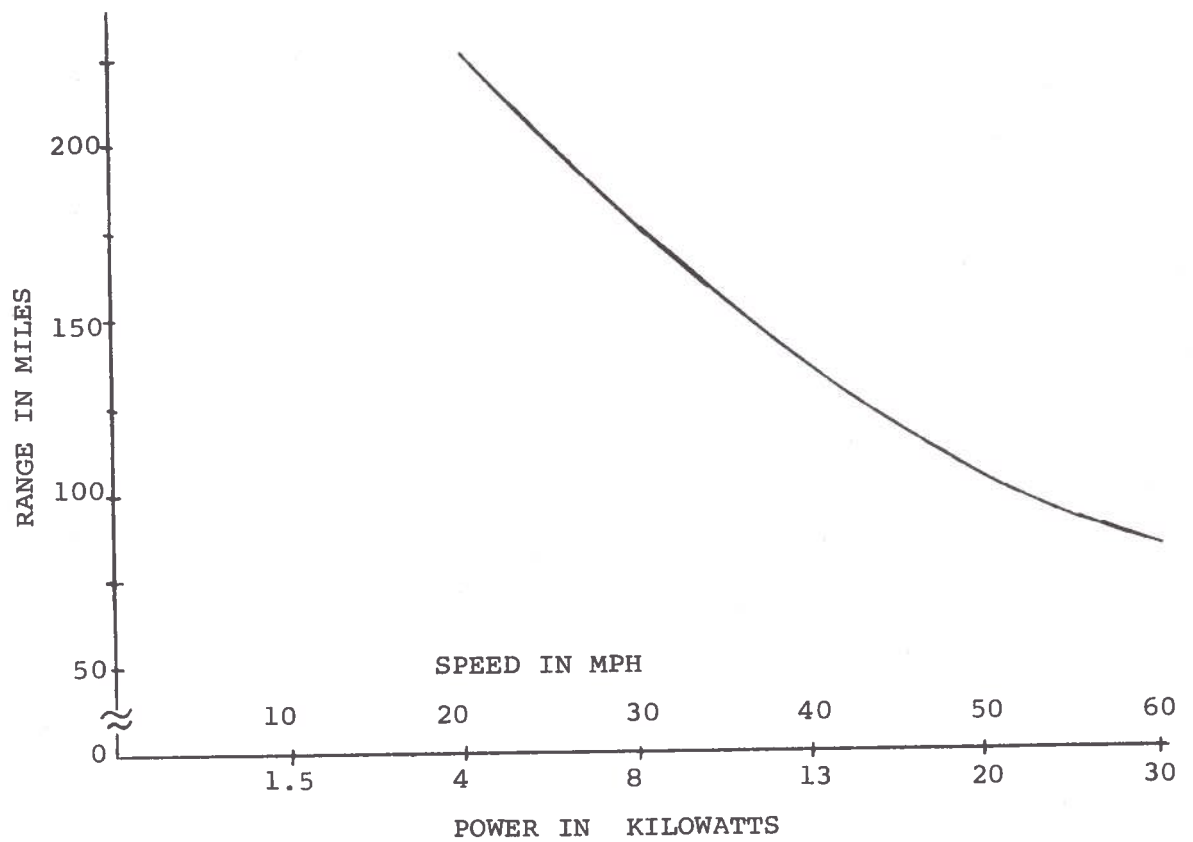


Figure 6. Range of a Compact Size (3400 lb) Electric Vehicle Powered by a Nominal 42 kw-hr Battery

TABLE 4. THE EFFECT OF CHARGING TIME UPON SELECTED BATTERY PARAMETERS (42 kw-hr nominal output)

	5	2	1	0.5	0.25
CHARGING TIME, hr	5	2	1	0.5	0.25
CHARGING CURRENT, A	58	147	300	686	1457
AVERAGE CHARGING VOLTAGE, V	186	197	207	215	250
POWER TO CHARGE, KW	10.8	29	62	147	365
OVERALL ENERGY EFFICIENCY, %*	80	74	69	56	46
HEAT GENERATED ON CHARGING, KW	-0.17	0.24	3.5	20	102
CURRENT DENSITY, A/cm <sup>2</sup>	0.05	0.13	0.30	0.63	1.33
TEMPERATURE RISE OF CELL CENTERLINE, °C	-0.07	0.1	2.0	8.2	41.5

\*Based on a two-hour discharge rate.

rise in the battery. There would be a correspondingly higher heat generation on discharge that would be available for heating the interior of the car and possibly for cooling the car with an absorption-cycle air conditioning system.

#### Task B. Testing and Evaluation of Prototype Battery Cells

The objective of this portion of the study is to test engineering-sized lithium-aluminum/metal sulfide cells in the laboratory, by subjecting the cells to the variable power demands that a battery would experience during use as the power source for automobile propulsion. An automobile requires high power peaks for acceleration, with much lower power required to overcome wind resistance and rolling friction. The inability of commercially available batteries to supply acceleration power throughout a substantial portion of the total capacity is one factor limiting their application in electric vehicles.<sup>1</sup> This factor is particularly important in safety considerations because a vehicle must perform satisfactorily near the end of its range, as well as when fully charged, to avoid becoming a hazard to other traffic. One way that this problem is avoided with presently available systems is by severely derating the range of the vehicle, and using only a portion of the total available capacity. The result is a vehicle with an excessive battery weight and a restricted driving range. Testing of the Li-Al/FeS<sub>2</sub> and Li-Al/FeS cells under realistic power demands will aid in the optimization of cell design to obtain good peak power performance over the entire discharge period. Testing of cells in the AEC program had been primarily with constant charge and discharge currents.

Many organizations have published curves of vehicle speed as a function of time that a car would follow under the various conditions of urban, suburban, and highway driving. Some of the associated power profiles are very complicated with frequent changes in vehicle speed. Initial testing of cells for this program has utilized the relatively simple SAE-J227 metropolitan driving profile, which has approximately the same energy usage per mile<sup>2</sup> as the more complicated EPA emission test profile.<sup>3</sup> The velocity-*vs.*-

time data of the driving profile has been converted to the power required at the battery using drag coefficients, acceleration equations, and rolling resistance equations published by A. D. Little<sup>4</sup>, and by assuming a conversion efficiency of battery power to power at the wheels of 75%. The velocity-time and battery power-time curves are presented in Figure 7 for a compact car.

### 3. DESCRIPTION OF TEST APPARATUS

A specialized test apparatus is being used to allow testing of the cells in the laboratory under conditions of rapid change in the power demand from the cell. Computer control of the cell operation was chosen to allow the greatest flexibility in matching the requirements of rapidly changing operating parameters. The test system is shown schematically in Figure 8. The cell voltage and the voltage across a current shunt are transformed into digital signals for the computer by a digital voltmeter. These values are multiplied by the computer to obtain the cell power. At frequent intervals, a comparison is made between the cell power and the required power as a function of time; the latter is stored in the memory unit. If necessary, a signal is sent to the digital-analog converter and power supply to increase or decrease the cell current and thus bring the cell power into agreement with the power profile. Voltage and current readings and current adjustments may be made as often as every 50 milliseconds. The current, voltage, and time increments are stored in memory to allow accumulation of the capacity (A-hr), energy (W-hr), cycle time, average current, etc. This information is punched on paper tape to allow further data analysis.

The test system was initially used to test a commercial lead-acid battery.\* These experiments served two purposes. First, the computer control program was debugged and it was verified that the system could operate reliably while unattended. Secondly, data were obtained on the response of the commercial lead-acid battery to the same driving profile that would be used to test the Li-Al/FeS<sub>2</sub> cells. This information provided a base-line performance against which the advanced cell performance could be tested. The response of the lead-acid battery to the driving profile is shown

---

\*Universal, Task Force 900 Fleet Line, 6 V, 190 A-hr, 41 kg.

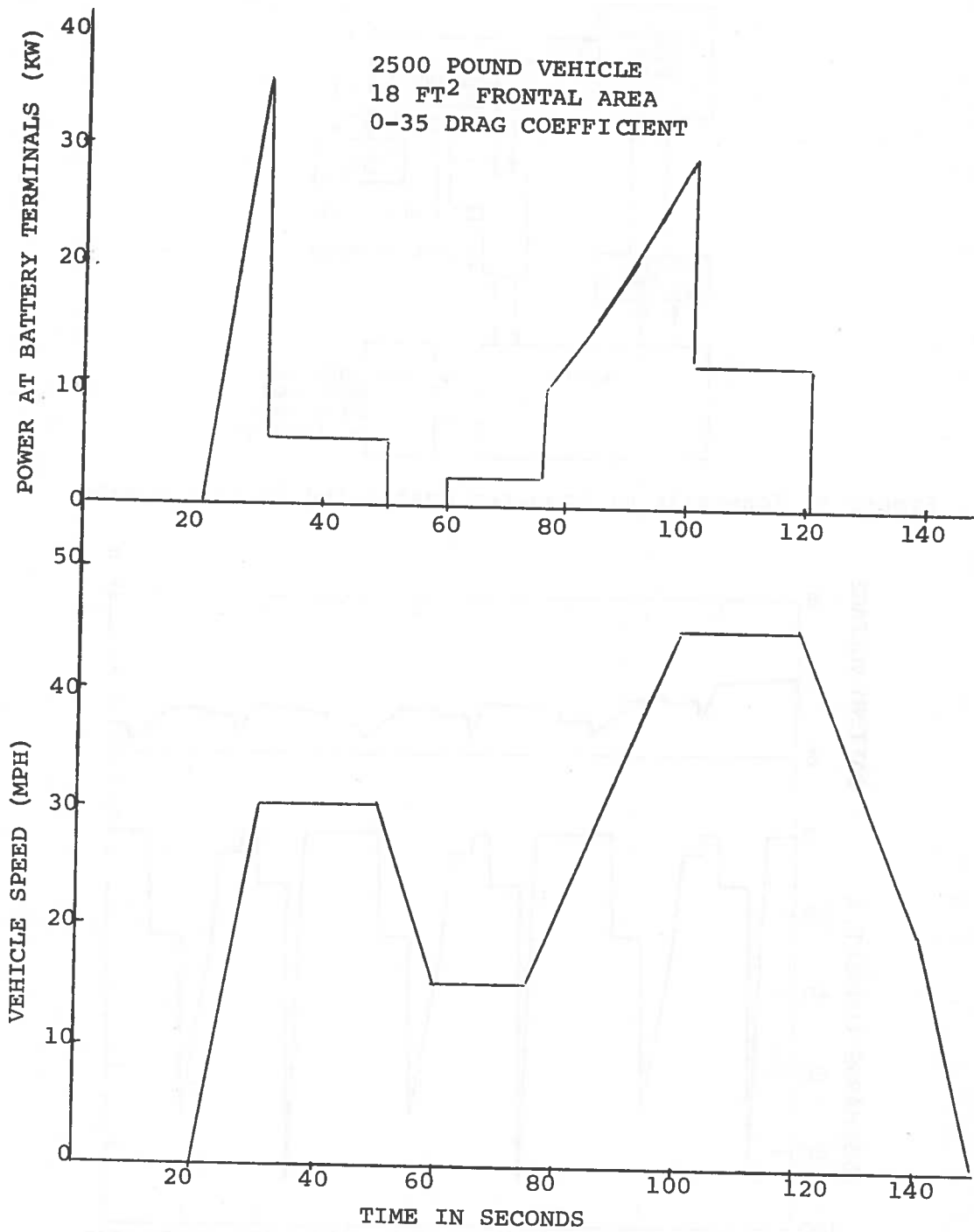


Figure 7. SAE-J227 Metropolitan Velocity-Time Curve and Corresponding Power-Time Curve

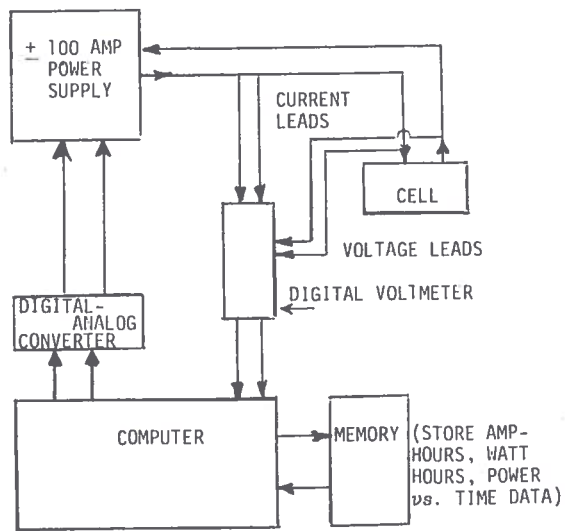


Figure 8. Schematic of Computer Controlled Cycling System

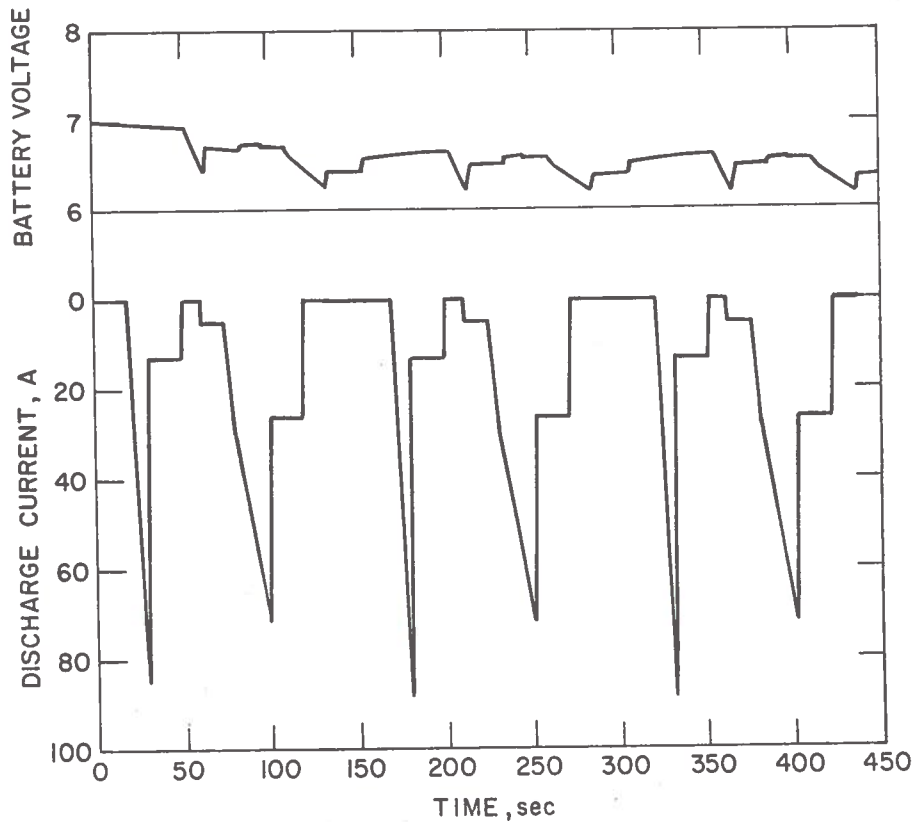


Figure 9. Response of Lead-Acid Battery to SAE-J227

in Figure 9. The voltage and current responses were dynamically obtained while the battery provided power in accordance with the driving profile. To obtain a smooth response of the control system to rapid changes in power requirements, it was necessary to sample the voltage and current every 200 milliseconds.

#### 4. DESIGN AND CONSTRUCTION OF LITHIUM/METAL SULFIDE BATTERY CELLS

A schematic diagram of the type of cell that has been developed in the AEC program and is being tested in this program is shown in Figure 10. The iron housing is 13-cm in diameter and 4-cm high. The cell contains two negative electrodes (Li-Al) and one positive electrode ( $\text{FeS}_2$ ). The  $\text{FeS}_2$  active material is contained in a stainless steel screen enclosure that is in direct contact with the negative electrodes. A separator of boron-nitride fabric and a particle retainer of zirconia fabric are inside the steel screen enclosure. Overlap of the separator cloths prevents active material from shorting to the screen support. The positive electrode current collector consists of three molybdenum screens welded to a molybdenum hub and a molybdenum current lead.

Cell W-9 which was constructed in the AEC program appeared to be particularly well suited for testing in the DOT cell evaluation program. A description of the physical characteristics for that cell is given in Table 5.

The cell was designed to have 100 A-hr of usable capacity; excess  $\text{FeS}_2$  capacity was provided to allow operation on only the upper voltage plateau, which results from conversion of  $\text{FeS}_2$  to FeS. Previous tests of cell performance had shown that using only the upper voltage plateau should allow better performance for electric-vehicle application.

#### 5. TESTING OF LITHIUM/METAL SULFIDE BATTERY CELLS

The computer-controlled cycling system has been utilized to test the engineering-scale Li-Al/ $\text{FeS}_2$  cell (W-9) to determine its potential for use in an electric vehicle. The first series of tests involved the determination of the peak power capability of the cell as a function of the state of charge. These data were obtained by rapidly (in <5 seconds) increasing the power withdrawn from the cell while plotting voltage as a function of current.

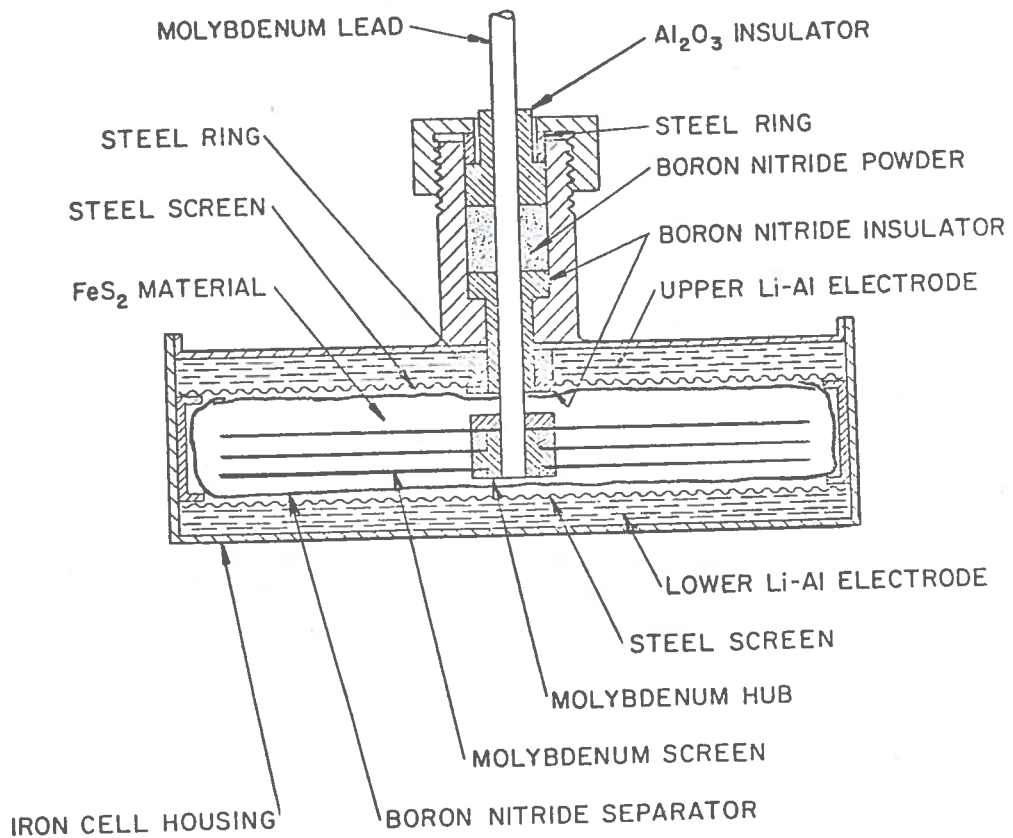


Figure 10. Li-Al/FeS<sub>2</sub> Engineering Test Cell

TABLE 5. DESCRIPTION OF CELL W-9

Design Capacity.....	100 A-hr
FeS <sub>2</sub> Capacity.....	204 A-hr
	(both voltage plateaus)
Li-Al Capacity *.....	112 A-hr
Electrode Area.....	241 cm <sup>2</sup>
Cell Diameter.....	13 cm
Cell Height.....	4 cm
Current Lead Diameter.....	0.476 cm
Cell Weight.....	1800 g

\* Li-Al electrodes were formed electrochemically from pressed plaques of aluminum wire.

This was repeated periodically during the discharge of the cell at a normal power of 20 w. These voltage-*vs.*-current curves were then used to calculate the peak power delivered by the cell. The results, which are based on measurements taken during the 12th discharge of this cell, are shown in Figure 11. The cell demonstrated an ability to deliver high peak power during discharge of 70% of the theoretical capacity of the cell.

After 1100 hours of operation and many additional cycles, the peak power data were again obtained. These data, which are also shown in Figure 11, indicate a reduction in the ability of the cell to produce a high power pulse throughout the discharge. Tests are in progress to determine if the performance can be restored by removing gas from the cell or by adding electrolyte.

After the initial set of peak power data were obtained (cycle 12), the cell was run during cycle 13 on the SAE-J227 driving profile (Figure 12) using a maximum power draw of 50 w. The cell completed 112 repetitions of the driving profile before reaching the cut-off voltage during a power spike on car acceleration. The response of the cell to the power profile demands is shown in Figure 12. The instantaneous cell voltage and current, as a function of time are presented for the 104th repetition of the 112 repetitions completed on discharge 13. At that time, as is evident from Figure 12, the cell was near the end of discharge, because the peak power requirement (50 w) is very near the maximum power that the cell can deliver, and therefore large currents are required and rapid polarization of the cell occurs.

A total of 30 A-hr was withdrawn from the cell; this might be expected from the results shown in Figure 11, which were obtained by the simple means of pulsing the power occasionally during discharge at steady power. The peak power for the next series of driving profile discharges was then lowered to 45 w. The cell completed 275 cycles and 67.5 A-hr capacity was withdrawn. This is also in good agreement with Figure 11.

Cell W-9 had impressive specific energy on the driving profile, even when operated on driving profiles that drew peak powers of 45 and 50 w, which are near its maximum short-term power output. However, the specific power output of the cell was inadequate for a reasonable battery weight,



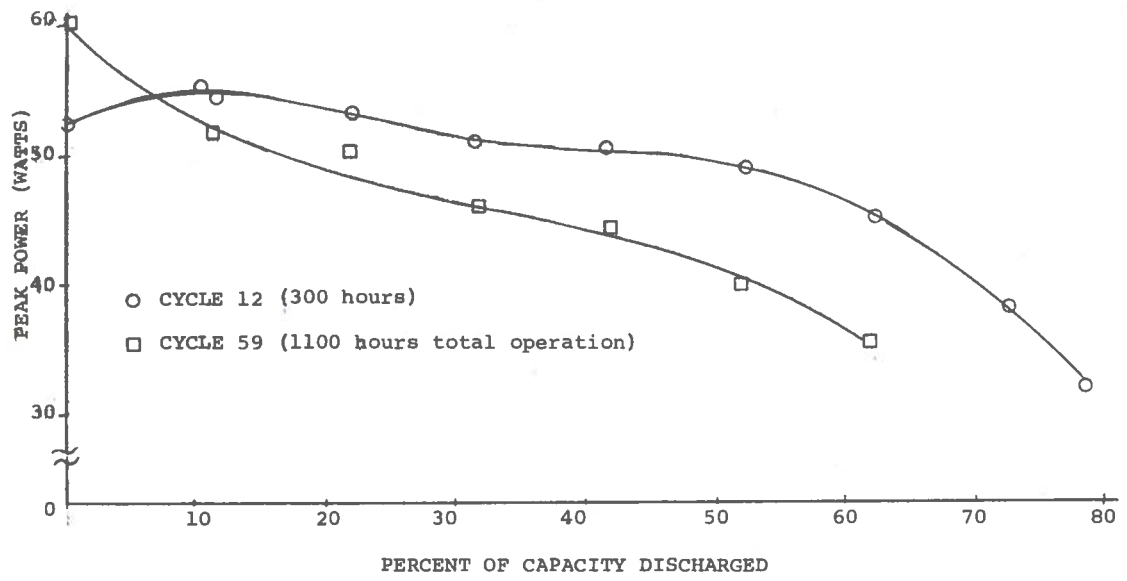


Figure 11. Peak Power versus Utilization Cell W-9

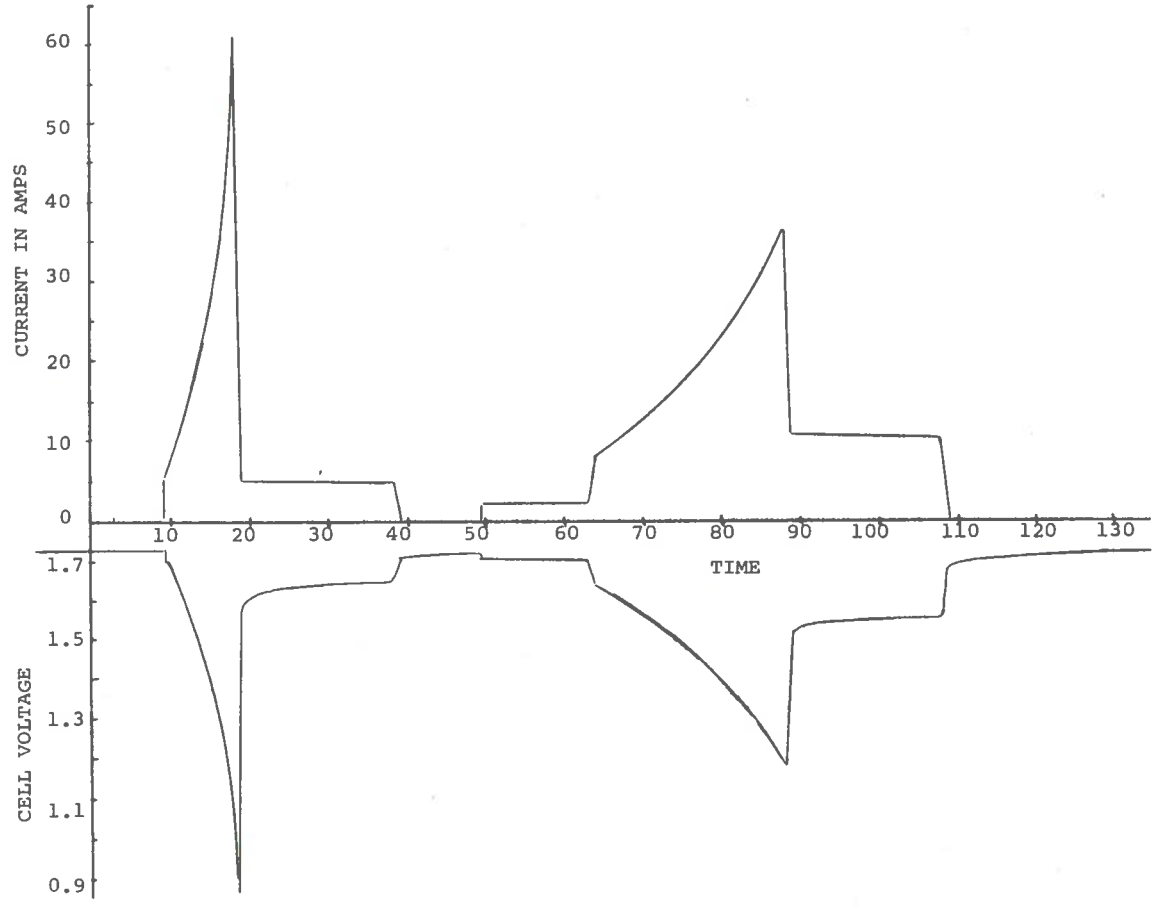


Figure 12. Response of Cell W-9 to SAE-J227 Driving Profile cell

because the electrodes were too thick (the  $\text{FeS}_2$  electrode of Cell W-9 is almost 2 cm thick). The power output of the lead-acid battery was also inadequate. Therefore, the range of a 2500-lb car equipped with these batteries was calculated by selecting a battery weight of 600 lb and assuming that the power of the battery could be increased (by about threefold in the case of the Li-Al/ $\text{FeS}_2$  battery and by about tenfold in the case of the lead-acid battery); this could be accomplished for the Li-Al/ $\text{FeS}_2$  battery by decreasing the thickness of the electrodes. It was further assumed for this calculation that the specific energy would remain the same as was measured in the driving profile tests. The calculated ranges of electric cars derived by this method are shown below:

CELL SYSTEM	PEAK POWER (watts)	CELL WEIGHT (kg)	CAR RANGE (miles)
Li-Al/ $\text{FeS}_2$	50	1.8	36.0
	45	1.8	79.7
Lead Acid Battery	500	41 (battery)	19.5

It is expected that the required specific power can be met by improved cells with thinner electrodes and that even higher specific energies can be obtained. Correspondingly, the range of the electric car will be longer than those shown in the above table.

## 6. FUTURE WORK

### Task A. Design and Assessment Studies

The battery design study is nearing completion. However, work remains to be done on heat-transfer calculations for the battery, and these may necessitate small modifications in the design. Also, further work will be done on calculations involving utilization of the waste heat generated during battery discharge, for heating of the interior of the car and for use

in absorption cycle air conditioning systems. Correction of minor inconsistencies in the calculations on utilization of the waste heat will be included in the annual report for this program, which is to be submitted to DOT about May 1, 1975.

Task B. Testing and Evaluation of Battery Cells

The testing of two or three additional cells under the fluctuating power conditions typical of urban and suburban automobile driving is planned. It is anticipated that these cells will have higher specific powers and higher specific energies than the W-9 cell which is now being tested. Various driving profiles, as suggested by DOT, will be used in these cell tests. The weight of battery required to drive a Mustang II, as calculated in the design study, will also be determined in cell tests under the various driving profile conditions. The results of these tests will be reported in the annual report submitted to DOT on May 1, 1975.

REFERENCES

1. Foote, L.R. et al., Electric Vehicle Systems Study, Scientific Research Staff, Ford Motor Company, Report No. SR-73-132, October 1973.
2. Private Communication from Charles Pax, EPA.
3. Federal Registration , Vol. 37, No. 221, pp.24316-24318, Nov.15,1972.
4. George,J.H.E.;Stratton,L.J.;and Acton, R.G., Prospects for Electric Vehicles, A Study of Low Pollution-Potential Vehicles-Electric, Contract No. PH-86-67-108, Dept. of Health, Education and Welfare, May 15,1968.

AERODYNAMIC DRAG REDUCTION TESTS ON A FULL-SCALE  
TRACTOR-TRAILER COMBINATION WITH  
SEVERAL ADD-ON DEVICES

Lawrence C. Montoya and Louis L. Steers  
Flight Research Center

ABSTRACT

Aerodynamic drag tests were performed on a conventional cab-over-engine tractor with a 45-foot van-type trailer and five commercially available or potentially available add-on devices using the coast-down method. The tests ranged in velocity from about 30 mph to 65 mph and included some flow visualization. A smooth, level runway at Edwards Air Force Base was used to perform the tests, with deceleration measurements taken with both accelerometers and stop watches. This paper presents an evaluation of the drag reduction results obtained with each of the five add-on devices.

INTRODUCTION

Because of the recent fuel oil crisis, the conservation of fuel oil products has become a matter of greater concern to everybody. The resulting high prices and sometimes limited quantities of gasoline and diesel fuel have caused increased interest in ground vehicle efficiency. In the past, when ground vehicle fuel was comparatively inexpensive and readily available, the aerodynamic drag (wind resistance) of some high volume carriers during design was considered unimportant. The high aerodynamic drag of these designs (i.e., box shapes) was merely overcome by more powerful engines, with resulting increases in fuel consumption.

In the fall of 1973, in response to the fuel crisis and increased interest in the aerodynamic drag of ground vehicles, the NASA Flight Research Center began a drag reduction program on a representative box-shaped ground vehicle (refs. 1 and 2). After baseline data were obtained for the vehicle with all square corners, the vehicle was modified by rounding the corners and sealing the undercarriage. The resulting reduction in aerodynamic drag exceeded 50 percent, which is equivalent to a fuel savings of approximately 15 percent to 25 percent at highway speeds.

Another aerodynamic drag ground vehicle study was initiated in the spring of 1974. Sponsored jointly by NASA and the Department of Transportation, the program was to assess the performance gains on a tractor-trailer combination due to the addition of different low cost drag reduction devices. These add-on devices, which are commercially available, or potentially available, were developed by private business concerns to reduce the aerodynamic drag of existing tractor-trailer combinations with only minor modifications.

A representative cab-over-engine tractor-trailer combination without any devices attached (the basic vehicle) was tested first. The tests were then repeated with the add-on devices installed.

This paper presents an evaluation of the drag reduction results obtained with each of five add-on devices using the coast-down technique.

The authors would like to acknowledge Ralph H. Sparks, who maintained the test vehicle, installed all the add-on devices and flow visualization system, helped with the instrumentation layout and installation, and was our dependable driver.

### SYMBOLS

$A$	frontal cross-sectional area (does not include the undercarriage and tires), 94 square feet
$C_{D_a}$	aerodynamic drag coefficient, $\frac{D_a}{qA}$
$D$	drag
$g$	local acceleration of gravity
$q$	dynamic pressure, $0.5\rho V^2$
$\Delta t$	time increment
$V$	velocity
$\Delta V$	velocity increment
$W$	vehicle weight during each test
$x$	distance between back of cab and front of trailer, 40 inches or 62 inches
$\rho$	air density
Subscripts:	
$a$	aerodynamic
$m$	mechanical
$t$	total

### TEST VEHICLE

The tractor-trailer combination test vehicle (fig. 1) consisted of a cab-over-engine tractor and a 45-foot-long, two-axle, smooth-sidewall trailer. The front vertical corners of the trailer had a 12-inch radius. The total gross weight of the test vehicle was approximately 32,000 pounds. General specifications of the test vehicle are given in table 1.

## METHOD

The drag data were obtained by using the coast-down method under carefully controlled conditions. Tire pressure was kept nearly constant by filling the tires with nitrogen, which reduces temperature effects. Vehicle weight was determined for each day of testing and was not permitted to vary significantly to keep mechanical or rolling drag as constant as possible between tests. By keeping mechanical drag constant, any changes in drag resulting from the addition of the devices would be aerodynamic in origin.

For this study, total drag is considered to be the retarding force that can be directly derived from the deceleration of the vehicle. The components of the total drag and its definition are as follows:

$$D_t = D_m + D_a = \frac{\Delta V}{\Delta t} \frac{W}{g}$$

where the total drag is the sum of the mechanical drag ( $D_m$ ) and aerodynamic drag ( $D_a$ ). By setting the manual transmission in neutral during each deceleration run, the mechanical drag consisted of (1) the tractive drag of the tires and bearings and the gear resistance back through the drive line to the transmission and (2) the thrust from the rotational inertia of the wheels and tires.

The test vehicle was accelerated to a few miles per hour above the starting velocity of each test, and the manual transmission was then disengaged. The time it took for the truck to slow to given speeds was recorded and used to calculate the total drag from the above-stated definition. A more complex approach to the coast-down method is described in reference 3.

## TEST CONDITIONS

The tests were conducted on an Edwards Air Force Base runway, which had a concrete surface with a constant elevation gradient of 0.125 percent. The effect of this small gradient was eliminated by averaging successive runs in opposite directions. The tests ranged in velocity from approximately 30 miles per hour to 65 miles per hour. Most of the tests were made in calm wind conditions.

During the tests, ambient pressure, temperature, and wind velocity and direction were recorded.

Tests were performed with a gap of either 62 inches or 40 inches between the front of the trailer and the back of the top part of the cab (fig. 1).

During the first tests, it was found that the position of the thermostatically controlled radiator cooling shutters had a considerable effect on the drag measurements.

To eliminate this variable, a cover that prevented airflow through the shutters was put over the radiator opening before each run (fig. 2).

## INSTRUMENTATION

A  $\pm 0.1g$  accelerometer with 0.001g resolution was used to measure deceleration along with a bank of five 0.1-second stopwatches and a calibrated precision speedometer with a 0.1-mile-per-hour readout capability. The speedometer was driven by a fifth wheel. The velocity and distance of the fifth wheel was displayed digitally inside the truck's cab (fig. 3) along with the bank of stopwatches. The time increments corresponding to preselected velocity intervals in miles per hour (i.e., 60 to 55, 55 to 50, 50 to 45, 45 to 40, and 40 to 35) were obtained by starting all the stopwatches simultaneously at the starting test velocity and stopping them individually at the end of the desired velocity interval. The stopwatch data were hand recorded. The accelerometer and fifth wheel velocity outputs were recorded on tape and identified with an event marker during each test.

## DEVICES TESTED

The five add-on devices which were tested are shown as the crosshatched areas in figure 4.

Three of the devices (devices A, B, and E) were cab mounted and designed to deflect more of the flow over the trailer. The other two devices (devices C and D) were mounted on the trailer. It appears that device C was designed to make the air flow smoothly around the trailer, and apparently device D was designed to maintain attached flow over the top of the trailer.

Device A, which was cab mounted, was 67 inches wide and 32 inches high. Device B, also cab mounted, was 52 inches wide and 27 inches high, with a 6.5-inch gap between the device and the cab. Device C was trailer mounted and extended a maximum of 24 inches forward of the trailer. Device D was mounted on the top front edge of the trailer, with a 6-inch gap between the front edge of the device and trailer and a 1.5-inch gap between the rear edge of the device and trailer. Device E was 60 inches wide, cab mounted, and extended vertically 48 inches above the cab in the stored position and 38 inches above the cab in the fully deployed position, which is shown in figure 4. The deployment and storage of device E were automatic and depended on the impact pressure and its variation with velocity. Data for this device were acquired only for the fully deployed position and the rear trailer location (62-in. gap).

The manufacturers chose the device of the best size available at the time of purchase for the test vehicle. All the devices were installed according to manufacturer's instructions.

## RESULTS

### Baseline Configuration

Typical results for the baseline configuration from several stopwatch runs and one accelerometer run are shown in figure 5 in terms of total drag versus truck velocity. The data show that the two methods of measuring deceleration (i.e., stopwatch precision speedometer and accelerometer) are consistent with each other. Repeatability is shown by the stopwatch data, which were obtained on separate days by two different people.

Baseline data for the two trailer positions (gaps of 62 in. and 40 in.) are presented in figure 6. It is apparent that the total drag was lower when the distance between the cab and trailer was shorter. At 55 miles per hour, the total drag was reduced approximately 7 percent, which is equivalent to a reduction in aerodynamic drag of approximately 10 percent.

### Modified Configurations

The total drag with the various add-on devices installed is shown in figures 7(a) to 7(e). In figures 7(a) to 7(d) the crosshatched region represents the drag range for the baseline vehicle; the lower bound is for the 40-inch gap and the upper bound is for the 62-inch gap. In figure 7(e) baseline data for only the 62-inch gap are shown because device E was tested only with a 62-inch gap.

The difference in total drag between the modified and baseline configurations is summarized in figure 8 for the two trailer positions at a speed of 55 miles per hour. As shown, the total drag reduction ranged from 18 percent for device A for the rear trailer position to approximately 2 percent for device D for both trailer positions. (The letters A, B, and so forth were assigned to the devices according to the chronological testing sequence and not according to rank.)

As mentioned before, total drag consisted of aerodynamic plus mechanical drag. The tractive portion of the mechanical drag is shown in figure 9. The data point at approximately 1 mile per hour represents a value that was measured using two methods, the coast-down and tow methods, and the solid curve extrapolation is based on Hoerner's semiempirical equation for rolling resistance (ref. 4). Using these data and accounting for the thrust from the rotational inertia of the wheels and tires, the aerodynamic drag was calculated by the relationship given on page 77. The resulting values of aerodynamic drag reduction are listed in table 2 together with the corresponding drag coefficients,  $C_{D_a}$ , for the two trailer positions. The

drag coefficients were based on a frontal cross-sectional area of 94 square feet, which does not include the projected areas of the undercarriage and tires. The aerodynamic drag reduction ranged from 24 percent for device A for the rear trailer position to 2 percent for device D for the forward trailer position.



As shown in table 2, the drag coefficients range from 1.17 for the baseline configuration for the rear trailer position to 0.89 for device A for both trailer positions. The drag coefficients obtained from wind tunnel tests (refs. 5 and 6) for cab-over-engine tractor-trailer combinations in the baseline configuration range from approximately 0.9 at the high end (i.e., approximately the same as the full-scale vehicle of this study with the best add-on device) to approximately 0.7 at the lower end. The drag coefficients from reference 5 are based on a frontal projected area and in reference 6 on the area based on the trailer's height above the ground times the width. A direct comparison with the results of either of these studies is not possible because of model configuration differences that are not readily definable (e.g., cab height, trailer size, corner radius, and distance between trailer and tractor).

A full-scale drag coefficient of approximately 1.04 is obtained for the baseline configuration of this study if the tire rolling resistance data of reference 7 (rotating drum tests) are applied instead of the extrapolation for velocity effects from reference 4. This drag coefficient is still above 1, whereas the majority of the wind tunnel data are well below 1.

#### Effect of Crosswinds

The data presented thus far are for zero wind conditions. Limited data were also obtained with crosswinds for the basic configuration and for some modified configurations. These data show that the drag of the configurations with add-on devices was sensitive to crosswinds, whereas the drag of the basic configuration exhibited little if any change. Figure 10 presents the total drag results for a 2- to 3-mile-per-hour crosswind at an angle of  $11^\circ$  relative to the longitudinal axis of the vehicle for the basic configuration and devices A, B, and C. These results are for the rear trailer position and represent the average of runs in two directions. Although the data do not define wind effects in detail, they indicate that in general the crosswinds reduced the ability of the add-on devices to decrease drag.

Figure 11 compares the total drag reduction due to the add-on devices for the rear trailer position as determined under conditions of crosswinds and zero wind (fig. 8). The total drag reduction decreased from 18 percent to 16 percent for device A, from 11 percent to 4 percent for device B, and from 8 percent to 6 percent for device C. These data were limited and should be substantiated by additional testing.

#### Flow Visualization

Some flow visualization pictures were taken of the truck at approximately 55 miles per hour (figs. 12(a) to 12(f)). The airflow was made visible with powder (diatomaceous earth), which was emitted at the top front edge of the cab. The powder was pumped out of a sandblaster hopper inside the trailer. Although the photographs do not define the details of the stream tube paths, they give a general idea of the flow's behavior with and without the add-on devices. It should be noted that the diatomaceous earth used in figures 12(a) and 12(e) produced a low density dispersion. The same general flow pattern resulted when diatomaceous earth that

produced a high density dispersion was used. Crosswinds ranged from 2 miles per hour to 5 miles per hour when the pictures were taken.

### CONCLUDING REMARKS

This study showed that moving the trailer forward from 62 inches to 40 inches reduced the aerodynamic drag for the baseline configuration approximately 10 percent at zero wind conditions.

The maximum aerodynamic drag reduction realized from an add-on device at zero wind conditions was approximately 24 percent for the rear trailer position (62 in.). Some add-on devices provided only small reductions in drag.

Limited data obtained for some of the devices showed that their ability to decrease drag was reduced by the presence of crosswinds.

*Flight Research Center*

*National Aeronautics and Space Administration*

*Edwards, Calif., December 9, 1974*

### REFERENCES

1. Saltzman, Edwin J.; and Meyer, Robert R., Jr.: Drag Reduction Obtained by Rounding Vertical Corners on a Box-Shaped Ground Vehicle. NASA TM X-56023, 1974.
2. Saltzman, Edwin J.; Meyer, Robert R., Jr.; and Lux, David P.: Drag Reductions Obtained by Modifying a Box-Shaped Ground Vehicle. NASA TM X-56027, 1974.
3. White, R. A.; and Korst, H. H.: The Determination of Vehicle Drag Contributions from Coast-Down Tests. SAE 720099, Jan. 1972.
4. Hoerner, Sighard F.: Fluid-Dynamic Drag. Publ. by the author (148 Busted Dr., Midland Park, N. J.), 1965.
5. Flynn, Harold; Kyropoulos, Peter: Truck Aerodynamics. SAE Transactions 1962, Vol. 70, c.1962, pp. 297-308.
6. Sherwood, A. Wiley: Wind Tunnel Test of Trailmobile Trailers. Wind Tunnel Rept. No. 85, Univ. Maryland, June 1953.
7. Davisson, J. A.: Design and Application of Commercial Type Tires. SP-344, SAE, Jan. 1969.

TABLE 1.—VEHICLE CHARACTERISTICS

The tractor-trailer combination used in this study was one of many that could have been used. Specifications are given herein for completeness only.

Tractor:

Make . . . . .	White Freightliner
Year . . . . .	1974
Type . . . . .	Cab over engine (with sleeper)
Number of axles . . . . .	3
Tire size . . . . .	10.00-22
Engine—	
Type . . . . .	350 Cummings Turbocharged
Model . . . . .	NTC-350
Displacement, in <sup>3</sup> . . . . .	855
Horsepower at 2100 rpm . . . . .	310
Transmission—	
Type . . . . .	Fuller Roadranger
Model . . . . .	RTO-9513

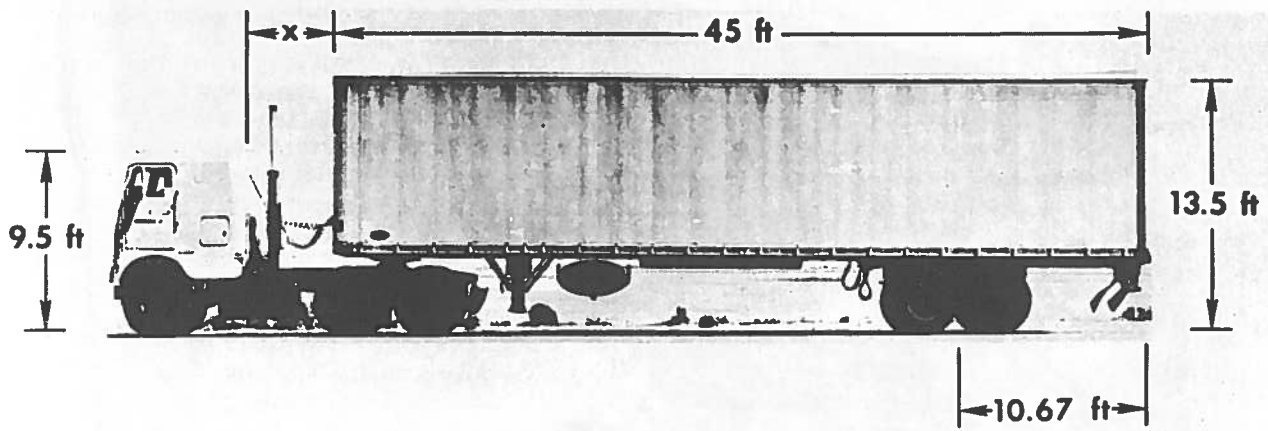
Trailer:

Make . . . . .	Strick
Year . . . . .	1972
Length, ft . . . . .	45
Type . . . . .	Smooth sidewall
Number of axles . . . . .	2
Tire size . . . . .	10.00-22

TABLE 2.—AERODYNAMIC DRAG REDUCTION AND DRAG COEFFICIENTS

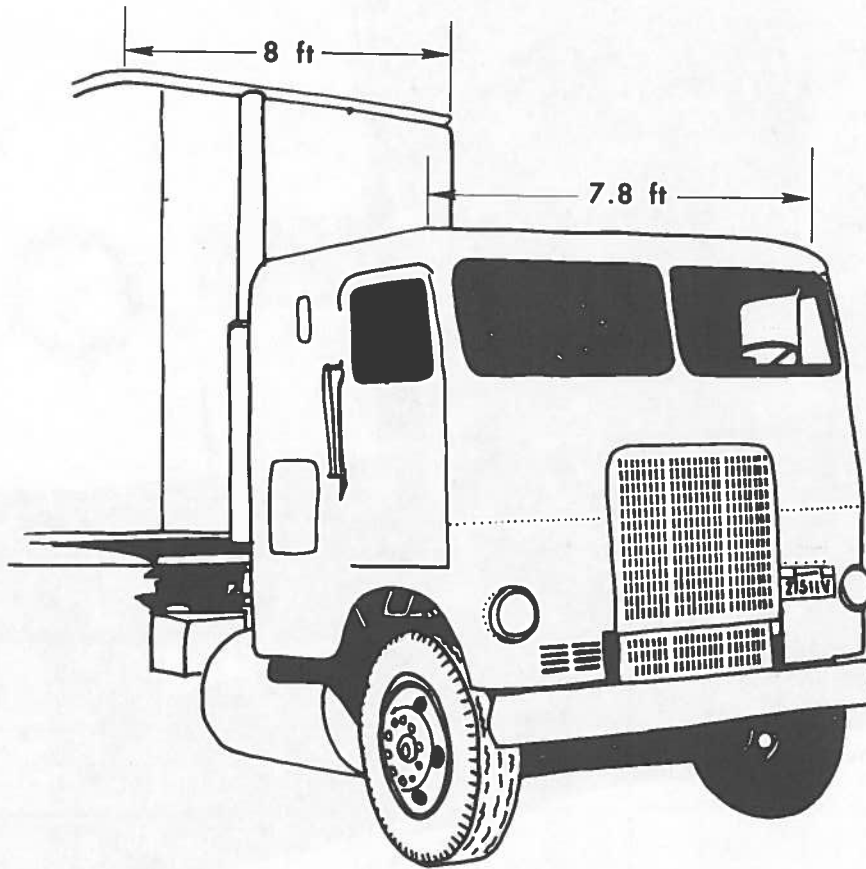
55 mph, zero wind conditions

Configuration	x, in.	Aerodynamic drag reduction, percent	Drag coefficient
Baseline	62	--	1.17
	40	--	1.06
Device A	62	24	0.89
	40	16	0.89
Device B	62	14	1.00
	40	11	0.94
Device C	62	11	1.04
	40	11	0.94
Device D	62	3	1.13
	40	2	1.04
Device E	62	19	0.95



(a) Side view .

E-27320



(b) Three-quarter front view .

Figure 1. Test vehicle .



Figure 2. Cover over radiator opening.



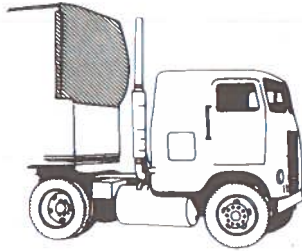
Figure 3. Instrumentation layout inside cab.



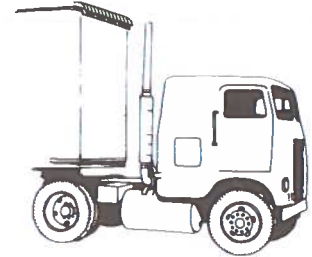
**DEVICE A**



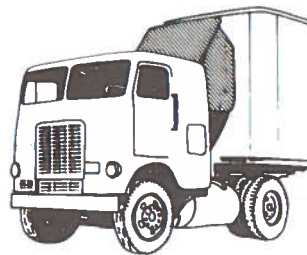
**DEVICE B**



**DEVICE C**



**DEVICE D**



**DEVICE E**

Figure 4. Devices tested.

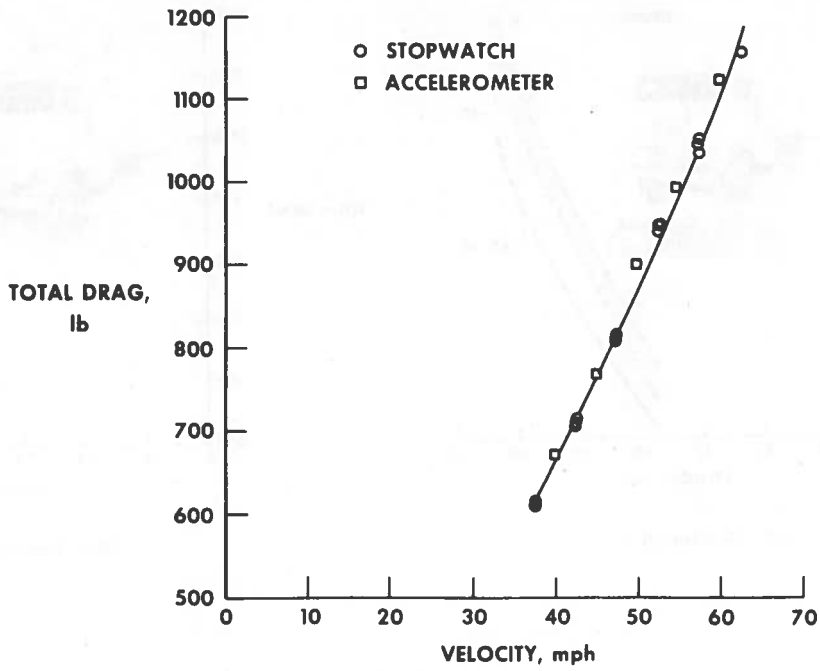


Figure 5. Typical total drag for baseline configuration.  $x = 62$  inches, zero wind conditions.

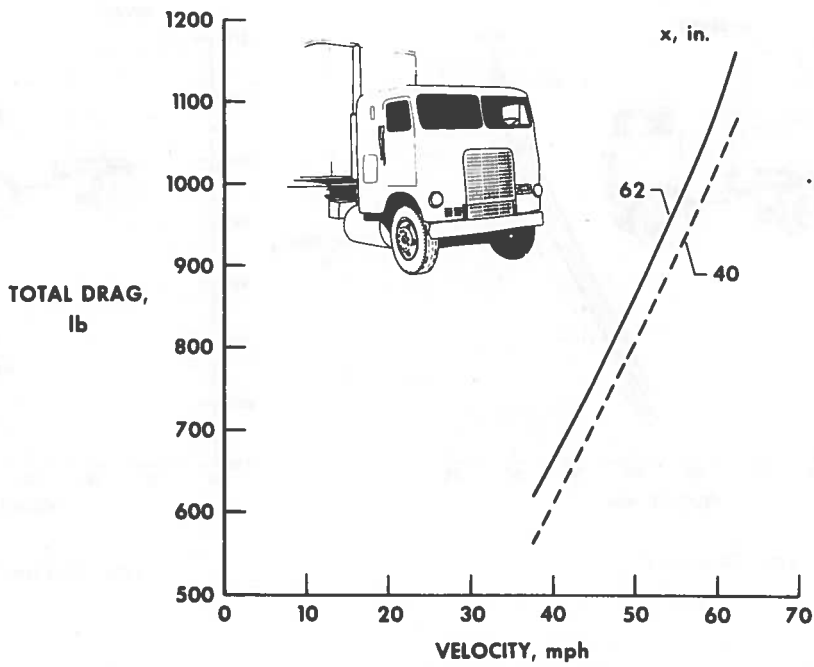
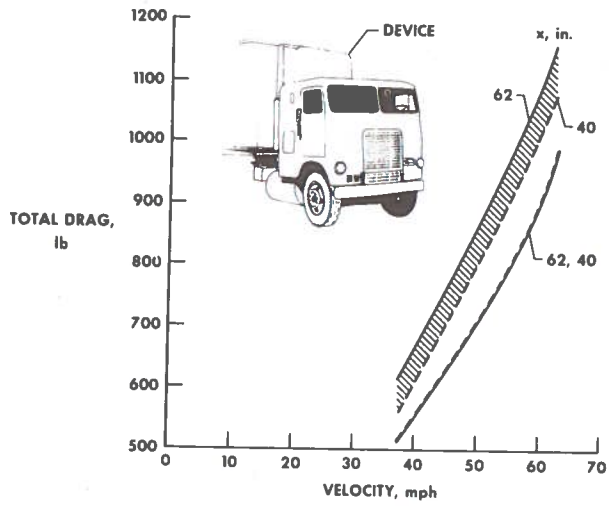
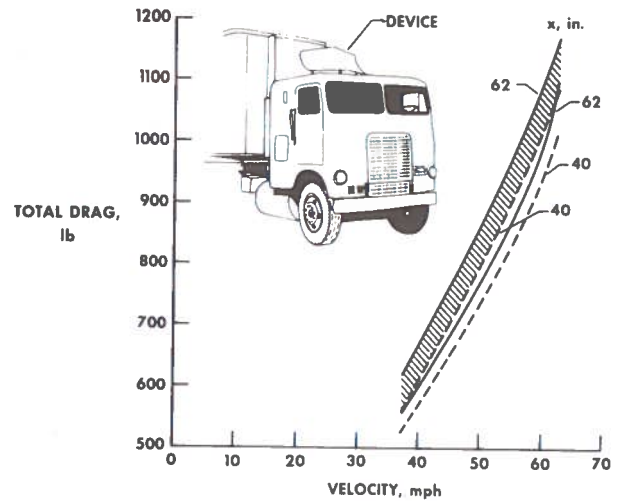


Figure 6. Total drag for baseline configuration for two trailer positions. Zero wind conditions.



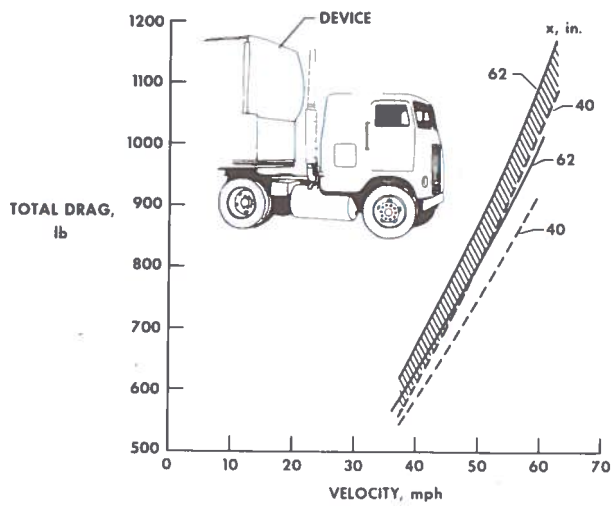


(a) Device A.

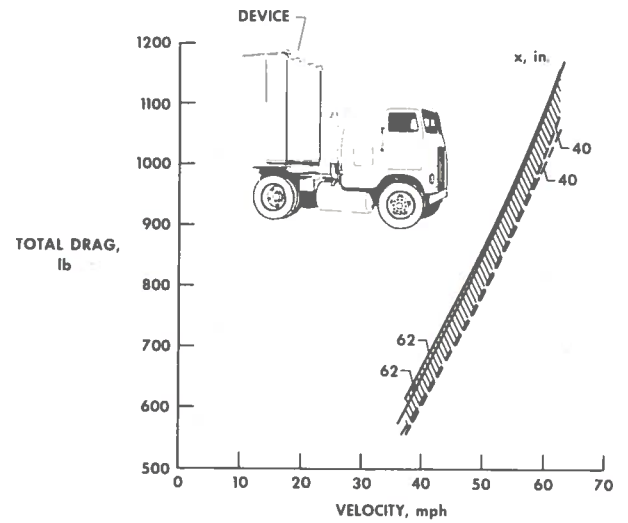


(b) Device B.

 BASELINE CONFIGURATION

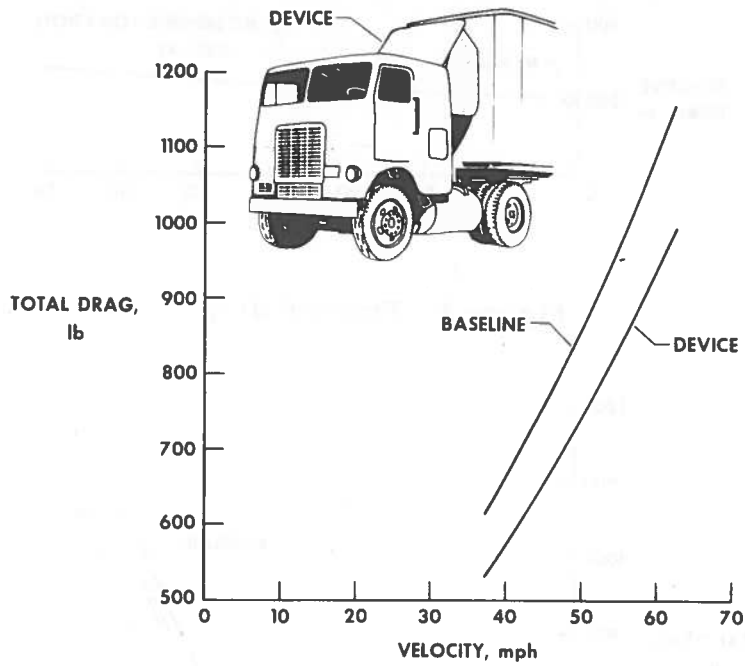


(c) Device C.



(d) Device D.

Figure 7. Comparison of total drag with and without add-on devices. Zero wind conditions.



(e) Device E.  $x = 62$  inches.

Figure 7. Concluded.

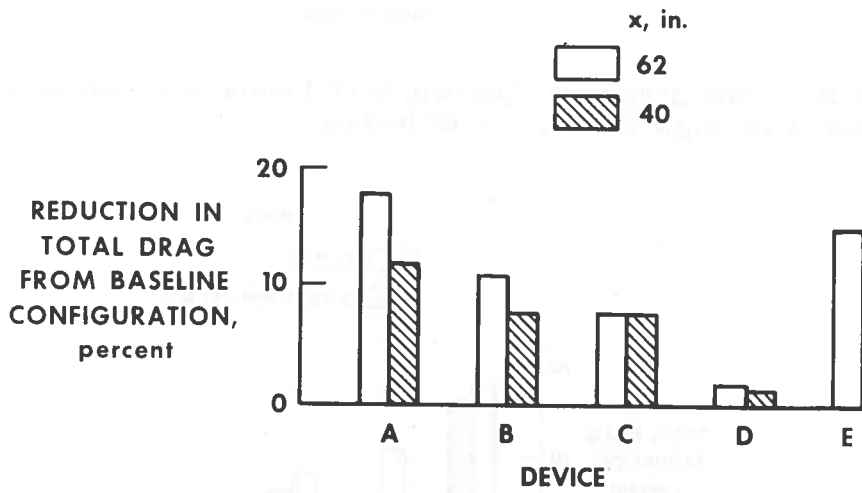


Figure 8. Reduction in total drag for the devices.  $V = 55$  miles per hour, zero wind conditions.

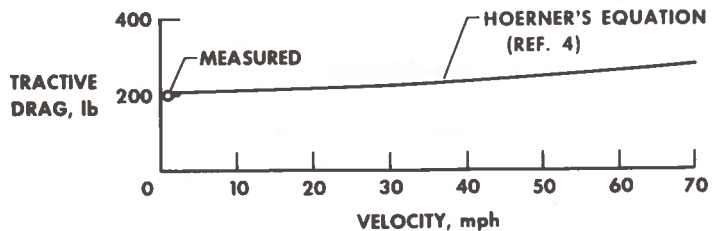


Figure 9. Tractive drag.

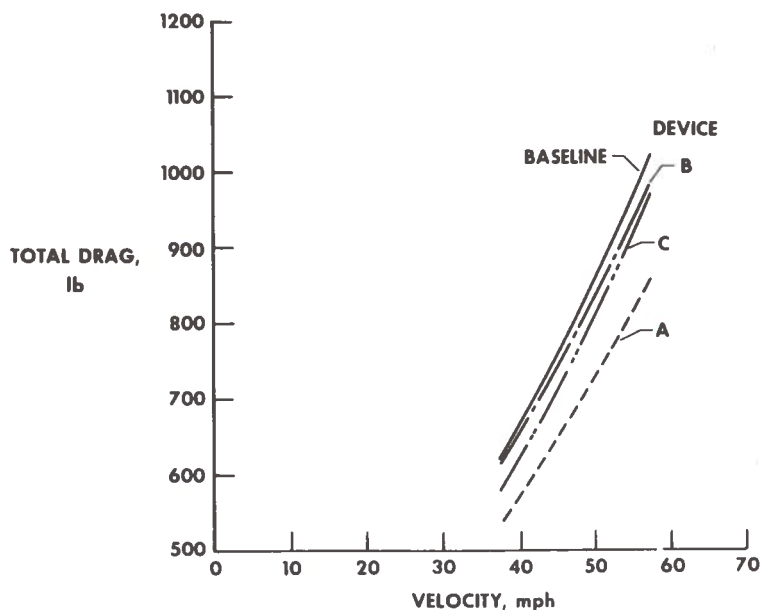


Figure 10. Total drag with crosswinds of 2 miles per hour to 3 miles per hour at an angle of  $11^\circ$ .  $x = 62$  inches.

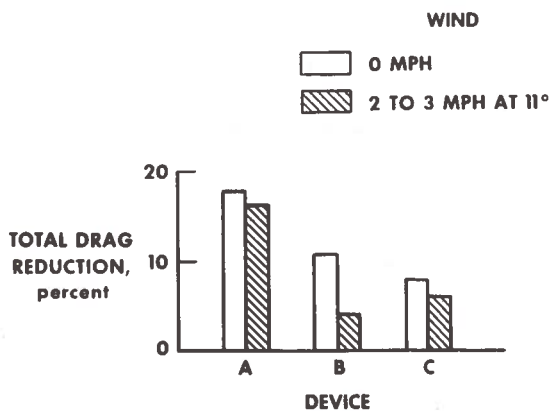


Figure 11. Reduction in total drag for devices A, B, and C with and without crosswinds.  $x = 62$  inches;  $V = 55$  miles per hour.



(a) Baseline configuration.



(b) Device A.

Figure 12. Flow visualization for baseline configuration and configurations with add-on devices.



(c) Device B.



(d) Device C.

Figure 12. Continued.

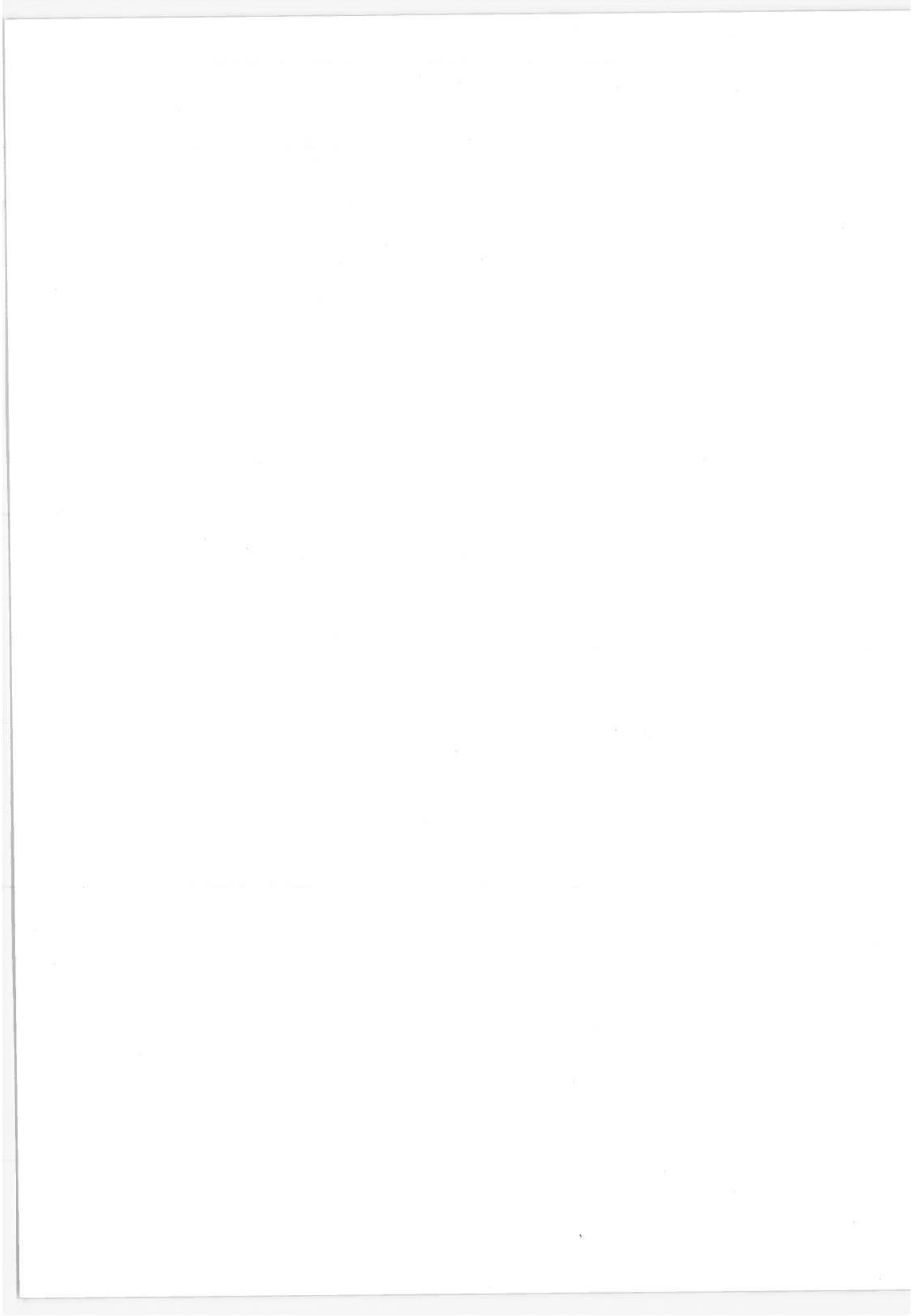


(e) Device D.



(f) Device E.

Figure 12. Concluded.



## STUDY OF AUTOMOTIVE AERODYNAMIC DRAG

Jack E. Marte and Bain Dayman, Jr.

Jet Propulsion Laboratory

California Institute of Technology

Pasadena, California

### ABSTRACT

Sub-scale and full-scale wind tunnel tests on three popular American cars have demonstrated that drag reductions in the range of 20-30% are possible by means of add-ons and relatively simple (from an aerodynamicists point of view) design changes. The initial results from a preliminary road test using a coast-down technique with a 1975 Chevrolet Impala Sport Sedan have shown that this technique can be used to obtain accurate and realistic aerodynamic drag and rolling resistance information which is representative of an actual vehicle under real operating conditions. This is demonstrated by the small scatter in the inferred resistances and the small deviation in the base raw data.

### 1. PURPOSE AND OBJECTIVES

The Jet Propulsion Lab (JPL) Automobile Aerodynamic Drag Reduction Program has the following general purposes:

- A. To demonstrate that a significant decrease in the aerodynamic resistance of automobiles can be practically achieved.
- B. To provide the necessary means to include aerodynamic considerations in the development and design cycle of automobiles.
- C. To develop the techniques necessary to quantify the aerodynamic resistance of actual automobiles.

This report is concerned with the progress which has been accomplished in Phase I of this program, a 9 month effort which began August 5, 1974. The purpose of Phase I is to experimentally validate the reduction in aerodynamic drag possible through add-on devices and minor design changes to existing types of autos with the overall goal of reducing fuel consumption.

The specific objective of Phase I is to demonstrate that a 25-30% reduction in aerodynamic drag can be achieved in a practical manner. Based on a reasonable mix of two EPA urban cycles and their highway cycle, a decrease in overall fuel consumption of approximately 5% can be expected when the Phase I goal is reached.



This amounts to 100-150 million barrels of gasoline per year for a 100 million car fleet, assuming 10,000 miles per year at 15 miles per gallon. The elements for Phase I of the project are diagrammed in Figure 1.

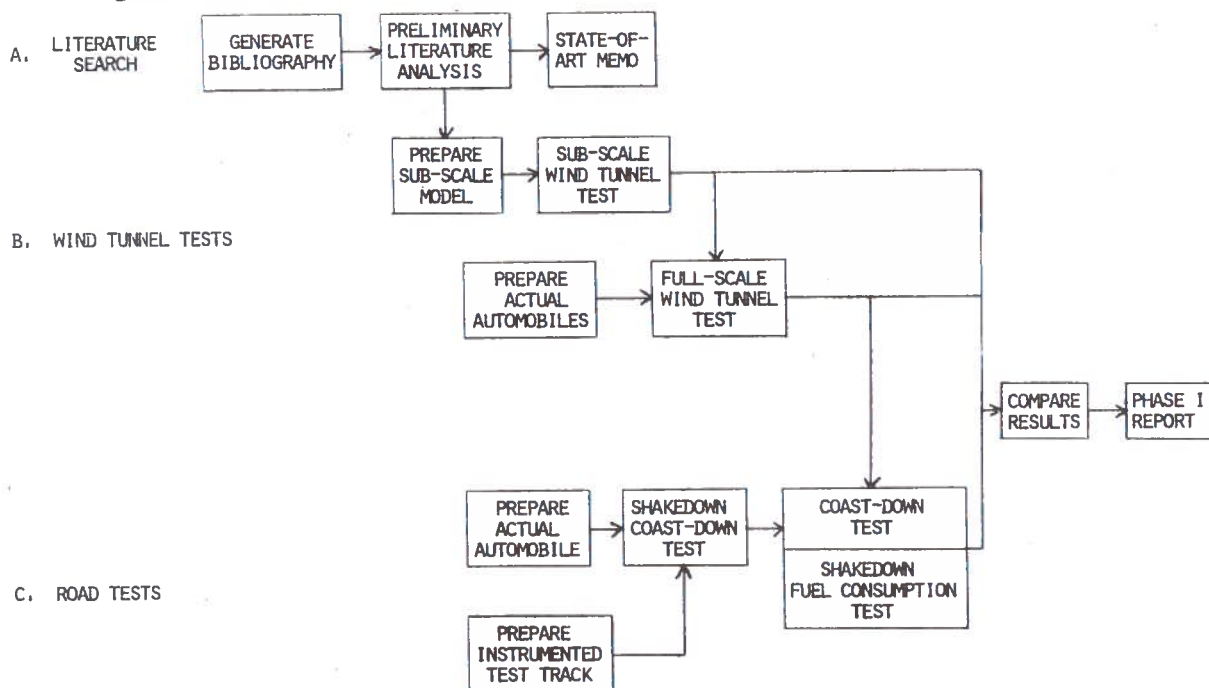


Figure 1. Project Elements (Phase 1)

The search of the open literature on automotive aerodynamics and related subject areas culminated in an informal report to the Transportation Systems Center and bibliography which was organized under the following subject headings:

- Aerodynamics
- Cooling Systems
- Engine Performance
- Fuel Economy
- General, Books, Proceedings
- Noise
- Stability and Handling
- Facility Test

- Road Test
- Tires and Rolling Resistance

The results contained in the informal report can be summarized as follows:

Reliable drag data on modern American automobiles available in the open literature has always been very scarce. The Motor Industries Research Association (MIRA) has, in a continuing series of reports, measured in their wind tunnels drag coefficients on some British, European and American cars dating back to 1926. The mean drag coefficient for the tested American cars in the 1960 to 1965 model years is given as 0.465 (0.421 to 0.510) for the radiator-open case. Equivalent values for British and European cars were 0.452 and 0.433, respectively. While the use of these values as absolute numbers may be inadvisable<sup>1</sup>, their relative magnitudes can be used and indicate that for the cars tested, the American models showed consistently higher drag than either the British or European models. A tendency to increase slightly with time was also noted.

## 2. DRAG DATA

One of the most recent sets of drag data on modern American automobiles in the public domain was presented at a recent SAE Meeting<sup>2</sup> and is reproduced in Tables 1 and 2.

- 
1. Although self-consistent, drag data from the MIRA wind tunnels is persistently slightly lower than equivalent data obtained in a number of American wind tunnels. These differences are thought by American automobile aerodynamicists to be due to differences in testing techniques but the matter is still an open question at this time. The reader is, therefore cautioned against making direct comparisons between MIRA and American drag data, although relative and incremental values of MIRA data are very useful.
  2. This data was assembled and presented during a prepared discussion by Mr. Gary Romberg of Chrysler Corporation at the International Automobile Engineering and Manufacturing Meeting in Toronto, Canada on October 21st to the 25th, 1974.

TABLE 1 DRAG COEFFICIENTS

Car	Wind Tunnel Facility*	$C_D A$
1973 Plymouth B-Body 2-Door H.T.	1	12.25
1975 Plymouth B-Body 4-Door Sedan	2	12.50 ( $C_D = 0.53$ )
1969 Dodge "Daytona" B-Body Race Car	2	6.94 ( $C_D = 0.32$ )
1975 Plymouth C-Body 4-Door Sedan	2	11.95
1974 G.M. Vega	1	9.46
1974 Ford Pinto	1	11.29
1974 Audi Fox	1	10.05

\*Note 1. Wind tunnel facility 1 is the Wichita State 7 x 10 ft wind tunnel, and 3/8-scale models were used; facility 2 is the Lockheed-Georgia 16 x 23 ft Low Speed Wind Tunnel using full-size cars.

Where the reference areas are known, the values for drag coefficients are given in parentheses. Road test data was also presented and, in general, showed correlation in the 2-3% range. Since various road test techniques were used, this level of correlation may have been fortuitous. The data presented in Table 1 is in no way definitive, but was presented only as a collection of what could be assembled to date.

A quantitative estimate of the effect of various drag-reduction measures is difficult. However, some values based on the experimental results of numerous investigations have been tabulated in Table 2 below. Items from the table can be considered additive if only one entry from item 6 is used. The exact values of the increments are, of course, dependent on the baseline design to which they are applied.

TABLE 2 IMPROVEMENT POTENTIAL

Improvement Potential (Relative to typical 1975 notch-back sedan)	$\Delta C_D$ (%)
1. Interference or parasite drag	4-9
2. Increased front-end radii	5-10
3. Windshield slope and fairing	3-6
4. Rear deck and window modifications (fast-back = 11%)	5-7
5. Engine Cooling	1-2
6. a. Full belly pan	15
b. Belly pan to front axle	9
c. Skirt	

### 3. SUB-SCALE WIND TUNNEL TESTS

The sub-scale wind tunnel test was run in the Guggenheim Aeronautical Laboratory, California Institute of Technology (GALCIT) 10 ft Wind Tunnel in Pasadena, California. A 40%-scale model of a 1974 Mustang II notch-back coupe was loaned to the program by the Ford Motor Company. The model was tested with two modified noses, full and partial underpans, front skirts or dams and rear trunk spoilers. The later two items were optimized for drag effect by varying skirt ground clearance and spoiler height, respectively. Car attitude and ground clearance were varied. Reynolds number effects were investigated and found to be insignificant in the range of road operation where all data were taken.

The greatest drag reduction actually measured during the test was 24% at zero yaw for a configuration which included a streamlined nose, a front skirt having 8.5 in (full scale) ground clearance at the front bumper and a 2-in. high (full-scale) spoiler at the rear of the trunk lid. For this configuration, the incremental improvement decreased to 18% at 12° yaw. By synthesis, i.e., the addition of incremental drag reductions from various runs with compatible configurations and extrapolation to the road vehicle conditions at 55 mph, a reduction in drag of as high as 30% at zero yaw can be obtained for configuration which included the streamlined nose, full underpanning, the 2-in. spoiler and moderate nose-down tilt of the body.

Figures 2 and 3 show the model installed in the GALCIT wind tunnel with some of the modifications. Note that the noses shown in these figures were mounted forward of the actual model nose in order to avoid permanently modifying the model contours. This practice is often followed in automobile aerodynamic testing and has been found to be a reasonable approximation of the effect of the same changes built into the car. It is, of course intended that there would be little or no change in the overall car length if the noses shown were incorporated in a real vehicle. In the case of the short rounded nose, the modification did, in fact, extend only to the front bumper. On both nose modifications the area of the air inlet was arbitrarily reduced approximately 10% on the assumption that improved inlet fairing could produce the same mass flow of air in the reduced area.

#### 4. FULL-SCALE WIND TUNNEL TEST

The full-scale wind tunnel test was run at the Lockheed-Georgia Low Speed Wind Tunnel in Marietta, Georgia on all three cars. The following results were obtained for configurations which included a skirt at the front bumper with 5.5 inch to 8.5 inch ground clearance, a rounded nose (not the more highly streamlined nose mentioned above in the GALCIT test), a right-angle "hard" corner at the trunk rear edge for the Impala and Valiant and a 2-inch high spoiler for the Mustang II:

	$\frac{\Delta C_D}{C_{D_{STD}}}$	$C_{D_{STD}}$
Impala	21%	0.55
Valiant	19%	0.60
Mustang II	17%	0.57

$$(\text{where } \Delta C_D = C_{D_{STD}} - C_D)$$

An additional 3-4% decrease can be obtained if the car body can be nosed down 2°. Figures 4, 5, and 6 show various configurations of the three cars as installed in the Low Speed Wind Tunnel.



Figure 2. Scale Model of Mustang II with Long Nose and Underpan as Modifications

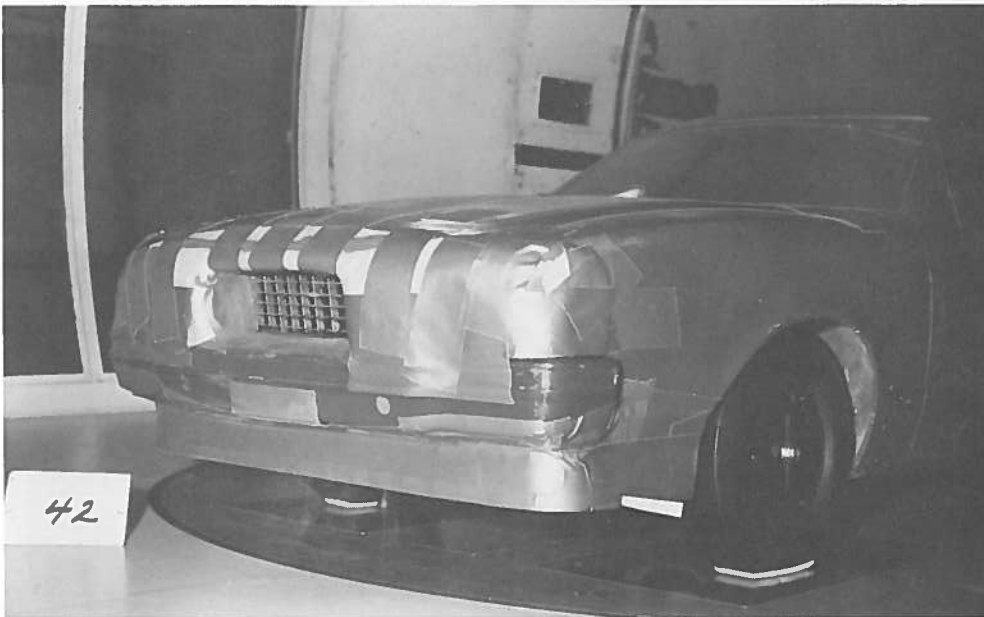


Figure 3. Scale Model of Mustang II with Short Nose and Front Skirt as Modifications



Figure 4. Impala Sedan with Short Nose, Window Fairings and Underpan as Modifications



Figure 5. Plymouth Valiant with Short Nose, Square Back, and Front Skirt as Modifications



Figure 6. Mustang II with Short Nose, Short Underpan and Square Back as Modifications

## 5. COMPARISON OF TUNNEL TESTS

A detailed comparative analysis of the Mustang II data from the two wind tunnel tests has not yet been carried out. For the configuration described above which resulted in a drag decrement of 17% in the GALCIT tunnel, a corresponding value of 19% was obtained in the Lockheed tunnel. However, in terms of absolute level, the agreement is not so satisfactory. A value of  $C_D = 0.50$  was measured in the GALCIT test and a corresponding value of  $C_D = 0.57$  in the Lockheed tunnel. The same type of buoyancy corrections and wind tunnel wall corrections which account only for the effective increase in the air-flow velocity due to the presence of a model whose frontal area is some 5-7% of the tunnel test section area were used to correct the raw data in both tests. At this time the discrepancy is unexplained but variations in model details, attitude, height or differences in tunnel flow or boundary layer could separately or in combination account for the difference. Further analysis is required.



## 6. SHAKEDOWN COAST-DOWN TEST

The shakedown coast-down test on a 1.6 mile runway at the Edwards AFB, Flight Test Center has also been completed. The objective of this shakedown test was to evaluate the test procedures, instrumentation, and quality of the data obtained. This objective was achieved; the test procedures, the instrumentation and the quality of the data were all good. It was not the purpose of the shakedown test to obtain an absolute value of the aerodynamic drag coefficient. For the sake of expediency, uncalibrated tires were used and the rolling resistance was far from minimal. During this test, data was obtained on a standard configuration Chevrolet Impala Sport Sedan which was accelerated to velocities as high as 80 mph before entering a series of eleven accurately located electric switches which start and stop a pair of interval counters. The resulting series of times between the 500 ft intervals are reduced by means of a computer program to drag coefficients. Many simplifying approximations were used in the initial data reduction. However, even this simplified data reduction was adequate to demonstrate that all test procedures were good since the reduced data showed an average RMS duration of only 0.04 sec. (which converts to a velocity error of 0.05 mph) for the seven acceptable runs of the 18 attempted. Most of the 18 runs were made with a wind velocity of less than 200 ft per min. parallel to the test course. Even though the initial data reduction accounted for this steady wind, it appears that minor gusts at these low mean velocities are the largest error source in this test technique. Assuming that the rolling resistance of the radial tires used matched that which appears in the literature, the seven-run average value of  $C_D = 0.545$  results. But if the rolling resistance characteristics of the tires used deviated appreciably from the value given in the literature; say to the degree that the to-be-used tires which have been calibrated at the Central Research Laboratories of the Firestone Tire and Rubber Company do, then the actual  $C_D$  would be lower by 0.035. There is no plan to calibrate these standard equipment tires since all objectives of this shakedown coast-down test were achieved and the absolute value of  $C_D$  will be obtained during the final series of coast-down tests.

At this time no implications should be drawn from the comparisons of the drag coefficients obtained from the coast-down test and the wind tunnel tests. The concerns about the coast-down  $C_D$  (which could bring the 0.545 down to 0.510) was discussed above. The value of  $C_D = 0.55$  from the test in the Lockheed Georgia Low Speed Wind Tunnel does not have the controversial streamline curvature correction included. If it were included, the drag coefficient would be decreased to  $C_D = 0.51$ . At this time there is no reason to expect even the final road-test data (coast-down) to agree with correctly reduced full-scale wind tunnel data. Conditions, such as the fixed tunnel floor with its thick boundary layer and the differences in vehicle attitude and height due to both aerodynamic lift and inertial forces, may lead to a significant difference in the data from these two techniques. In the final analysis, the data from the coast-down test if properly obtained (good test procedure and proper reduction techniques performed), would be the more meaningful result since the testing environment most nearly matches that for the actual case of an automobile in operation. We are sufficiently encouraged by these preliminary results to believe that this coast-down technique may be the best method currently available to obtain absolute drag levels for cars and trucks under real-life operating conditions.

Figure 7 and 8 show the test vehicle and some of the equipment at the test site. In the second period of road testing the standard and a low-drag configuration of the same car will be tested under conditions for which mechanical and tire resistances will be both minimized and measured or carefully estimated as a function of velocity in an attempt to improve on the good data of the first test period.



Figure 7. Impala Field Test Car at Edwards AFB



Figure 8. Field Test Instrumentation Van

## ROLLING RESISTANCE OF PNEUMATIC TIRES

S.K. Clark

University of Michigan

Ann Arbor, Michigan

### ABSTRACT

Since the power losses of an automobile which are directly attributable to its tires have been estimated to be approximately one-fourth of the total automobile power losses, potential improvements in tire power transmission efficiency are important and worth seeking. Summaries of tire rolling resistance as influenced by tire construction and design, tire materials, and tire operating conditions indicate clearly that current trends toward smaller, lighter automobiles and increasing usage of radial tires, in addition to reduced speed levels are positive contributions in the effort to reduce tire rolling losses.

### 1. INTRODUCTION

It is useful to think of the tires on the drive wheels of an automobile or truck as power transmission devices, since they transmit power from the engine to the roadway in order to propel the vehicle. This is accomplished with an efficiency which may vary from nearly 100% to zero, although under normal conditions of good traction and steady-state running the efficiency of the pneumatic tire is quite high, being of the same order of magnitude as that of other power transmission components in the vehicle. The unpowered or free rolling wheels on a vehicle may be thought of as a special case of powered wheels, but now with zero torque applied from external sources.

The assessment of the mechanical efficiency of a tire, and particularly a pneumatic tire, is made difficult by the interaction of tire losses with a variety of other factors, such as velocity, pressure, and temperature. This interaction may be partially clarified by the following set of considerations:

- (a) It is generally agreed by all who have studied the problem that the total mechanical loss incurred in a pneumatic tire is made up of three components:
- (i) Friction between the road and tire surface due to slipping at the tire road interface
  - (ii) Windage or aerodynamic losses in the tire itself.
  - (iii) Hysteretic losses within the tire due to action of the rubber and cord components of the tire, both of which have their individual loss characteristics.
- (b) Under conditions of free rolling or steady state driving, where external torque applied to the wheel is not large, it is generally conceded that the hysteretic component of the total tire loss is the dominant one, making up something more than 90% of the total mechanical losses in the tire. Aerodynamic drag of the tire itself and friction between the tire and roadway are minor components.
- (c) The hysteretic loss characteristics of most of the materials used in the tire construction, namely rubber and polymeric cord, are quite sensitive to the temperature level at which the loss characteristics are measured. Steel and glass cords are less sensitive to temperature effects.
- (d) Starting from rest at ambient temperature, the temperature of the rolling tire begins to rise as the vehicle starts in motion due to the fact that the hysteretic losses inside the material generate heat. Due to the poor thermal conductivity of rubber it takes a relatively long time for the tire to come into temperature equilibrium. For example, a normal passenger car tire under passenger car vehicle loads requires at least 30 minutes to reach steady-state temperature beginning from rest. Eventually this equilibrium is attained. This higher temperature is not uniform throughout the tire body but varies according to geometric and material design. Due to mixing, the air inside the tire cavity will have a

higher average temperature than at the beginning of the rolling process. This results in a higher pressure than the original inflation pressure of the tire, due to the increased temperature of the trapped air. This rise in pressure causes a reduction in the deflection of the tire. Since the following loss is strongly dependent upon the tire deflection as well as upon the material temperatures in the tire body, then these factors both influence the equilibrium state rolling loss value.

## 2. THE INFLUENCE OF TIRE CONSTRUCTION AND DESIGN

While there has been some controversy concerning the exact quantitative differences between rolling losses in different types of tire constructions, there seems to be general overall agreement that among the three major types, the bias tire, the bias-belted tire and the radial tire, that the radial tire exhibits the lowest rolling resistance in general, the bias-belted tire the next lowest and finally the bias tire the highest. The exact values are highly dependent upon other factors and cannot be assigned numerically in a general way. Partly this is due to the materials used in typical radial and bias tire constructions but is also partly due to their detailed design characteristics such as belt stiffnesses and cord angles.

With regard to tire material selection, two major components must be discussed here. The first of these is the tire cord, which may range all the way from rayon or nylon, both relatively high loss materials, to glass or steel, both of which perform as nearly linearly elastic materials when used in pneumatic tire service. The choice of cord materials is not generally considered to be a major influence in determining tire rolling loss, in most cases.

The choices of rubber compounds used in the tire seem to be more important than the choice of tire cord. A number of different rubber compounds are used inside a pneumatic tire for different

specific purposes. The two most important from the point of view of tire rolling loss are the carcass compounds, used to encase and insulate the reinforcing cords from mechanical contact with one another, and the tread compound which is used to provide scuff protection for the tire carcass as well as to give optimum traction and wear characteristics. It is hardly surprising that different rubber compounds would be used for service conditions which are so different from one another. Generally speaking, one could conclude that the choice of low loss rubber compounds would be beneficial in reducing the rolling loss of pneumatic tire, and this is indeed true.

As can readily be imagined, the relative importance of the reinforcing cords and the rubber compounds in contributing to tire rolling loss is the subject of considerable interest. Willett and Collins et al. have both attempted to define the role of various tire component materials in the overall hysteretic heating process. Since this process is so intimately tied to tire rolling resistance, the conclusions applying to one will apply to the other. Both writers approach this problem from the point of view of selective compounding and construction, that is to say, by building tires using rubber or textiles of varying loss characteristics while all other materials were held constant. Free rolling losses were then measured in these tires in an effort to define the role of each of the tire components in the overall loss process. The data of both Collins and Willett are combined in Table 1. Both writers conclude that approximately 20 to 40% of the total loss in a pneumatic tire may be attributed to losses in the cord reinforcing system.

There is some information in the literature comparing rolling loss characteristics of bias, bias-belted, and radial tires for the same size and load carrying abilities. Representative data for passenger car tires are given by Elliott in Fig. 1.

It may very well be asked whether the apparent advantages of the radial tire design can be translated into improved fuel economy. Data on this have been presented by Bezbatchesko, whose results are shown in Table 2.

### 3. TIRE MATERIALS

Rubber compounds play a relatively large role in controlling the loss characteristics in pneumatic tires. Curtiss gives data on two tires identical in all respects except for their rubber compounds. This is shown in Fig. 2, where it is seen that at higher speeds the high hysteresis material (low rebound) exhibits a lower rolling loss than the low hysteresis material (high rebound). This is undoubtedly because of the onset of dynamic and vibratory effects, which are more efficiently suppressed by a high damping material than by a low damping material. Nevertheless, the conclusion seems to be that within the normal speed range significant improvements can be made by variations in rubber compounding in a tire.

In Fig. 3 Roberts shows that for three sets of tires made with high- and low-loss compounds, the initial or room temperature rolling resistance values differ markedly, probably by close to a factor of 2 to 1 or 2.5 to 1. However, their equilibrium temperatures under running conditions also tend to be different, with the higher loss compound running at a higher equilibrium temperature. Under these conditions of equilibrium the comparative loss values of the two tires differ by not more than 20%. From this it must be concluded that while fundamental improvements are possible by the use of low-hysteresis rubber compounds, care must be taken in assessing the magnitudes of the potential gains. They will certainly not be as large a factor as might be anticipated by consideration of their room temperature hysteretic properties alone.

### 4. TIRE OPERATING CONDITIONS

It is well known that a cold tire starting from rest will slowly build-up temperature, and become hotter as time goes on. Eventually the heat generated in the tire is balanced by heat loss, primarily due to conduction with the surrounding air, and temperature equilibrium is achieved. Since the hysteretic properties are strongly influenced by temperature then it is not surprising that tire drag also changes as temperature changes. This has been shown clearly from the work of Evans given in Fig. 4, for passenger car tires



of conventional size and construction. The general conclusion seems to be that times of the order of 20 to 30 minutes are needed for complete temperature equilibrium to be achieved.

Tire rolling resistance may increase slightly with speed or remain essentially constant with speed in the region of moderate speed range. At higher speeds the rolling resistance tends to increase at a faster rate. Typical data on this phenomenon have been presented by Curtiss whose results are given in Fig. 5. These results indicate the average or idealized response to be expected over a variety of tire types.

All the information reported in the literature agrees that the larger the tire deflection the greater the rolling resistance. This is primarily due to the fact that from 90 to 95% of the power consumption in the rotating tire is caused by hysteresis of the materials and of the tire structure, and that both of these effects are proportional in some fashion to the deformation state of the tire.

Increasing tire inflation pressure decreases the rolling resistance at all speeds on smooth hard surfaces. This occurs because the deflection at a fixed load is less at higher pressure, therefore reducing the hysteresis loss which is partly tire deformation dependent. This is summarized in Fig. 6 from Curtiss.

At fixed speed and inflation pressure the rolling resistance of a pneumatic tire increases with increasing vertical load. This is mostly due to the increased deflection resulting from the increased load.

The rolling loss of pneumatic tires is essentially independent for all hard surface roads, although some test data seem to indicate a slight increase in rolling resistance for asphalt vs. concrete. Clearly, rolling loss is substantially greater for vehicles which operate on unpaved roads and for off-the-road vehicles. Walter and Conant give data for typical rolling loss values for several common surfaces. These are given in Table 3. The ranges of values given here are so broad that no specific detailed conclusions can be made about rolling resistance as influenced by road surface type.

## REFERENCES

1. Bezbatchenko, W., 'The Effect of Tire Construction on Fuel Economy', SAE 740067, 1974.
2. Collins, J. M., Jackson, W. L. and Oubridge, P. S., 'Relevance of Elastic and Loss Moduli of Tyre Components to Tyre Energy Losses', Trans. Inst. Rub. Ind. 40, No. 6, 239, 1964.
3. Curtiss, W. W., 'Low Power Loss Tires', SAE 690108, 1969.
4. Elliot, D. R., Klamp, W. K. and Draemer, W. E., 'Passenger Tire Power Consumption', SAE 710575, 1971.
5. Evans, R. D., 'Factors Affecting the Power Consumption of Pneumatic Tires', Proc. 2nd Rub. Tech. Conf., W. Heffer and Sons, (London), 438-452, 1948.
6. Roberts, G. B., 'Power Wastage in Tires', Proc. I.R.C., Amer. Ch. Soc., 57-72, 1959.
7. Walter, J.D., and Connant, F. S., 'Energy Losses in Tires', The Firestone Tire and Rubber Company.
8. Willett, P. R., 'Hysteric Losses in Rolling Tires', Rub. Chem. and Technol., Vol. 46, No. 2, 425-441, 1973.

Table 1. LOSS CONTRIBUTION OF TIRE COMPONENTS

	9.00-20 Truck Tire	2.25-8 Industrial Tire	6.95-14 4-Ply Bias Passenger Car Tire
<b>Rubber:</b>			
Tread	59%	51%	72%
Other	12%	9%	11%
<b>Cord:</b>			
Reference	[2]	[2]	[8]

Table 2. FUEL CONSUMPTION

Tire	Gasoline Consumption, mpg		
	35 mph	50 mph	75 mph
Steel belt/rayon body radial tire	18.758	18.403	13.681
Rayon belt/rayon body radial tire	18.143	17.718	(13.298)
Glass belt/polyester body bias-belted tire	(17.614)*	(17.068)	(13.024)
4-ply nylon body bias tire	(17.636)	(17.207)	(13.102)
Limits for significant difference at 95% confidence	0.408	0.462	0.376

\*The bracketed figures show less than 95% confidence.

Table 3. ROLLING RESISTANCE  
ON DIFFERENT ROAD SURFACES

Surface	Lb/1000 Lb
	Vehicle Weight
Concrete	10-20
Asphalt	12-22
Dirt	25-37
Sand	60-150

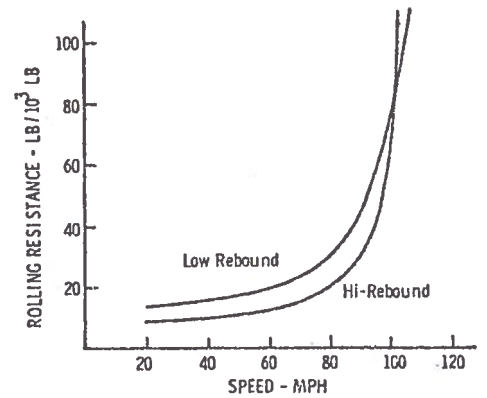


Fig. 2. Rolling resistance vs. speed for high- and low-hysteresis compounds.

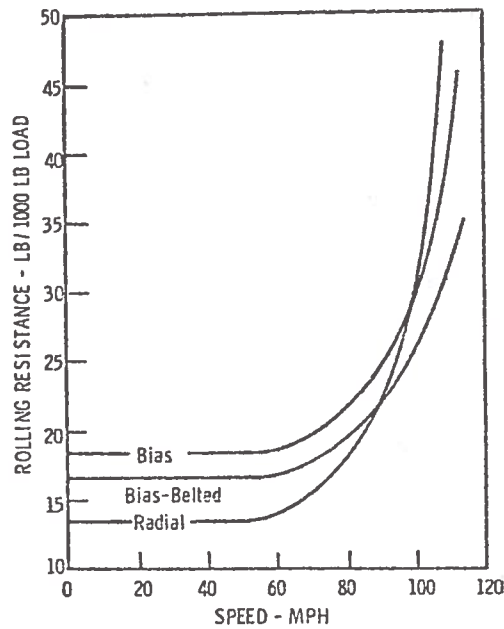


Fig. 1. Rolling resistance vs. speed for different tire construction types (passenger car tires).

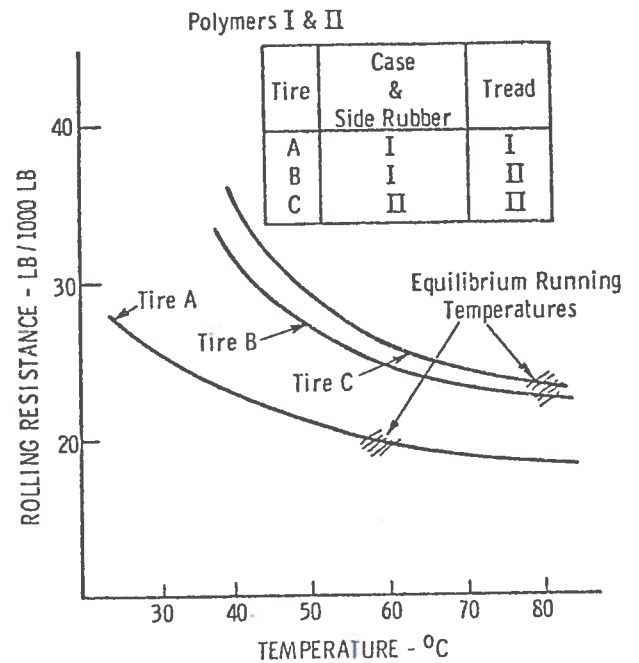


Fig. 3. Rolling resistance vs. temperature for a production polymer (I) and an experimental high-hysteresis polymer (II).

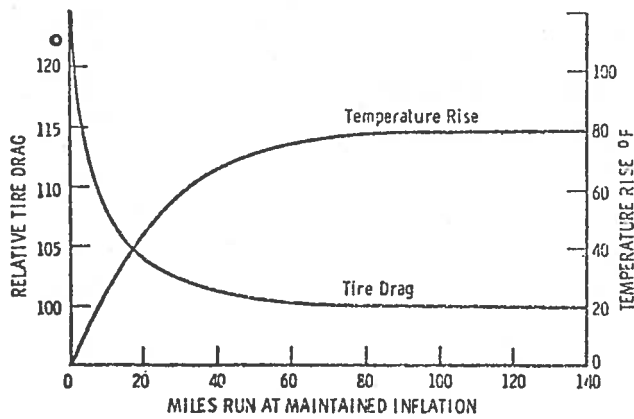


Fig. 4. Relative tire drag (proportional to rolling resistance) and tire temperature increase vs. miles traveled.

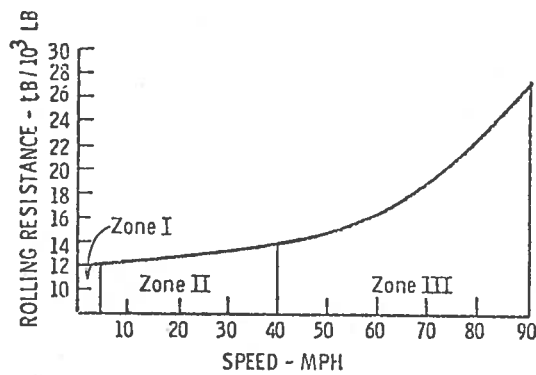


Fig. 5. Rolling resistance vs. speed.

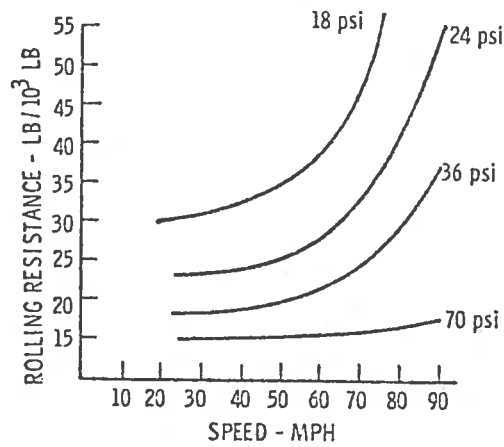
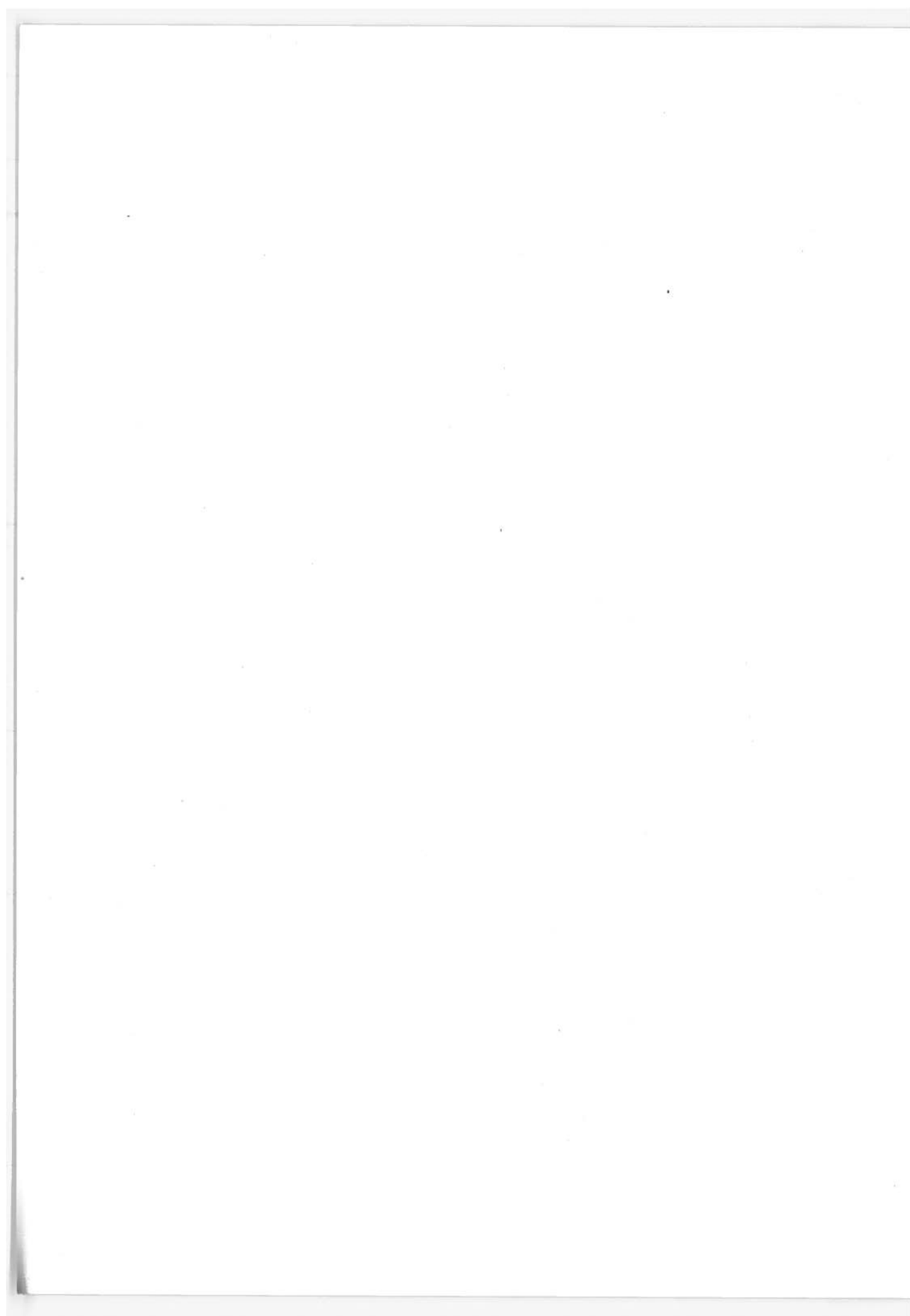


Fig. 6. Rolling resistance vs. speed for different inflation pressures.



## AUTOMOTIVE FUEL ECONOMY EVALUATION

Carlos W. Coon, Jr.  
Southwest Research Institute  
San Antonio, Texas

### ABSTRACT

This study was initiated in mid 1973 with a program dedicated to experimental characterization of 1973 standard and intermediate size vehicles and to identification and evaluation of possible methods of improving fuel economy. Typical results from the experimental program are presented, and a summary of the results from the improvement evaluation program is included.

A comparison of gravimetric, volumetric, and carbon balance fuel measurement techniques was conducted during chassis dynamometer operation, and a brief outline of the techniques and results is presented.

The current phase of the investigation involves characterization of 1974 subcompact vehicles; road tests, stationary dynamometer tests, and chassis dynamometer tests are being conducted on representative automobiles.

In addition, the rolling resistance of several sets of tires is being determined using a mobile facility that minimizes the effect of aerodynamic drag.

A series of chassis dynamometer tests to evaluate the effect of warm-up on fuel economy will be conducted.

Another group of tests will involve a comparison of intake port fuel injection and carburetion on otherwise comparable vehicles.

The present study included experimental characterization of the fuel economy of 1973 model year vehicles, identification and evaluation of individual improvements, and the synthesis of vehicle designs that incorporated combinations of compatible improvements.

The experimental portion of the program involved six 1973 vehicles representing three major manufacturers and both standard and intermediate sizes. The vehicles were subjected to a series of tests during which fuel economy was measured on the road and on the chassis dynamometer. In addition, engine fuel map data and accessory power consumption data were acquired.

Another phase of the program involved the identification and evaluation of a series of individual improvements that might be placed in 10% of vehicle production by 1980. Several constraints were applied; vehicles were to be comparable in performance to 1973 model year vehicles, the 1976 interim emission standards were to be attained, and all applicable safety and noise standards were to be met. Among the improvements considered were the following:

1. Turbocharged spark ignition engines
2. Diesel engines, naturally aspirated and turbocharged
3. Stratified charge engines
4. Lean mixture engines
5. Automatic transmissions with overdrive and lock-up clutch
6. Continuously variable transmissions
7. Tire modifications
8. Aerodynamic modifications
9. Weight modifications
10. Accessory drive modifications.

The improvements were evaluated using an analytical procedure to estimate the probable fuel economy increase; the method included a compensating factor based upon difficulty of emission control. The diesel and stratified charge engines emerged as the most desirable power systems; and other devices, such as the lock-up clutch, showed considerable promise.

The improvements were combined in synthesized vehicle designs that would allow the advantages of each to be favorably displayed. It was suggested that fuel economy improvements on the order of 50% could be obtained from vehicles having the proper configuration.

A comprehensive interim report covering the individual improvement program is presently in the final stage of publication.

Following the program dedicated to evaluation of improvements, a brief experimental project was initiated that was dedicated to the comparison of various fuel measurement techniques on

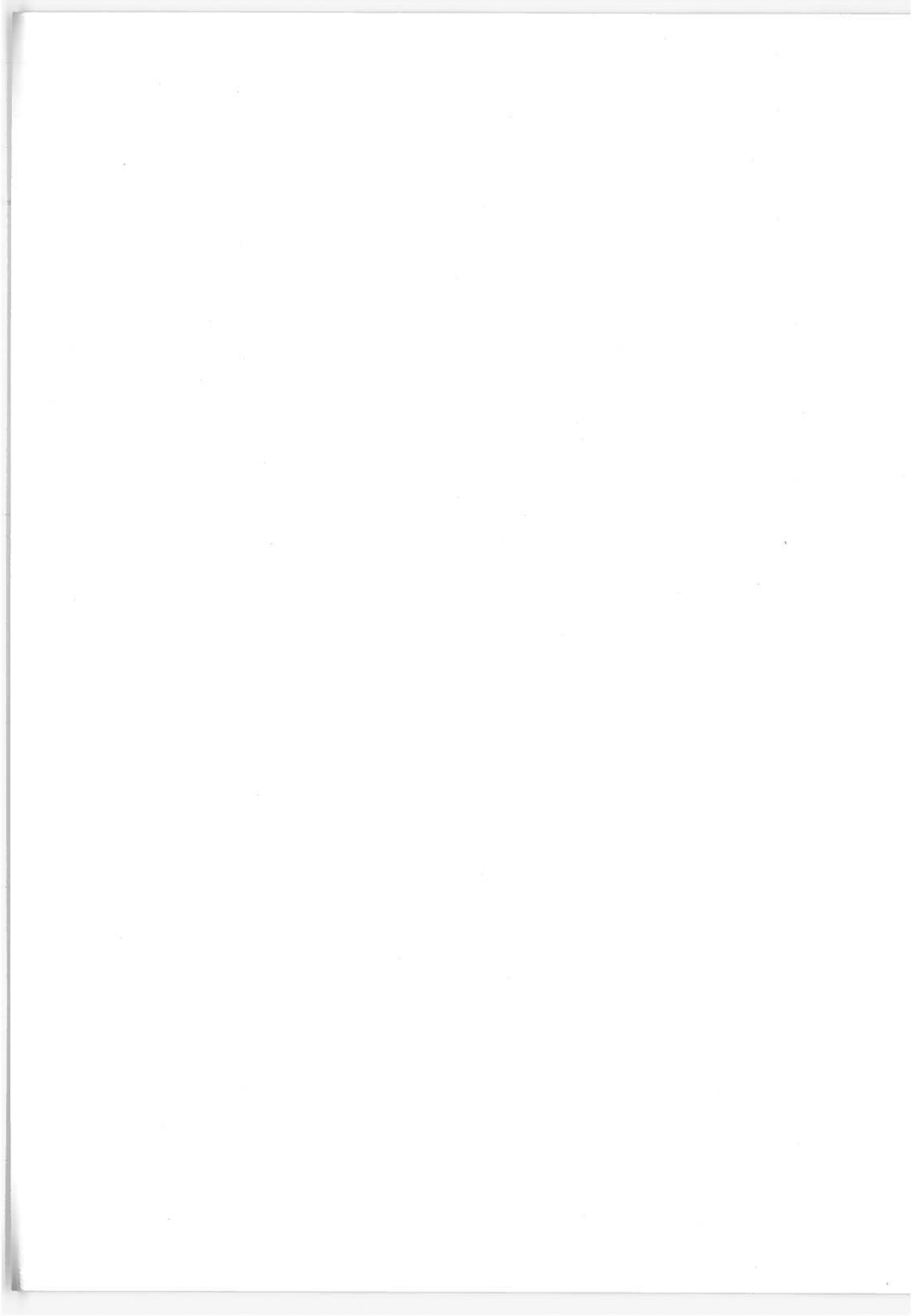
the chassis dynamometer. Road load data were acquired by the coastdown technique, and gravimetric, volumetric, and carbon balance fuel consumption data were acquired during a comprehensive dynamometer driving schedule which included LA-4 cycles, EPA highway cycles, and steady speed operation. Statistical comparisons of the results were obtained, and the advantages and disadvantages of each technique during each mode of vehicle operation were assessed.

The present phase of the program involves characterization of 1974 model year subcompact vehicles. Two domestic and two foreign vehicles are being subjected to engine tests, chassis dynamometer tests, and road load fuel economy tests; acquisition of data is approximately 50% complete. Similar tests are also planned for a passenger car powered by a diesel engine.

In addition, tests are being conducted to determine tire rolling resistance in the absence of aerodynamic drag. These data are being acquired through the use of a special trailer chassis shielded by an enclosure attached to a separate hitch.

A comparison of intake port fuel injection with standard carburetion is also planned, as is an assessment of the effect of vehicle warm-up on fuel consumption.





## EVALUATION OF AUTOMOTIVE FUEL FLOWMETERS

Baldwin Robertson  
National Bureau of Standards  
Washington, D.C.

### ABSTRACT

Flowmeters measure the gasoline consumed by an engine either on the road or on a dynamometer. NBS is surveying commercially available meters and find which are most suitable, to determine the environment in which they will be ultimately used, and to measure their accuracy in a laboratory simulation of that environment.

This paper discusses: (1) the different kinds of flowmeters; (2) the environment of the flowmeter in an automobile (flowmeter temperature; fuel temperature, pressure, density, viscosity, color, opacity, flow pulsations, back flow, and swirl due to elbows; line voltage fluctuations; electromagnetic radiation from ignition; vehicle attitude with respect to the vertical; and vibration); and (3) plans for a test set-up for evaluating and calibrating these meters in the laboratory under conditions simulating the automotive environment.

### 1. INTRODUCTION

The Transportation Systems Center (TSC) is presently developing a series of fuel economy measurement procedures. This work is in support of the Automotive Energy Efficiency Program of the Department of Transportation. The procedures will be used in the test and evaluation phases of projects directed toward improving our understanding of the fuel consumption of modern highway vehicles. The evaluations will involve not only component tests (improved engines, for example) but also tests of an entire vehicle which incorporates an alleged improvement. The engine tests will be done on an engine dynamometer, and the vehicle tests on a chassis dynamometer or on a road test. All of these tests will require fuel measurements.

TSC has asked the National Bureau of Standards (NBS) to survey commercially available fuel flowmeters and find those most suitable for the different fuel economy tests conducted by TSC. By searching published literature and other sources, NBS is to determine the various environmental conditions in which these meters will be ultimately used. NBS will then measure the accuracy of the meters in a laboratory simulation of a representative sample of these conditions. Finally, when the measurements are completed,

NBS will specify for each acceptable flowmeter a calibration technique and an operating procedure for use in tests by TSC.

## 2. AVAILABLE FLOWMETERS

The flow rate of gasoline to the carburetor of automobiles can be as low as .4 gal/hr (.4 cm<sup>3</sup>/sec) for a small car at idle. It can be as high as 22 gal/hr (22 cm<sup>3</sup>/sec) for a large car at full-load going up hill at high speed. This is a range of over 50 to 1.

The environment of a flowmeter in an automobile is sufficiently hostile so that the flowmeter is not likely to measure fuel flow very accurately unless specially designed for this purpose. In our initial series of tests we will evaluate only the flowmeters that are advertised for automotive use.

The flowmeters range in price from \$40 to \$8,600. They range in readability from .1 gal to 10<sup>-5</sup> gal, and have a claimed accuracy as good as 1/4%. Not all of them cover the necessary 50 to 1 flow range. Several are available as miles-per-gallon meters as well as instantaneous gallons-per-hour or total fuel used meters. Miles-per-gallon meters could ultimately be sold as optional or even standard equipment on automobiles. The fuel consumption versions range in weight from about 1 to 25 lbs (in mass from .5 to 11 kg) and in size from what just fits in your hand up to about a cubic foot (a cube 30 cm on a side). Some have remote readouts that are to be put on the dashboard to make it easy to record the measured results.

Regardless of where the flowmeter is placed, its input and output lines usually have to be connected between the fuel pump and the carburetor. Many cars have a fuel pump with three fuel lines connected to it. One line comes from the tank, one goes to the carburetor, and a vapor diverter line goes back to the tank. The diverter is an orifice on top of a fuel passage. The orifice is too small to let most of the liquid gasoline go through. But bubbles will rise to the top of the gasoline in the passage and go through the orifice. Then the diverter line carries them back to the tank. This helps prevent vapor lock. However, the diverter

line also carries a relatively large flow of liquid gasoline back to the tank. If the flowmeter were connected into the line from the tank to the pump, it would measure the flow to the carburetor plus the flow back to the tank. On these cars the flowmeter must be connected so that the fuel flows from the pump to the flowmeter and then to the carburetor. Only then will it measure just the flow to the carburetor.

The various types of flowmeters will be described in the order of increasing price. The \$40 one is a variable area flowmeter. It uses a light beam shining through the gasoline to detect the position of the ball. The light passes through a mask that is shaped so that the reading is proportional to the flowrate.

A \$90 flowmeter has a ball that travels through a toroidal passage, i.e., a passage shaped like the dough of a donut. The ball is pushed along by a jet of fuel every time it comes around the toroid. The fuel travels three-fourths of the way around the toroid behind the ball and then exits while the ball coasts along to where it gets pushed again. Each time the ball goes around the toroidal passage it interrupts a light beam and is counted.

There is a \$200 flowmeter which uses a toothed disk. The fuel flows from a jet aimed tangentially at the toothed disk causing it to rotate. As the disk rotates, its teeth interrupt an infrared light beam and is counted.

Another flowmeter (\$240) uses an automatically filled .01 gallon container. The contents of the container are dumped on demand into a reserve tank that holds three times as much as the container. A pump at the outlet of the reserve tank pumps the fuel to the carburetor. The number of times the container is filled is counted.

The next flowmeter (\$280) uses a tiny turbine meter with a bypass line around it and a diaphragm blocking the bypass line. The bypass line is intended to smooth out the flow through the turbine meter. A light beam is interrupted by the blades of the turbine rotor every time one goes by. The resulting signals are counted.

The last flowmeter in this price range uses a positive displacement flow transducer.

More sophisticated flowmeters are available at higher costs. There is a \$2370 positive displacement flowmeter which is a calibrated piston pump run by a variable speed motor. The volume displaced per piston stroke times the number of strokes gives the flow measurement. The speed of this calibrated pump is automatically varied to maintain constant output pressure. Input pressure is boosted and held constant by another pump. A vapor diverter purges bubbles from the fuel before metering.

A mass flowmeter is available (\$3465) which uses four matched orifices in a Wheatstone bridge arrangement. This flowmeter is the only one which reads mass flow directly. All others respond to volume flow. However, it uses an internal pump whose rate must be held constant. This requires a synchronous motor running on 115 volts, 60 Hz AC which is easily supplied if the meter is used for dynamometer testing. For mobile testing, a converter must be used, and this weighs 60 lbs and draws about 50 amps at 12 volts.

Still another flowmeter (\$3975) uses four pistons in a radial arrangement connected to the same crank shaft. The fuel flow causes the crank to turn continuously. A vapor eliminator is incorporated in the inlet. The crank shaft is magnetically coupled to a device which senses both the magnitude and direction of the rotation. An up-down counter is used so that back flow is subtracted automatically. The readout also displays fuel temperature.

Finally, the \$8600 flowmeter is a positive displacement meter using pumps.

These ten flowmeters operate on a variety of principles and are to be placed in a variety of locations on a car. The range of environmental conditions under which they maintain their optimum accuracy no doubt varies from meter to meter. Our laboratory test set-up should be designed to determine this range and reveal the weaknesses of each meter.

### 3. FLOWMETER ENVIRONMENT

The environment of the flowmeters in an automobile is complex and rather hostile. It is complex because there are several possible locations in which to place the flowmeters, physical variables to be considered, different makes and models of cars, and a broad range of conditions under which the cars will be operated. In principle, the environment could be expressed more simply in terms of the flowmeter locations, the physical variables, and the range of values that these variables take for these locations. The problem is in getting the data for the normal operating conditions that will occur in the tests by TSC.

Unfortunately we cannot solve the problem by simply measuring the variables. First, many of the measurements would have to be made on 1975 cars since they differ in several important ways from earlier ones. Second, the tests would have to be performed on a representative sample of makes and models of cars. Third, they would have to be performed under a complete range of weather conditions. Fourth, we do not have the time nor all of the instruments. The time and expense involved is obviously enormous. We must rely on measurements taken by others and these appear to be somewhat limited.

We do have the recommended standards and test methods published by the Society of Automotive Engineers<sup>1</sup> and other sources.<sup>2</sup> Unfortunately, much of the data either applies to 1972 or earlier cars or applies to test conditions that are much more extreme than will occur in the tests by TSC. Conversations with several knowledgeable people<sup>3</sup> in the research laboratories of automobile manufacturers as well as others provided data which applies to the conditions of the planned TSC tests.

The temperature of the fuel in the fuel lines can range at least between 15°F (-10°C) and 150 to 170°F (65 to 77°C). This results in a 10 percent change of density and a change by a factor of 2 in the kinematic viscosity. This will certainly affect the performance of some of the flowmeters. However, there are potentially much larger effects at the higher temperatures. Depending

on what week of the year and in what part of the country the gasoline is purchased, vapor bubbles can form in the fuel line at temperatures above 120°F (50°C) to 160°F (70°C). These bubbles or even ordinary air bubbles in the fuel reduce the average density of the fuel much more than ordinary thermal expansion of the liquid. If bubbles are in the fuel measured, they can cause errors of 5 to 20 percent in the reading of most flowmeters, even apart from the backflow effect to be described later. Some flowmeters have vapor diverters, which are intended to eliminate the bubbles just before the fuel is metered. Even so, bubbles can form again inside the meter. If they do, the measured flowrate can be inaccurate.

If there are no bubbles in the fuel which is measured, there can be an even larger effect due to bubbles formed in the fuel line between the meter and the carburetor, i.e., downstream of the meter. On hot days it is not unusual to find 50 to 80 percent of the volume inside the fuel line occupied by the bubbles. The effect of this on the flowmeter is due to the pulsating fuel pump pressure, which can vary in the range from 3 to 7 psi (.2 to .5 std. atm.) on cars with a vapor diverter. When the pressure drops, due to flow back through the vapor diverter, the gas bubbles get larger according to the perfect gas law. New bubbles may even form since the solubility of the more volatile components in the gasoline has been lowered by the decrease in pressure. The increase in volume of the fuel, because of the bubbles, causes fuel to flow backwards through the meter. Some flowmeters will not count this backflow, others will count it as if it were ordinary forward flow. Then on the next fuel pump stroke, the pressure increases, the bubbles collapse and may even disappear, and the fuel that once flowed backward now flows forward through the flowmeter, getting counted once again. This can cause a 20 to 30 percent error in flowmeter reading.

The effect is particularly large when the engine is turned off which causes the fuel line pressure to drop to zero. The bubbles and gravity can then cause the entire contents of the fuel line (more than 10 cm<sup>3</sup>) to flow backwards through the flowmeter.

There is another possible cause of pulsations in fuel flow which can occur even when bubbles are not present. The needle valve in the float bowl of the carburetor may tend to be either appreciably open or closed entirely, rather than somewhere in between. Thus the flow may tend to stop and start and this may affect the accuracy of some meters.

Besides the change in fuel density and viscosity due to temperature, there can be a change of roughly 3 percent in density and 25 percent in kinematic viscosity depending on the week and place of purchase.

Another property of the gasoline may also affect flowmeter performance - its opacity due to its color: red for premium, orange for regular clear for unleaded, and brown for tax-free off-road use. If the gasoline is unusually strongly colored, the light beam going through it in some flowmeters may not be intense enough to be detected. These flowmeters will then give erratic readings or record no flow at all.

Turbine meters may be affected by swirl in the fuel flow. The swirl can be generated by centrifugal force if the fuel flows through elbows. This swirl may add to the rotating motion of a turbine rotor.

All of the meters described use electrical power from a 12-volt battery. If the car battery is used there may be undesirable effects due to fluctuation in the voltage supplied to the meter. These voltage fluctuations may affect flowmeter accuracy. However, the effect of the noise and transient voltages can be reduced if the flowmeter is connected directly to the battery.

Another possible source of flowmeter inaccuracy is the electromagnetic radiation from electronic ignition systems in normal operation. This may disturb the electronic circuitry in some flowmeters which are not properly shielded.



Some meters may have their accuracy affected by a change in attitude of the meter with respect to the vertical as the car goes up or down hill or around a banked turn. The maximum grade on a hill is usually 9 percent, and the maximum banking on a curve is usually 6 percent (10 percent if in a location where ice and snow is unlikely)<sup>4</sup>.

Assuming that it is a rigid body, the flowmeter as a whole has six vibrational degrees of freedom: three translational and three rotational; one about each of the three axes. Each of these modes of vibration can have many frequencies and intensities. The details depend strongly on the exact location of the flowmeter in the car, the make and model of the car, wheel balancing, the smoothness of the road, engine, and the speed of the car.

A vibration level has been proposed by the Packaging Committee of ASTM in a test procedure for packages shipped on a truck. This test procedure specifies vibrating at .5 g acceleration. However, the suspension of an unloaded truck is much stiffer than that of an automobile. So the amplitude of the vibration is probably larger than expected for a flowmeter inside the car during the TSC tests.

A much lower vibration level has been measured by the Noise, Vibration and Harshness Division of an automobile manufacturer. They<sup>5</sup> report a peak acceleration of .05 g on the dash of a car on a nearly perfectly smooth road with wheels balanced dynamically. A reasonable test procedure for our purposes would be to vibrate at a level somewhere between the two.

In the tests planned by TSC, it is desirable that the flowmeter not affect the performance of the car. There are three ways in which the flowmeter could affect the performance: (1) the pressure drop across the meter might be an appreciable fraction of the fuel pump pressure. The engine could be deprived of fuel, and its performance affected, 2) some flowmeters smooth out the pressure pulses from the fuel pump. The effect of this might be to lower the fuel level in the carburetor float bowl, and that could affect engine performance or fuel economy, 3) the extra load on the engine due to the electric power drawn from the car's electric

system by one of the flowmeters is about one horsepower. This will affect fuel economy measurements. This can be avoided by powering the flowmeter by separate batteries, but the battery mass plus the flowmeter and its converter might affect the performance of the car, especially if it is a small car.

#### 4. TEST PROCEDURE

It is essential to use gasoline for our tests. This requires a specially vented laboratory with special electrical fittings throughout in order to meet the electric code. Every electrical part used must be either in an explosion proof box, in an ordinary box that is purged with fresh air, or in a nearby room in which there is no gasoline. This adds considerably to the expense and difficulty of purchasing equipment for our test set-up.

A schematic of our planned test set-up is shown in figure 1. The flowmeter is connected between an automobile fuel pump and the float bowl of a carburetor. Gasoline is pumped from the storage tank through the meter, through the needle valve and float bowl and through the flow adjusting valve to the weigh tank.

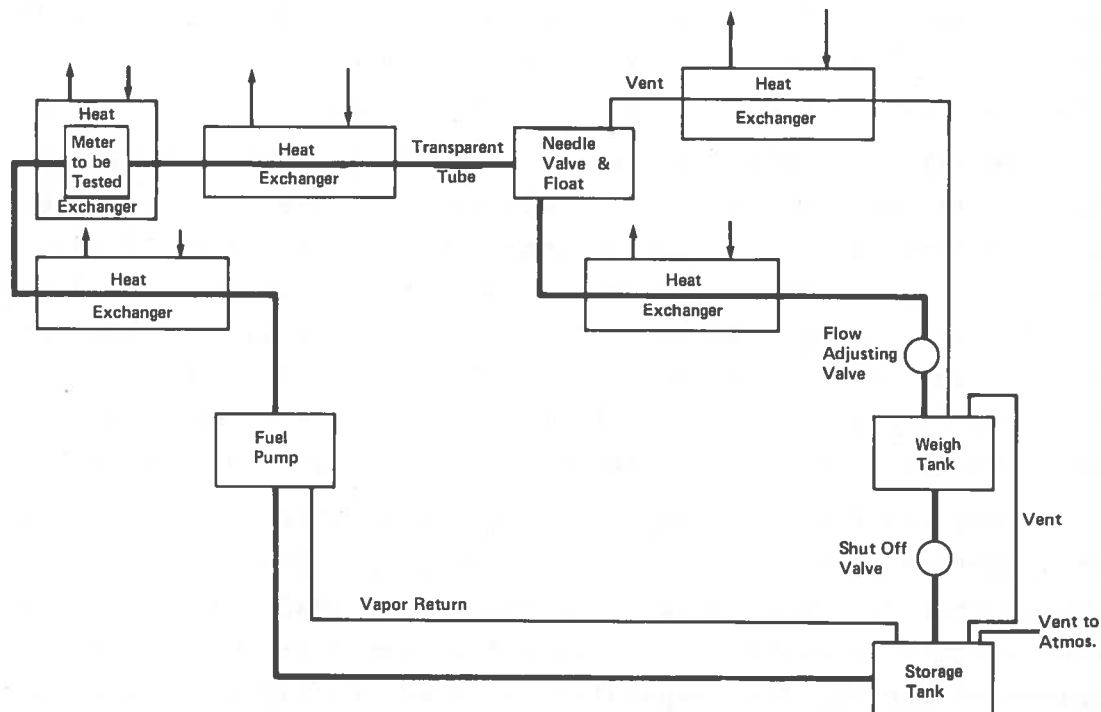


Figure 1. Flowmeter Test Setup

The fuel pump is a mechanical one that is normally driven by a cam on the cam shaft. This rotates at half engine speed, and so the pump should be driven in the range 225 ppm (pulses per minute) to 1800 ppm. We will use an explosion-proof motor connected to a variable speed drive with an automobile cam on it. The fuel pump has a diverter line leading back to the storage tank. This line can be closed off in order to simulate automobiles without a diverter.

The needle valve, float, and bowl assembly is one that can be purchased separately as a replacement part for an automobile carburetor. The open side where the bowl attaches to the carburetor will be covered with a transparent plastic plate so that we can observe the liquid level during nonsteady flow experiments. For steady flow, at least, the fuel pump will supply enough fuel so that the liquid level in the float bowl will be very nearly constant, regardless of the flowrate.

The flowrate for the entire flow around the system is set by the flow adjusting valve. Since the liquid level in the float bowl is constant, the pressure drop across the valve is constant, and the flowrate depends only on the setting of the valve. The resulting flow is spilled into the weigh tank.

We will use substitution weighing of the fuel collected. The tank is suspended on a load cell which is used only to detect when the tank is full. This is done with a comparator. First, the flow is permitted to reach a steady state with the fuel draining out the tank through the shut off valve and fuel line at the bottom and spilling into the storage tank. The pipes are arranged so that they do not interfere with the weighing. A weight whose mass equals the mass of gasoline to be measured hangs from the tank.

Once the flow is steady, the shut off valve is closed. Gasoline starts to fill the tank. When enough gasoline is in the tank so that the comparator connected to the load cell passes its mark, a timer is started. The weight is immediately removed. Because of the way the comparator is wired, no signal is given to the timer when the comparator passes its mark on the way down.

Meanwhile gasoline continues to fill the tank. When the tank is full, the comparator passes its mark again, and the timer is stopped. The shut off valve is immediately opened draining the tank. When the tank is empty the weight is hung back on the tank. This completes the weighing. The flowrate is the mass of the weight divided by the time difference.

This technique eliminates errors due to inertia and due to the hysteresis and nonlinearity of the load cell. The major source of error in our measurement will come from not having a perfectly steady flow condition. Experience in our laboratory at similar flow rates suggests that we would be lucky if our system uncertainty due to this were smaller than 1/4 percent at .4 gal/hr (.4 cm<sup>3</sup>/s). At higher flowrates, the uncertainty should decrease. One of the most important parts of our evaluation will be to see how accurate the flowmeters are when there are bubbles in the fuel. Nitrogen can be bubbled into the storage tank, and the vapor diverter on the fuel pump blocked.

Alternatively, with the vapor diverter in use, the gasoline can be heated by hot water in the heat exchangers on the left. The temperature will be increased until 50 percent of the volume in the fuel line is occupied by bubbles. This will be determined approximately by visual inspection through the transparent solid plastic tube. The gasoline will be cooled by the heat exchangers so that it is at room temperature when it is weighed. Alternatively, the gasoline and the meter will be cooled on the left and warmed on the right. Temperatures will be measured throughout. We expect to work in the range between approximately 15°F (-10°C) and approximately 140°F (60°C) to 160°F (70°C).

Gasoline is a mixture of a number of components with different boiling points, densities, and viscosities. The components with the lowest boiling points are dissolved in the mixture. As the temperature is raised these most volatile components are driven off. As a result the properties of the gasoline will change with time.

We will control this by cooling the hot vapor from the float bowl to  $-22^{\circ}\text{F}$  ( $-30^{\circ}\text{C}$ ). In addition the entire system will be vapor tight with the only vent to the atmosphere coming from the storage tank. This vent is necessary in order to keep the pressure in the vent lines equal to atmospheric pressure. An oil filled circular moat with a concentric inverted cup in it will be used at the top and bottom of the weigh tank in order to have it both vapor tight and unhindered for weighing.

At the top of the tank, the inverted cup will have the rigid tubing going through it, and so it will be fixed. The lips of the cup will dip into the oil in the circular moat, which will be attached to the weigh tank. Since there will be no pressure difference between inside and out of the tank there will be no gurgling of vapor through the oil.

At the bottom of the tank, the inverted cup will have the rigid tube from the shut-off valve going through it. It will swing free with the weigh tank and shut-off valve. This time the oil-filled circular moat will be fixed.

In spite of our efforts the gasoline will probably change its properties. We will measure its Reid vapor pressure, and its density and viscosity at room temperature frequently. For some tests we may use heptane with butane dissolved in it by bubbling it through.

For some flowmeters we will use gasoline of a deep color. For others we will put two elbows just upstream of the flowmeter. For all the flowmeters we will measure pressure upstream and downstream of the flowmeter. We will tilt the flowmeter 10 percent, vary the supply voltage, add electrical noise to the line voltage, and bring an electronic ignition system near the meter and its readout module. All of this will be done while the flowmeter is operating to determine the effect on its accuracy.

With steady flow the meter reading is proportional to the flowrate. For unsteady flow the totalized reading of the flowmeter would be expected to equal the total quantity of fluid that was

metered during the time of measurement. This will be checked directly by starting with a steady low flowrate, then quickly increasing the flowrate, and finally letting the system settle down to a steady high flowrate. The totalized flowmeter reading (corrected) should equal the mass weighted. Alternatively, we will similarly decrease the flow. During these tests we will inspect the float level to make sure the flowmeter would not deprive an engine of fuel.

We propose also to do vibration testing while the flowmeter is in operation to determine if its accuracy is affected. The flowmeter and/or the float bowl should be vibrated vertically and in both horizontal directions. Consideration of vibration is important for TSC since even a low level of vibration may affect flowmeter accuracy more than the accuracy limits determined in other tests. More importantly a flowmeter might be unaffected by the vibration on most cars, but significantly affected by the vibration on a particular car. This seems entirely possible since vibration frequencies and intensities can vary so much from car to car. Since each car is unpredictably different, this failure in flowmeter accuracy might not be detected in on-the-road testing with one or two cars. Thus the vibration testing should be done in the laboratory where the conditions can easily be varied over the range possible in any car.

#### REFERENCES

1. "Preliminary Recommended Environmental Practices for Electronic Equipment Design" proposed by the Environmental Standards & Test Methods Subcommittee of the Electronic Systems Committee, Society of Automotive Engineers and presented at the International Colloquium on Automotive Electronic Technology, October, 1974, (SAE, 1974).
2. H.I. Wilson, "Fuel System Time-Temperature Histories During Specified Car Use Patterns." Paper No. 720080, Trans. SAE (1974).
3. Milton Baker, James Callison, (private communication).
4. American Association of State Highway and Transportation Officials.
5. Ernest Johnson (private communication).

## AUTOMOTIVE DATA BASE AND IMPACT ASSESSMENT

L.H. Lindgren  
Rath & Strong, Inc.  
Lexington, Massachusetts  
and  
Merrill L. Ebner  
Boston University  
Boston, Massachusetts  
ABSTRACT

The Automotive Data Base is the basic computer system used for simulations and analyses of investments, vehicle costs, and total costs to the customer for the implementation of various vehicles and engines.

Included in the Automotive Data Base are:

- Vehicles and Components
- Facilities and Machinery
- Vendors
- Maintenance
- Fuel Economy

The Automotive Data Base is a computer based development resulting from studies performed for the National Academy of Sciences Committee on Motor Vehicle Emissions and the Department of Transportation Systems Center in Cambridge, Massachusetts.

This contract includes the transfer of the data and the methodology used in the development of the data base. It also includes supplementary data of actual production facilities, tooling and equipment manufacturers, and the resource data base used in the studies. An analysis of the conversion costs and the lead times required to make changes in the industry of engines and vehicles is developed for a group of alternate piston engines.

The discrete data developed is used to evaluate the aggregate impacts of alternative governmental automotive policy decisions. Two impacts are assessed: that on the automotive manufacturers and that on the driving public. Impact on the industry is expressed as total yearly investment to implement a policy and as the investment per car for the various types of cars likely to be produced under the policy. Impacts on the public are expressed as aggregate yearly costs for fuel, maintenance and sticker price.



Under the current contract, the technique is being refined, documented and used on selected studies.

## 1. INTRODUCTION

The Automotive Data Base is a development resulting from studies performed for the National Academy of Sciences Committee on Motor Vehicle Emissions (NAS/CMVE) and the Department of Transportation/Transportation Systems Center (DOT/TSC) in Cambridge, Massachusetts.

The original concept of the automotive data base and the Manufacturing Impact Model was presented in a DOT/TSC document "Planning Document for the Evaluation and Impact of Various Mass Produced Automotive Implementation Plans" (February 1972). The purpose of the project was to define the basic concepts, the data base, and the methodology for impact studies in automotive manufacturing. This methodology became the basis for the data gathering and reporting used by the NAS/CMVE I panel No. 5 consultants for Manufacturability and Costs. The long-term goal for the DOT/TSC was to inherit the NAS data base, to enhance the data base, to provide the capability for future studies, and to provide a continuing monitoring system for transportation studies. As the project progressed from the concept stage to the application stage, a more definitive manual was provided for DOT/TSC. This manual, known as the "Application Manual for the Use of a Computer Data Base to Aid in the Evaluation of the Impacts of Various Automotive Implementation Plans" (June 1972), defined the computer retrieval numbering system for products and resources and it depicted the specific output documents needed for investment analysis.

As the data gathering of NAS/CMVE I, which extended from August, 1971 to December, 1972 was completed, the data base became available for use by DOT/TSC. The first study using the NAS data base was contracted by DOT/TSC to simulate the impact on manufacturing of the various fuel economy model mix production plans. The objective of the study was to evaluate the manufacturing investment costs of the conversion to small vehicles, and the subsequent fuel economy benefits.

The CMVE II study by NAS which included an update of automotive technology to achieve both emissions controls and fuel economy, began in 1973. The manufacturability and costs (M/C) panel enhanced the CMVE I model with an expanded vehicle and engine configuration data file. The M/C panel also developed detailed resource data to support the configurations and included the capacities of the manufacturers of tooling and equipment. The investment programs were designed to allocate the time phased investments over each configuration in the scenario.

The NAS/CMVE II data base completed in October 1974 is the data base that is being expanded in this contract (DOT/TSC 803) to include more significant data and a more definitive structure capability to allow DOT/TSC to have a data source for future costs analysis and impact studies.

This manual of the "Manufacturing Assessment Model" contains the following:

- A. Model description and the concepts which comprise the design;
- B. A description of the model data bases-
  - 1) Product/Resource master data base
  - 2) Configuration data base
  - 3) Product/Cost data base
  - 4) Resource/Investment data base;
- C. A set of instructions for use of the files with an identification of the input-output documents.

The purpose of this manual is to provide DOT/TSC with an automotive data base as developed for NAS/CMVE II and to have the capability to expand the data to include other segments of the transportation sector.

The manual provides the descriptive material of the model data base at this stage of development and the operating instructions for its use as a data source and the maintenance of the data base.

## 2. HISTORY AND OVERVIEW

The Manufacturing Assessment Model (MAM) is a development over a three-year period that is based on the concept that the automotive industry could be analyzed by identifying the significant products, components, and the supporting resources used in the manufacturing and assembly of vehicles.

The purpose of the development of MAM was to provide a computer based methodology to evaluate the impact on manufacturing resources in the automotive and truck industry of various alternative vehicles and implementation plans. Because of the complexity of the industry and the permutations of products it was necessary to provide a significant reduction of the complexities and still retain a representative image of the real world. The basic concept used in this data reduction process was to group the products and resources according to how the product was made rather than how it is described, sold, or used. This concept allows for the grouping of similar company products such as Pintos and Vegas into a single category called subcompact.

Once this concept was defined it was possible to identify the basic data requirements of the model. These basic data requirements are:

Product Data Base - The identification of the vehicles and the components that make up each vehicle. The supporting information for each component includes descriptive data, production data and cost data.

Resource Data Base - The identification of the manufacturing facilities and resources required to produce each component identified in the product data base.

Product-Resource Structure - The cross reference or chaining of the product to the resources which would establish the proper relationship of product requirements to the demand on the resources. This file is the source file used in the generation of the time-phased requirements resulting from a simulated implementation or production plan.

In the initial stages of development these data files or data bases were used for the NAS/CMVE I study in which the technological feasibility of meeting the requirements of the Clean Air Act 1970 in the automotive manufacturing sector was evaluated.

During this phase of development the computer vased system was designed to utilize a software development called Time Phase Requirements Inventing Management (TRIM). This system was designed to provide complex manufacturing operations a means to maintain precise control of configurations, inventory, and costs in a discrete time phased production environment. The TRIM system used three basic files: 1) item master which contained the product and resource data base; 2) the product structure which contained both the product and resource structures; and 3) the requirements file which contained the detailed time phased production requirements generated from the end item or vehicle production plan.

The model entered a 2nd generation of development during NAS/CMVE II. The IBM 360-20 TRIM version was redesigned to run on the IBM 360-50 at BU. It was at this time that Mr. L.Lindgren and Dr. M. Ebner of Boston University combined their resources to enhance the original design to provide improved investment computation and a vehicle in use total costs capability. In order to use the IBM 360-50, which did not have the bill-of-material processor capability, we reprogrammed the model to submodels which had some of the capabilities of the original TRIM that were necessary to give the desired outputs needed for the NAS/CMVE II study. Mr. Lindgren and Dr. Ebner were consultants on the Manufacturability and Costs subpanel of the NAS/CMVE II committee.

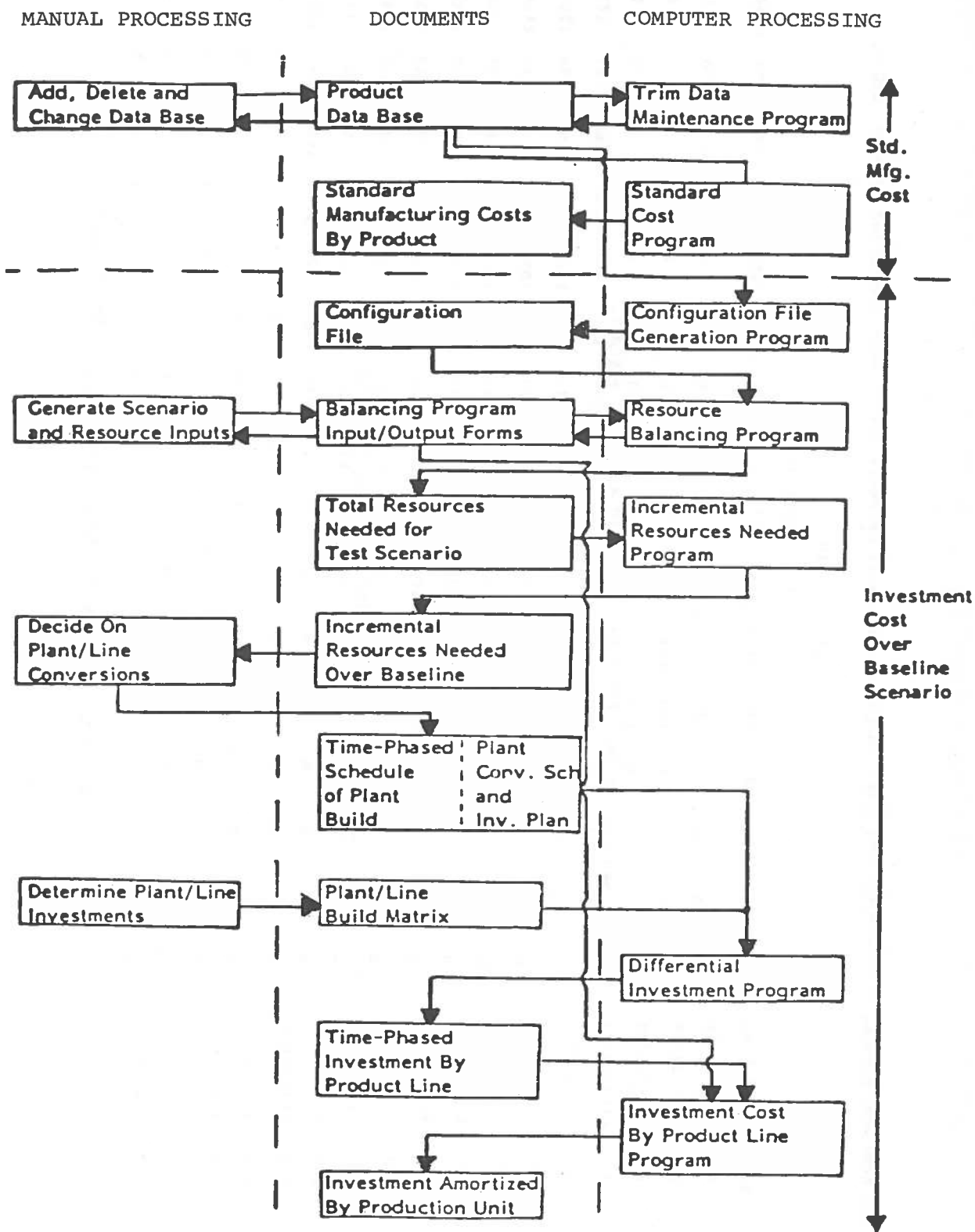
During the NAS/CMVE II phase of development, the DOT/TSC specified a third generation of the model. Since the NAS/CMVE II was limited to emissions technology, the DOT/TSC requirements were to expand the model capability to include fuel economy and safety capabilities, as well as reliability, maintenance and aftermarket capabilities.

The NAS/CMVE II data base includes about 276 vehicle configurations and about 285 resources. The product data includes about

2,000 components with detailed costs and lead times. The requirements of this contract is to convert the NAS/CMVE II data base to include the following:

1. Costs - manufacturing labor and material
2. Lead times
3. Reliability data
4. Maintenance data
5. Aftermarket data

In addition to the general purpose for the model development, this contract provides the specific data base interface for the Boston University contract DOT/TSC 805 "Assessment of Impacts on Automotive Manufacturing Due to Changes in Vehicle and Engine Designs."



DOT CONFIG-DOT820-062 RSIMR-LHL820-063 SCNR-ESD/EDT-164 DALPM-47 NETPM-38 INVPM1 -045 INVPM2-162 8/24/74 SEC A.

S.NO.	VEHICLE NO.	TEST SCENARIO																
		TIME PHASED REQUIREMENT																
		1970	1971	1972	1973	1974	1975	1976	1977	1978	1979	1980	1981	1982	1983	1984	1985	
61	1144126234	0	0	0	0	575	2499	1783	0	0	0	0	0	0	0	0	0	
62	1154127234	0	0	0	0	388	1658	1203	0	0	0	0	0	0	0	0	0	
63	1164128234	0	0	0	0	279	1172	762	0	0	0	0	0	0	0	0	0	
64	1111121124	OC	VEN/CARB	AI/PEGR/HCAT/EFE	MINI 14	90-CID	M/TR .4HC	3.4CO 2.	14	39	152	154	159	160	164	166	169	172
65	1121122124	0	0	0	0	9	40	193	710	815	925	1062	1124	1150	1168	1186	1204	
66	1134123124	0	0	0	0	7	34	379	1622	1834	1953	2124	2034	2082	2114	2146	2180	
67	1144125124	0	0	0	0	15	69	500	1825	1834	1740	1593	1605	1644	1669	1694	1720	
68	1144126124	0	0	0	0	50	217	801	2738	2650	2570	2549	2569	2630	2672	2712	2753	
69	1154127124	0	0	0	0	20	87	405	1318	1018	925	956	962	986	1001	1017	1032	
70	1164128124	0	0	0	0	21	80	330	912	917	925	956	962	986	1001	1017	1032	
106	1111221121	OC	AV/CARB	ECU/OZ/AI/PEGR/HNCCAT	MINI 14	90 CID	M/TR .4HC	3.4CO	24	152	152	154	159	160	164	166	169	172
107	1121222121	0	0	0	0	0	0	149	710	815	925	1062	1124	1150	1168	1186	1204	
108	1134223121	0	0	0	0	0	0	0	0	0	0	0	0	0	0	0	0	
109	1144225121	0	0	0	0	0	0	0	0	0	0	0	0	0	0	0	0	
110	1144226121	0	0	0	0	0	0	0	0	0	0	0	0	0	0	0	0	
111	1154227121	0	0	0	0	0	0	0	0	0	0	0	0	0	0	0	0	
112	1164228121	0	0	0	0	0	0	0	0	0	0	0	0	0	0	0	0	

A Section of a Typical Scenario (ESTD/EDOT)

AUTOMOTIVE INDUSTRY LOAD DISTRIBUTION STATISTICS

181. RESOURCE NO: 6300110141  
OH 1970 1971 1972 1973 1974 1975 1976 1977 1978 1979 1980 1981 1982 1983 1984 1985 TREND

TEST SCENARIO  
PLANT  
UTILIZATION  
PLANTS OR  
LINES  
RESOURCES  
NEEDED

0.0	0.0	0.0	0.0	32.64	1.59	1.76	0.86	0.93	0.96	0.99	0.98	1.01	1.02	1.04	1.06
0	0	0	0	0	1	1	2	2	2	2	2	2	2	2	2
0.0	0.0	0.0	0.0	0.33	1.59	1.76	1.72	1.85	1.91	1.98	1.97	2.02	2.05	2.08	2.11
															2.14

182. RESOURCE NO: 6300110150  
OH 1970 1971 1972 1973 1974 1975 1976 1977 1978 1979 1980 1981 1982 1983 1984 1985 TREND

TEST SCENARIO  
PLANT  
UTILIZATION  
PLANTS OR  
LINES  
RESOURCES  
NEEDED

0.0	0.0	0.0	0.0	32.64	1.59	1.76	0.86	0.93	0.96	0.99	0.98	1.01	1.02	1.04	1.06
0	0	0	0	0	1	1	2	2	2	2	2	2	2	2	2
0.0	0.0	0.0	0.0	0.33	1.59	1.76	1.72	1.85	1.91	1.98	1.97	2.02	2.05	2.08	2.11
															2.14

183. RESOURCE NO: 6300107044  
OH 1970 1971 1972 1973 1974 1975 1976 1977 1978 1979 1980 1981 1982 1983 1984 1985 TREND

TEST SCENARIO  
PLANT  
UTILIZATION  
PLANTS OR  
LINES  
RESOURCES  
NEEDED

0.0	0.0	0.0	0.0	0.0	0.0	0.0	0.0	0.0	0.0	0.0	0.0	0.0	0.0	0.0	0.0
0	0	0	0	0	0	0	0	0	0	0	0	0	0	0	0
0.0	0.0	0.0	0.0	0.0	0.0	0.0	0.0	0.0	0.0	0.0	0.0	0.0	0.0	0.0	0.0
															1.00

184. RESOURCE NO: 6300020036  
OH 1970 1971 1972 1973 1974 1975 1976 1977 1978 1979 1980 1981 1982 1983 1984 1985 TREND

TEST SCENARIO  
PLANT  
UTILIZATION  
PLANTS OR  
LINES  
RESOURCES  
NEEDED

0.0	0.0	0.0	0.0	53.32	2.29	2.15	0.99	0.92	0.88	0.89	0.90	0.92	0.93	0.95	0.96
0	0	0	0	0	1	1	2	2	2	2	2	2	2	2	2
0.0	0.0	0.0	0.0	0.53	2.29	2.15	1.99	1.83	1.77	1.78	1.80	1.84	1.87	1.90	1.93
															1.70

185. RESOURCE NO: 7300070139  
OH 1970 1971 1972 1973 1974 1975 1976 1977 1978 1979 1980 1981 1982 1983 1984 1985 TREND

TEST SCENARIO  
PLANT  
UTILIZATION  
PLANTS OR  
LINES  
RESOURCES  
NEEDED

0.0	0.0	0.0	0.0	53.32	2.29	2.15	0.99	0.92	0.88	0.89	0.90	0.92	0.93	0.95	0.96
0	0	0	0	0	1	1	2	2	2	2	2	2	2	2	2
0.0	0.0	0.0	0.0	0.53	2.29	2.15	1.99	1.83	1.77	1.78	1.80	1.84	1.87	1.90	1.93
															1.70

A Section of the Resource Loading Output (ESTD/EDOT)



VEHICLE DESCRIPTION: OC STD/CAR: AI/EGR INTA V8 290-CID A/TR 3-4HC 39CO 3.0NOX

SER. RESOURCE NO.	VEHICLE NUMBER	DESCRIPTION	INVESTMENT/VEHICLE		TOTAL INTEREST	TOTAL	76-79 MAX
			PRINCIPAL	INTEREST			
	44115655		2.7821	0.2156	2.9977	4.3252	
			PRINCIPAL	INTEREST	TOTAL	TOTAL	76-79 MAX
274.	52000 710	PLANT ALUMINUM BODY COMPONENTS	0.7560	0.0709	0.8269	1.1635	
275.	58030 706	PLANT RADIAL TIRES	1.1927	0.0820	1.2748	1.9227	
277.	54000 701	PLANT 4 SPEED LOCK UP AUTO TRANS	0.8333	0.0626	0.8960	1.2390	

An Illustrative Investment by Car Output (ESTD/EDOT)

INCREMENTAL COST SUMMARY REPORT

SCALE FACTOR= 1.000 08

	1970	1971	1972	1973	1974	1975	1976	1977	1978	1979	1980	1981	1982	1983	1984	1985
INC FUEL COST	0.00	-0.68	-4.47	-10.93	-15.95	-21.21	-26.09	-31.53	-36.39	-40.58	-44.33	-47.30	-49.85	-51.93	-53.71	-55.23
PV. FUEL COST	0.00	-0.65	-4.13	-9.73	-13.63	-17.44	-20.62	-23.97	-26.59	-28.51	-29.95	-30.73	-31.13	-31.19	-31.01	-30.67
INC MAINT COST	0.00	-0.00	0.00	0.00	-0.00	-0.00	-0.00	0.00	0.00	-0.00	-0.00	0.00	-0.00	-0.00	0.00	0.00
PV. MAINT COST	0.00	-0.00	0.00	0.00	-0.00	0.00	0.00	-0.00	0.00	0.00	-0.00	-0.00	0.00	0.00	0.00	-0.00
INC STKR PRICE	-0.00	-0.24	-1.36	-2.43	-2.21	-2.71	-2.81	-2.99	-2.98	-2.94	-2.94	-2.96	-3.03	-3.07	-3.12	-3.17
PV. STKR PRICE	-0.00	-0.24	-1.26	-2.16	-1.89	-2.23	-2.22	-2.27	-2.17	-2.06	-1.98	-1.92	-1.89	-1.84	-1.81	-1.76
INC INVESTMENT	-0.0	-0.0	-0.0	-0.0	-0.0	-0.0	-0.0	-0.0	-0.0	-0.0	-0.0	-0.0	-0.0	-0.0	-0.0	-0.0
PV. INVESTMENT	-0.0	-0.0	-0.0	-0.0	-0.0	-0.0	-0.0	-0.0	-0.0	-0.0	-0.0	-0.0	-0.0	-0.0	-0.0	-0.0
INC U.S. COST	-0.00	-0.93	-5.82	-13.37	-18.16	-23.93	-28.90	-34.53	-39.37	-43.53	-47.27	-50.26	-52.87	-55.00	-56.83	-58.40
PV. U.S. COST	-0.00	-0.89	-5.38	-11.88	-15.52	-19.67	-22.84	-26.24	-28.77	-30.58	-31.94	-32.65	-33.02	-33.03	-32.81	-32.42

TOTAL COST OF SCENARIO		INCREMENTAL COST OF SCENARIO	
TOT FUEL COST	6524.91	INC FUEL COST	-490.18
PV. FUEL COST	4077.58	PV. FUEL COST	-329.95
TOT MAINT COST	585.29	INC MAINT COST	0.00
PV. MAINT COST	425.54	PV. MAINT COST	0.01
TOT STKR PRICE	7679.16	INC STKR PRICE	-38.97
PV. STKR PRICE	5746.70	PV. STKR PRICE	-27.71
TOT INVESTMENT	0.0	INC INVESTMENT	0.0
PV. INVESTMENT	0.0	PV. INVESTMENT	0.0
TOT U.S. COST	14789.36	INC U.S. COST	-529.16
PV. U.S. COST	11049.80	PV. U.S. COST	-357.64

Incremental Cost Summary for Scenario ESTD/EDOT.

## BIBLIOGRAPHY

1. DOT 1 - Planning Document for the Mass-Produced Automotive Advanced Engine Implementation Study DOT/TSC-3784
2. DOT 2 - Application Manual for the Computer Based Model for Simulation of the Automotive Implementation Study DOT/TSC-4199
3. DOT 3 - Planning Document for a Preliminary Study of Automated Station Vehicle Diagnostic Centers DOT/TSC-4460
4. NAS/CMVE I Report, Dec. 1972
5. NAS/CMVE I Panel 5 Report, March, 1973
6. DOT 4 - Technical Planning Document for the Simulation of Impact on Resources of Automotive Mass-Produced Conversion to an Assumed Model Mix Manufacturing Plan DOT/TSC-6002
7. DOT 5 - Planning Document for the Petroleum Portion of the DOT Study of Energy for Transportation DOT/TSC-6439
8. DOT 6 - Planning Document for Cost Estimates for Bumper Study DOT/TSC 7609
9. NAS/CMVE II Report, December 1974
10. NAS/CMVE II Manufacturability and Cost Panel Report, Dec. 1974
11. DOT/TSC Boston University Contract DOT/TSC 803, "Assessment of Impacts on Automotive Manufacturing Due to Changes in Vehicle and Engine Designs."
12. EPA/CALSPAN-460/3-73-005 "Technical Evaluation of Emission Control Approaches and Economies of Emission Reduction Requirements for Vehicles Between 6000 and 14000 lbs. GVW."
13. SWRI/EPA "Technical Evaluation of Emission Controls of Heavy Duty Vehicles 14,000 lbs. to over 33,000 lbs."
14. NSF/RAND R1650NSF, Oct. 1974, "How to Save Gasoline--Public Policy Alternatives for the Automobile."
15. NAS - Committee on Cost Benefits, Chairman Dr. John Meyer, Vol. 4, Chapter 2, Dr. D. Duwees "Costs and Benefits of Automobile Emissions Control ".

## SAFETY IMPLICATIONS OF SMALL CAR USAGE

H. C. Joksch

The Center for the Environment and Man  
Hartford, Connecticut

### ABSTRACT

This paper summarizes the state-of-the-knowledge on the relation between automobile size and motor vehicle accidents. The results of the Center for the Environment and Man (CEM) study of the open questions are presented. They are:

1. The influence of car size in single car accidents;
2. The influence of car size in accidents involving more than two cars;
3. The influence of car size in car-truck accidents;
4. The influence of car size in pedestrian and bicycle accidents;
5. Interactions between car size and speed; and
6. The influence of car size upon fatalities (different from fatal and serious injuries).

The limitations of the data bases and the results are discussed. Changes in car occupant deaths resulting from a shift in the car-size mix over the next 10 years are projected. The effects of the speed limit and changing vehicle use are discussed.

### 1. OBJECTIVE

The ultimate objective of this study was to estimate how the number of motor vehicle accident deaths would change over the next ten years under various assumptions on the use of small cars, on travel speed reductions, and on changes in vehicle use, which might result from a limited availability of gasoline.

As a basis for such estimates:

- Relations between automobile weight and the frequency and severity of accidents had to be established.
- Potential automobile improvements which might affect this relation had to be identified;

- A model had to be developed to calculate deaths and injuries as functions of the automobile population characteristics;
- Relations between accidents (and their severity) and automobile use in quantitative (vehicle miles of travel) and qualitative (speed, time of day and week) terms had to be established; and
- An approach to estimate the impact of changing automobile use on accidents and their severity had to be found.

## 2. SCENARIOS

The Transportation Systems Center provided the following "scenarios" for which estimates and projections were to be made:

- Four alternative compositions (in terms of "subcompact," "compact," "intermediate," "standard," and "luxury" cars) of car sales from 1972 through 1985.
- Assuming optional and mandatory installation of air cushion restraint systems.
- Reduction of travel by
  - elimination of all Sunday travel;
  - a 10% reduction in commuter traffic;
  - a 20% reduction in commuter traffic;
  - a 30% reduction in commuter traffic.
- The 55 mph speed limit
  - enforced as currently done;
  - enforced;
  - rescinded and enforced at previous levels.

## 3. SCOPE

The scope of the study was limited to considering cars of essentially current design and construction, and improvements and minor modifications, but no basic changes or major modifications. Time and available funds limited the extent to which new data could be developed and the depth of the analyses. Most analyses had to be based on published or easily available information.

#### 4. FACTORS CONSIDERED

The purpose of this study was to estimate how the number of motor vehicle accident deaths would change over the ten years 1975-1985 with possible changes in four factors:

1. The composition of the passenger-car fleet. The study included four possibilities, ranging from a slightly increasing proportion of standard-size cars sold compared to the years 1972-1975 to a doubling of the proportion of subcompact cars sold by 1980.

2. Air-cushion restraint systems. Two alternatives were considered: no use and mandatory installation.

3. Reduction in travel. Four cases were studied: eliminating Sunday travel, and reducing commuter travel by 10, 20, and 30 percent.

4. The 55-mile-per-hour speed limit. Three possibilities were examined: enforcement as at present, strict enforcement, and the limit rescinded with enforcement returning to previous practices.

There are many difficulties and uncertainties associated with the relevant available data and the models that can be derived. However, for the purposes of this summary, it suffices to say that the best estimates obtainable by combining these data and models with CEM's best judgement yield these results (all figures quoted being ratios of the risks of a fatality for the whole population of car occupants related to 1972 experience):

##### A. Each of the four factors considered separately.

1. The composition of the passenger-car fleet. Of the four possibilities considered, all but the one with a doubling of the proportion of subcompact sales yielded comparable results; thus, the relative risks can be summarized this way:

- For single-car crashes (50% of all car occupant deaths), the relative risk by 1985 declines to 0.91 for the doubling-subcompact-sales case, but to an average of 0.85 for the other cases.

- For car-car and car-truck crashes (50% of all car occupant deaths), relative risk by 1985 declines to an average of 0.97 for the other cases; for the doubling-subcompact-sales case, the single-car risk declines to 0.91, but the car-car relative risk rises to 1.23 and the car-truck relative risk to 1.35.
- For all crash types combined, the relative risk by 1985 declines to between 0.88 and 0.91 for the other cases; for the doubling-subcompact-sales case, the relative risk rises to between 1.01 and 1.14. The ranges indicate the effects of uncertainty in basic data.

2. Air-cushion restraint. CEM's estimate is that cars equipped with air-cushion restraints reduce the risk of fatality in all crashes by 35%. For mandatory restraints for all new cars beginning in 1978, this estimate yields a relative risk estimate for the total passenger-car fleet by 1985 of 0.84 for the doubling-subcompact-sales case and 0.70 for the other cases.

3. Reduction in travel. Various factors (such as displacement of forbidden travel to nonforbidden times, the relative insensitivity of risk ratios to the marginal changes of the proposed cases, and the relatively low sensitivity of occupant deaths to volumes of commuter travel) make it impossible to estimate separate risk ratios for the marginal travel reductions proposed for consideration. Rather, the changes in risk that would ensue from the proposed travel reductions appear to be so small as to be buried in the variability of the phenomena under consideration. In effect, therefore, the relative risk ratios for the changes considered here are too close to unity to be differentiated from it, in view of the variability present in the rest of the problem.

4. The 55-mile-per-hour speed limit. Relative to the risk of fatality for an accident at 40 mph, the risk ratio for an accident at 60 mph is two, for one at 70 mph it is four and for one at 80 mph it is over 10. The year 1974 and its pattern of enforcement, which continues at present (January 1975), saw a significant downward shift in the distribution of travel speeds. To achieve a

strict-enforcement case, we assume for the speed distribution that there is no change for speeds below 40 mph, but that 85% of the speeds are 55 mph or less. Combining these speed distributions with the risk ratio as a function of speed, we get the following results (which can apply to any future year):

- For the actual 1974 speed reduction, the fatal risk ratio relative to the previous year may be as low as 0.88 to 0.93, but could be as high as 0.97.
- For strict enforcement of the 55 mph speed limit, the fatal risk ratio relative to 1973 to 0.83 to 0.88.

B. The factors considered together.

Considering all the factors together (which, practically, means uniting the results of paragraphs 2 and 4 above), we obtain these results (which assume mandatory air-cushion restraints and strict enforcement):

- For the doubling-subcompact-sales case, the relative risk ratio declines to between 0.68 and 0.85.
- For the other cases, the average risk ratio declines even further to between 0.59 and 0.68.

## 5. CONCLUSIONS

In sum, depending on the composition of the fleet in 1985, the relative risk ratio is reduced between 15 and 41%. The 1985 fleet in the doubling-subcompact-sales case contains about one-third subcompacts; for the other cases it averages one-fifth subcompacts.

In retrospect, the compositions of the fleet exhibit contrary influences, some reducing the risk ratio as much as 10%, others increasing it (the most notable of the latter being the subcompact in car-truck crashes, which can increase it by as much as 45%). Imposition of the 55 mph speed limit reduced risk to an unknown extent up to 12%; strict enforcement could reduce it by 15%, to possibly 10%. The dominant influence could be the mandatory installation of the air-cushion restraint system which would



reduce the risk ratio by 23% in 1985 (and by 35% once the entire automobile population is equipped with it). Thus, strict enforcement of the 55 mph speed limit and mandatory installation of the air-cushion restraint system would more than compensate for the effects of increasing sales of small cars.

Some other subsidiary conclusions are worth noting:

- The tendency of the subcompact car to raise the risk ratio arises largely from the presence of this car in a fleet dominated by heavier cars; if the fleet were entirely composed of subcompacts, this tendency would be much reduced.
- The relative insensitivity of the risk ratio to levels of commuter traffic is a surprising result that clearly calls for further inquiry.

The results of this study are based on data and models of varying reliability, and the structure of the analysis is forced into relative crudity by this fact. Thus, it is clear that all of the phenomena and questions studied here warrant much further study; initial steps to this end are detailed in the body of the main report not included here.

INCREASED FUEL ECONOMY IN TRANSPORTATION  
SYSTEMS BY USE OF ENERGY MANAGEMENT

N. H. Beachley & A. A. Frank

Co-Principal Investigators

University of Wisconsin

Madison, Wisconsin

ABSTRACT

The basic goal of the research is to investigate energy management techniques within the engine-transmission system of an automotive vehicle which have the potential of producing significantly better fuel mileage than is currently obtainable. In addition, techniques for accurately predicting the transient emissions of internal combustion engines under all types of operation are being studied. As part of the investigation, computer simulation models for standard type vehicles as well as advanced concepts have been and are being developed. One of the energy management techniques that is currently being pursued in detail, because of very favorable preliminary evaluation, is the use of a powerplant system combining a prime mover with a highspeed flywheel for energy storage. With this concept, it is possible to use the prime mover only under near-ideal conditions, and efficient regenerative braking is possible.

1. OBJECTIVES

A. Overall Program and Objectives

The basic objective of the program is to study and evaluate methods for improving fuel utilization efficiency in automobiles. The methods being emphasized are those based on Energy Management, a term applied to advanced powerplant concepts in which the generation, storage, and application of energy for the propulsion of the vehicle is done in a manner which will optimize the overall fuel efficiency for a given driving cycle. The ultimate Energy Management systems will include an energy storage device and control system which causes the prime mover to operate at maximum efficiency or not at all.

B. Past Program and Objectives

To study fuel efficiency, it is necessary to be able to describe in every detail all elements of an automobile with respect to the production or transmission of power. The main objective of the first year's effort was to develop computer simulation

techniques and programs which allow the study of vehicles with respect to both fuel consumption and emissions. This computer simulation system has been named the Automotive Propulsion Simulator (APS).

A study was also made of the fuel-saving potential of replacing the present-day automatic transmission with an optimized continuously-variable transmission (CVT).

#### C. Current Program and Objectives

The first objective of the current year's effort is to use the APS developed in the first year to study methods of improving fuel efficiency by relatively straightforward modifications of present-day hardware. Such variations as improved torque converters, different transmission and rear axle ratios, overdrives, improved tires, etc., are assessed. The effect of these changes on emissions has been included.

Another task of the current contract is to develop and define techniques and methods of computing the transient emissions produced by automobiles following a given driving cycle, such as the EPA-CVS cycle. The most promising of these techniques will be presented and discussed.

The third and final objective of the current effort is the simulation and evaluation of Energy Management powerplant systems consisting of a prime mover, a high-speed flywheel, and a continuously-variable transmission. The fuel economy and emissions characteristics of a number of variations of this concept in different-sized vehicles are being investigated. Included in this effort is the design of a realistic control system to allow such a system to operate with the convenience of the present-day automatic vehicle.

#### D. Future Program and Objectives

Based on the results of the current research and the experience of the research team in constructing vehicles and power transmission systems, a hardware design and development phase will be undertaken. A standard automobile chassis will be fitted with an engine-flywheel-CVT Energy Management system. Hardware

components will be ones already proven by previous development. Tentative design features and system potentials will be discussed.

## 2. FIRST YEAR PROGRAM (1973-74)

- A. Collection of data on vehicles, components, continuously-variable transmissions (CVT's), flywheels, etc.
- B. Development of Automotive Propulsion Simulator (APS), a true dynamic simulation (Figure 1)
  - a) All-digital version
  - b) Hybrid real-time version, with driver compartment simulator
  - c) Complete documentation, and aid to users
- C. Study of fuel-saving potential of CVT's (Table 1 and 2)

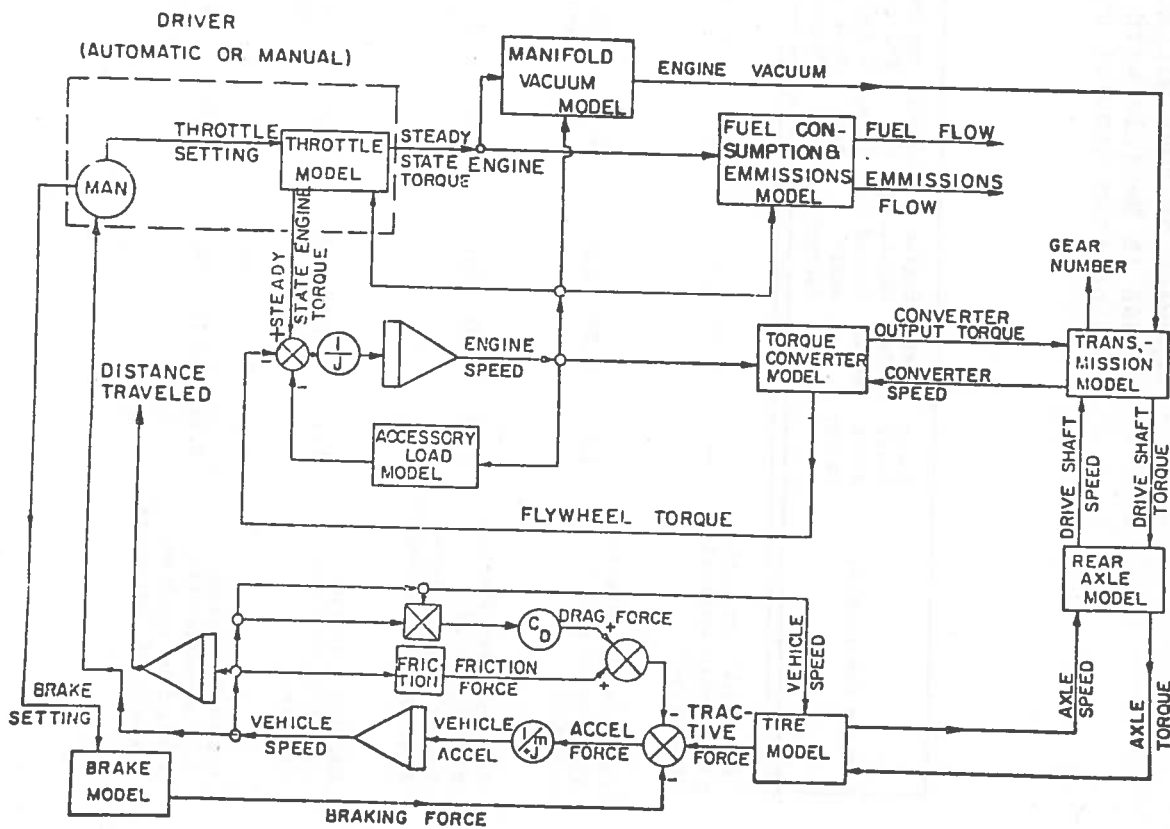


Figure 1. Automotive Propulsion Simulator

TABLE 1 SUMMARY OF FUEL MILEAGE SIMULATIONS  
 (4800 lb Vehicle with 430 cu. in.  
 engine from Simulations #1 and #2)

Vehicle Description	Power-Plant Scale Factor	Rear Axle Ratio	Engine Displ., in. <sup>3</sup> (based on scale factor)	50-70 mph time, sec.	mpg over EPA cycle; % improvement over "Benchmark"	mpg at steady speeds; % improvement over "Benchmark"					
						30mph	40mph	50mph	60mph	70mph	80mph
"Benchmark" car with present-day automatic transmission	--	2.75	430	5.1	12.5	20.4	20.6	19.4	17.3	13.4	12.9
Car with hydrostatic power-split CVT, unscaled	1.0	1.00	430	4.8	12.0 (-4%)	18.3 (-10%)	20.0 (-3%)	22.2 (14%)	19.8 (14%)	17.9 (34%)	15.2 (18%)
Car with hydrostatic power-split CVT, scaled to match performance of "Benchmark"	0.92	1.07	394	5.1	12.6 (1%)	18.4 (-10%)	20.8 (1%)	22.4 (15%)	20.3 (17%)	18.2 (36%)	15.2 (18%)
Car with toroidal traction-drive CVT, unscaled	1.0	1.75	430	4.0	13.1 (5%)	24.8 (22%)	27.8 (35%)	24.7 (27%)	20.1 (16%)	17.9 (34%)	14.9 (16%)
Car with toroidal traction-drive CVT, scaled to match performance of "Benchmark"	0.80	2.10	343	5.1	14.7 (18%)	28.7 (41%)	29.0 (41%)	24.3 (25%)	20.5 (18%)	18.0 (34%)	15.1 (17%)

TABLE 2 SUMMARY OF FUEL MILEAGE SIMULATIONS  
 (3150 lb Vehicle with 250 cu. in.  
 engine - from Simulation #3)

Vehicle Description	Power-Plant Scale Factor	Rear Axle Ratio	Engine Displ., in. <sup>3</sup> (based on scale factor)	50-70 mph time, sec.	mpg over EPA cycle; % improvement over "Benchmark"	mpg at steady speeds; % improvement over "Benchmark"					
						30mph	40mph	50mph	60mph 70mph 80mph		
"Benchmark" car with present-day automatic transmission	--	2.79	250	11.8	12.6	23.0	21.9	20.2	18.5	15.7	12.9
Car with toroidal traction-drive CVT, unscaled	1.0	2.25	250	9.9	15.3 (21%)	27.9 (21%)	29.8 (36%)	23.9 (18%)	21.4 (16%)	18.2 (16%)	15.6 (21%)
Car with toroidal traction-drive CVT, scaled to match performance of "Benchmark"	0.89	2.52	222	11.8	16.2 (28%)	30.4 (32%)	28.9 (32%)	23.4 (16%)	21.3 (15%)	18.6 (19%)	15.4 (20%)

### 3. SECOND YEAR PROGRAM (1974-1975)

- A. Refinements to APS
- B. Study of effect on fuel economy and emissions of straight-forward drivetrain changes. The purpose of this is to be able to compare advanced concepts with improved present-day systems (Figure 2)
- C. Development of mathematical models to accurately predict transient emissions (Figures 3 - 8).

#### Goal:

To develop a modeling technique that will permit instantaneous values of CO, NOX, and HC emissions to be accurately predicted for any point of any realistic driving cycle.

#### Background:

Transient (instantaneous) emissions over the EPA-CVS cycle have been found to be quite different from values taken from a steady-state engine emissions map. This is due to several factors:

- 1) Engine thermal condition at any instant of the cycle is different from that of the corresponding point on the steady-state emissions map.
- 2) Emissions maps to be used are to have engine rpm & engine torque as coordinates, with contours of constant brake specific emissions. The emission values at each point on the map will not be the steady-state values, but a weighted average value of all engine thermal conditions from "very cold" to "very hot".

A-MID-SIZED VEHICLE/OVERDRIVE & LOCKUP  
 B-MID-SIZED VEHICLE/OVERDRIVE/  
 C-MID-SIZED VEHICLE/BASE  
 D-FULL-SIZED VEHICLE/OVERDRIVE & LOCKUP  
 E-FULL-SIZED VEHICLE/OVERDRIVE  
 F-FULL-SIZED VEHICLE/BASE

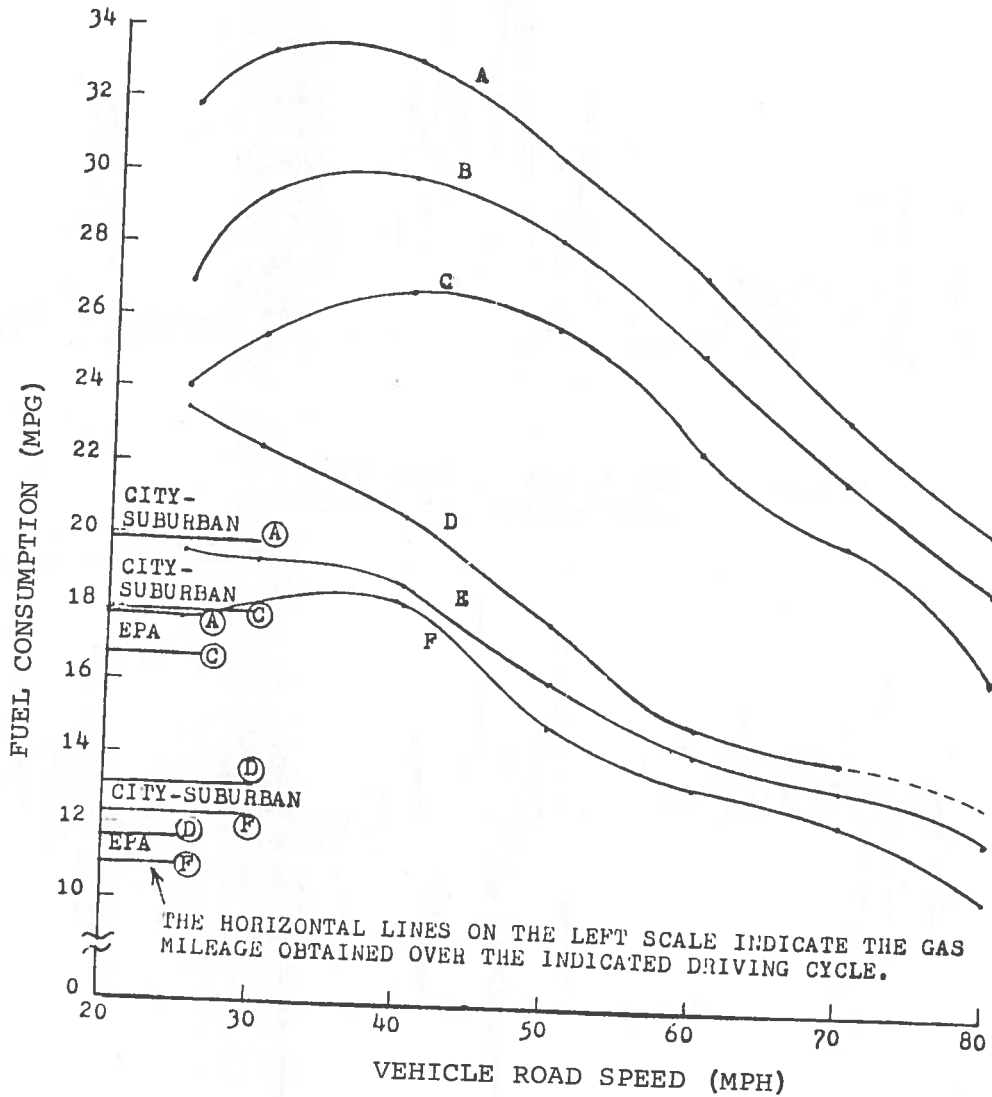


Figure 2. Fuel Economy versus Steady-State Road Speed



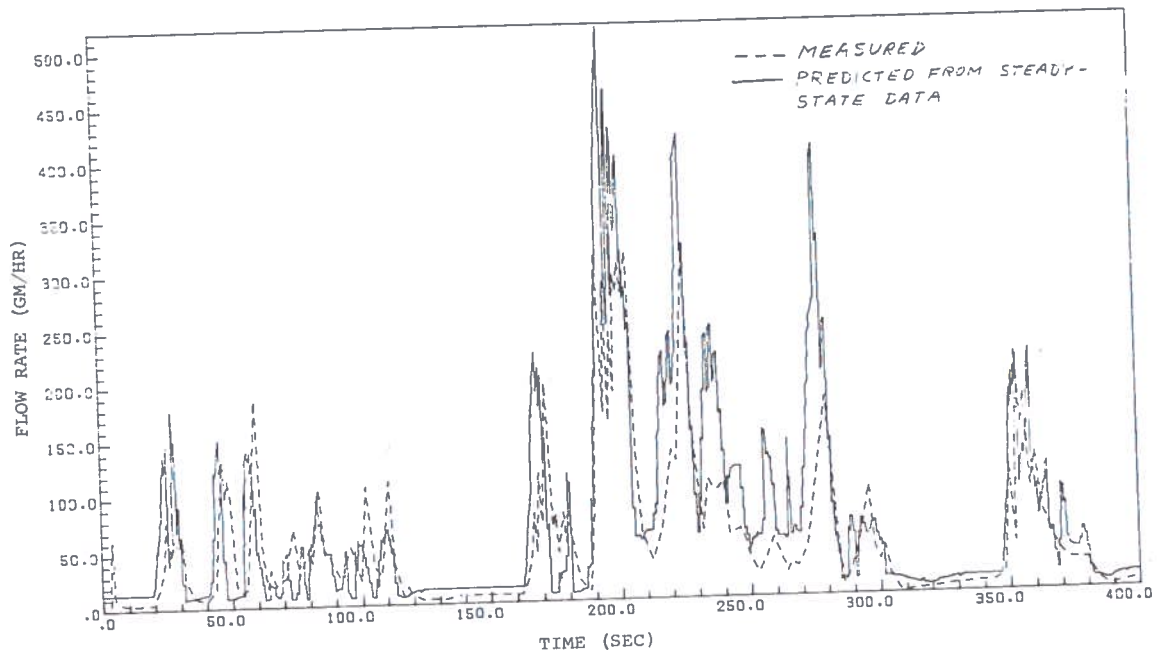


Figure 3. NOx Emission Flow Rate  
(400 Seconds of EPA Cycle)

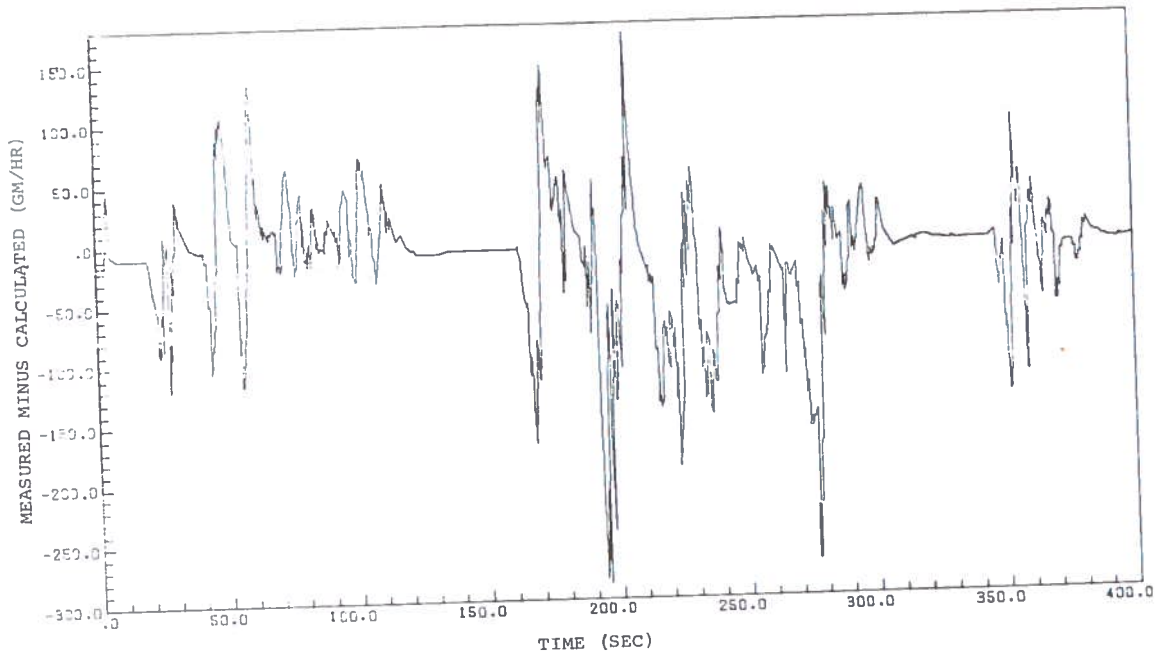


Figure 4. NOx Measured Emission Minus Calculated  
(400 seconds of EPA Cycle)

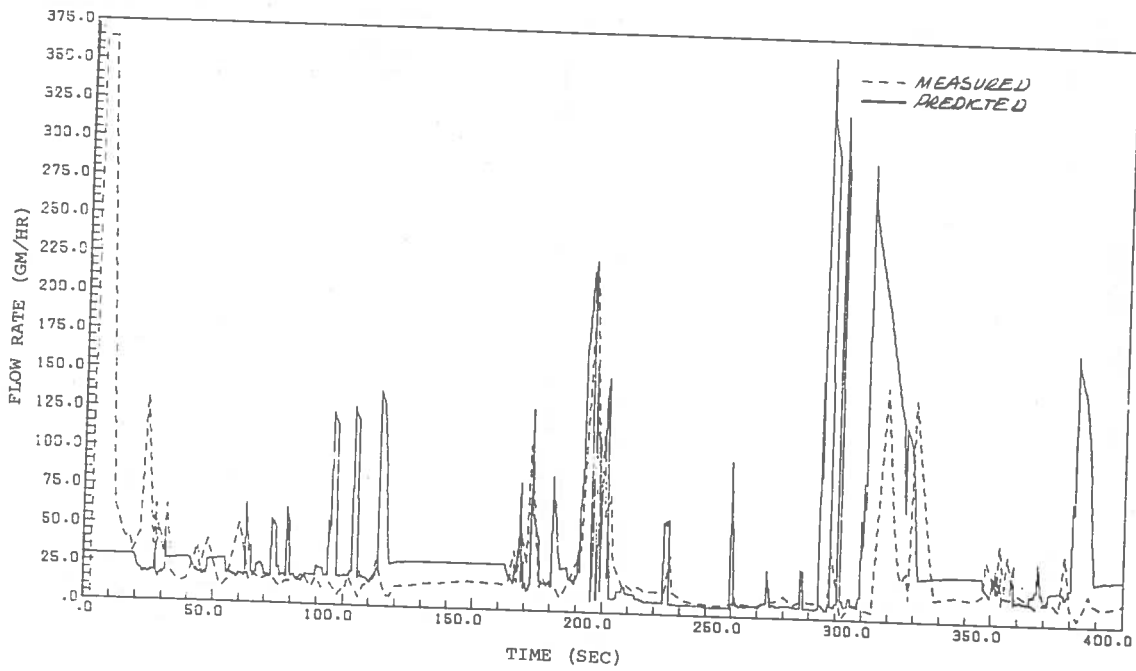


Figure 5. HC Emission Flow Rate  
(400 Seconds of EPA Cycle)

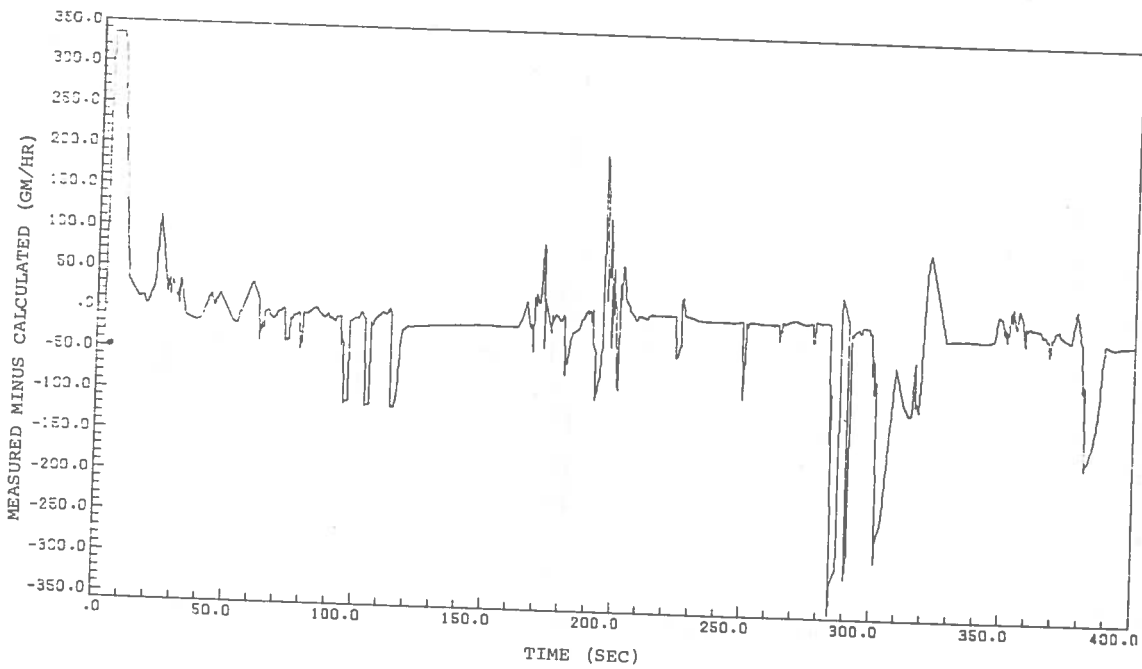


Figure 6. HC Measured Emission Minus Calculated  
(400 Seconds of EPA Cycle)

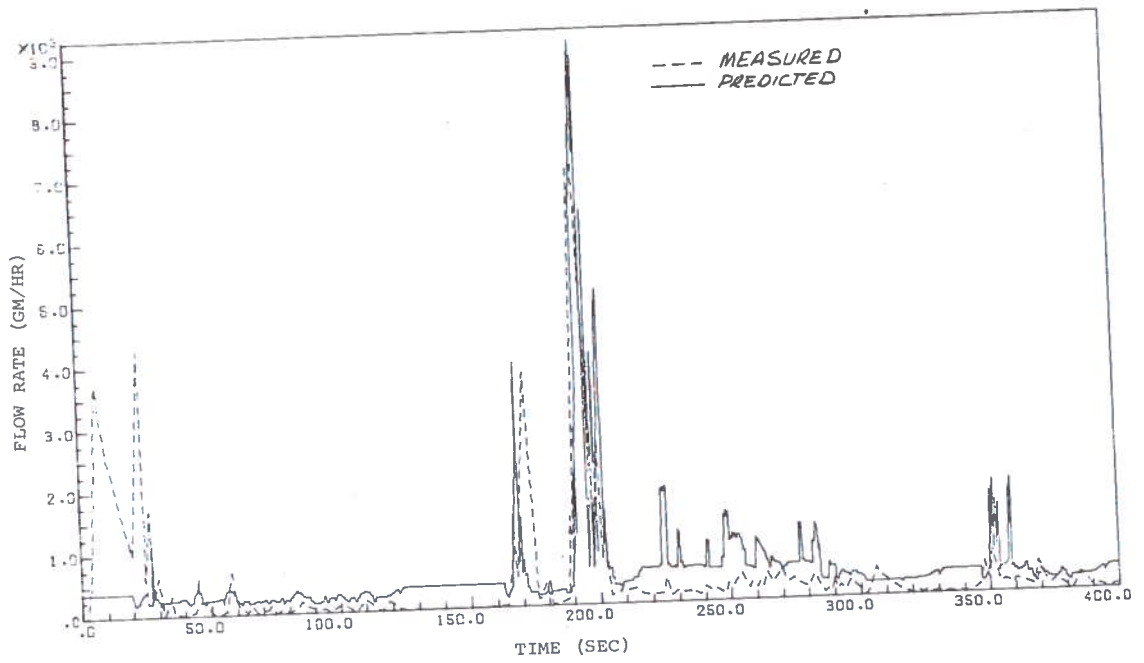


Figure 7. Emission Flow Rate  
(400 Seconds of EPA Cycle)

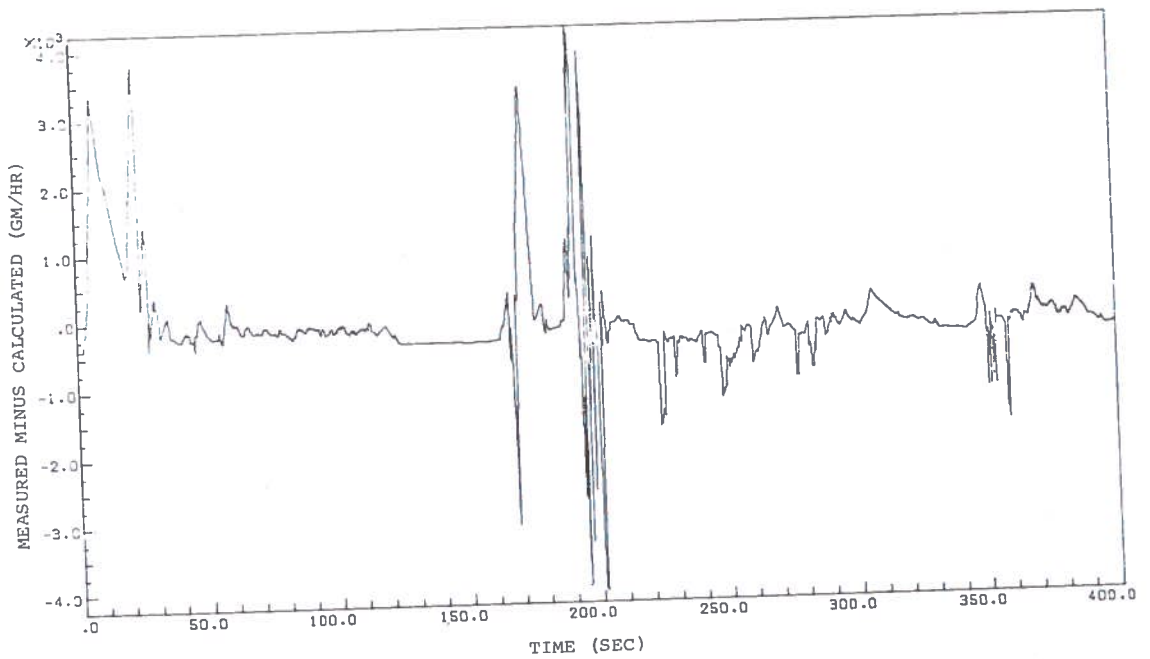


Figure 8. CO Measured Emission Minus Calculated  
(400 Seconds of EPA Cycle)

- 3) To calculate emissions at any instant of time;
  - a) Get emission values from the weighted average maps
  - b) Calculate engine thermal condition from recent past history of operation
  - c) Determine a correction factor, from the thermal condition, to be added to the map values
  - d) Add short term transient corrections.

Testing Procedure to Develop "Weighted Average Emissions Maps"

- 1) Define "very cold" in terms of steady-state operation at a particular point of power and speed (e.g., idle). Define "very hot" in terms of steady-state operation at a particular point of high torque and high speed.
- 2) Choose a grid of points on the map to adequately cover the engine operating area (about 50 points should be adequate).
- 3) Make two runs for each point on the map:
  - a) Starting with a "very cold" engine thermal condition, hold torque and speed at the given point until steady-state conditions are reached. Record continuously emission rates of all three pollutants.
  - b) Starting with a "very hot" engine thermal condition, repeat (a) above.
- 4) Using continuous data from (3) above, emission values for the given point on the map can be determined for any engine "thermal condition".
- 5) Above best done, if practical, with realistic under-hood conditions.
- 6) In lieu of above, it may be possible to develop the required emissions data from an EPA-CVS test in which continuous emission rates are measured for all three pollutants..

D. Computer simulation and optimization of flywheel hybrid design (based on principle of energy management). See Figures 9 - 14.

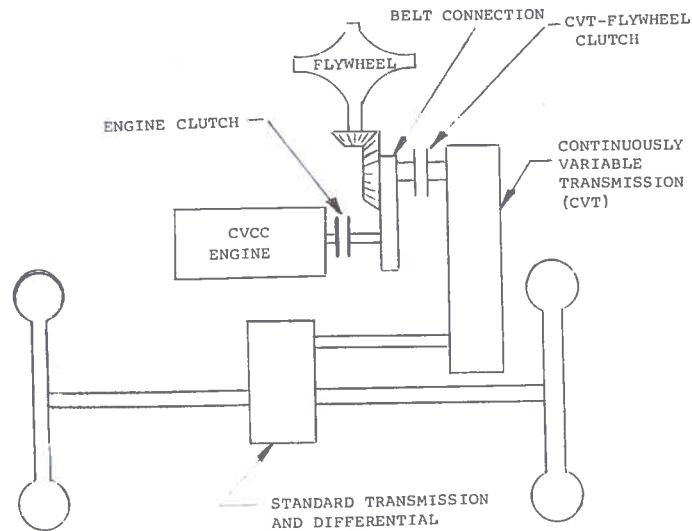


Figure 9. Flywheel-CVCC Vehicle Schematic

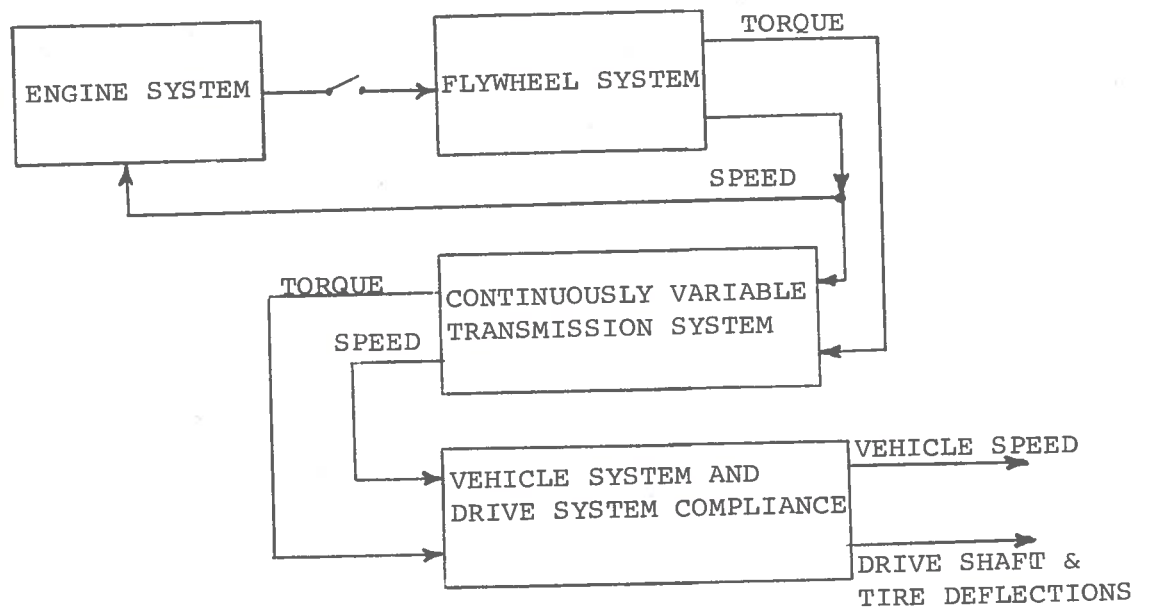
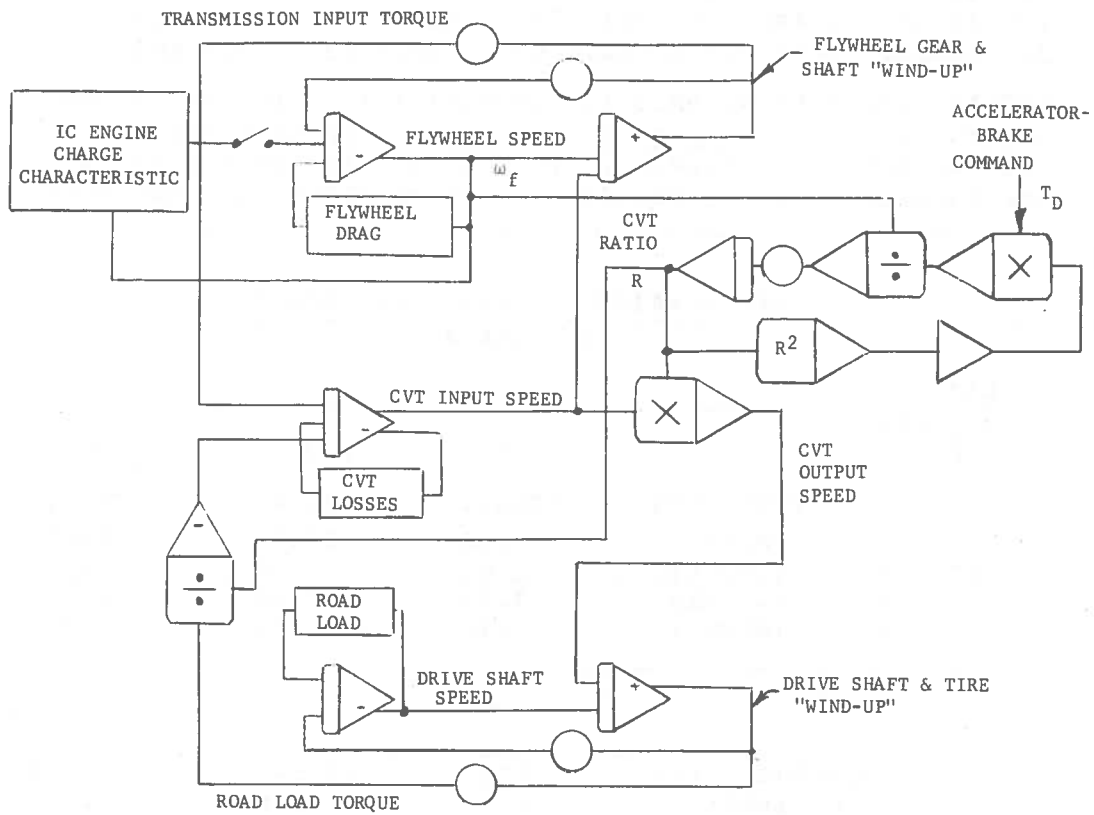


Figure 10. Basic Simulation Block Diagram



CONTROL EQUATION

$$\dot{R} = K \frac{T_o (I_c / I_f + R^2)}{I_c \omega_f}$$

Figure 11. Simplified Flywheel Drive Simulation

HYBRID FUEL ECONOMY AND EMISSIONS  
1973 5000 POUND CAR ON EPA DRIVING CYCLE

BASE CAR 10.5 MPG

THE ROAD LOAD IS 5468.2 HORSEPOWER SECONDS  
THE BRAKING LOSS IS 5529.9 HORSEPOWER SECONDS  
THE FLYWHEEL LOSS IS 1372.0 HORSEPOWER SECONDS

THE TOTAL DISTANCE TRAVELED IS 7.5 MILES  
THE AVERAGE REAR AXLE EFFICIENCY ASSUMED IS 95 PERCENT  
THE AVERAGE GEAR BOX EFFICIENCY ASSUMED IS 99 PERCENT

THE AVERAGE BSFC ASSUMED IS .50 POUNDS PER HORSEPOWER HOUR  
THE AVERAGE BSNO ASSUMED IS 2.0 GRAMS PER HORSEPOWER HOUR  
THE AVERAGE BSCO ASSUMED IS 16.0 GRAMS PER HORSEPOWER HOUR  
THE AVERAGE BSHC ASSUMED IS .6 GRAMS PER HORSEPOWER HOUR

REGENERATIVE BRAKING EFFICIENCY  
(PERCENT)

CVT				
EFFICIENCY				
(PERCENT)				
		70	80	90
	ENERGY (HP SEC)	13447.5	12894.5	12341.5
	FUEL (MPG)	24.50	25.55	26.69
80	NOX (GM/MI)	1.00	.96	.91
	CO (GM/MI)	7.97	7.64	7.31
	HC (GM/MI)	.30	.29	.27
	ENERGY (HP SEC)	12509.5	11950.5	11403.5
	FUEL (MPG)	26.33	27.55	28.89
85	NOX (GM/MI)	.93	.89	.84
	CO (GM/MI)	7.41	7.09	6.75
	HC (GM/MI)	.28	.27	.25
	ENERGY (HP SEC)	11675.7	11122.7	10569.7
	FUEL (MPG)	28.21	29.62	31.16
90	NOX (GM/MI)	.86	.82	.78
	CO (GM/MI)	6.92	6.59	6.26
	HC (GM/MI)	.26	.25	.23

Figure 12. Hybrid Fuel Economy, Emissions, and Regenerative Braking Efficiency (Base Car 10.5 mpg)

HYBRID FUEL ECONOMY AND EMISSIONS

~~1973 3150 LB CAR ON EPA DRIVING CYCLE~~

BASE CAR 16.6 MPG

~~THE ROAD LOAD IS 5353.9 HORSEPOWER SECONDS~~  
~~THE BRAKING LOSS IS 2863.6 HORSEPOWER SECONDS~~  
~~THE FLYWHEEL LOSS IS 1372.0 HORSEPOWER SECONDS~~  
~~THE TOTAL DISTANCE TRAVELED IS 7.5 MILES~~

~~THE AVERAGE REAR AXLE EFFICIENCY ASSUMED IS 95 PERCENT~~  
~~THE AVERAGE GEAR BOX EFFICIENCY ASSUMED IS 99 PERCENT~~

~~THE AVERAGE BSFC ASSUMED IS .50 POUNDS PER HORSEPOWER HOUR~~  
~~THE AVERAGE BSNO ASSUMED IS 2.0 GRAMS PER HORSEPOWER HOUR~~  
~~THE AVERAGE BSCO ASSUMED IS 16.0 GRAMS PER HORSEPOWER HOUR~~  
~~THE AVERAGE BSHC ASSUMED IS .6 GRAMS PER HORSEPOWER HOUR~~

REGENERATIVE BRAKING EFFICIENCY  
(PERCENT)

CVT				
EFFICIENCY (PERCENT)				
		70	80	90
	ENERGY (HP SEC)	10292.3	10005.5	9718.6
	FUEL (MPG)	32.00	32.92	33.89
80	NOX (GM/MI)	.76	.74	.72
	CO (GM/MI)	6.10	5.93	5.76
	HC (GM/MI)	.23	.22	.22
	ENERGY (HP SEC)	9649.5	9362.6	9075.8
	FUEL (MPG)	34.14	35.18	36.29
85	NOX (GM/MI)	.71	.69	.67
	CO (GM/MI)	5.72	5.55	5.38
	HC (GM/MI)	.21	.21	.20
	ENERGY (HP SEC)	9078.1	8791.2	8504.4
	FUEL (MPG)	36.29	37.47	38.73
90	NOX (GM/MI)	.67	.65	.63
	CO (GM/MI)	5.38	5.21	5.04
	HC (GM/MI)	.20	.20	.19

Figure 13. Hybrid Fuel Economy, Emissions, and Regenerative Braking Efficiency (Base Car 16.6 mpg)



HYBRID FUEL ECONOMY AND EMISSIONS

2000 LB CAR ON EPA DRIVING CYCLE

BASE CAR 23.9 MPG

THE ROAD LOAD IS 2450.7 HORSEPOWER SECONDS  
 THE BRAKING LOSS IS 1951.6 HORSEPOWER SECONDS  
 THE FLYWHEEL LOSS IS 1372.0 HORSEPOWER SECONDS  
 THE TOTAL DISTANCE TRAVELED IS 7.5 MILES

THE AVERAGE REAR AXLE EFFICIENCY ASSUMED IS 95 PERCENT  
 THE AVERAGE GEAR BOX EFFICIENCY ASSUMED IS 99 PERCENT

THE AVERAGE BSFC ASSUMED IS .55 POUNDS PER HORSEPOWER HOUR  
 THE AVERAGE BSNO ASSUMED IS 1.5 GRAMS PER HORSEPOWER HOUR  
 THE AVERAGE BSCO ASSUMED IS 4.0 GRAMS PER HORSEPOWER HOUR  
 THE AVERAGE BSFC ASSUMED IS .2 GRAMS PER HORSEPOWER HOUR

REGENERATIVE BRAKING EFFICIENCY  
 (PERCENT)

CVT		EFFICIENCY (PERCENT)		
		70	80	90
80	ENERGY (HP SEC)	5856.9	5661.7	5466.6
	FUEL (MPG)	51.13	52.89	54.78
	NOX (GM/MI)	.33	.31	.30
	CO (GM/MI)	.87	.84	.81
	HC (GM/MI)	.04	.04	.04
	<hr/>			
85	ENERGY (HP SEC)	5512.7	5317.6	5122.4
	FUEL (MPG)	54.32	56.31	58.46
	NOX (GM/MI)	.31	.30	.28
	CO (GM/MI)	.82	.79	.76
	HC (GM/MI)	.04	.04	.04
	<hr/>			
90	ENERGY (HP SEC)	5206.8	5011.6	4816.5
	FUEL (MPG)	57.51	59.75	62.17
	NOX (GM/MI)	.29	.28	.27
	CO (GM/MI)	.77	.74	.71
	HC (GM/MI)	.04	.04	.04

Figure 14. Hybrid Fuel Economy, Emissions, and Regenerative Braking Efficiency (Base Car 23.9 mph)

E. Analysis and preliminary system design of power plant controls (Figure 15 - 18)

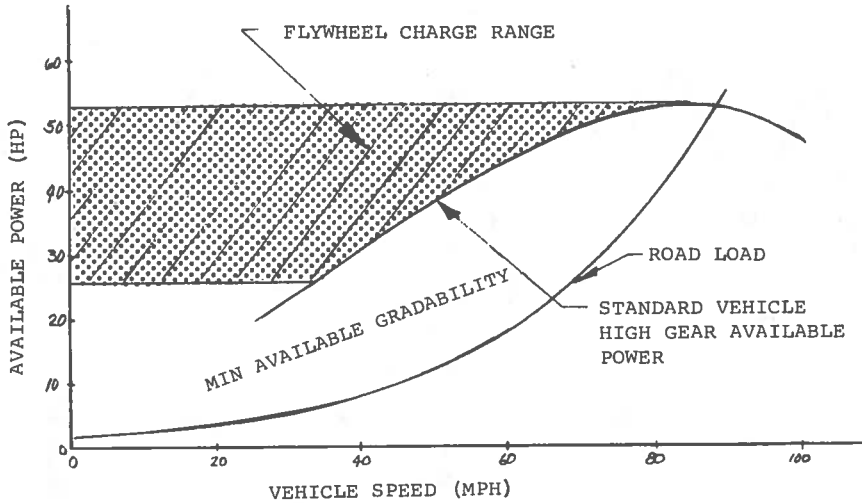


Figure 15. Determining Flywheel Change Criteria

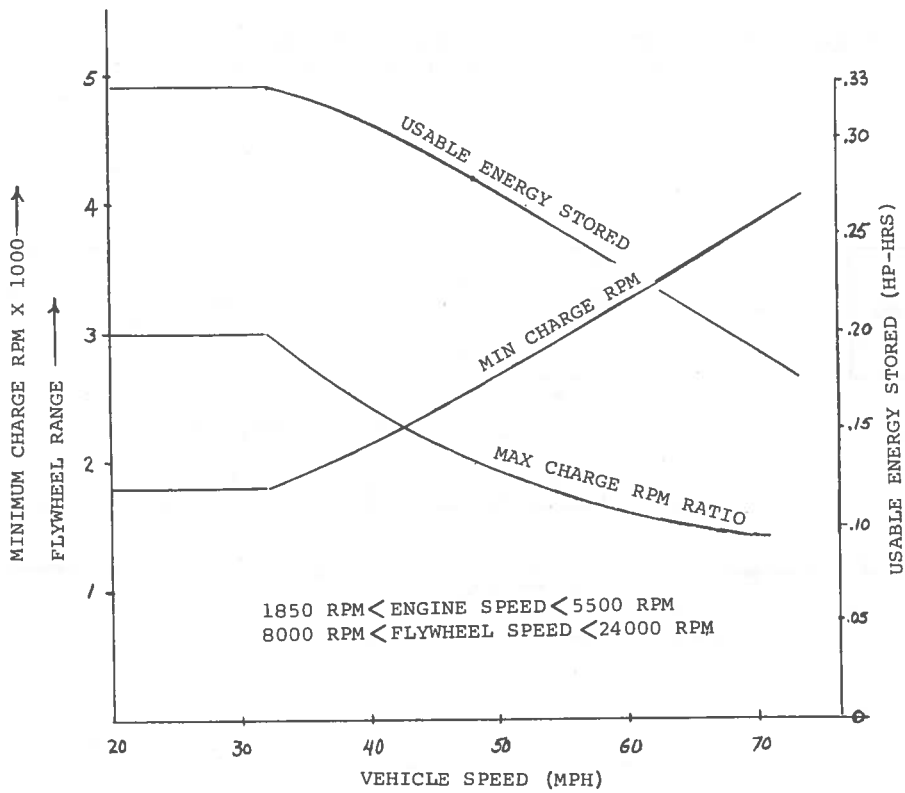


Figure 16. Maximum Charge Ratio for Standard Vehicle Gradability

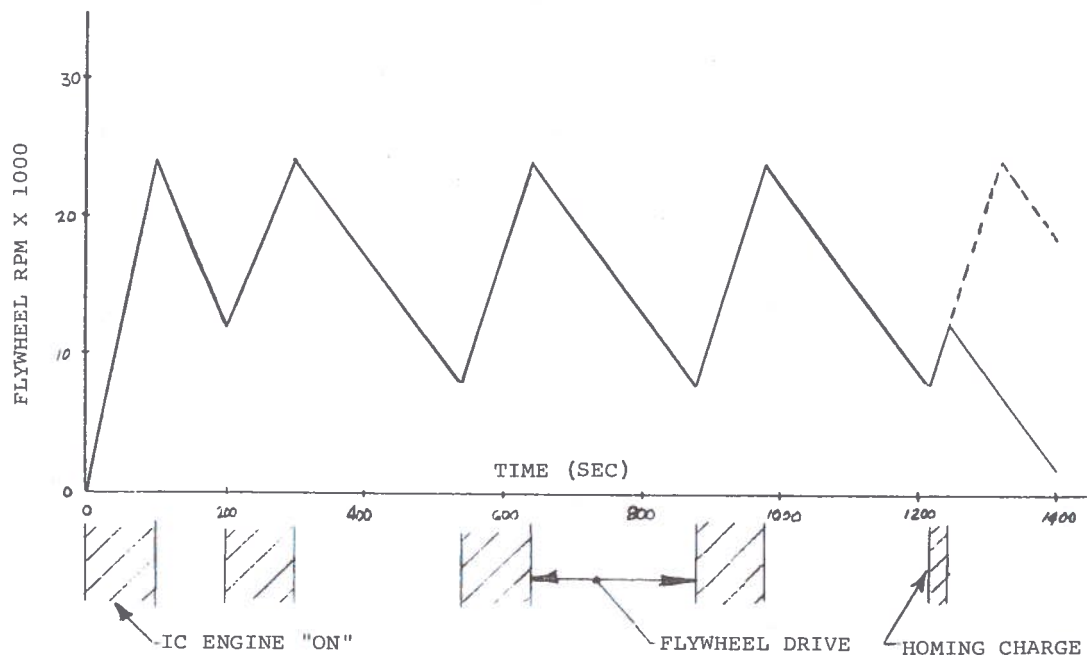


Figure 17. Estimated Flywheel-IC Engine Cycles During an EPA-CVS Test

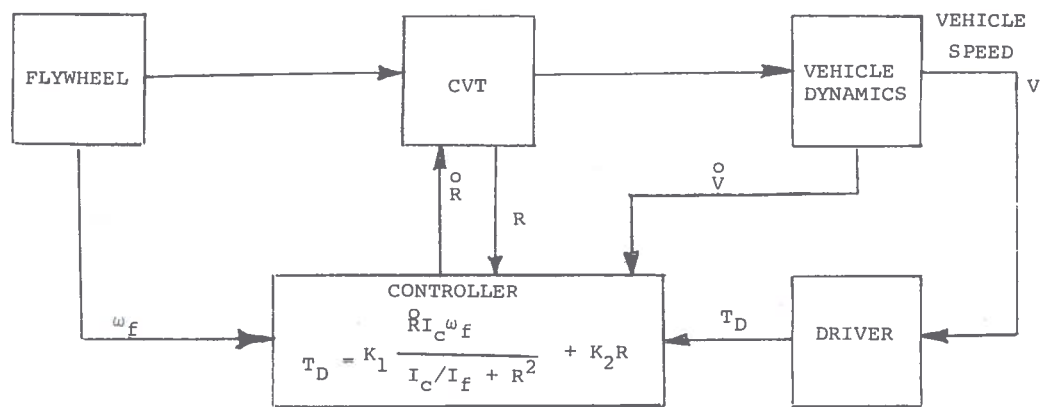


Figure 18. Vehicle Dynamic Controller

4. THIRD YEAR (BEGINNING MAY 1, 1975)

- A. Mechanical design of flywheel-I.C. engine powerplant and control system (Figure 19).
- B. Procurement of flywheel package on a subcontract basis.
- C. Construction and testing of powerplant system.
- D. Installation in vehicle, fuel mileage and emissions Testing.

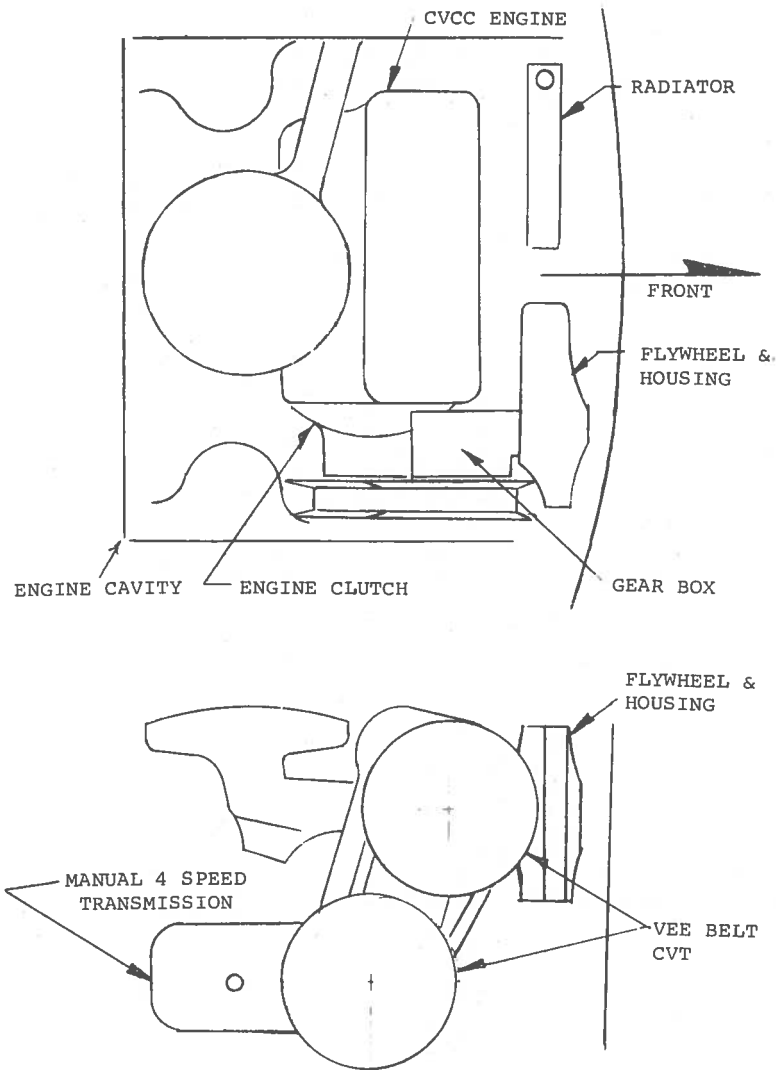
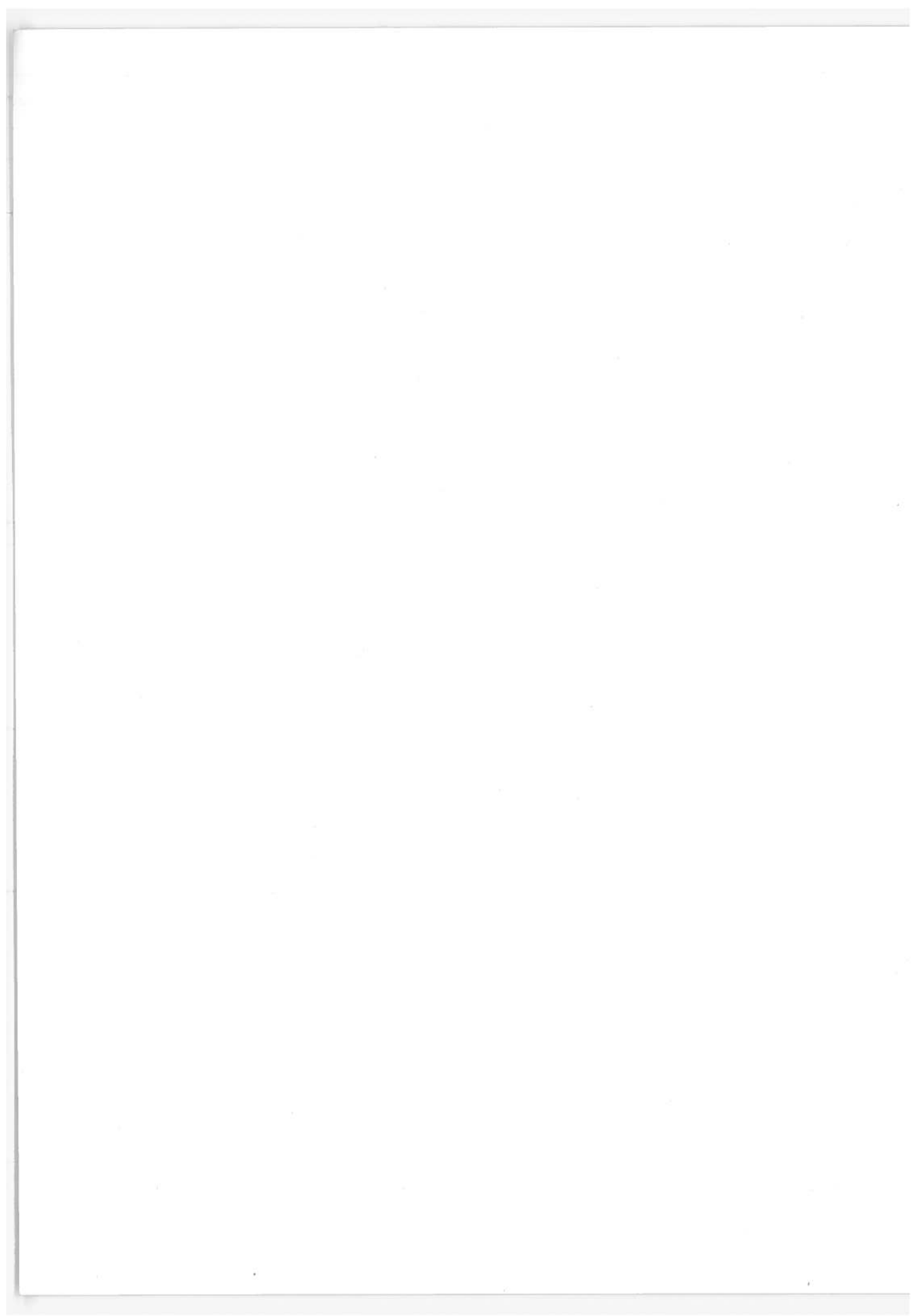


Figure 19. Flywheel-CVCC Vehicle Layout



## CLOSED-LOOP CONTROL OF SPARK TIMING

J. David Powell  
Stanford University  
Palo Alto, California  
and

Mont Hubbard  
University of California  
Davis, California

### ABSTRACT

Investigations at Stanford are currently underway which are aimed at reducing the degradation of spark advance settings with time and providing automatic adjustments of spark timing to changing engine and environmental conditions. The status of the project will be reviewed with particular emphasis on the measurements being made and the mechanization of the control. A promising measurement for spark advance control that will be discussed is the crank angle location of the peak cylinder pressure.

### 1. INTRODUCTION

Figure 1 shows the fundamental difference between open-loop and closed loop control for a fuel control system; namely, that open loop control relies on known relationships that exist in a nominal engine between certain output quantities and the desired controlled input. As atmospheric, fuel, or engine conditions change, these nominal functions are incorrect and an error results. In a closed loop controller, a parameter directly related to the quantity being controlled ( $O_2$  in this case) is measured and compared with the desired fuel/air (f/a) ratio, then used to drive the f/a to the correct value. The virtues are (1) less sensitivity to changing conditions and (2) more accuracy.

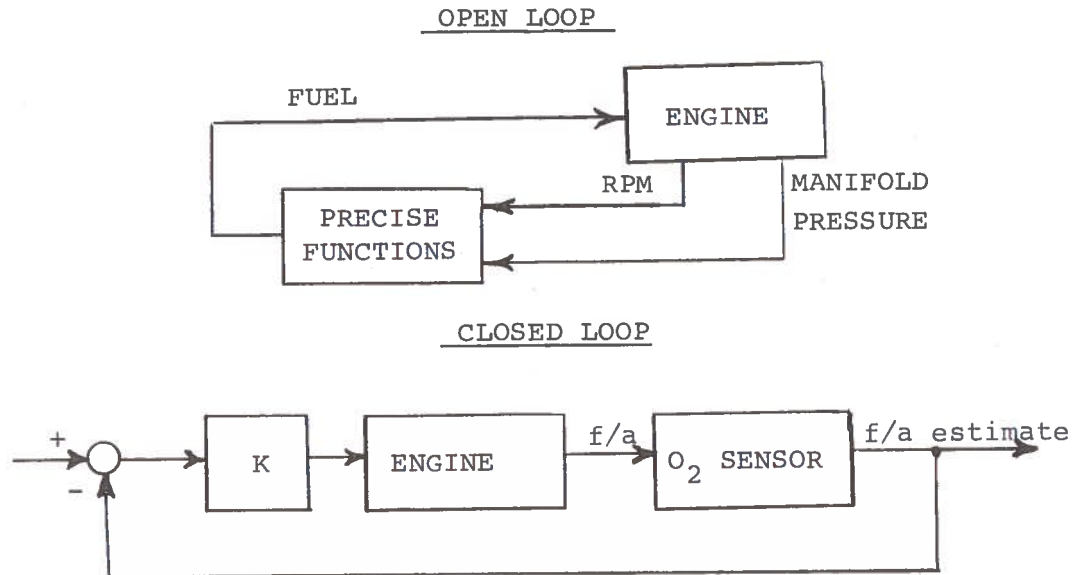


Figure 1 Open Loop and Closed Loop Control for Fuel Control System

## 2. FUEL-AIR RATIO CONTROL

The first year's support by the University Research Program is described in detail in the final report.<sup>1</sup> Figure 2 demonstrates the accuracy and insensitivity characteristics of the controller. The figure illustrates that, before the airflow decreases, the equivalence ratio is held to within  $\pm 0.5\%$  with peak excursions of about  $\pm 1\%$ . The introduction of an airflow decrease produced no noticeable effect on the equivalence ratio, although the fuel flow (ANALOG PULSE WIDTH in Figure 2) was modified by the closed loop control. Figure 3 demonstrates the ability of the controller and sensor to provide the same consistent equivalence ratio at a lean condition. However, since the sensor output is somewhat temperature dependent at lean mixture ratios, the accuracy of the controller would ultimately depend on a compensation of the sensor based on measured exhaust temperatures.

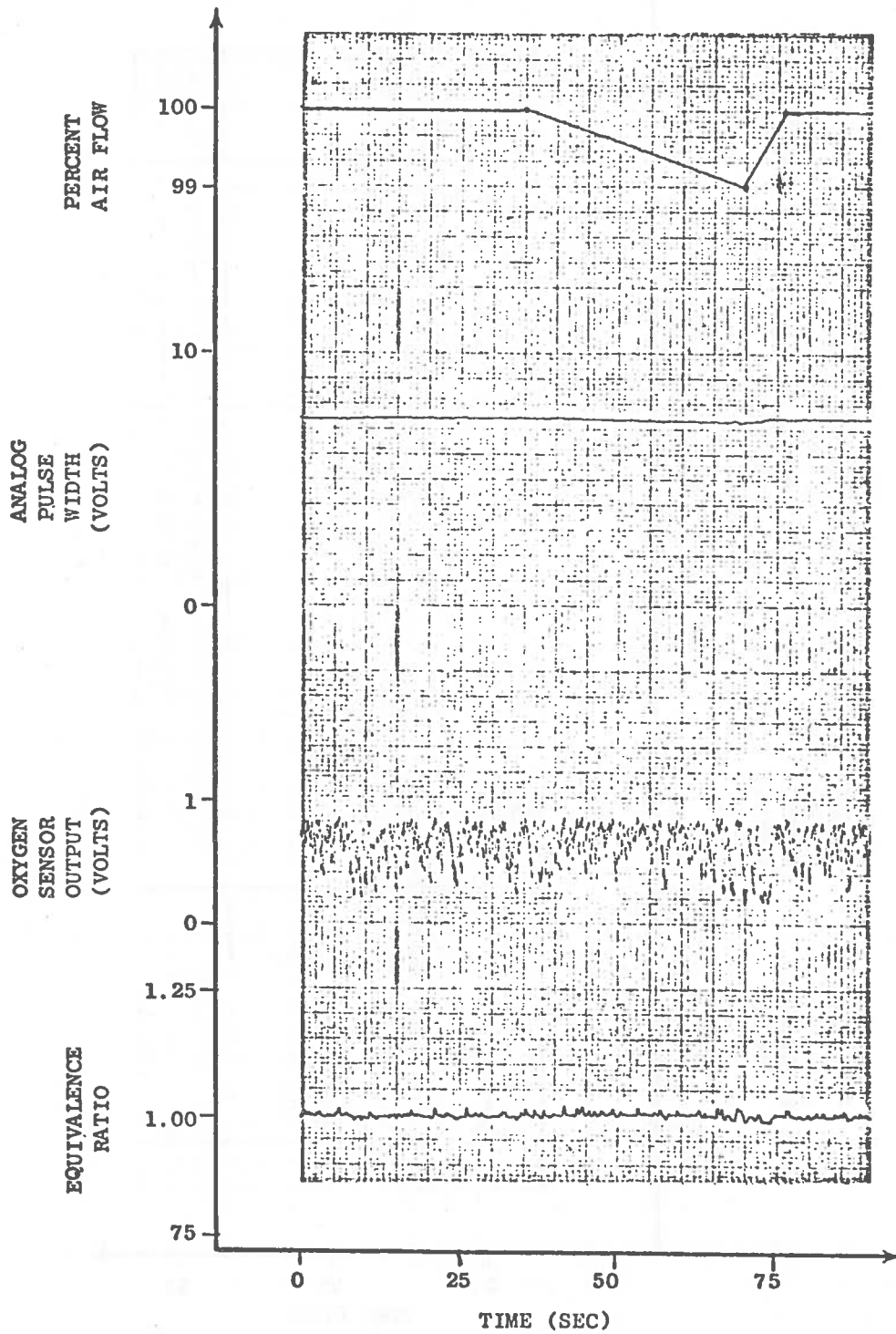


Figure 2 Accuracy and Insensitivity of Closed-Loop Controller



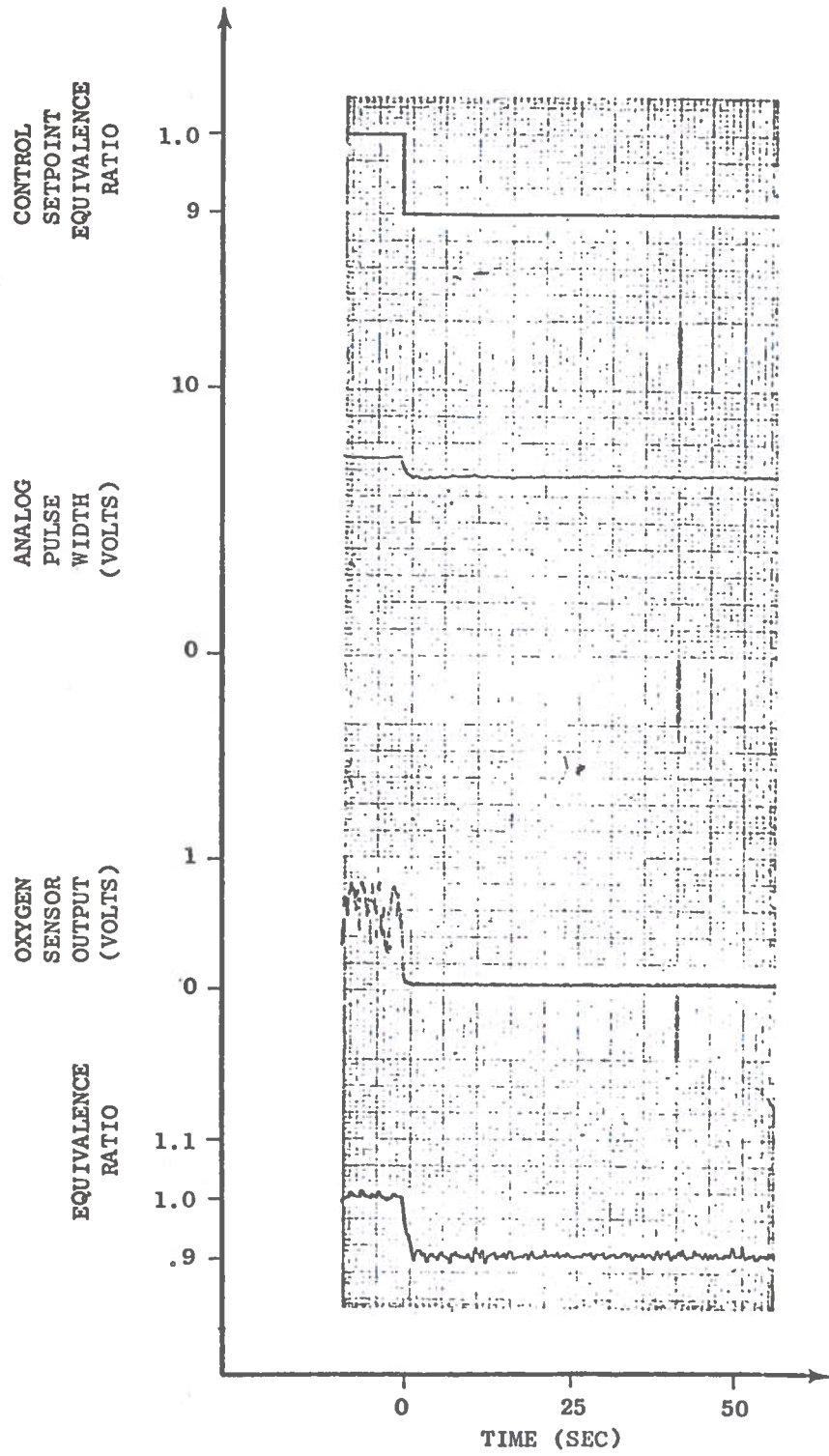


Figure 3 Accuracy and Insensitivity of Closed-Loop Controller Under Lean Conditions

### 3. SPARK ADVANCE CONTROL

Figure 4 depicts open and closed-loop schematics for spark advance systems. Current production spark advance schedules are typically based on RPM and manifold vacuum; therefore, for any condition other than that used to determine the schedule, the spark advance will be different than that intended. The question to be answered in designing a closed loop control is: what should be fed back? The factors that influence desirable spark advance schedules include f/a, humidity, gasoline characteristics, altitude, and ambient temperature. In the case of humidity SAE paper 690166<sup>2</sup> indicates that the optimum spark advance shifts  $10^\circ$  from dry to moist air (90% relative humidity at  $100^\circ\text{F}$ ). Furthermore, if the spark advance is not adjusted for this effect, a loss in brake specific fuel consumption (bsfc) of 2-3% will result. Since this is just one of many factors which change the optimum spark advance, the combined effect of all factors could easily result in a 5% bsfc loss if not accounted for in the spark schedule.

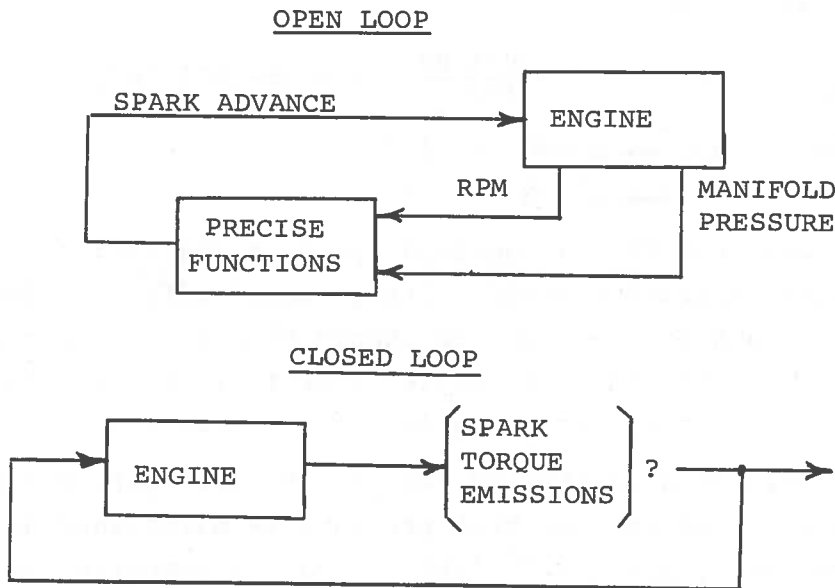


Figure 4 Open and Closed Loop Diagram for Spark Advance Systems

To determine an appropriate quantity for a self adjusting spark advance controller, we ran our CFR single cylinder engine at 5 RPMS, (600 → 1800), 3 airflows (50% → 100%), 5 fuel-air ratios, ( $\phi = 1.1 \rightarrow .7$ ), and 4 spark advances (MBT,  $-10^\circ$ ,  $-20^\circ$ , and  $+10^\circ$ ). At each control setting, we measured CO, Hc,  $\text{NO}_x$ , Bsfrc, Bmep, peak cylinder pressure, and position of peak cylinder pressure (PPSN). The data collected were fit to the following analytical model of engine performance for later use in control scheme evaluations:

$$Y = A + B_i U_i + C_i U_i^2 + D_i U_i^3 + E_i U_i^2 U_j + F_i U_i^2 U_j \quad (1)$$

where

$$\begin{aligned} U_1 &= \text{engine RPM} \\ U_2 &= \% \text{ throttle} \\ U_3 &= \phi \\ U_4 &= \text{spark advance} \end{aligned}$$

Because cylinder pressure is a relatively simple measurement, we were particularly interested in its relationship to spark advance.

The analytical model of PPSN at the optimum (MBT) spark advance is as follows:

$$\text{PPSN}_{\text{opt}} = 15.7 - \frac{\text{RPM}-1200}{400} - 4.5 (\phi - .97)^\circ \text{ATDC} \quad (2)$$

$$\begin{aligned} \Delta \text{RPM} &= 600 \longrightarrow \Delta \text{PPSN} = 1.2^\circ \\ \Delta \phi &= .1 \longrightarrow \Delta \text{PPSN} = .5^\circ \end{aligned}$$

The model shows that PPSN at optimum spark is practically constant over the engine operating range. The greatest effect is due to RPM which is shown by the model to change PPSN by  $1.5^\circ$  for a change of 600 RPM. The model shows a smaller effect of  $\phi$ . All other terms were omitted since they were even less significant.

We postulated a control system whereby the spark advance is continually adjusted so that peak pressure is maintained at the mean value of the model, i.e.  $15.7^\circ$  ATDC. Figure 5 compares the spark advance schedule so obtained with the optimum (MBT) curves. Note that the PPSN controlled spark advance is typically within one degree of MBT and the largest difference is  $2^\circ$  (at 600 RPM, 50% airflow). Figure 6 shows the percent loss in bsfc vs. the value

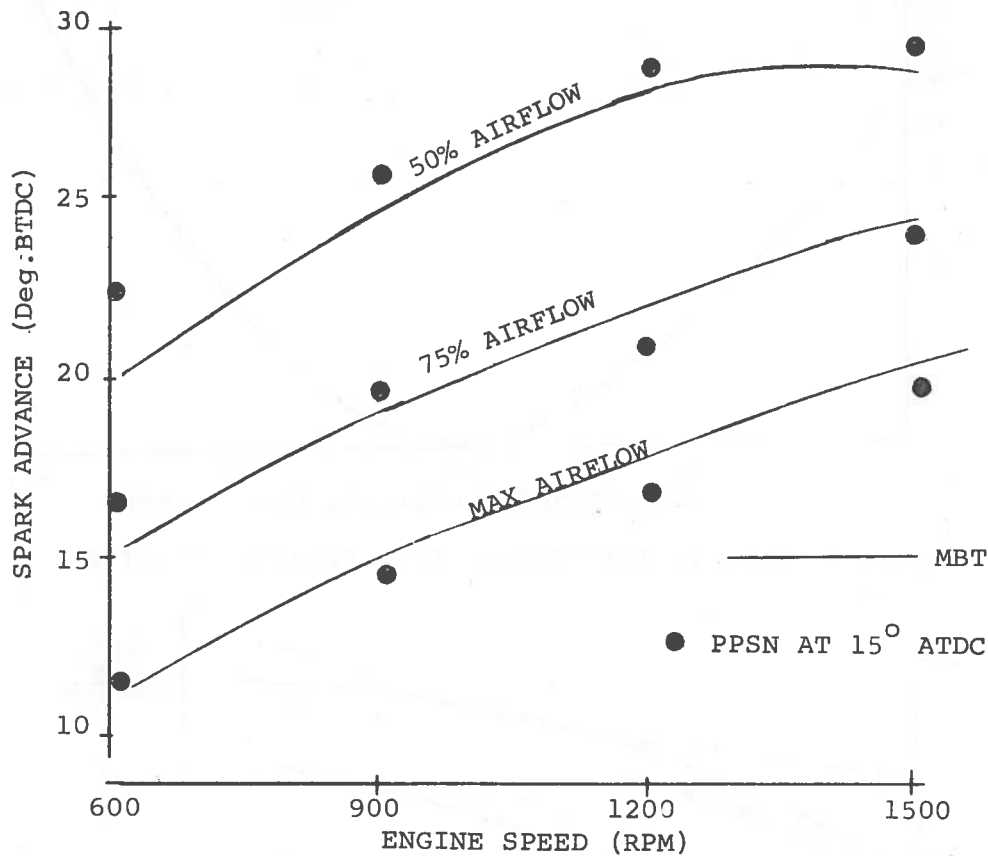


Figure 5 Relationship of Spark Advance to Engine Speed of PPSN used as a set point for PPSN control. The most important feature of this curve is that the minimum (at  $15.7^\circ$ ) represents a small fraction of 1% loss in bsfc.

To be of value as an insensitive controller, i.e. to behave in a closed loop manner, the system must adjust to the optimum at different engine conditions. Figure 7 shows the behavior for an off nominal fuel/air ratio. The solid lines are the MBT spark advance curves, while the dashed curves are the spark advance resulting for PPSN controlled to  $15.7^\circ$  ATDC. The dashed curves move from the schedules shown by dots in Figure 5 to the schedule approximating the  $\phi = .9$  MBT one, in other words the system does adjust to the changed fuel-air ratio. This adjustment is due to the leaner mixture causing a slower flame speed, which requires more spark advance for a constant PPSN.

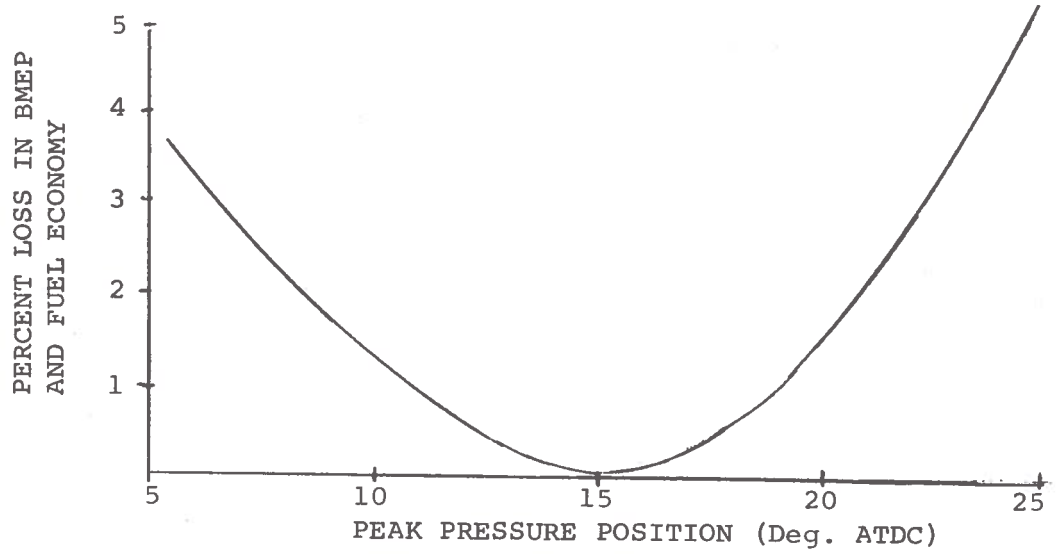


Figure 6 Loss in BMEP Versus Peak Pressure Position

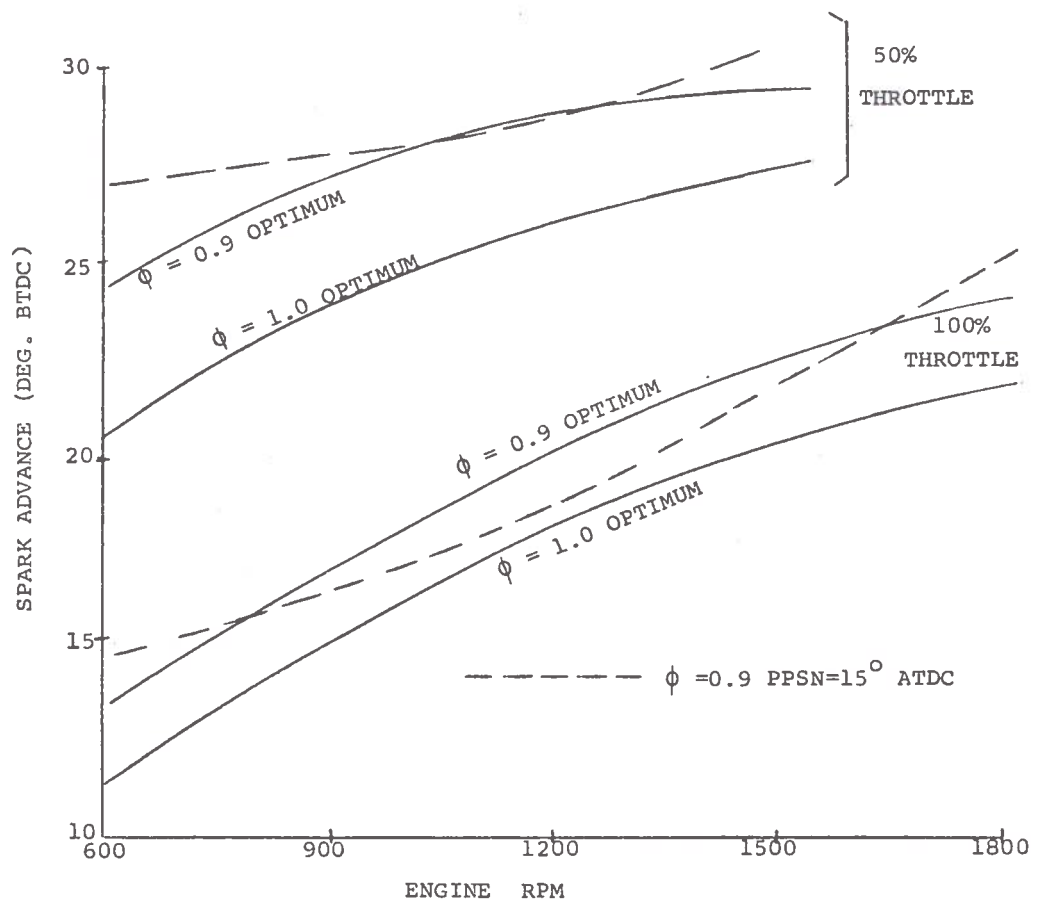


Figure 7 Optimum Spark Advance Versus Engine RPM for Off Nominal F/A Ratio

Changes in atmospheric humidity can change engine performance markedly. The first effect of humidity is the displacement of a portion of the unit air charge which could otherwise be used to oxidize additional fuel. This decreases brake output.

A second effect of humidity is that at a constant speed, load and equivalence ratio, the value of the optimum spark advance increases. This is due to a decrease in the turbulent flame propagation speed with increased humidity. Even if the spark is readjusted to the new optimum value, the combustion takes place over a larger crank angle which increases time losses and hence decreases brake output. If the spark is not readjusted to its new optimum value engine performance suffers even more.

The average winter humidity generally differs from the average summer humidity and there may be even larger daily variations. Saturation specific humidity (in lbs of moisture per lb of dry air) increases roughly exponentially for temperatures below 140°F. For example, in saturated air at 100°F, the vapor pressure of H<sub>2</sub>O is about 1.0 psi, or about 7% of total barometric pressure is due to water vapor.

Nakajima, et al,<sup>2</sup> studied the effects of atmospheric conditions including humidity on engine performance. Figure 8 shows the optimum spark timing versus humidity for their four cylinder gasoline engine. The optimum spark changes are independent of speed and are on the order of 10 degrees spark advance for a change in H<sub>2</sub>O vapor pressure of 1.0 psi. This sensitivity might change slightly from engine to engine.

We have recently run similar humidity tests in our laboratory. Engine intake humidity was varied at a constant intake temperature of 125°F by mixing small amounts of saturated steam with ambient air. Optimum spark advance was determined for each humidity, and engine power and peak pressure position were measured at the optimum spark advance.

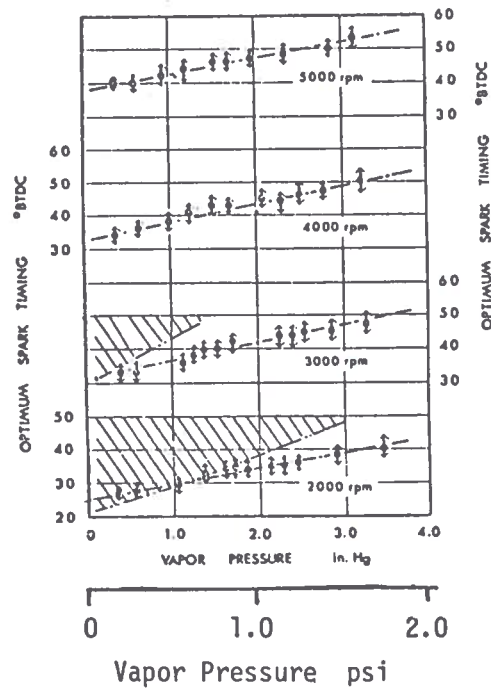


Figure 8 Optimum Spark Timing at Various Humidities (Shaded Areas Show The Region Where Knocking Occurs, Arrowheads Indicate Points Where Output decreases as Much as 0.5% From Maximum Value)

Figure 9 shows the results of these tests. At 1500 RPM the sensitivity is approximately 6-7 degrees of advance for an increase in  $H_2O$  vapor pressure of 1.0 psi. The above tests were run at constant equivalence ratio (closed loop fuel-air ratio control) while Nakajima's data was with a carburetor whose air-fuel ratio changed slightly with humidity. This could explain the different sensitivities observed.

The second half of Figure 9 shows that the position of the pressure peak changed little over a fairly wide range of atmospheric humidities when the spark was set to its optimum value. This verifies that closed loop spark control based on peak pressure position continues to provide optimum spark advance even with reasonably large variations in ambient humidity and therefore the control scheme is said to be insensitive to changes in humidity.

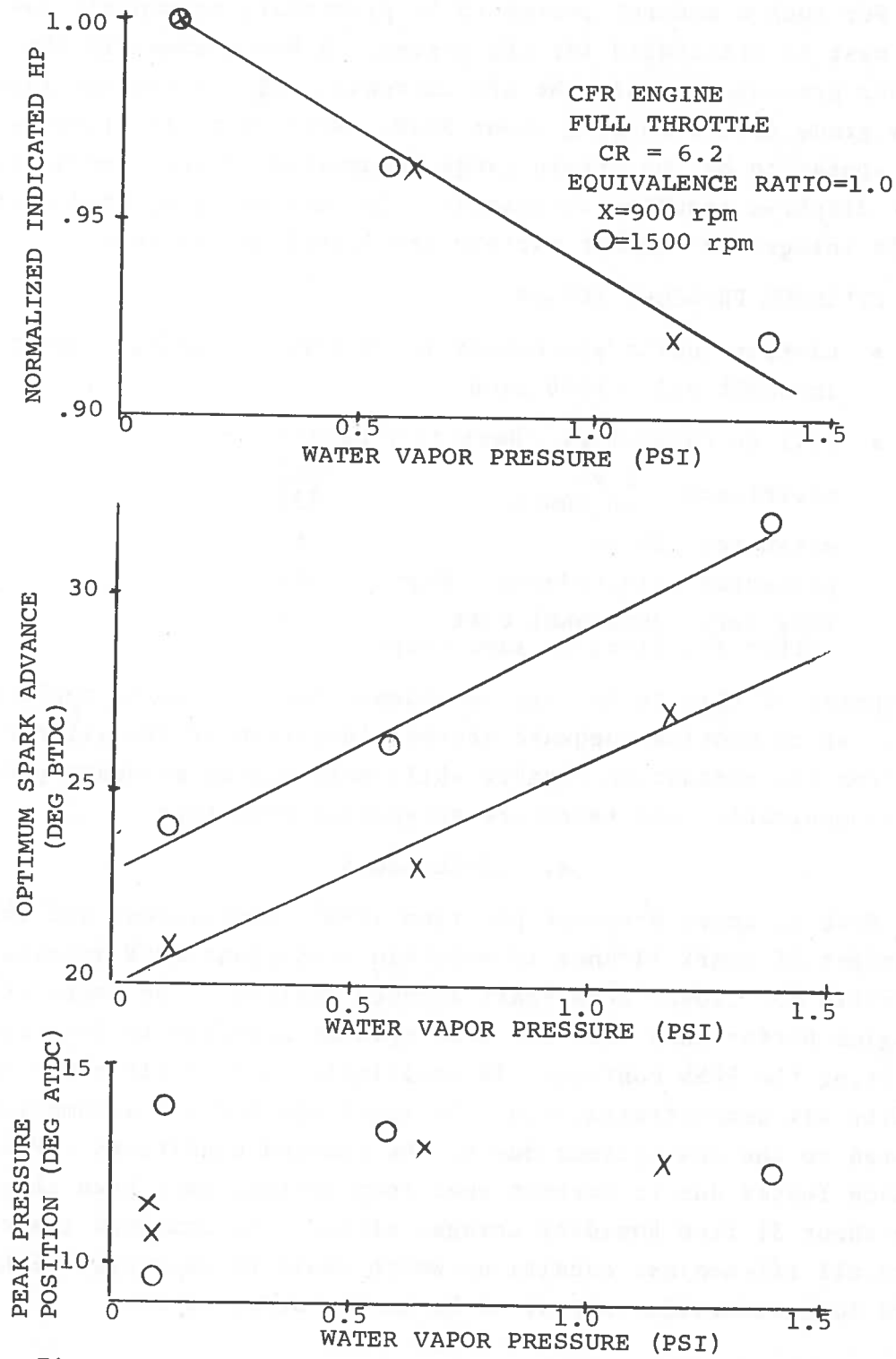


Figure 9 Power, Optimum Spark Advance and Peak Pressure Position Versus Intake Humidity ( $H_2O$  vapor pressure)



For such a control system to be practical, reasonably low costs must be attainable for the system. A key element is the cylinder pressure sensor. We are currently using a Kistler laboratory grade device costing about \$500. More cost effective devices appear to be the strain gauge integrated circuit techniques or the diaphragm inductor techniques. Current and projected costs for the integrated circuit variety are listed as follows:

#### CYLINDER PRESSURE SENSOR

- Kistler quartz piezoelectric (laboratory model, vibration insensitive) ~ \$500 each
- Silicon technology --Resistive device
 

advertised	1/yr	~\$65
	10,000/yr	~\$35
estimated	1M/yr	~\$7
projected with redesign	1M/yr	~\$3
long term functional cost		~\$1
(other functions on same chip)		

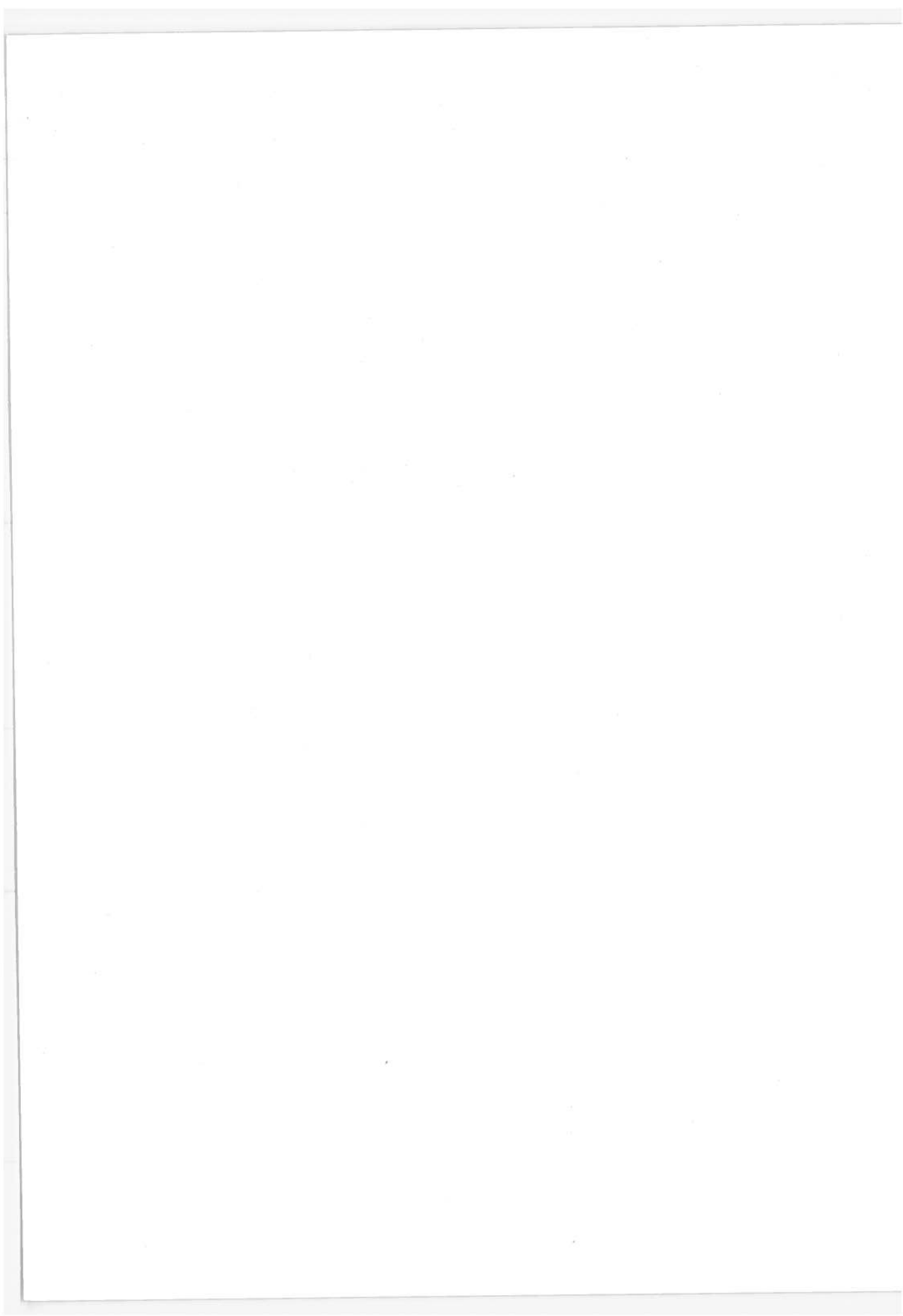
Development of this technology is planned for the engine application so as to provide adequate thermal isolation of the silicon chip from the combustion chamber while maintaining adequate pressure communication and therefore acceptable bandwidth.

#### 4. CONCLUSIONS

Peak cylinder pressure position (PPSN) measurement and the adjustment of spark advance to maintain a constant PPSN appears attractive for closed loop spark advance control. The degradation in engine performance over the true optimum schedule is less than 0.1% using the PPSN control. Insensitivity to fuel-air ratio and humidity was demonstrated, i.e. the spark advance was automatically adjusted to the new optimum due to the changed conditions. Performance losses due to current open loop systems have been shown to be about 3% from humidity changes alone. The combined losses due to all off-nominal conditions which could be recovered with a closed loop controller appear to be on the order of 5%.

#### REFERENCES

1. Hubbard, Mont, and Powell, J.D., "Closed-Loop Control of Internal Combustion Engine Exhaust Emissions", Stanford Univ., SUDAAR Report No. 473, Feb. '74.
2. Nakajima, Shinoda, Onoda, "Toyota Paper on Atmospheric Effects", Society of Automotive Engineers, SAE 690166.



## DEVELOPMENT OF THE VALVED HOT-GAS ENGINE

Joseph L. Smith  
Massachusetts Institute of Technology  
Cambridge, Massachusetts

### ABSTRACT

The Massachusetts Institute of Technology (MIT) valved hot-gas engine is a closed-regenerative-cycle engine using helium or hydrogen as the working fluid and a reciprocating compressor/expander. By utilizing a low molecular weight gas at a high mean pressure, high power densities and high efficiency (similar to the Stirling engine) can be achieved with moderate heat transfer surface. Actual thermodynamic operation of the MIT hot-gas engine is nearly the same as for the Stirling engine, with comparable mean pressure, pressure ratio, operating temperatures, power density and efficiency. The major difference is in the heat transfer components. The MIT engine employs heat exchangers with steady (in multi-cylinder configurations) unidirectional flow at constant pressure, where as the Stirling machine uses heat exchangers (and regenerator) with oscillating flow and pressure. The advantages for the MIT engine are greater design flexibility (a single direct heater) and direct cooling, since increased heat exchanger gas volume does not degrade engine performance. In addition the heat load on the regenerator is reduced. The engine employs poppet valves in the expander and check valves in the compressor. By adding variable timing to the valves the engine will have rapid response to load changes and should be capable of good efficiency at part load and with frequent changes in load.

The objective of the development program is a rapid advancement toward the full potential of this engine concept. The current work on the project is to obtain maximum information from the existing engine. Analytical and experimental work is underway to explain more fully the observed engine performance characteristics. Additional work on a new heater will allow high power operation of the experiment. An investigation of variable valve timing for power control will be started soon.

### 1. INTRODUCTION

A new valved, hot-gas engine (VHGE) has been under investigation at MIT since 1969 when the late Dr. Vannevar Bush renewed his long standing interest in hot-gas engines. The ultimate objective of the project is the development and commercial realization of a power plant for transportation vehicles which will provide low emission of pollutants while achieving highest energy conversion efficiency.

In the early part of the program the concept for the VHGE was evolved, and an analytical basis for the design was formulated. Later an experimental VHGE was constructed and tested. The encouraging results were reported by Fryer<sup>1</sup> and Hankard<sup>2</sup> and were presented at the 1973 IECEC<sup>3</sup>.

Based on this preliminary work, the present DOT Office of University Research program was initiated to bring the state of knowledge of the VHGE system to the level of other systems currently under investigation so that the relative merits and potentials can be evaluated.

## 2. DESCRIPTION OF THE ENGINE

The MIT, valved, hot-gas engine is a closed-regenerative-cycle engine which uses helium or hydrogen as the working fluid and employs a reciprocating expander/compressor, as shown in Figure 1. The six major components of the engine are: compressor, expander, burner/heater, regenerative counterflow heat exchanger, cooler, and a crankcase/crosshead mechanism. The expander and compressor are on opposite ends of an elongated piston (displacer-piston). The expander employs mechanically operated poppet valves and the compressor employs spring loaded check valves.

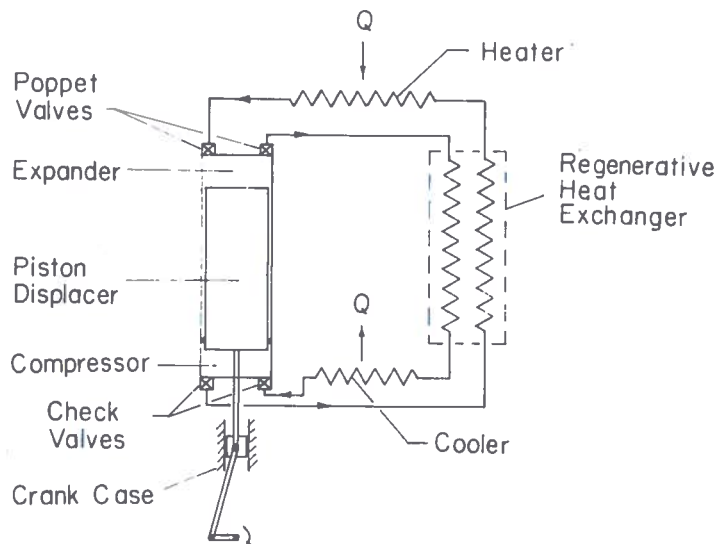


Figure 1. Schematic of the Valved Hot-Gas Engine

The VHGE operation closely follows an ideal Brayton cycle. Hot, high-pressure gas from the burner/heater is expanded nearly reversibly and adiabatically in the expander. Low-pressure exhaust gas from the expander is first cooled in the regenerative heat exchanger and then in the cooler. Cool, low-pressure gas from the cooler is compressed nearly reversibly and adiabatically in the compressor. The high-pressure gas is then preheated in the regenerative heat exchanger and then heated to maximum temperature in the burner/heater. The clearance volume in the compressor is adjusted to provide the desired pressure ratio of about two to one. The entire cycle operates at a mean pressure in the range of 1000 to 3000 psi. The back-to-back arrangement of the compressor and expander allows direct flow of the compressor work from the expander so that the crank mechanism need be designed only for the net power of the engine. In addition only one set of double acting piston rings are required.

In the final developed configuration, the engine is expected to have multiple expander/compressor cylinders (perhaps four) connected with a single heater, a single regenerator and a single cooler, each operating with steady (rather than pulsating) gas flow. By utilizing a low molecular-weight gas flowing steadily at a high mean pressure, the VHGE can achieve a high power density and a high efficiency with a moderate requirement for heat transfer surface. The VHGE has the low-pollution and multifuel capability of an external combustion system. In addition, preliminary work has indicated that the VHGE system should be able to offer high efficiency under frequent and rapid changes in power as required in vehicular applications. The concept is to use variable valve timing to reversibly vary the mass of gas circulated, rather than using an irreversible pump-up, blow-down system to change the gas charge in the engine.

### 3. COMPARISON OF VHGE AND STIRLING ENGINE

In spite of different ideal thermodynamic cycles, the thermodynamic operation of the VHGE is in reality reasonably close to the operation of practical Stirling engines. The ideal isothermal Stirling cycle consists of reversible isothermal compression and

expansion with constant volume regeneration. The ideal cycle for the VHGE is the closed Brayton cycle with reversible adiabatic expansion and compression with constant pressure heat exchanges. Since the idealizations introduce false differences, it is best to compare on the basis of operating, open-system components for each thermodynamic function.

As is shown in Figure 1, the double acting piston-cylinder of the VHGE is quite similar to that of the four-cylinder double acting Stirling engine. In addition the two engines each have three heat exchange components to perform heating, regeneration and cooling functions as shown in Figure 2 and Figure 3. In the heat exchange components of the Stirling machine, the gas flows at different pressures and are separated in time (the gas pressure within changes with time). In the BHGE, the gas flows at different pressures are separated in space (the gas pressure within is constant in time). Thus the VHGE must have expander and compressor valves and a two-passage, counter-flow heat exchanger for regeneration. However, the gas within the heat exchange components of the Stirling engine must be expanded and compressed each cycle. Thus, the gas volume (dead volume) must be kept very small in the Stirling engine. In a multicylinder Stirling, each cylinder requires a separate set of heat-exchange components.

The advantage of the VHGE is that the heat exchange components are single steady-flow units which can be designed and arranged without the dead volume limits of the Stirling engine. For example the working gas can be used directly in the radiator without a cooling water system. The heater can be designed with adequate air side surface and can be arranged for optimum burner design.

Another advantage of the VHGE is shown by the temperature distributions shown in Figure 2 and Figure 3. In the Stirling engine the high temperature end of the regenerator is nearly at the maximum temperature for the cycle. Thus the high pressure gas is already nearly at inlet temperature a before it enters the heater h. The temperature of the gas drops during expansion

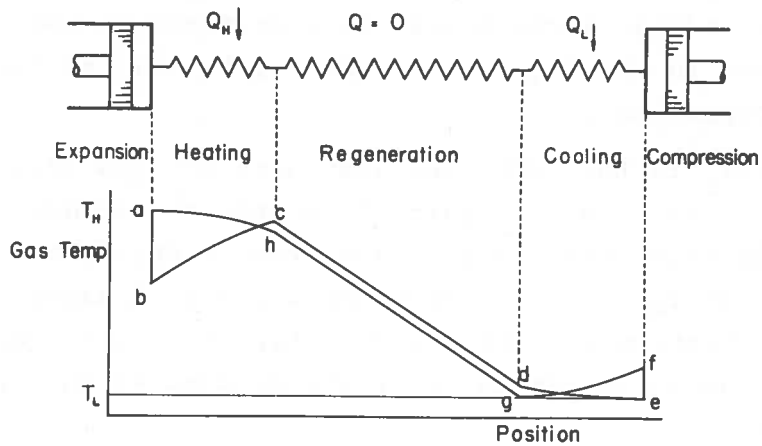


Figure 2. Temperature Distribution for Stirling Engine

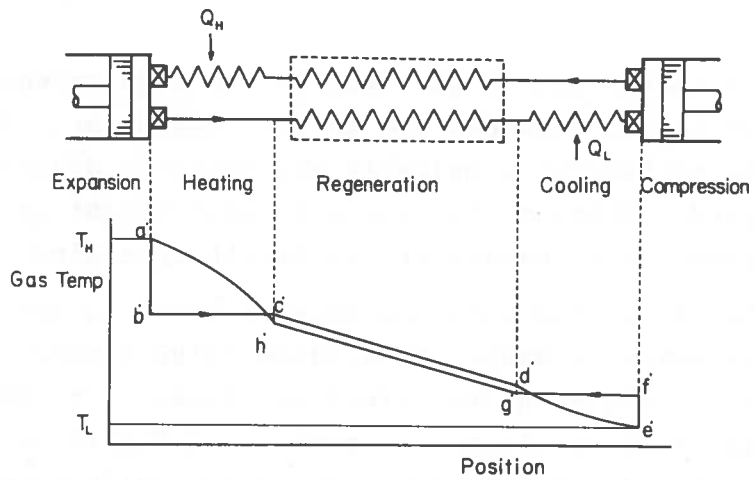


Figure 3. Temperature Distribution for Valved Hot-Gas Engine



from a to b, Figure 2, so that the cooler exhaust gas is heated as it passes through the heater from b to c, nearly back to  $T_H$ . The low pressure gas is then re-cooled during regeneration. Thus, most of the heat added in the heater is transferred to the low pressure gas then to the regenerator and finally to the high pressure gas ready for expansion.

In contrast, in the VHGE, the high pressure gas leaves the regenerative section at h', (Figure 3), nearly at expander exhaust b'. The high pressure gas is heated in the heater from h' to a' nearly up to  $T_H$ . The cooler exhaust gas b' bypasses the heater and enters the regenerative section directly c'. This reduces the heat transfer load on the regenerator and eliminates one flow pass through the heater.

In the same manner the VHGE cools the low pressure gas d' to c' before it enters the compressor rather than cooling the compressor discharge f to g which must then be immediately reheated in the regenerator.

The VHGE has the advantage over the Stirling engine in directly heating expander inlet gas and compressor inlet gas, which reduces the heat load and temperature span on the regenerative section.

The major disadvantage of the VHGE is the requirement for mechanical valves in the expander and in the compressor. The valves add to the mechanical complexity and impose a dynamic limit on the engine speed. However, the low molecular weight gas requires smaller valves than for a comparable air breathing engine.

On the other hand, the valves provide a means to realize control of engine power by means of variable valve timing. The power is adjusted by changing the effective displaced volume of the expander and compressor as shown in Figure 4 and Figure 5. This changes the mass circulated (and thus the power) while maintaining constant pressures and temperatures throughout the engine. The flow into the expander is reduced by adjusting the cut off from c to c' and the exhaust valve is opened at R' rather than R to avoid over expansion of the reduced mass of gas. The exhaust valve

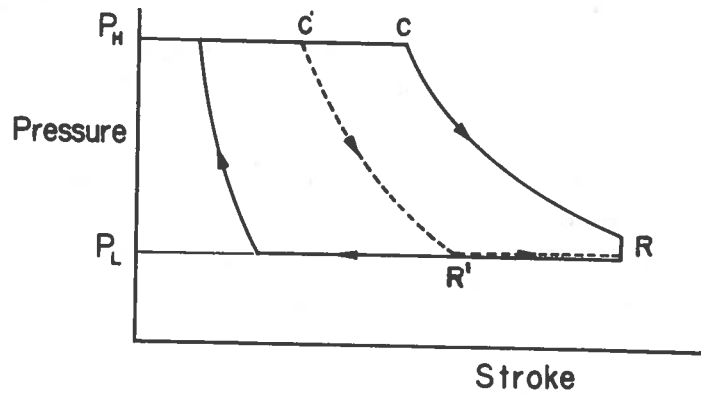


Figure 4. Expander Diagram with Variable Valve Timing

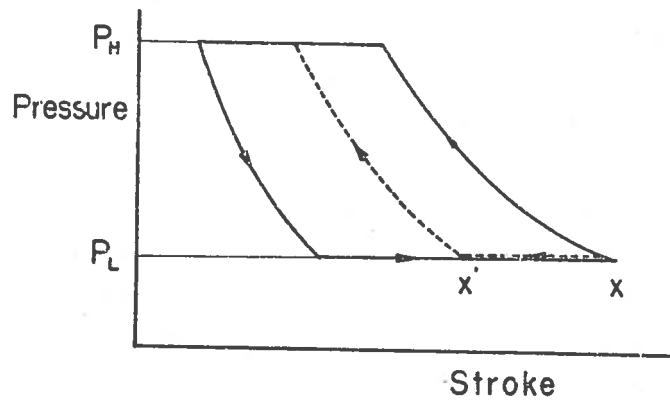


Figure 5. Compressor Diagram with Variable Valve Timing

breathes freely from  $R'$  to  $R$  with inflow of low pressure gas, which is then reexhausted on the exhaust stroke. The flow into the compressor is reduced the same amount by keeping the compressor inlet valve open from  $x$  to  $x'$  with the excess gas flowing back out the inlet valve. With this system the engine power can be changed in only a few strokes without blowing down high pressure gas or drawing on an auxiliary reservoir of high pressure gas. Since no blow-down and pump-up are required to change power, the VHGE could change power frequently (as in automotive applications) without loss of efficiency. The development of the mechanism for variable valve timing is a significant challenge and will require considerable effort.

#### 4. SCOPE, PROGRESS AND RESULTS FOR PRESENT PROGRAM

The first part of the program is to obtain maximum information from the present experimental engine. The preliminary tests of the experimental engine performance did not reach expectations. The first task was to determine the reason and improve the analysis. The symptom was that the indicated compressor power was 1.8 times the expected value. In addition the compressor clearance volume adjustment had to be set at the minimum value in order to achieve rated pressure ratio. The compressor diagram was, however, nearly ideal for the clearance volume setting. The expander power and the expander diagram were about as expected. The problem was first thought to be gas leakage from high pressure to low pressure. Static tests revealed no fixed leaks in the system and a static seal leakage much too small to produce the observed effects. A series of dynamic piston ring leakage tests were run in an attempt to verify the leakage. None of the tests clearly showed evidence of enough leakage to explain the problem. Then the engine is run at various speeds and mean pressure levels, the expander and compressor indicator diagrams are always similar. This indicates that the leakage, if present, must be proportional to speed and mean pressure and must occur for the most part while valves are simultaneously open in both expander and compressor. Otherwise the indicator diagrams would have to be far from ideal. In spite of considerable effort the cause of the problem is still not positively identified.

At the present time, work is underway to provide transient gas temperature measurements at the gas ports inside the compressor and the expander. These measurements are expected to evaluate the influence of heat transfer between the gas and the ports and the cylinder wall. This should allow the influence of leakage to be separated from reduced volumetric efficiencies caused by wall-to-gas heat transfers.

The experimental engine is also being improved to allow operation over a wider range of speeds and pressures. The engine has previously been rearranged and adequate mechanical support provided for heat transfer components. Presently the engine can be operated regularly to 1000 RPM with 1200 RPM a maximum because of the unbalanced crank base.

A new electric heater of 60 kW has been designed and is now being constructed for the experimental engine. Fabrication of parts is now complete and final assembly into the pressure case will begin in the near future.

The second part of the present program is the continued development of an accurate and reliable model for calculating the performance of a VHGE of a given design. Work is currently underway to develop a method of following the unsteady processes in the expander and the compressor by means of a numerical step-by-step integration. The effects of wall-to-gas heat transfer and of piston ring leakage will be included. The current experimental effort is directed toward measurements in the engine which will supply basic data for the analysis.

The third part of the present project is an investigation of variable valve timing for improved power control of the VHGE as has been described previously. The influence of variable valve timing will be included in the analytical model for the operation of the VHGE. The various options for achieving variable valve functions will be investigated analytically and experimentally. Work on this part of the project will be started in the near future.

## 5. FUTURE PLANS

It is expected that the results of the present work will establish the basis for the future design of a fully optimized VHGE. The projected performance of this design can then be compared with other alternate engine systems. A favorable comparison will justify the construction and testing of an optimized prototype VHGE.

## REFERENCES

1. "Design, Construction and Testing of a New Valved, Hot-Gas Engine", B.C. Fryer, MIT Sc.D. Thesis, October 1972.
2. "Instrumentation and Testing of a Closed, Reciprocating, Brayton Cycle Engine", T.R. Hankard, MIT S.M. Thesis, May 1973.
3. "Design, Construction, and Testing of a New Volved Hot-Gas Engine", B.C. Fryer and J.L. Smith, Jr., Proceedings of the Eighth Inter-Society Energy Conversion Engineering Conference, AIAA, August 1973, pp. 174-181.

## ALCOHOLS AS VEHICLE FUEL EXTENDERS

R. T. Johnson  
University of Missouri  
Rolla, Missouri

### ABSTRACT

The major purpose of this study can best be described as a characterization program. The major objectives are to provide a basically unbiased report of the effects of adding alcohol to unleaded gasoline to increase the volume of liquid fuel for vehicle use. Areas being examined include:

1. Octane characteristics of alcohol-gasoline blends.
2. Engine parameter studies to determine if spark timing and other engine variables can be adjusted to maintain fuel economy and control emissions.
3. A brief study of the relationship between exhaust aldehydes and fuel alcohol content including the effect of a platinum oxidizing converter.
4. A simulation of the Federal Test Procedure (FTP) for emission certification to determine the effect of fuel alcohol on emissions and fuel economy for this well recognized data form.

Methyl alcohol or Methanol was chosen as the most important alcohol to be used in this study because the technology now exists to manufacture it from coal.

The octane test program for methanol-gasoline blends has been completed and a brief summary of these results will be presented. In addition, a brief description of the methods being used for other phases of the program will be given.

### 1. INTRODUCTION

Alternate fuels research at the University of Missouri - Rolla (UMR) began a few years ago when we started examining total system efficiency from raw materials to vehicle wheels. The basis for this study was to identify alternate energy sources which might provide some relief to the liquid petroleum shortage we expected to occur. The decision to examine methyl alcohol (methanol) as the first of these liquid fuels was based on a variety of information. The available literature indicated that technology existed

to manufacture methanol from coal, garbage, and other resources that were abundant in this country. In addition, the sketchy information available in the open literature indicated that the expected thermal efficiency for manufacturing methanol from coal was between 50 and 70 percent compared to the possible 50 percent efficiency indicated for synthetic crude oil processes.

## 2. PRESENT CONCEPT

Our initial, and present, concept was to consider methanol as a gasoline extender. It could simply be a bulk liquid to extend the gasoline pool. We consider methanol to have no particular advantages as a liquid fuel. Rather, it is a way to get the needed liquid energy into our transportation system within the next 5 to 10 years. Our position is neither pro nor con. We simply want to be sure that information concerning the emissions, fuel economy, and other characteristics of this fuel is available in literature used in the decision making process.

## 3. PROGRAM DETAILS

The present program at UMR is basically a characterization program. In that program we have elected to use small displacement engines and light vehicles. We feel that shortages and high fuel costs will make this type of vehicle a larger portion of automobile population in the next few years. Current work is divided into two basic programs. One program is to characterize emission, fuel economy, etc., for small displacement vehicles using a simulation of the Federal Test Procedure (FTP) for emissions from light duty vehicles and the LA-4 driving cycle. The second program is a single cylinder engine study examining the effects of engine parameter changes on the emissions, etc. of the methanol-gasoline blends.

## 4. FEDERAL TEST PROCEDURE SIMULATION

The Federal Test Procedure (FTP) simulation requires additional explanation. The normal emission test procedure for light duty vehicles collects a diluted exhaust sample in bags during various phases of the test. At the end of each phase the concentration of pollutants in the bag is analyzed and used to compute

the emissions on a mass basis. This system gives average results for the entire test but no specific information about how various operating modes influence emissions and fuel economy. Our desire for more specific information and our lack of capital to acquire a Constant Volume Sample system dictated a different approach to measuring emissions during the LA-4 driving cycle. Our approach is to monitor the undiluted exhaust, acquire time history data of the emissions, fuel flow, etc., and use a modal analysis technique to determine the mass emissions and fuel economy.

In terms of equipment, we are using the engine and drive train from a small vehicle and a chassis dynamometer to simulate a vehicle on the dynamometer during the test. The analysis instruments used are rapid response, on-line analyzers. Figure 1 is a schematic of the analysis instrument system. In the setup and calibration of our instrumentation system we are developing techniques for calibration and reporting of the approximate methanol content of exhaust hydrocarbons.

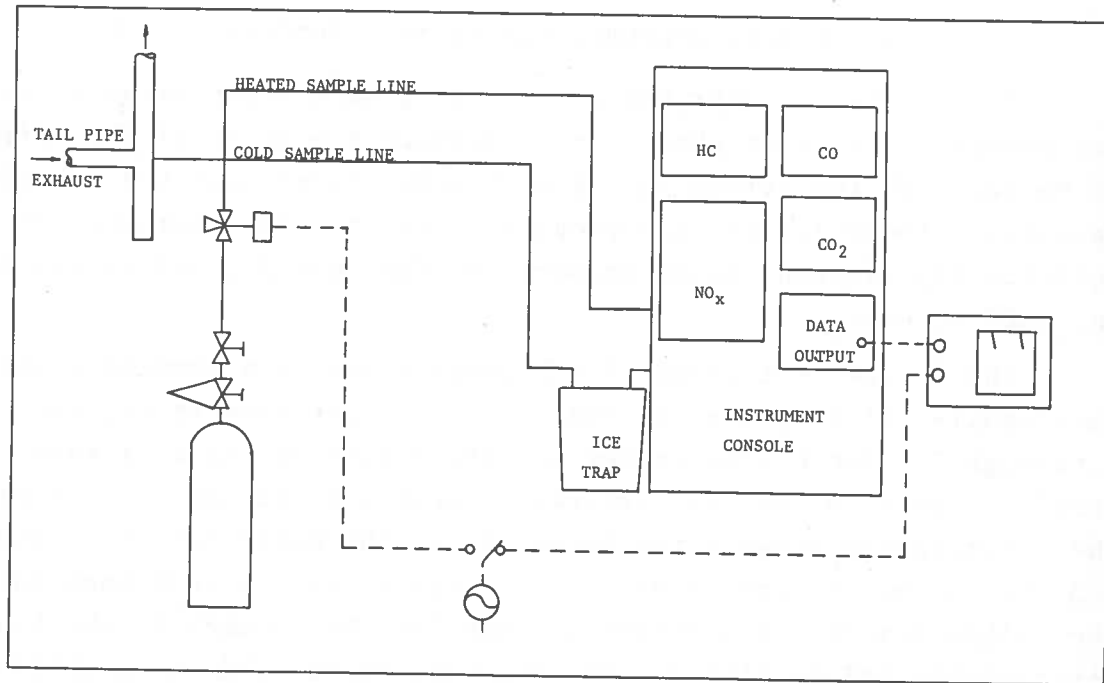


Figure 1. Diagram of the Analysis Instrument System



In order to use modal analysis to determine the mass emissions from undilluted exhaust gas, an enormous amount of data must be taken. A data acquisition system is a necessity for this type of analysis. In an effort to meet our specialized needs within reasonable cost constraints, we designed and constructed a data acquisition system that allows us to monitor HC, CO, CO<sub>2</sub>, NO<sub>x</sub>, fuel flow, vehicle speed, an ignition key synchronization signal, and up to nine additional channels of information. Figure 2 is a schematic of this data acquisition system.

In order to effectively process the data acquired during a simulated emissions test, the digital data recorded on the test tape must be entered into the computer. Figure 3 is a schematic representation of the process used to enter this data into the computer system. Once the data is in the computer system, it is corrected for instrument calibration. Time response and computations for grams/mile of the measured pollutants are then made. Results for each mode are presented below in addition to emission fuel economy results for the entire test.

#### 5. SINGLE CYLINDER ENGINE TEST PROGRAM

The single cylinder engine test program was separated into two phases. The first phase was to develop a picture of the effect of methanol on the octane rating of blends of methanol and unleaded gasoline. Phase two of this program is related to examining the relationship between engine parameters, fuel blends, and emissions and fuel economy.

The octane test phase of the program has been completed and the results are displayed in Table 1 and illustrated in Figures 4 through 7. Table 1 describes the properties of the four base gasolines used in the test program. Figures 4 through 7 illustrate the relationship between the Research and the Motor octane ratings and the volume percent of methanol in the blend for each base fuel. The volume percent of methanol is based on the volumes of the two constituents before mixing. For the base fuels used it is obvious than methanol has a significant effect on the research octane rating of the blend. However, it is also apparent that the motor

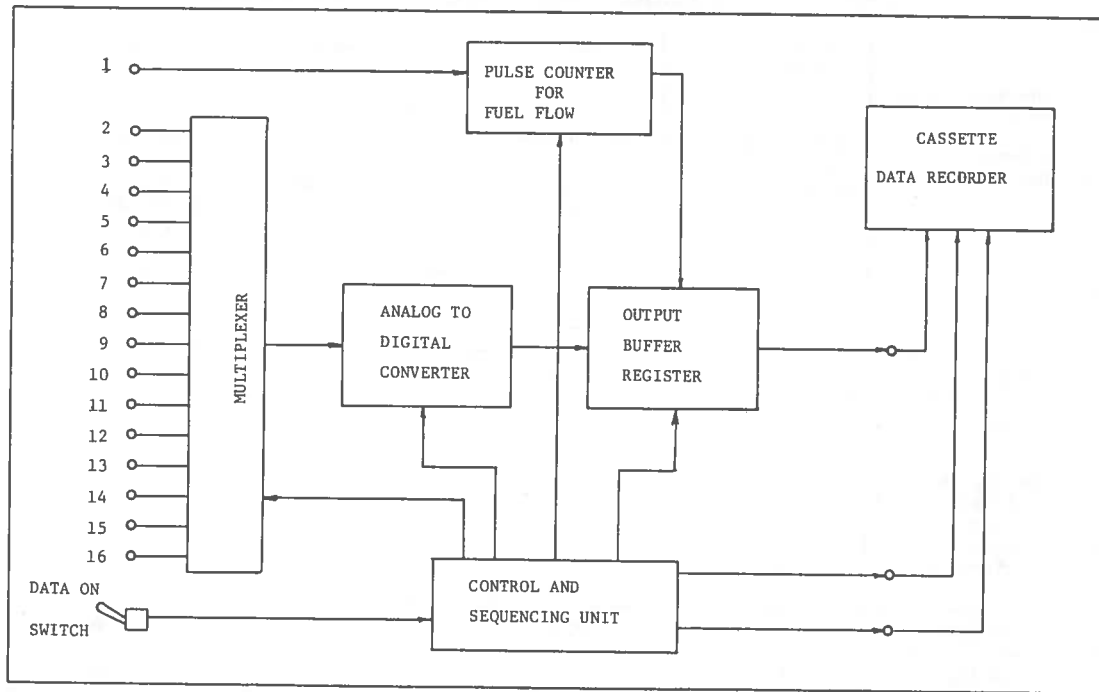


Figure 2. Diagram of Data Acquisition System

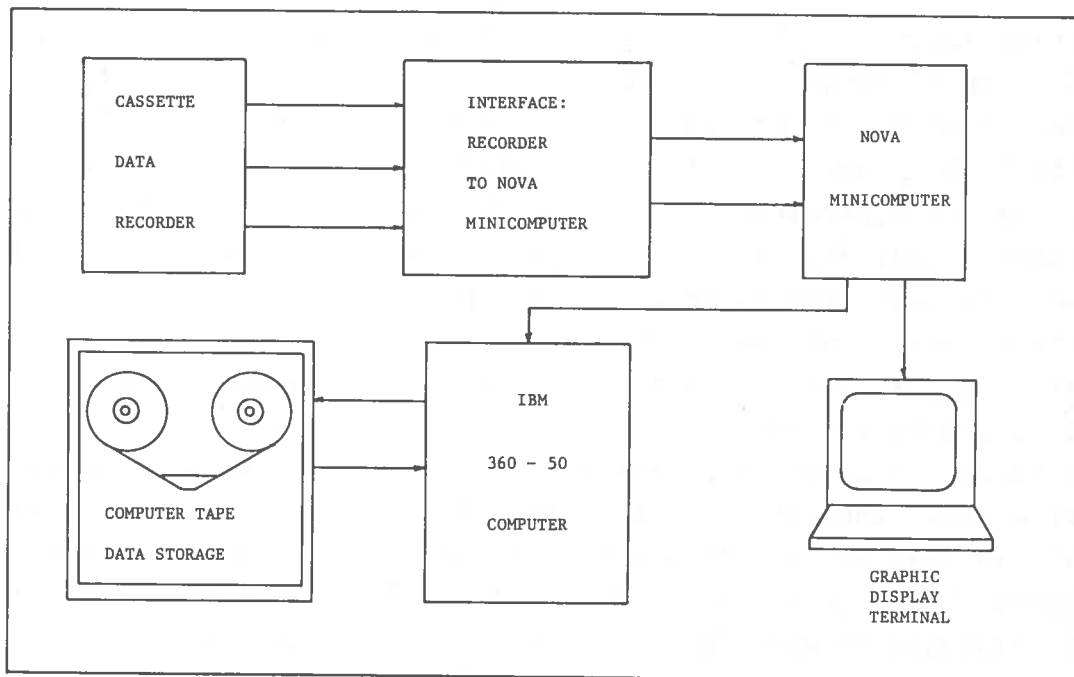


Figure 3. Diagram of Computer Input Process

TABLE 1 GENERAL BASE FUEL CHARACTERISTICS

characteristic	Base Fuel A	Base Fuel B	Base Fuel C	Base Fuel D
General Description	Summer blend of regular grade gasoline without TEL	Summer blend of regular unleaded gasoline commercially available	Summer blend of premium type unleaded gasoline for 1975 & later vehicles	Indolene (6) unleaded, reference fuel specified for use in vehicle emission certification
RON	81.1	89.9	95.8	98.1
MON	75.5	82.1	87.1	87.6
Nominal HC Distribution (%)				
Olefins	1.0	12 - 15	1.0	10
Aromatics	31.0	20 - 25	27.5	35
Saturates	68.0	68 - 60	71.5	55
$\Delta N$ (RON)	30.35	20.85	14.05	12.00
$\Delta N$ (MON)	10.65	4.10	1.96	0.66
K (RON)	0.02759	0.02583	0.03426	0.02896
K (MON)	0.03743	0.02919	0.0251	0.0345

octane rating of the blend is not affected substantially by the addition of methanol. The Blending Octane Value (BOV) for different concentrations of methanol in one base fuel is shown in Figure 8. This figure shows that the BOV changes with methanol concentration and is not a parameter which depends only on the base fuel. The octane number data were applied to a simple first order exponential equation using two parameters. The parameter  $\Delta N$  is called the octane number increment and is an asymptotic quality. A second parameter, K, the base fuel response factor, gives an indication of how sensitive the base fuel is to small concentrations of methanol. A large value for K indicates a large octane increase for a small concentration of methanol. Figure 9 illustrates the relationship between  $\Delta N$  and the octane number of the base fuels tested. This information implies that for the fuels tested methanol produced no degradation of the octane ratings and in fact provided an increase in the octane ratings of the lower octane base fuels.

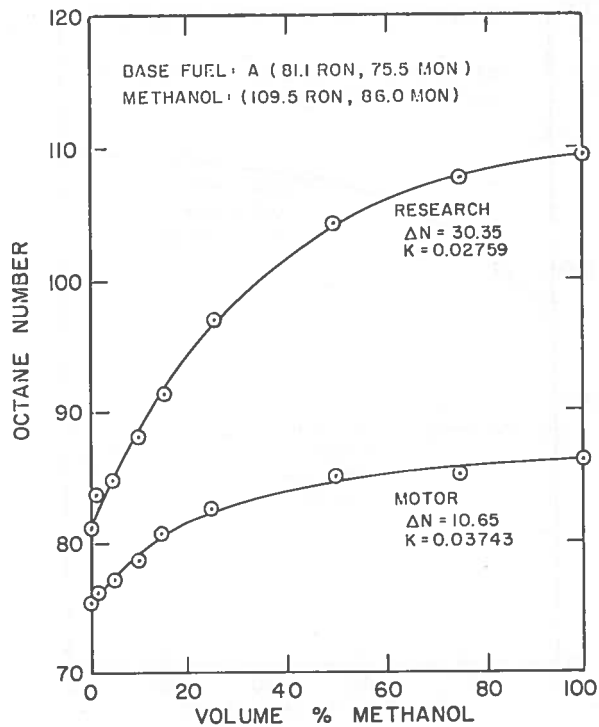


Figure 4. Relationship Between Octane Number and Volume of Methanol-Base Fuel A

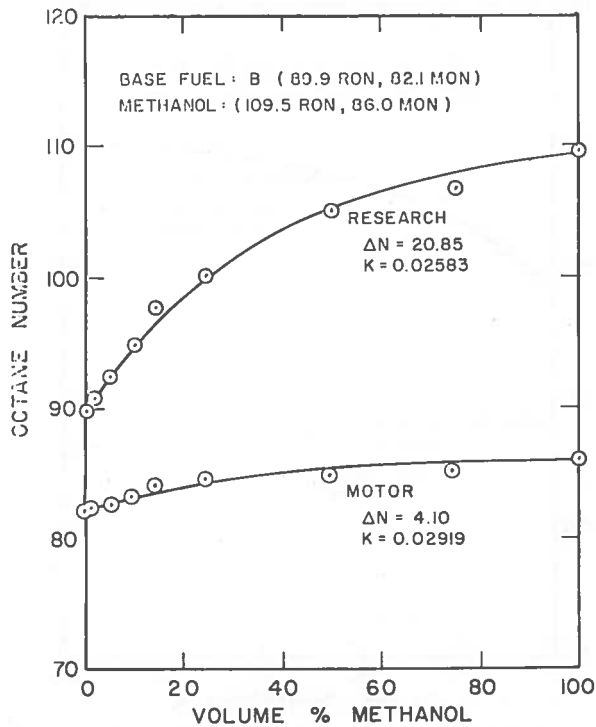


Figure 5. Relationship Between Octane Number and Volume of Methanol-Base Fuel B

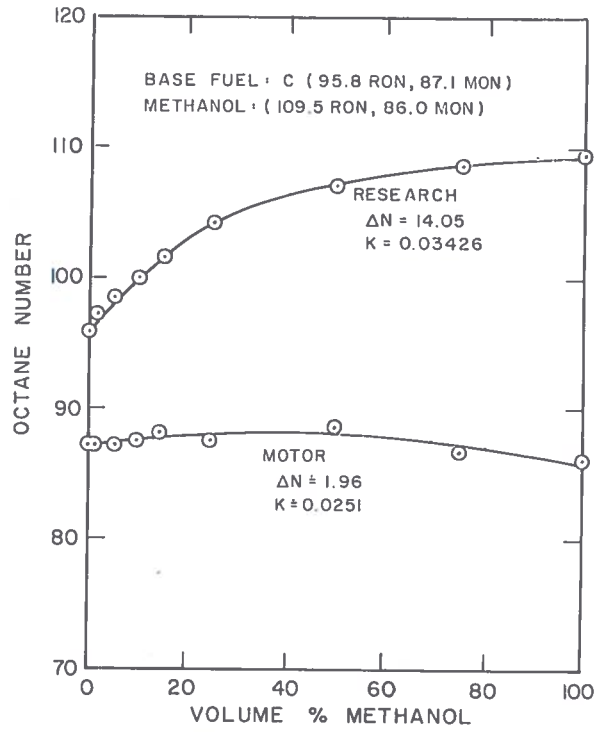


Figure 6. Relationship Between Octane Number and Volume of Methanol-Base Fuel C

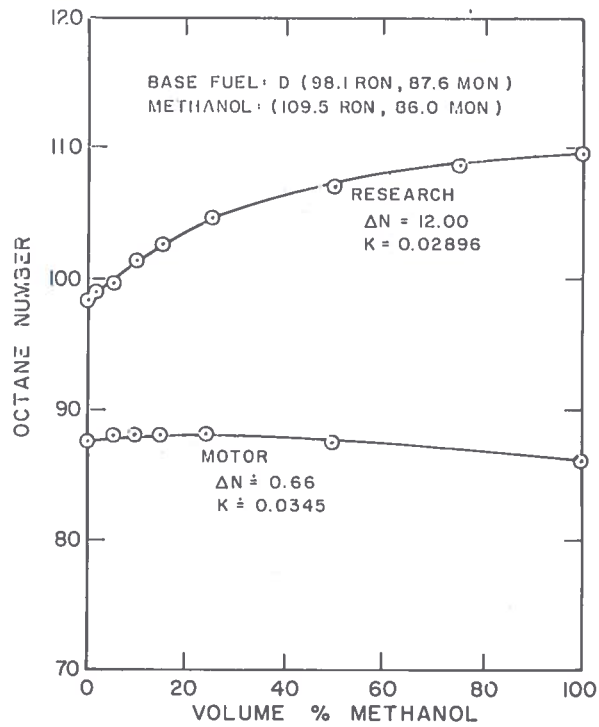


Figure 7. Relationship Between Octane Number and Volume of Methanol-Base Fuel D

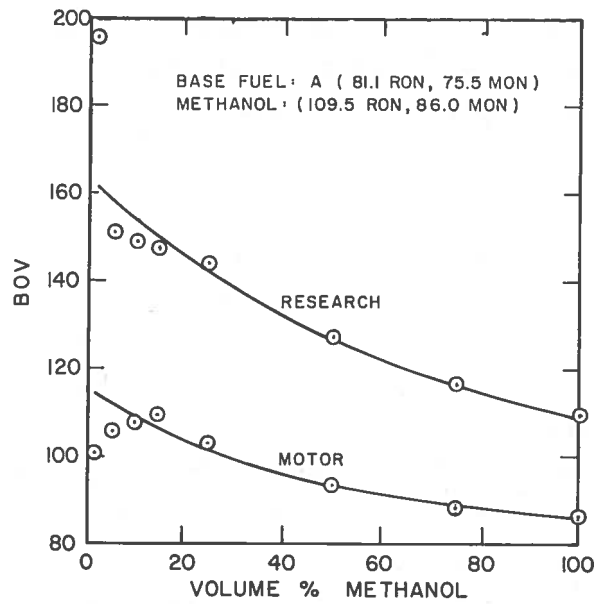


Figure 8. Blending Octane Value (BOV) versus Volume of Methanol-Base Fuel A

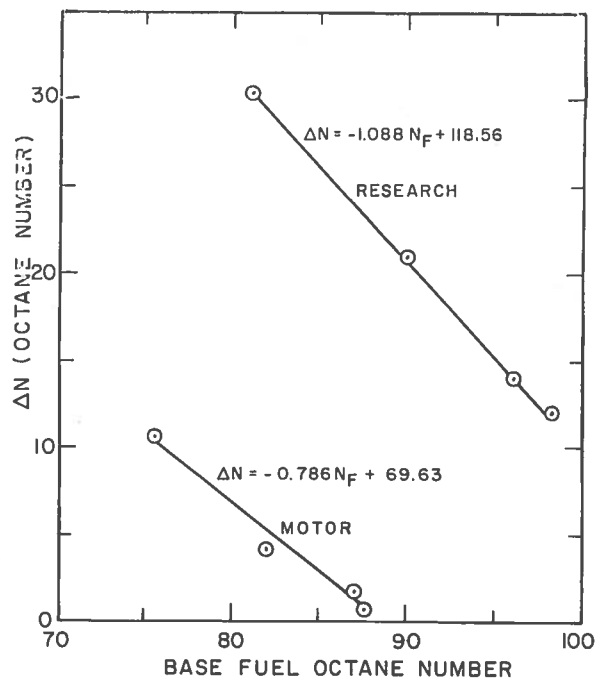


Figure 9. Relationship Between  $\Delta N$  (Octane Number) and Base Fuel Octane Number

The results of the octane test program have been used to modify the planned test program for engine and fuel parameters. In examining the motor octane data, it appears that there is little to be gained in examining higher compression ratios or methanol concentrations.

In addition to examining the effects of variations in spark timing, air-fuel ratio, and compression ratio on the emissions and fuel economy of several methanol-gasoline blends, this program is designed to examine the possible increase in aldehydes from fuels containing methanol. The DNPH gravimetric method is being used. Very preliminary data indicate that about 70% of the aldehydes in the sample are formaldehyde and the results are being presented as formaldehyde. Although the data are insufficient for any conclusions, preliminary results show a 33% increase in aldehydes with 10% methanol in one of the base fuels. After complete baseline data for the aldehydes emissions from selected mixtures is obtained, duplicate data will be taken with a platinum converter in the exhaust to determine if there is a significant effect on the aldehydes.

At the conclusion of the single cylinder engine test program any substantial gains in emission control or fuel economy will be verified using the FTP simulator.

## PERFORMANCE AND EMISSIONS OF HYDROGEN FUELED INTERNAL COMBUSTION ENGINES

P. C. T. de Boer, W. J. McLean and H. S. Homan  
Cornell University  
Ithaca, New York 14850  
U.S.A.

### ABSTRACT

A description is given of the differences between hydrogen engines and engines running on hydrocarbon fuels. The differences arise from properties of hydrogen such as high flame speed, a very low lean flammability limit, low ignition energy and high ignition lag times for auto-ignition at high pressures. These properties provide the potential of high thermal efficiency at part load, by operating the engine unthrottled with lean mixtures. They also are the cause of pre-ignition and backfiring problems. The latter problems can be solved in a number of ways, among which are the use of either direct cylinder fuel injection, or of lean mixtures, or of low compression ratios. Direct cylinder injection has the additional advantage of providing a high maximum power output. A detailed discussion is given of the thermal efficiency of hydrogen engines. Also discussed are phenomena leading to irregular engine operation such as surface ignition and spark knock. While spark knock occurs only at very high compression ratio, and generally does not appear to have very serious consequences in hydrogen engines, it may cause the engine to run rough. Even at moderately high compression ratios, combustion in hydrogen engines is accompanied by pressure waves. A detailed analysis is given of NO production. For lean mixtures the NO emissions are limited by the rate of formation, and for rich mixtures by the rate of decomposition during the expansion process. NO emissions are negligibly small for fuel-air equivalence ratios below about 0.55. Peak NO emissions occur at equivalence ratios near 0.8, and are of the same order as for gasoline engines. It is concluded that the hydrogen engine is a practical possibility, likely to find a number of applications within the next few decades.

### 1. INTRODUCTION

The idea of using hydrogen as a fuel for internal combustion engines occurred very early in the development of these engines. Hydrogen always seemed attractive from several points of view: it mixes easily with air, the resulting mixture has wide flammability limits, is easily ignited, and has a large flame speed. In addition, the product of combustion, water, is non-polluting, non-odorous, and not objectionable in other ways. Furthermore, the heat of combustion per unit mass is much higher for hydrogen than for any other fuel. Using a gaseous fuel such as hydrogen rather than a liquid one obviates such problems as achieving fuel atomization and evaporation during cold start and warm up, uneven distribution of fuel to different cylinders arising from the existence of a liquid film on the walls of the intake manifold, and unwanted variations in air-fuel ratio during transient conditions such as acceleration and deceleration. While it has appeared that the problems cited with liquid fuels can be overcome without great difficulty, this was not obvious during the early phases in the development of the internal combustion engine.



The first investigator of record proposing the use of hydrogen as an engine fuel was the Rev. W. Cecil, who presented a paper "The application of hydrogen gas to produce a moving power in machinery" to the Cambridge Philosophical Society in the year 1820. At the time, engines of the vacuum principle were being developed. In Cecil's engine, an explosion of hydrogen and air heated the mixture, which was allowed to expand to atmospheric pressure. Cooling the mixture then created a partial vacuum, and the actual work was provided by the atmospheric pressure on the piston. The engine is reported to have run satisfactorily. However, engines of the vacuum principle never were used on a large scale, and were later displaced by engines where the motive power was derived from the pressure rise resulting from combustion.

Interest in hydrogen was revived in the 1920's, by which time the internal combustion engine had been developed to a large extent in its current form. Investigators of note were Ricardo and Burstall, who established that hydrogen could be used successfully as an engine fuel, but that it tended to pre-ignite and to cause backfiring into the carburetor. Pre-ignition could be avoided by keeping the compression ratio low (below about 5 or 6).

A very active program on hydrogen engines was pursued by Erren, first in Germany and later in England. Erren documented many important ideas in the form of patents. Among other topics, he considered the possibility of fuel injection, stressing that this should solve the pre-ignition and backfire problems. He also considered the possibilities of constant pressure combustion by regulating rate of injection, of "quality regulating" the power output of an unthrottled engine, and of high pressure electrolyzers to generate hydrogen. Erren published very few papers in technical journals. Of these, only one [Erren and Campbell, 1933] provided detailed technical information, consisting mainly of theoretical considerations. This paper was presented at a meeting of the Institute of Fuel in London. When asked what IMEP (indicated mean effective pressure) had been obtained, Mr. Campbell replied that "the authors had the figures for the high efficiency engines, but all the high efficiency engines turned out so far were not their property, and the figures were not their property. Such an engine was being erected in London, however, so that those who were interested could see for themselves." However, no publications have followed about the latter engine. Recently, additional information about Erren's work has been given by Weil, who was Technical Director of the "Deutsche Erren Gesellschaft" in Germany until 1938. [Weil, 1972]

Detailed results on hydrogen engines with direct cylinder fuel injection were published by Oehmichen in 1942. Using a single-cylinder engine with a fuel injector mounted in the sidewall of the cylinder, about midway between top and bottom, he obtained many results on thermal efficiency, the effect of equivalence ratio, knock limitations, the cylinder pressure as a function of time, etc. He also considered the practicality of hydrogen production. Oehmichen concluded that "hydrogen might be used in exceptional cases for special purposes, or in stationary engines, provided large quantities would be available either as a byproduct, or where it could be produced inexpensively." We discuss Oehmichen's work in further detail later on.

Further work on carbureted hydrogen engines was done by R.O. King and associates. Captain King had been present at the meeting of the Institute of Fuel mentioned before. After Herr Erren claimed that "he could demonstrate

that one could get nearly twice as much power with hydrogen as with petrol, and that he had had to make the tests to satisfy the German patent office, because it would not grant him the patent if he could not prove the claim," Captain King replied that "it was difficult to deal with a claim of that sort; anyone making it should support it with figures, a description of the experimental methods and sufficient details to enable the critic to form an opinion. That had not been done in this case." The argument continued with a discussion of the possibility that the increase in power might be due to the super-charging effect of hydrogen cylinder injection. King also expressed the opinion that if one used mixtures which were 20% or more lean, it apparently was not necessary to use injection. In his later work, King followed up this idea in great detail. He and his collaborators proved that by keeping the engine scrupulously clean, compression ratios as high as 14 could be used for chemically correct mixtures without the occurrence of pre-ignition, back-firing or knock. At higher compression ratios, pre-ignition occurred when the mixture was chemically correct, but compression ratios of 20 were usable at equivalence ratios less than about 0.50.

In recent years, hydrogen engines have come to the forefront first of all because of their low pollution characteristics, and secondly because of the potential use of hydrogen as a synthetic fuel. The only harmful pollutant caused by the combustion of hydrogen with air is nitric oxide. Murray and Schoepel [1972] were the first to measure NO levels in the exhaust of a hydrogen engine. Using direct fuel injection during the last part of the compression stroke, they found that peak NO levels were about 14 times smaller than peak NO levels of an engine running on gasoline, and about 5 times smaller than those for benzene. These figures have been cited in many recent reports on the future of hydrogen as an alternative fuel. They also found that the lean operation which is possible on hydrogen yields extremely low NO concentrations. Subsequent work by other investigators [Stebar and Parks, 1974, de Boer et al, 1974, Billings and Lynch, 1973] has substantiated the latter conclusions, but unfortunately has shown the former finding to be incorrect. Stebar and Parks used a carbureted CFR engine with a compression ratio of 8, running on either hydrogen or iso-octane. They state that "the maximum NO emission measured with hydrogen was almost twice that obtained with iso-octane. (This trend is consistent with a higher flame temperature for hydrogen than for iso-octane). However, ultra-lean operation consistent with hydrogen's wide flammability limits permitted dramatic reduction in NO<sub>x</sub>. Emissions of NO<sub>x</sub> were extremely low for equivalence ratios less than 0.55". The work of Billings and Lynch [1973] is in agreement with this conclusion, as is our own work [de Boer et al, 1974, also present paper].

In recent years, various groups have converted automobiles to operation on hydrogen. Swain and Adt [1972] and Adt et al [1973] avoided the back-fire problem by introducing the hydrogen through a hole in the seat of the intake valve. They note that the performance of their vehicle (a 1971 4-cylinder Toyota 1600 stationwagon) is not noticeably different from that of a similar gasoline fueled vehicle. They also converted a 4-cylinder Pontiac engine to operation on hydrogen. Finegold et al [1973, 1974] created the "UCLA hydrogen car", which showed a marked increase in brake thermal efficiency as compared to gasoline (25-100% for quality governed operation on hydrogen). Finally, Billings and Lynch [1973] converted various vehicles to operation on hydrogen, trying out many important new ideas.

From the information available at the present time, a number of definitive general conclusions can be drawn. One of these is that engine operation on hydrogen is quite feasible. The thermal efficiency of hydrogen engines tends to be significantly better than that of comparable gasoline engines. Safety does not appear to be a more serious problem than with liquid petroleum fuels. Pre-ignition, backfiring and knock may be prevented by suitable engine modifications. Fuel injection of hydrogen provides the possibility of a high power output, but such a high power output is accompanied by high NO emissions. For mobile engines, storage of hydrogen presents severe but solvable problems. The main problem with application of hydrogen engines on a large scale is that of cost. In the following sections, these points are discussed in more detail.

## 2. DIFFERENCES BETWEEN HYDROGEN AND HYDRO-CARBON FUELED ENGINES

Before discussing the performance of engines running on hydrogen, it is useful to consider the various principles according to which such engines can operate. In general, these principles are the same as the ones applying to engines running on hydro-carbon fuels. In the following lines, emphasis will be on the ways in which hydrogen engines are or should be different. The differences arise from properties of hydrogen such as high flame speed, very wide flammability limits, low ignition energy, and low heat content per unit volume. Before discussing these differences, we briefly summarize the definitions of various important engine parameters.

The fuel-air equivalence ratio  $\phi$  is defined by  $\phi = (F/A)/(F/A)_S$ , where F stands for the percent of fuel in the mixture, A for the percent of air, and subscript S denotes stoichiometric conditions. F and A may be expressed either in percents by volume, or in percents by mass. For hydrogen, the value of  $F_S$  is 29.5% by volume, while

$$\phi = 2.39 x / (100-x),$$

where x is the percent by volume of hydrogen in the mixture. Conversely,

$$x = 100\phi / (2.39 + \phi)$$

In some of the older literature, use is made of the concepts percent weak and percent rich. A mixture which is y% weak by definition contains sufficient fuel to combine with 100-y% of the oxygen available in the air [cf. Ricardo, 1924, p. 334]. Thus,

$$\begin{aligned} \text{percent weak} &= 100 (1-\phi) \text{ for } \phi < 1 \\ \text{percent rich} &= 100 (\phi-1) \text{ for } \phi > 1 \end{aligned}$$

Sometimes, still another definition of mixture strength is used, i.e., percentage of correct [Leah, 1949], defined as  $x/x_S$ . Obviously, care must be taken in distinguishing between these various definitions. The compression ratio is defined as the ratio of cylinder volumes when the piston is at bottom dead center and at top dead center, respectively. The difference between these volumes is the displacement. The net work done per cycle on the piston is called the indicated work  $W_i$ . Dividing this work by the heat of combustion  $Q_i$

of the amount of fuel introduced into the cylinder per cycle gives the indicated thermal efficiency  $\eta_i$ . Dividing the net work  $W_i$  by the displacement gives the indicated mean effective pressure IMEP. Subtracting engine friction losses from the corresponding indicated quantities provides brake quantities such as brake thermal efficiency  $\eta_b$ , brake mean effective pressure BMEP, etc.

We now consider the effects of the high flame speed of hydrogen-air mixtures (see Fig. 1). The most conspicuous of these is backfiring into the carburetor, a phenomenon which early investigators of hydrogen engines were quick to observe. [Ricardo, 1924, Burstall, 1927]. The backfiring tendency is enhanced by the low ignition energy of hydrogen (see Fig. 2) and by the small quenching distance (Fig. 3).

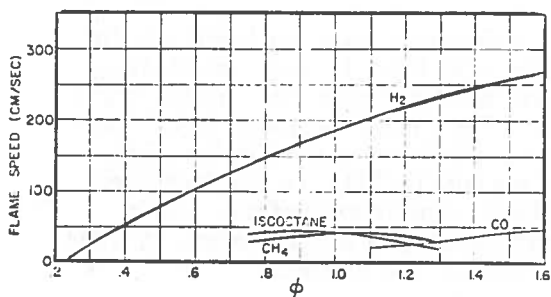


Fig. 1. Laminar flame speed as a function of fuel-air equivalence ratio  $\phi$ , for hydrogen, methane, isooctane and carbon monoxide [Gibbs and Calcote, 1959]. Initial temperature 300K, initial pressure  $p = 1$  atm.

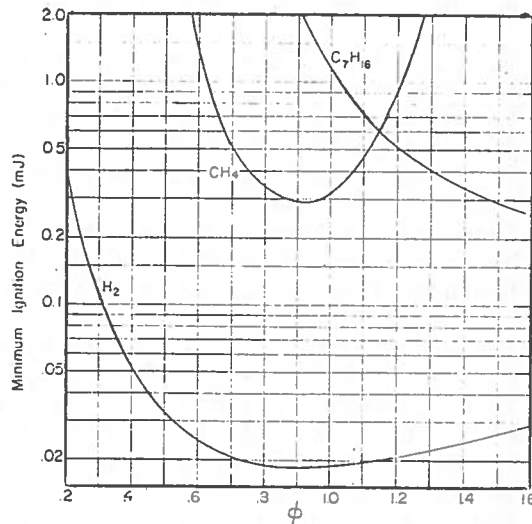


Fig. 2. Minimum spark ignition as a function of fuel-air equivalence ratio  $\phi$ , for hydrogen-methane-and heptane-air mixtures at room temperature and at  $p = 1$  atm. [Blanc et al, 1947; cf. also Lewis and von Elbe, 1961, Ch. V, Sec. 13].

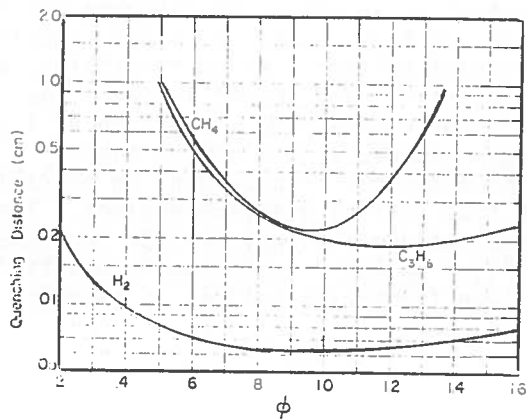


Fig. 3. Quenching distance as a function of fuel-air equivalence ratio  $\phi$ , for hydrogen-methane-and propane-air mixtures at room temperature and  $p = 1$  atm. [Blanc et al, 1947, cf. also Lewis and von Elbe, 1961, Ch. V, Sec. 13]

While backfiring can be eliminated by keeping the engine scrupulously clean [King et. al., 1958], this does not appear to be a very practical solution. Instead, it is possible to prevent backfiring by using lean mixtures, by using exhaust gas recirculation, or by using water injection. All of these measures reduce flame speed and increase ignition energy and quench distance. Any other modification resulting in these effects also should reduce or eliminate backfiring into the carburetor. Of course, the entire problem does not arise if the hydrogen is injected directly into the cylinder (direct fuel injection), rather than carbureted. Cost of injection equipment is significantly higher than cost of a carburetor. In most gasoline engines, therefore, the fuel is introduced with carburetors rather than with injectors. For Diesel engines, on the other hand, injection is a necessity. The high cost here is at least partially offset by economic operation, and is not a major consideration for large engines.

It would appear that fuel injection is preferable over carburetion for hydrogen engines. While direct cylinder injection is most promising, it may be that injection into the intake manifold near the intake port ("port injection") would be acceptable. The latter requires much lower injection pressures, and can therefore be achieved with simpler, less expensive equipment. Another interesting possibility is the hydrogen induction technique of Swain and Adt [1972] mentioned before. This technique uses regulation of the hydrogen pressure as the means to vary hydrogen flow rate, and hence power output of the engine.

The wide flammability limits of hydrogen make it possible to use very lean or very rich mixtures. Flame propagation experiments in a tube yield a lean flammability limit for a mixture at room temperature and 1 atm pressure of  $\phi = 0.10$  ( $x = 4\%$ ) for upward propagation of a coherent flame and of  $\phi = 0.23$  ( $x = 9\%$ ) for downward propagation, as well as for upward propagation of a noncoherent flame. [Coward and Jones, 1952, Egerton, 1953] The latter limit is the one most applicable to combustion in engines. However, a more practical lean limit for combustion in engines is about 0.30; below this limit, flame speed and hence thermal efficiency drop off drastically, [cf. Fig. 1; and Oehmichen, 1942]. The rich flammability limit is at  $\phi = 7.0$  ( $x = 75\%$ ).

Rich mixtures are unattractive for engine operation, except in certain special cases such as space applications where both oxygen and hydrogen must be carried. On the other hand, the use of lean mixtures is very attractive because it leads to high thermal efficiency. In addition, it provides the possibility of controlling the power output of an engine by changing the fuel flow rate, while keeping the air flow unthrottled. This is called "quality regulation", as opposed to "quantity regulation" provided by throttling, and has the very important advantage of eliminating air pumping losses. The latter account for a significant fraction of engine power output under light load and idle conditions where many engines operate most of the time. Consequently, quality regulation has the potential of providing an overall engine efficiency which is much higher than that of gasoline engines. The difference may be as large as 50% in indicated efficiency or 100% in brake efficiency [Finegold and Van Vorst, 1974]. Quality regulation is unsatisfactory for gasoline engines because the lean flammability limit of gasoline is

at an equivalence ratio  $\phi$  of about 0.75, at which point the indicated power output has dropped off only about 30% from its maximum. In contrast, Diesel engines often are quality regulated, as are gas turbines.

Much of the fundamental work on knock phenomena has been done in hydrogen engines. Hydrogen is a logical choice for this type of work because the hydrogen-air combustion process is relatively well understood. In general, the conclusions are that hydrogen is highly susceptible to knock caused by surface ignition. Usually, this causes preignition (ignition before occurrence of spark ignition), but it may also lead to post-ignition (ignition after occurrence of the spark, at a location not yet reached by the flame). At very high compression ratios (16 or above for chemically correct mixtures), spark knock may occur. Spark knock is caused by auto-ignition of the end mixture, after this mixture has been compressed and thereby heated as a result of combustion elsewhere in the cylinder, but before it has been reached by the flame front. The severity of spark knock depends on spark timing. Spark knock can be eliminated by retarding the spark, in contradistinction to surface ignition knock. All knock phenomena are objectionable, because they can lead to rough running, loss in thermal efficiency and power, run-on, runaway, ping and rumble. Spark knock is especially undesirable, because it is accompanied by rapid pressure and temperature rises, which may lead to destruction of engine parts.

Fuels having a low tendency to cause spark knock generally are not very suitable for compression ignition engines [see e.g., Lichty, 1967, Ch. 8], because they exhibit long ignition lag times. Compression ignition of hydrogen indeed is notoriously difficult to achieve [Gerrish and Foster, 1935]. As a matter of fact, there is no technical documentation of any engines ever having operated this way in a controlled manner. The closest approximation to a compression ignited hydrogen engine is that achieved by Karim and Klat [1965] and by Karim and Watson [1971], who raised the compression ratio of a motored CFR engine until auto-ignition occurred at top dead center. Apparently, the experiment was terminated once this point was achieved. Gerrish and Foster [1935] found that injection of even a minute amount of Diesel oil simultaneous with hydrogen injection solved the compression ignition problem.

In spark-ignited hydrogen engines, best ignition results are obtained by reducing spark gap settings to about 1/2 to 1/3 of those customary for gasoline engines. It seems likely that the need for these reductions is connected with the long ignition lags that also prevent compression ignition. On the other hand, the possibility of using such small gaps arises from the low ignition energy and the small quench distance of hydrogen (see Figs. 2 and 3).

The low heat content per unit volume of hydrogen causes a reduction in maximum output power of normally aspirated hydrogen engines as compared to gasoline engines (normally aspirated here means carbureted, non-supercharged). In a stoichiometric mixture of hydrogen and air, hydrogen takes up about 30% of the volume, while the corresponding figure for gasoline vapor is only about 2%. It follows that less oxygen can be introduced per engine cycle into the cylinder of a carbureted hydrogen engine than

of a gasoline engine. Using the heats of combustion of hydrogen and gasoline it can be shown that this results in a reduction of about 20% in maximum power output. Again, direct fuel injection of hydrogen offers a significant advantage in this connection. Its supercharging effect leads to a maximum power output that is about 10% larger than can be obtained by running the same engine on gasoline. Of course, some power is needed to inject the hydrogen, making the comparison less favorable in case this power is to be derived from the output of the engine. Other ways for obtaining the power needed for injection would be the use of high pressure containers, or conversion of liquid hydrogen to high pressure gaseous hydrogen by the use of exhaust heat.

For a number of special applications, it is preferable to use hydrogen-oxygen rather than hydrogen-air engines. A prime example is that of auxiliary power units for space applications, where it would be useless to carry air instead of oxygen. Such power units exhaust into vacuum, which enhances thermal efficiency. Valuable experience with this type of operation has been gained by Cameron and Morgan [1964], Morgan and Morath [1965], Brattan [1966] and Arao et al. [1967]. Another application for which hydrogen-oxygen engines would be attractive is that of stationary engines, in a situation where both oxygen and hydrogen are available [Escher, 1972]. Such a situation would arise if hydrogen is produced from the electrolysis of water.

Gas turbines appear to be particularly suitable for operation on hydrogen, as was proven by extensive investigations in the mid-1950's at NASA-Lewis Research Center [Silverstein and Hall, 1965; Lewis Laboratory Staff, 1967; Kaufman, 1967, Friedman et al., 1956; Rayle et al., 1967; Jones and Rayle, 1958; Smith and Grobman, 1958]. The weight advantage of hydrogen over kerosene (JP) fuel makes application to aircraft particularly attractive. Flight tests with a B-57 aircraft showed that a production J-68 turbojet engine could be made to run successfully on hydrogen by relatively simple modifications. Additional research involved the suitability of short length "swirl-can" combustors. Recent work on the application of hydrogen to gas turbines concerns the potential reduction in NO emissions that can be obtained [Jones and Grobman, 1973; Grobman et al., 1973]. One of the important conclusions of this work is that for aircraft designed to fulfill a given mission, the NO emission rate in kg/hr may be reduced 30% by using hydrogen rather than JP fuel. It is conceivable that further reductions may be obtained by taking advantage of the low lean flammability limit of hydrogen.

### 3. THERMAL EFFICIENCY AND POWER OUTPUT

The indicated thermal efficiency (ITE or  $\eta_i$ ) of a reciprocating combustion engine is given to a first approximation by

$$\eta_i = 1 - r^{-(\gamma-1)}, \quad (1)$$

where  $r$  is the compression ratio and  $\gamma$  the ratio of specific heats of the mixture. This formula is obtained from an air-standard analysis of the engine process [Lichty, 1967, Chap. 3], which neglects phenomena such as the detailed properties of the combustion gases, heat losses to the cylinder walls, finite opening times of valves, power losses arising from pressure drops across valves, etc. Eq. (1) provides a basis for understanding some fundamental aspects of the thermal efficiency of reciprocating combustion

engines. For  $r = 6$  and  $\gamma = 1.3$ , Eq. (1) yields  $\eta_i = 0.42$ ;  $\eta_i$  increases significantly as  $r$  increases and as  $\gamma$  increases. Relatively high values of  $\gamma$  can be achieved in hydrogen engines, because the wide flammability limits of hydrogen allow operation with a large excess of air ("lean operation"). In hydrogen engines, the compression ratio is limited primarily by the onset of preignition. If pre-ignition can be avoided, it is possible to use compression ratios that are much higher than would be acceptable for gasoline engines, and that are comparable to those used in Diesel engines. Thus, both the influence of  $r$  and of  $\gamma$  combine to give hydrogen engines the potential for high efficiency.

In order to improve on Eq. (1), account should first of all be taken of the properties of the combustion gases. A common modelling process used for this purpose is the "ideal engine process" [see, e.g., Lichty, 1967, Chap. 5]. In this process it is assumed that the gases are in equilibrium at all times, that combustion occurs instantaneously, and that heat losses and flow losses can be neglected. In spite of these simplifications, the process generally gives results that are quite acceptable; in many cases, they are within 20% of actual values (see e.g., Fig. 4).

Detailed comparisons between experimental results and calculated values for  $\eta_i$  based on the ideal engine process have been given by Oehmichen [1942]. In an extensive investigation, he established the dependence of  $\eta_i$  on equivalence ratio  $\phi$ , on compression ratio  $r$ , and on the engine speed (see Fig. 4). The upper solid line in each figure represents the theoretical result based on the ideal engine process, while the other solid lines represent results obtained by using direct fuel injection during the first half of the compression stroke, with an injection pressure of about 6 atm. The dotted lines in Fig. 4a and Fig. 4b represent Oehmichen's results when the engine was carbureted, while the dotted lines in Figs. 4e and 4f represent the results of King and Rand [1955], also for a carbureted engine. A number of conclusions can be drawn from Fig. 4. First of all, for  $\phi$  larger than about 0.4, the experimental results are fairly close to the theoretical result based on the ideal engine process. The differences probably arise to a large extent from heat losses to the cylinder walls, left out of account in the computations. Secondly, for  $\phi$  below 0.4, the actual thermal efficiency drops significantly below the calculated values. This trend is typical for all hydrogen engines, and arises largely from a reduction in flame speed. The resulting decrease in power output is so large that it is impractical to run a hydrogen engine near the lean flammability limit ( $\phi \approx 0.23$ ). Another observation is that indicated efficiency increased with engine speed, and that in general quality regulation gave higher efficiency than quantity regulation. In part, the latter differences must arise from the supercharging effect of hydrogen already mentioned before. The effect results in a larger equivalent compression ratio, and also yields additional expansion work. However, since in Oehmichen's engine the hydrogen was injected rather early in the compression cycle, this expansion work probably was not very large. From our computer program we have found that the difference in  $\eta_i$  for an injected and a carbureted engine typically is a few percent or less.



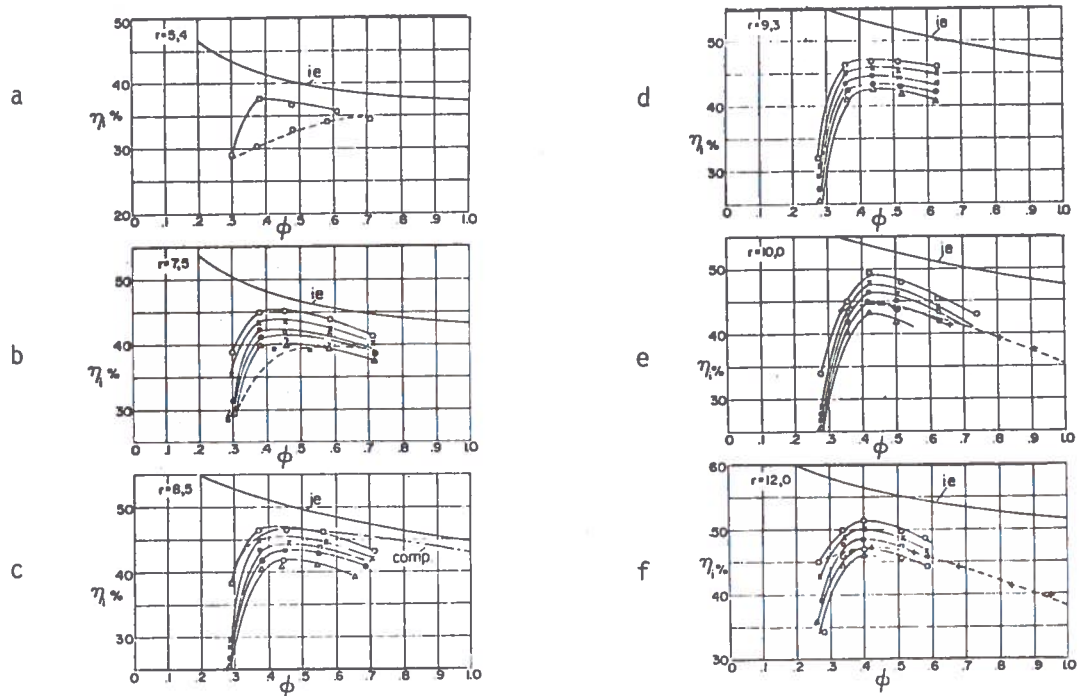
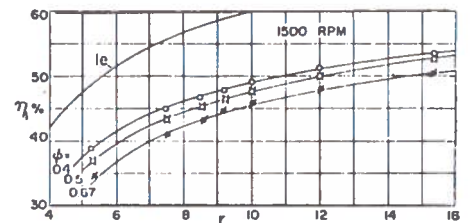


Fig. 4. Indicated thermal efficiency  $\eta_i$  as a function of equivalence ratio  $\phi$ , for various compression ratios  $r$  and various engine speeds. Solid curves and corresponding data points were obtained by Oehmichen [1942].  $\circ$  = 1500 rpm,  $\times$  = 1250 rpm,  $\square$  = 1000 rpm,  $\cdot$  = 750 rpm,  $\Delta$  = 500 rpm. Curves marked *ie* are theoretical results based on the ideal engine process. Also included are results obtained by King and Rand [1955] for  $r = 10$  and  $r = 12$  at 1500 rpm (dotted lines and points marked +). Curve marked *comp* in *c* is the result of a computer calculation taking account of the finite flame speed.

Fig. 5. Indicated thermal efficiency  $\eta_i$  as a function of compression ratio  $r$ , for various equivalence ratios  $\phi$  at an engine speed of 1500 rpm. Curve marked *ie* is a theoretical result based on the ideal engine process [Oehmichen, 1942].



Of course Oehmichen and King and Rand [1955] are not the only investigators of the thermal efficiency of hydrogen engines. Valuable results have also been reported by Ricardo [1924], Burstall [1927], King, Hayes et al., [1958], Swain, Adt, et al., [1972, 1973], Billings and Lynch [1973], Stebar and Parks, [1974]. Finegold [1974], and still others for carbureted engines, and by Murray and Schoepel [1971, 1972] for injected engines. A comparison between all of these was recently made by McAlevy et al., [1974]. In general, the data tend to fall somewhat below the results of Oehmichen [1942] and King and Rand [1955]. In this sense, the data shown in Fig. 4 represent the best values obtained with hydrogen engines as documented to date.

The data shown in Fig. 4 can be replotted with compression ratio  $r$  as the horizontal coordinate [Oehmichen, 1942]. One such plot is shown in Fig. 5. The increase in efficiency with compression ratio is quite obvious. Again, many other experimental results are available to confirm this trend.

Associated with Figures 4 and 5 are results obtained for IMEP as a function of compression ratio  $r$  and equivalence ratio  $\phi$  (see Fig. 6). As is to be expected, IMEP increases with  $r$  as well as with  $\phi$ . For complete combustion of all available fuel, IMEP is maximum at  $\phi = 1$ . In practice, the highest IMEP's frequently are obtained with values of IMEP larger than unity. The increase of IMEP with  $\phi$  is shown in Fig. 7, which is based on our own work. The engine used in this work is a modified CFR (Cooperative Fuel Research) engine with a Diesel head [de Boer et al., 1974]. While the thermal efficiencies and the IMEP's achieved are comparatively low, they were found to be the same for operation on hydrogen as for operation on Diesel oil. Since Diesel engines in general operate quite efficiently, this is a further indication of the potential for high efficiency of hydrogen engines.

Increases in the indicated thermal efficiency correspond to relative increases in the brake thermal efficiency that are significantly larger, for the obvious reason that power needed to overcome friction is independent of efficiency. Thus, while indicated efficiencies of a hydrogen engine may perhaps be 50% larger than of the same engine run on gasoline, the brake thermal efficiency with hydrogen may be 100% larger. [Finegold and Van Vorst, 1974].

Because of the high cost of hydrogen, brake thermal efficiency is one of the prime factors in determining the practicality of hydrogen engines. To illustrate this point, we include some rather approximate figures on the current cost of cryogenic hydrogen, based on informal statements by a spokesman for the Linde Company. The price one would currently pay for a tanker-truck full of liquid  $H_2$  would be \$1.20/lb, equivalent to \$23/10<sup>6</sup>BTU. Based on heating value, this would correspond to \$2.50/gallon of gasoline. When buying only a 50 liter Dewar, the price per pound would increase by a factor 5. At very large volumes, say about one half the total hydrogen produced in the U.S.A., the price would drop by a factor of 2, resulting in \$1.25 per gallon of gasoline. If the brake thermal efficiency

Fig. 6. Indicated mean effective pressure IMEP as a function of compression ratio  $r$ , for various values of equivalence ratio  $\phi$  [Oehmichen, 1942].

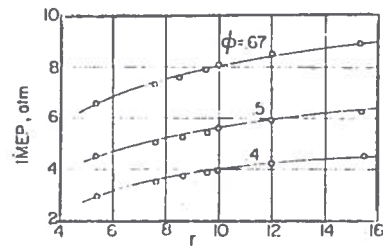


Fig. 7. Indicated mean effective pressure IMEP as a function of equivalence ratio  $\phi$ , for various compression ratios  $r$ , at an engine speed of 1200 rpm. Results were obtained with a CFR engine with Diesel head, using hydrogen or Diesel oil.

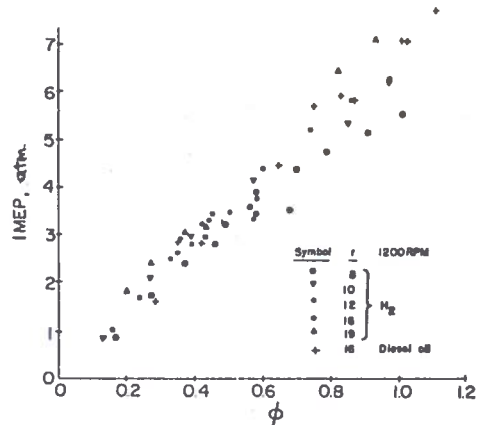


Fig. 8. Ignition timing for best torque as a function of equivalence ratio  $\phi$ , for various engine speeds and a compression ratio  $r=10$ . Also indicated are lines of constant IMEP. [Oehmichen, 1942].

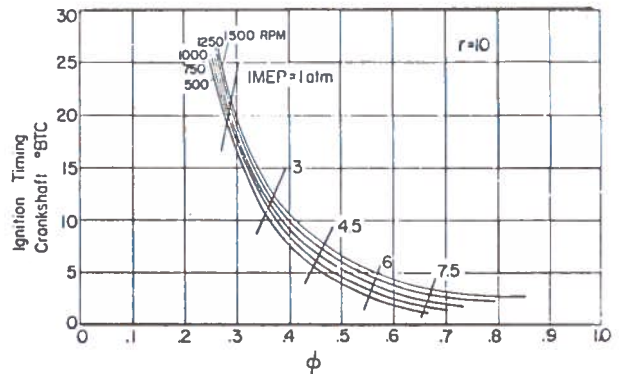
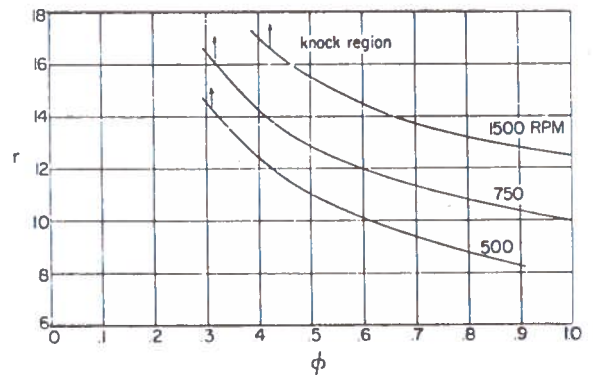


Fig. 9. Compression ratios  $r$  leading to knock as a function of equivalence ratio  $\phi$ , for various engine speeds [Oehmichen, 1942].



with hydrogen would be twice as high as that with gasoline, the resulting price would be \$0.60 per equivalent gallon of gasoline. The latter figure is of the order of the current price of gasoline in the U.S.A. (which includes taxes not included in the hydrogen figures!), and significantly lower than current gasoline prices in many European countries. Long term projections for the cost of hydrogen produced by thermochemical or other means hold out hope for reducing the cost to \$6-10/10<sup>6</sup> BTU, or \$0.70 - \$1.10 per equivalent gallon of gasoline on a heat of combustion basis.

Because of the decrease in flame speed at low  $\phi$ , it is necessary to advance the spark timing as a function of  $\phi$ . Typical spark timings used by Oehmichen to obtain maximum IMEP under the conditions specified are shown in Fig. 8. Also indicated are lines of constant IMEP. Oehmichen reports that in spite of the ignition advance, combustion became irregular at the lower values of  $\phi$ . In our own work we have been able to operate at values of  $\phi$  as low as 0.17, while retaining regular combustion as evidenced by the pressure history in the cylinder.

The best indicated efficiency was achieved at an equivalence ratio of  $\phi = 0.4$ , an engine speed of 2000 rpm and a compression ratio  $r = 15.4$ ; it amounted to 55%, which is very high indeed for an internal combustion engine (see Fig. 5). Comparable values were achieved by King, Hayes et al., [1958]:  $\eta_i = 51\%$  at  $r = 16$  and  $\eta_i = 52\%$  at  $r = 20$ , both at an engine speed of 1800 rpm and an equivalence ratio  $\phi = 0.38$ .

The difference in theoretical results obtained by the ideal engine process, and a computer model taking account of finite flame speed and valve timing [de Boer et al., 1974] is indicated in Fig. 4C. (The curve labeled comp was obtained by Mr. J.J. Fagelson). The latter model correctly accounts for the trend to lower efficiency at small  $\phi$ , but does not include heat losses, which are most important at larger  $\phi$ .

#### 4. BACKFIRING, PRE-IGNITION AND KNOCK

As mentioned in section II, the early investigators of hydrogen engines were confronted with backfire and pre-ignition problems. It was found that the highest usable compression ratio for stoichiometric mixtures generally was between 6 and 8, depending on the particular engine, on engine speed etc. Important contributions to the understanding of these problems were made in a series of papers by King and his collaborators (1948, 1955, 1958), who showed that compression ratios as high as 14 could be used in combination with stoichiometric mixtures provided the engine cylinder and piston are kept scrupulously clean. Apparently, the pre-ignition is caused by catalytic reactions at the cylinder surface, or at free floating particles liberated from the surface. The latter point was proved by showing that the introduction of dust particles into the mixture lead to pre-ignition.

A natural solution to the backfiring problem consists of keeping the hydrogen and the air separate until introduced in the cylinder using either fuel injection or an induction technique such as proposed by Swain and Adt (1977). The available documentation indicates that fuel injection also solves the problem of pre-ignition. For example, Oehmichen [1942] reports that in his

work auto-or pre-ignition was never observed, even though the compression ratios used were as high as 15.4. Apparently, this is related to long auto-ignition lag times of hydrogen-air mixtures at high pressures [Lewis and von Elbe, 1961]. The same effect is responsible for the difficulty in operating hydrogen engines with compression ignition.

Knock in hydrogen engines in principle is caused by the same phenomena as in engines operating on hydrocarbon fuels. Numerous investigations have shown that true "combustion knock" in spark ignition engines is caused by auto-ignition of the end mixture, after this end mixture first has been compressed as a result of combustion in the first part of the mixture. While the flame speed is much less than the speed of sound, the auto-ignition process is always accompanied by pressure waves travelling at least as fast as the speed of sound. In spite of their universal occurrence, the nature of these waves is not well understood, and the subject is controversial. A clear description of the situation is given by Obert [1950], who suggests that the high temperature of the mixture makes it possible that detonation waves are formed, even though such detonation waves are not encountered in tube experiments using the same mixture at lower temperatures.

Oehmichen [1942] reports that the knock-free region of operation is extended by increasing the engine speed (Fig. 9). Apparently, the limits shown were determined by judging the smoothness of operation of the engine. According to Oehmichen's findings, knock disturbances in a hydrogen engine only lead to difficulties when the engine is operated close to its rated power.

The presence of the waves mentioned before at a high compression ratio ( $r = 19$ ) is clearly seen in Fig. 10 obtained on our CFR engine. Even at a compression ratio of 8, the combustion is not entirely smooth. It appears that the combustion process is not completed upon passage of the first wave, so that there may be some kind of interaction between the combustion process and the waves. In spite of the rapid fluctuations in pressure, the noise generated by the engine at  $r = 19$  was not excessive, and did not resemble the sound of knock as emitted by hydrocarbon engines. Similar waves were observed by King, Hayes et al., [1958, Fig. 7] at compression ratios of 12 and 14, where the engine is reported not to have been knocking. Obert [1950], on the other hand, defines spark knock as the occurrence of waves of this type. At this time, it is not clear to what extent the presence of pressure waves is acceptable in hydrogen engines. The waves frequently show a rate of pressure rise larger than held commonly acceptable to prevent rough running (30-40 psi per crankshaft degree, see Lichty, 1967, Chap. 14). Complete clarification of this point probably requires extensive experimentation with engines in actual applications.

## 5. EMISSIONS

One of the most attractive features of the hydrogen fueled engine is its potential for low air pollution emissions. Since the fuel does not contain carbon, all emissions of carbon monoxide, carbon dioxide and hydrocarbons are essentially eliminated, assuming that lubricating oil consumption is not excessive. On the other hand, the combustion temperatures during constant

Fig. 10. Cylinder pressure as a function of crankshaft angle in hydrogen CFR engine with Diesel head. Traces on right represent the same event as those on left, on an expanded horizontal scale.

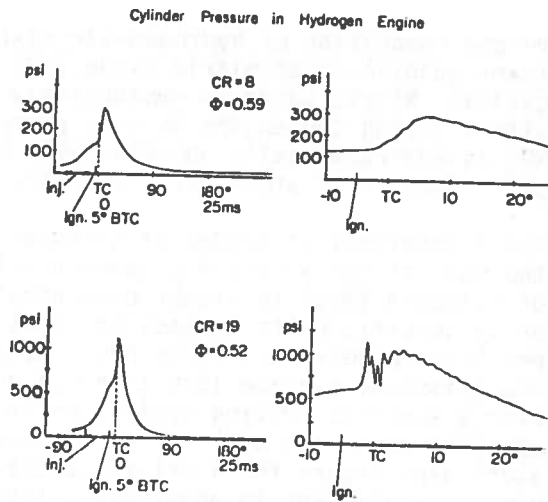


Fig. 11. Variations of NO Emissions with Equivalence Ratio for Different Equivalence Ratios.

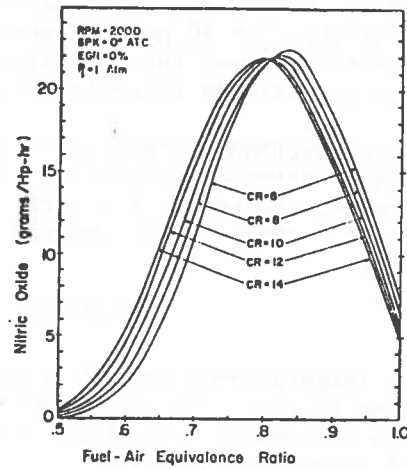
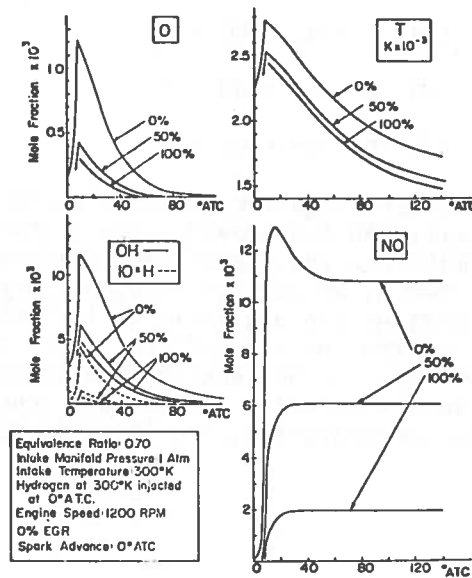


Fig. 12. Thermochemical Evolution of Burned Gases ( $\phi = 0.7$ )



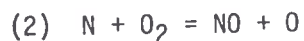
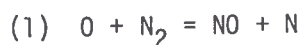
volume combustion of hydrogen-air mixtures are high enough to form significant quantities of nitric oxide (NO) during internal combustion engine cycles. Nitric oxide is subsequently converted to nitrogen dioxide (NO<sub>2</sub>) either during the engine exhaust process or in the atmosphere, and this NO<sub>2</sub> is environmentally objectionable both by itself and because of its participation in atmospheric reactions generating photochemical smog.

Total emissions of oxides of nitrogen from a given engine are equal to the sum of the NO and NO<sub>2</sub> concentrations and are reported as total oxides of nitrogen (NO<sub>x</sub>) in either concentration units as parts per million (ppm) or in specific units as mass per unit engine energy output, usually grams per horse-power-hours (g/hp-hr). Ultimate Federal standards require that NO<sub>x</sub> emissions average less than 0.4 g/mi determined by constant sampling over a specific driving cycle. While it is next to impossible to convert specific emissions at a series of steady operating points into an equivalent g/mi figure for a driving cycle, a rough rule of thumb is that 0.4 g/mi is equivalent to about 0.8 g/(bhp-hr) for a 3000 lb. vehicle [Blumberg and Kummer, 1971]. For the same vehicle this roughly corresponds to an average emission of 40 ppm. Lighter vehicles having smaller power requirements may meet the g/mi standard with relatively larger emissions in either specific or concentration units.

The present section reviews available analytical and experimental data on oxides of nitrogen emissions from hydrogen fueled spark ignited reciprocating engines with a view towards evaluating the potential environmental impact of hydrogen fueled vehicles in a future "hydrogen economy".

## 6. ANALYTICAL DATA

The high temperature chemical processes which form NO are reasonably well understood by now. The following three reactions, known as the extended Zeldovich mechanism, are responsible for NO formation in reciprocating internal combustion engines:



Due to the requirement for breaking an N-N bond, the first reaction, which produces NO and provides the N atoms for the subsequent reactions, is highly endothermic and significant NO formation thus requires high temperatures (> 2000 K) as well as available oxygen. In an engine cycle these formation conditions are available during the combustion process and in the burnt gases during the initial portion of the expansion process. In the later stages of the expansion NO reactions cease due to the low temperatures. Thus, the NO becomes chemically stable at a concentration well above its chemical equilibrium concentration, resulting in relatively high exhaust emissions.

Since the rate of the NO formation processes depend upon temperature and available oxygen, only, they occur primarily in the post flame gases. They depend indirectly on the type of fuel used, in the sense that the fuel type effects the flame temperatures and, through the stoichiometry, the available oxygen. Under engine conditions the NO is often formed in near equilibrium concentrations after combustion, and rapidly quenched thereafter. An approximate estimate of the NO emissions in an Otto cycle engine can be obtained by computing equilibrium NO concentrations immediately after constant volume combustion. This method is useful for obtaining an estimate of any large change in NO<sub>x</sub> emissions due to fuel differences. Starkman et al. [1970] have used such a procedure to estimate NO<sub>x</sub> emissions for various fuels. Their results show that on this basis hydrogen and gasoline give nearly the same NO<sub>x</sub> levels, indicating that gross differences in NO<sub>x</sub> emissions should not result from the fuel combustion properties alone.

We have carried out a much more detailed analysis of the production of NO<sub>x</sub> in a hydrogen fueled engine. In this work the chemical kinetic processes governing NO formation were followed throughout the Otto cycle by numerically integrating the appropriate non-linear chemical rate equations over the temperature and pressure conditions existing inside the engine cylinder. This model incorporates both the effects of finite burning rates and cylinder temperature gradients into the analysis. The details of the procedure and a comparison with experimental data are available elsewhere [Fagelson et al., 1975]; here we just summarize the major results. Figure 11 shows the predicted specific NO emissions as a function of fuel-air equivalence ratio for various compression ratio engines operating at the conditions noted in the figure. NO emissions reach maximum values of approximately 20 g/(ihp hr) for equivalence ratios near 0.8 and are substantially less for much leaner or richer mixtures. NO control to about 1 g/(ihp hr) can be achieved by operating lean with equivalence ratios limited to about 0.55. A brief description of the chemical processes controlling these emissions follows.

For mixtures leaner than  $\phi = 0.8$  the NO is limited by thermal quenching during the formation processes, while for mixtures richer than  $\phi = 0.8$  the net NO emissions are determined by quenching of NO decomposition reactions during the expansion stroke. Figures 12 and 13 illustrate these effects. The Figures show the mole fractions of O, OH, H and NO, and the gas temperature during the engine cycle for the first (0%), middle (50%) and last (100%) elements of charge to burn. The percentages given indicate the percent mass burned when that particular element burns. Figure 12 for  $\phi = 0.7$  shows that for this lean mixture the relatively high oxygen atom levels and moderate temperatures lead to NO mole fractions which are limited by thermal quenching of the NO formation reactions. Figure 13 for  $\phi = 1.0$  shows that in this stoichiometric mixture the high temperatures and resulting large free radical and atom concentrations greatly accelerate the NO reactions. The fast reactions, particularly the third reaction involving H and OH, allow the NO mole fraction to more closely follow chemical equilibrium, and substantial decomposition of NO is observed during the expansion stroke. This decomposition results in lower net NO emissions.



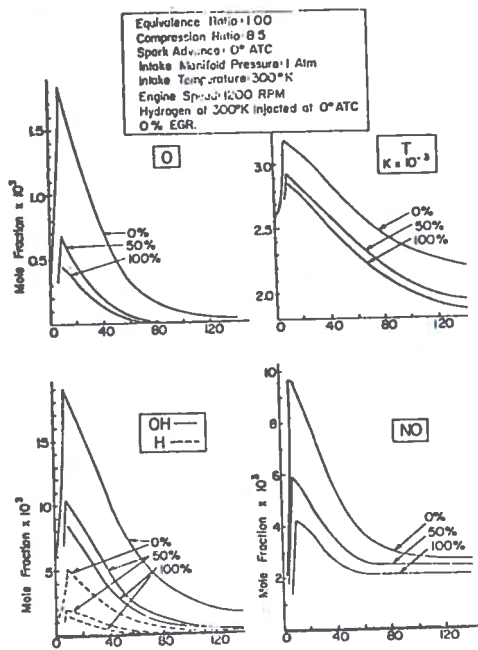


Fig. 13. Thermochemical Evolution of Burned gases ( $\phi = 1.00$ )

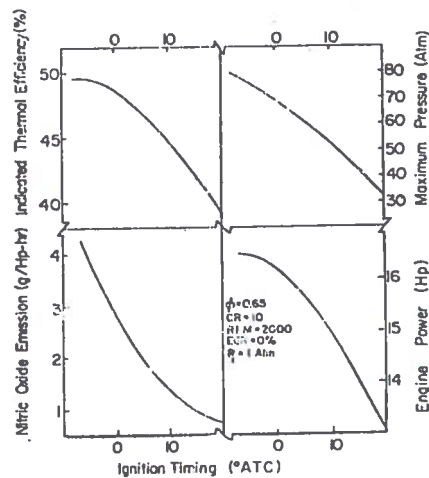


Fig. 15. Effect of Ignition Timing on Engine Characteristics.

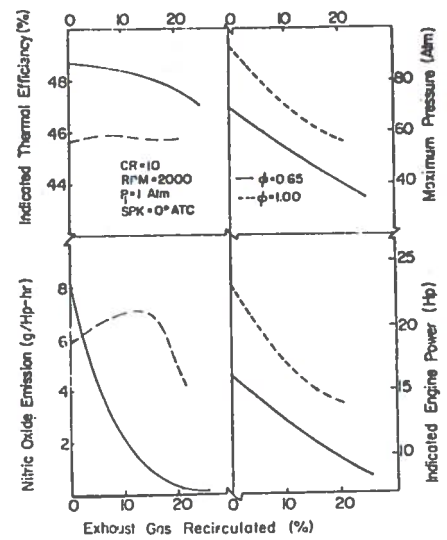


Fig. 14. Effects of Exhaust Gas Recirculation (EGR) on Engine Characteristics.

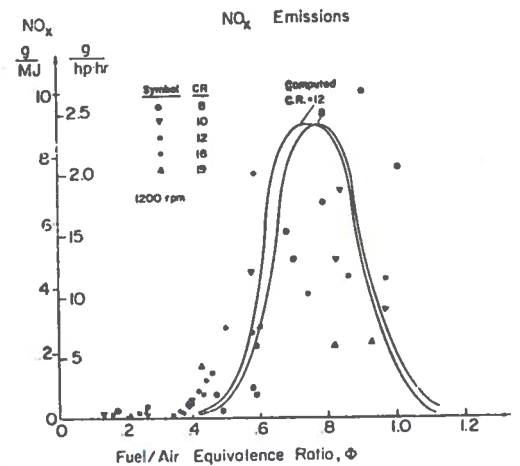


Fig. 16. Specific  $\text{NO}_x$  emissions as a function of equivalence ratio  $\phi$ , at various compression ratios  $r$  and an engine speed of 1200 rpm. Curves represent computer results obtained by Fagelson et al. [1975].

The analytical model can also be used to predict the effects of various NO<sub>x</sub> control techniques on engine performance and emissions. Effects of exhaust gas recirculation (EGR) and spark timing are shown in Figures 14 and 15, respectively. EGR is most effective in lean mixtures where it limits NO formation; in stoichiometric or rich hydrogen-air mixtures substantial percentages of EGR are required to effect the NO emissions. Spark retard is also effective in reducing NO emissions, but in contrast to EGR it has a deleterious effect on engine efficiency.

## 7. EXPERIMENTAL DATA

During the past few years, several of the different groups working with hydrogen fueled engines and/or vehicles have obtained NO<sub>x</sub> emissions data. Not surprisingly the data are not all consistent; we attempt here to summarize and evaluate available information.

Murray and Schoepfel at Oklahoma State University were the first to obtain NO<sub>x</sub> emissions data for a hydrogen fueled engine [Murray and Schoepfel, 1971], [Murray, et al., 1972]. Their initial results employing direct cylinder injection of hydrogen on a small (3.5 hp, 6.5:1 compression ratio) single cylinder air cooled engine indicated relatively low NO emissions ranging from 365 ppm at full power, near stoichiometric operation to 63 ppm at 30% power, lean operation. The exhaust sample was cooled and dried with a transit time of about 20 seconds, and any NO<sub>2</sub> present in the sample was not measured. Further data reported for this engine in water cooled operation gave specific emissions at "wide open throttle" from 2 to 6 g/(ihp hr) depending on fuel injection timing. Reported exhaust gas compositions (H<sub>2</sub>, O<sub>2</sub>, N<sub>2</sub>, CO, CO<sub>2</sub>, H/C, NO<sub>x</sub>) for these tests indicated that the "wide open throttle" data were recorded under quite lean fuel air mixtures, with  $\phi < 0.35$  for the compositions reported.

Unfortunately Murray and Schoepfel chose to compare their NO<sub>x</sub> emissions data with data from other engines operating with different fuels under different conditions. This comparison showed the emissions with hydrogen to be significantly less than for other fuels and led to widespread publication of comparisons claiming that with respect to NO<sub>x</sub> hydrogen was inherently "cleaner" than hydrocarbon fuels. Other test data referred to below do not sustain this conclusion. In fact, the data of Schoepfel [1971] obtained by using gasoline in the same engine show NO<sub>x</sub> emissions comparable to those obtained using hydrogen.

Billings and Lynch [1973] directly compared NO emissions for hydrogen and gasoline using a 6.65 CID single cylinder air cooled engine of 5.5:1 compression ratio. These tests were at fixed rather than best torque ignition ratings, but nevertheless enable comparison of the emissions potential of the two fuels. Gasoline gave peak NO emissions of 800 ppm at  $\phi = 0.93$  with the spark retarded with respect to best torque advance, while hydrogen gave maximum NO of 5000 ppm at  $\phi = 0.83$  with the spark advanced with respect to best torque. These tests would seem to indicate quite similar NO emissions for hydrogen and gasoline in near stoichiometric mixtures if the spark timing is optimum. In addition these tests confirmed the extremely low NO concentrations obtainable using very lean hydrogen air mixtures, concentrations less

than 100 ppm being obtained for  $\phi < 0.6$ . Very low NO emissions during engine operation with quite lean mixtures have also been confirmed by University of Miami investigators (Adt et al., 1973; Adt and Swain, 1974).

Comparative NO<sub>x</sub> emissions data for hydrogen and isooctane over a wide range of equivalence ratios have been obtained by Stebar and Parks [1974] using a carbureted CFR engine at constant speed and air flow with the spark timing adjusted for best torque. Peak specific NO<sub>x</sub> emissions for isooctane were 18 g/(ihp hr) at  $\phi = 0.95$ , while for hydrogen peak emissions of nearly twice that occurred near  $\phi = 0.8$ . Again the dramatic reduction in NO<sub>x</sub> obtainable with very lean hydrogen-air mixtures was confirmed.

Finegold and Van Vorst [1974] have reported NO<sub>x</sub> emissions with hydrogen fuel substantially lower than with gasoline for equal power outputs from a 350 CID V-8 engine. Tests were conducted using both stoichiometric hydrogen-air mixtures with water added (water/hydrogen mass ratio = 2) and quality regulated hydrogen air mixtures limited to equivalence ratios "in the neighborhood of 0.6" because of backfire problems. The very low emissions obtained with hydrogen fuel are apparently explained then by the cooling effect of the added water in the one case and by lean mixtures in the other.

Our own NO<sub>x</sub> emissions data obtained in tests on a CFR engine with hydrogen injected directly into the prechamber of the Waukesha Diesel head are summarized in Figure 16. Again quite low emissions are obtained for very lean mixtures with a rapid increase observed for  $\phi > 0.6$ . In agreement with the previously cited CFR engine data, near stoichiometric mixtures result in quite high NO<sub>x</sub> emissions. In this case, peak emissions exceeded 20 g/(ihp hr).

It is apparent that the chemical interactions controlling formation of oxides of nitrogen in hydrogen fueled engines are the same as in other combustion processes. Thus engines operated on hydrogen using near stoichiometric mixtures can be expected to produce substantial NO<sub>x</sub> emissions quite similar to those obtained with hydrocarbon fuels. Well known control techniques such as spark retard, exhaust gas recirculation, and water addition are effective in controlling NO<sub>x</sub> emissions. In addition, the extremely low-value of the lean flammability limit of hydrogen-air mixtures can be used to reduce NO<sub>x</sub> emissions to almost negligible amounts by restricting operation to equivalence ratios less than 0.6. Direct cylinder fuel injection may be employed to boost power without sacrificing emissions control at these lean mixtures.

## 8. CONCLUDING REMARKS

The material presented in the preceding pages indicates that the hydrogen internal combustion engine is a practical concept. Its potential for high thermal efficiency will be an important factor in determining the conditions under which it will be competitive with hydrocarbon fueled engines. The potential almost certainly has not yet been fully realized, because no engines have been optimized for operation on hydrogen. Features to be incorporated in such engines are a high compression ratio and high engine speeds. The latter are desirable because of the high flame speed of hydrogen, and also because they reduce spark knock. The problems presented by pre-ignition, backfiring, knock and NO-production are well understood, and can be solved in a number of ways. Injection of hydrogen remains an attractive possibility. The experience of Oehmichen [1942] as well as that of ourselves indicates that one of the practical difficulties with injection may be the achievement of a reliable, long lasting seal in the injector.

Another promising application of hydrogen to internal combustion engines is its use as a supplementary fuel, in combination with hydrocarbon fuels. This application is currently under active investigation at the Jet Propulsion Laboratory. Also under investigation in a joint program between the Jet Propulsion Laboratory and our own group at Cornell University is the application of hydrogen in Diesel engines, using a glow plug or a R. F. discharge plug to obtain ignition. Taking account of all of these factors, as well as of the hydrocarbon fuel shortage that is developing, it seems likely that the hydrogen engine will find a number of applications within the next few decades.

## ACKNOWLEDGEMENT

The present work was supported in part by the U.S. Department of Transportation, Office of University Research, under Contract No. DOT-OS-30113.

## REFERENCES

- Adt, R. R., Herschberger, D. L., Kartage, T., and Swain, M. R., 1973, "The Hydrogen-Air Fueled Automobile Engine (Part 1)", 8th Intersociety Energy Conversion Engineering Conference, p. 194-197, Paper No. 739092.
- Adt, R. R. and Swain, M. R., 1974, "The Hydrogen/Methanol Air Breathing Engine", Proceedings the Hydrogen Economy Miami Energy Conference, University of Miami, Florida.
- Arao, M., Chandler, B., and Goodhart, M., 1967, "Nonairbreathing Internal Combustion Engine", Intersociety Energy Conversion Conference, Miami Beach, Florida, p. 527.
- Billings, R. E. and Lynch, F. E., 1973, "Performance and Nitric Oxide Control Parameters of the Hydrogen Engine", Publication No. 73002, Energy Research, Provo, Utah.
- Blanc, M. V., Guest, P. G., von Elbe, G. and Lewis, B., J. Chem. Phys. 15, 798 (1947); Third Symposium on Combustion and Flame and Explosion Phenomena, p. 363, Williams and Williams, Baltimore (1949).
- Blumberg, P. and Kummer, J. T., 1971, Combustion Science and Technology, 4, p. 73.
- Brattan, A. I., 1966, "Reciprocating Engine for Space Power", Intersociety Energy Conversion Conference (IECEC), p. 284, Los Angeles, California.
- Burstall, A. F., 1927, Proc. Inst. Automobile Engrs. 22, 358.
- Cameron, H. M., Morgan, N. E., 1964, AIAA paper 64-756.
- Coward, H. F. and Jones, G. W., 1952, Limits of Flammability of Gases and Vapors, Bull. 503, Bur. Mines.
- de Boer, P.C.T., McLean, W.J., Fagelson, J.J. and Homan, H.S., 1974, "An Analytical and Experimental Study of the Performance and Emissions of a Hydrogen Fueled Reciprocating Engine," Proc. 9th Intersociety Energy Conversion Engineering Conference, paper 740956, San Francisco, Cal.
- Drell, I. L., and Belles, F. L., 1957, Survey of Hydrogen Combustion Properties, NACA Report 1383.
- Egerton, A. C., 1953, "Limits of Inflammability", Fourth Symposium (International) on Combustion, The Williams and Williams Co. (Baltimore), 4.

- Egerton, A., Smith, F. L. and Ubbelohde, A. R., 1935, Phil. Trans. Roy. Soc. London A 234, 433.
- Erren, R. A. and Campbell, W. H., 1933, J. Inst. Fuel 6, 277.
- Escher, W. J. D., 1972, "The Case for the Hydrogen-Oxygen Car", Escher Technology Associates, pm-21.
- Fagelson, J. J., McLean, W. J. and de Boer, P. C. T., 1975, "Analysis of Hydrogen as a Reciprocating Engine Fuel", Symposium on Chemistry of Combustion in Engines, American Chemical Society, April 1975.
- Finegold, J. G., and Van Vorst, W. P., 1974, "Engine Performance with Gasoline and Hydrogen: A Comparative Study", presented at the Hydrogen Economy Miami Energy Conference.
- Friedman, R., Norgren, C. T. and Jones, R. E., 1956, "Performance of a Short Turbojet Combustor with Hydrogen Fuel in a Quarter-Annulus Duct and Comparison with Performance in a Full-Scale Engine". NACA RM E56D16.
- Gerrish, H. G. and Foster, H. H., 1935, National Advisory Committee for Aeronautics, Publ. no. 535, 495.
- Gibbs and Calcote, 1959, J. Chem. Eng. Data 4, 226.
- Grobman, J., Norgren, C. and Anderson, D., 1973, "Turbojet Emissions, Hydrogen versus JP," NASA TMX-68258.
- Jones, R. E. and Rayle, W. D., 1958, "Performance of Five Short Multi-element Turbojet Combustors for Hydrogen Fuel in Quarter-Annulus Duct", NACA RM E58D15.
- Jones, R.E. and Grobman, J., 1973, "Design and Evaluation of Combustors for Reducing Aircraft Engine Pollution," NASA TMX-68192.
- Karim, G. A. and Klat, S. R., 1966, J. Inst. Fuel, p. 109, March 1966.
- Karim, G. A. and Watson, H. C., 1971, SAE Transactions, 80, p. 450.
- Kaufman, H. R., 1967, "High-Altitude Performance Investigation of J65-B-3 Turbojet Engine with Both JP-4 and Gaseous Hydrogen Fuels", NACA RM E57A11.
- King, R. O., Hayes, S. V., Allan, A. B., Anderson, R. W. P., Walker, E. J., 1958, Trans. Engineers Institute of Canada 2, no. 4, p. 143.
- King, R. O., and Rand, M., 1955. Can. J. Technol. 33, p. 445.
- King, R. O., Wallace, W. A., Mahapatra, B., 1948, Can. J. of Research F 26, p. 264.
- Leah, A. S., 1949, Engineering 168, 665.

Lewis, B. and von Elbe, G., 1961, Combustion, Flames and Explosions of Gases, 2nd edition, Academic Press, N.Y.

Lewis Laboratory Staff, 1967, "Hydrogen for Turbojet and Ramjet Powered Flight", NACA RM E57D23.

Lichty, L. C., 1967, Combustion Engine Processes, New York, McGraw-Hill.

McAlevy, R. F. III, Cole, R. B., Hollenberg, J. W., Kurylko, L., Magee, L., Weil, K. H., "Hydrogen as a Fuel", Semi-annual Technical Report AD787-484, available from National Technical Information Service, (NTIS), August 1974.

Morgan, N. E. and Morath, W. D., 1965, NASA CR-255.

Murray, R. G. and Schoepfel, R. J., 1971, Proc. 1971 Intersociety Energy Conversion Engineering Conference (IECEC), pp. 47-51, Paper no. 719009.

Murray, R. G., Schoepfel, R. J. and Gray, C. L., 1972, "The Hydrogen Engine in Perspective", Proceedings, 7th Intersociety Energy Conversion Engineering Conference, Paper no. 729216.

Obert, E.F., 1950, Internal Combustion Engines, 2nd edition, International Textbook Company, Scranton, Pa.

Oemichen, M., 1942, Verein Deutsche ingenieur, Deutsche Kraftfahrtforschung, Heft 68.

Rayle, W. D., Jones, R. E. and Friedman, R., 1957, "Experimental Evaluation of "Swirl-Can" Elements for Hydrogen-Fuel Combustion", NACA RM E57C18.

Ricardo, H. R., 1924, Further Note on Fuel Research, Proc. Inst. Automobile Engrs. 18, 337 (1923-24).

Schoepfel, R. J., 1971, Final Report EPA Contract EHS 70-103, "Design Criteria for Hydrogen Burning Engines", Oct. 1971.

Silverstein, A. and Hall, E. W., 1955, "Liquid Hydrogen as a Jet Fuel for High Altitude Aircraft", NACA RM E55C28A.

Smith, A. L. and Grobman, J., 1958, "Exploratory Investigation of Performance of Experimental Fuel-Rich Hydrogen Combustion System", NACA RM E58C19A.

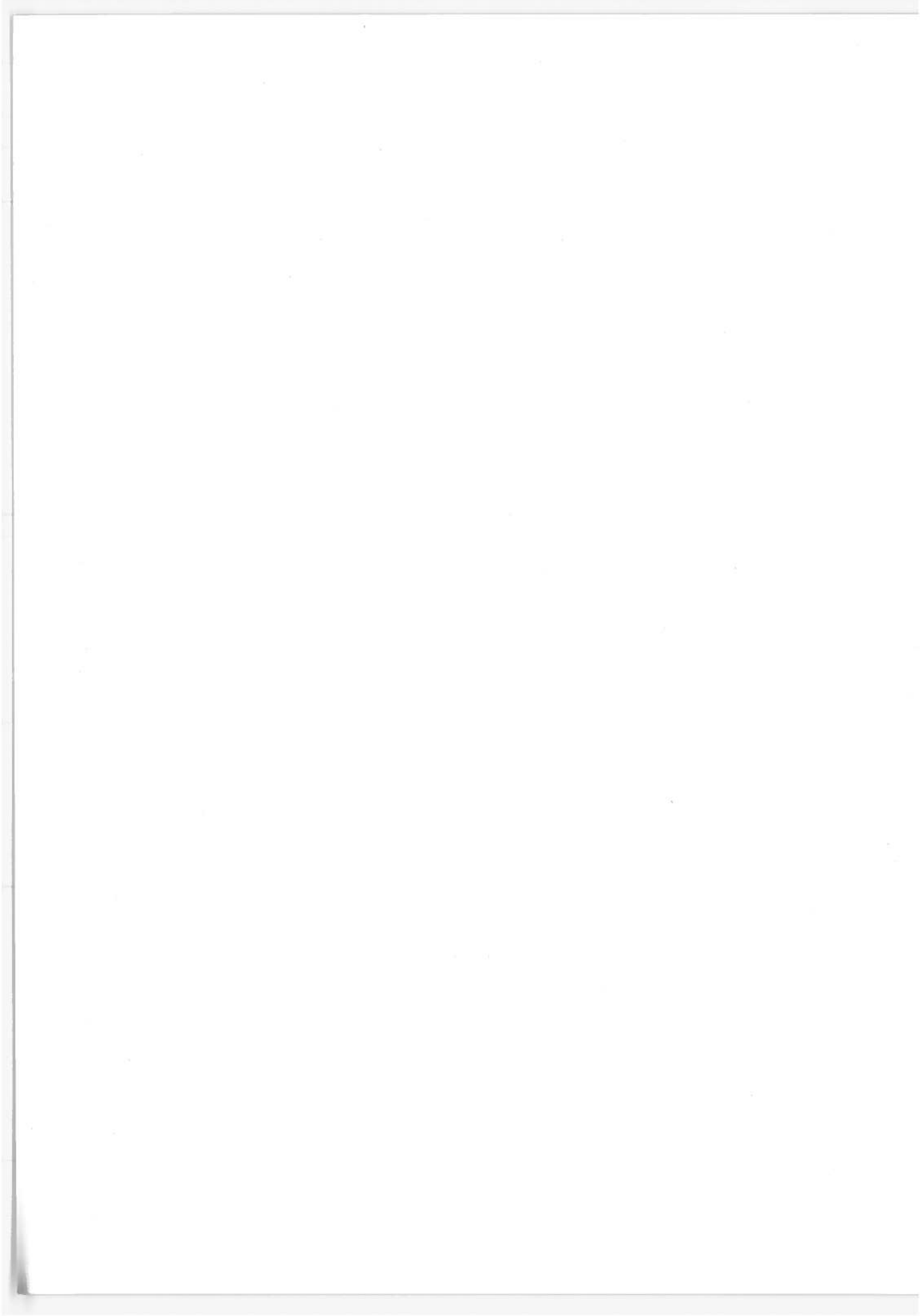
Starkman, E. S., et al., 1970, J. Air Pollution Control Association, 20, 87.

Stebar, R. F. and Parks, F. B., 1974, "Emission Control with Lean Operation Using Hydrogen-Supplemented Fuel", SAE Paper No. 740187, Automotive Engineering Congress and Exposition. (Also General Motors Research Publication, GMR-1537).

Swain, M. R. and Adt, R. R., 1972, "The Hydrogen-Air Fueled Automobile", Intersociety Energy Conversion Engineering Conference (IECEC) p. 1382 San Diego, California.

Weil, K. H., 1972, "The Hydrogen I. C. Engine-Its Origins and Future in the Emerging Energy-Transportation-Environment System", Intersociety Energy Conversion Engineering Conference (IECEC) p. 1355 San Diego, California.





## PERFORMANCE AND EMISSION MODELING FOR H<sub>2</sub> FUELED I.C. ENGINES

William J. McLean and Jean-Jacques Fagelson

Cornell University,  
Ithaca, New York 14850

### ABSTRACT

In considering hydrogen as a potential fuel for spark ignited reciprocating engines, it is of interest to estimate performance and emissions over a wide range of engine operating conditions so that particularly attractive operating regimes may be identified without extensive experimentation. A numerical model of the complete engine cycle has been constructed for the purposes of carrying out such estimates and also for elucidating in a fundamental way those processes which differentiate hydrogen fueled engines from gasoline engines.

An ideal fuel-air Otto cycle analysis has been used for initial estimates of the relative performance of hydrogen and gasoline. The analysis shows that in the same engine with a premixed stoichiometric fuel-air charge, gasoline and hydrogen give about the same thermal efficiency, but that gasoline gives 20% more power. If the hydrogen is instead injected directly into the cylinder, power is increased 40% so that a direct injection hydrogen engine gives about 20% more power than a carbureted gasoline engine with both at stoichiometric fuel-air ratios.

In order to estimate nitric oxide (NO) emissions from a hydrogen fueled engine, an adiabatic model for the combustion and burnt gas expansion processes has been developed. The combustion is modeled by employing a semi-empirical turbulent flame speed and by considering the burnt gases to be in chemical equilibrium except for NO. The burnt gases are assumed to remain unmixed and the NO is governed by the extended Zeldovich reaction mechanism. The model has been confirmed by comparison with available experimental data.

In general, the burnt gas properties are similar for hydrogen and hydro-carbon fuels so that similar levels of NO emissions are obtained under equivalent operating conditions. In the case of hydrogen, however, very lean mixtures can be used for part load operation and quite low levels of NO can be obtained under these conditions.

Well known NO control techniques such as exhaust gas recirculation and spark timing retard can also be used in hydrogen fueled engines.

It is concluded that, from a performance and emissions standpoint, a spark ignited reciprocating engine operating unthrottled with direct cylinder injection of hydrogen fuel is an attractive transportation powerplant in a future "hydrogen economy."

## 1. INTRODUCTION

The recent crisis in the worldwide petroleum supply system which caused brief but widespread gasoline shortages has focused attention on the vulnerability of our current energy systems and stimulated discussions of future system. One such future energy scenario is the "hydrogen economy" in which hydrogen serves as an energy carrier which is used directly as a combustion fuel in industry, commerce and the home, as well as in transportation power systems. The hydrogen of course is not the energy source but is generated from nuclear energy through electrolysis or thermal decomposition of water. Detailed discussions of such hydrogen energy systems can be found in the literature (1-6). The widespread use of hydrogen fuel would require nearly complete revamping of a large portion of our current energy supply and distribution system, and such enormous investments would only be made as hydrogen became cost competitive with dwindling fossil fuel supplies. Hydrogen is thus a long term energy option which is not expected to be cost competitive in the near future (7,8) when petroleum supplies will probably be supplemented by coal and shale derived fuels. In the longer term, however, we may well see widespread use of hydrogen as fuel. For example, one projection (9) forecasts peak production of fossil derived fluid fuels in 2010, with hydrogen production beginning in 1990 and surpassing fluid fossil fuels in 2050.

One of the major uses for hydrogen fuel in a future energy system would be in the transportation sector where it would fuel combustion engines for air, land and marine transportation. In the present work, automotive use of hydrogen is considered and the

spark ignited reciprocating internal combustion engine is the powerplant selected for analysis. Although various other types of automotive powerplants are under development, the reciprocating engine promises to retain a substantial portion of the engine market because of its low cost, high reliability, and relatively high specific power and efficiency (10,11). Hydrogen would be a particularly good fuel for IC engines because its wide flammability limits would permit high efficiency unthrottled engine operation. Engine emissions of hydrocarbons, carbon monoxide and carbon dioxide would be completely eliminated with only  $\text{NO}_x$  emissions to be controlled.

If we assume the widespread availability of hydrogen at some future date and consider not just the automotive powerplant but the overall vehicle system, the major drawback to the use of hydrogen is the onboard storage requirement (8,12). The low volumetric energy density of hydrogen leads to severe storage volume requirements if the vehicle is to carry as much energy as a standard gasoline tank. Developments in metal hydride solid phase storage and inexpensive cryogenic dewars for liquid hydrogen storage are required here. Any engine efficiency gain with hydrogen over gasoline of course reduces the hydrogen storage requirement for equivalent vehicle range. Various groups have recently converted several vehicles to run on hydrogen fuel in order to demonstrate the overall feasibility of operating present day engines on hydrogen (13-15).

The present paper results from an analytical investigation of hydrogen as a fuel for reciprocating engines. The objective of this study was to assess the potential performance and fuel economy of hydrogen fueled engines relative to the same engines fueled with gasoline, and to construct an analytical model for  $\text{NO}_x$  emissions from the hydrogen engine and assess these emissions and their controls in an unthrottled direct injection hydrogen engine.

## 2. HYDROGEN COMPARED WITH GASOLINE

In considering a given alternative fuel for reciprocating engine application, the power and efficiency of the engine using that fuel

are of primary importance. We consider here the performance of an engine fueled with hydrogen relative to the performance of the same engine fueled with the reference fuel, gasoline. For this analysis the gasoline is assumed to be isooctane, and the fuels are compared by analyzing their performance in an ideal fuel-air Otto cycle (16), where full chemical equilibrium and temperature dependent specific heats are used, but the combustion is taken to be instantaneous at the top center piston position. Such analyses overestimate power and efficiency (17), but are nevertheless useful for a relative comparison of various fuels. We also assume that power control with isooctane is obtained by throttling the inlet charge, whereas for hydrogen the wide flammability limits permit unthrottled engine operation and the power is controlled by "quality regulation", i.e., by varying the equivalence ratio ( $\phi$ ) through the amount of fuel supplied.

Figure 1 shows the ideal fuel-air cycle power and efficiency computed for a single cylinder 611 cm<sup>3</sup> displacement engine at a compression ratio of eight. Three cases are considered. For the

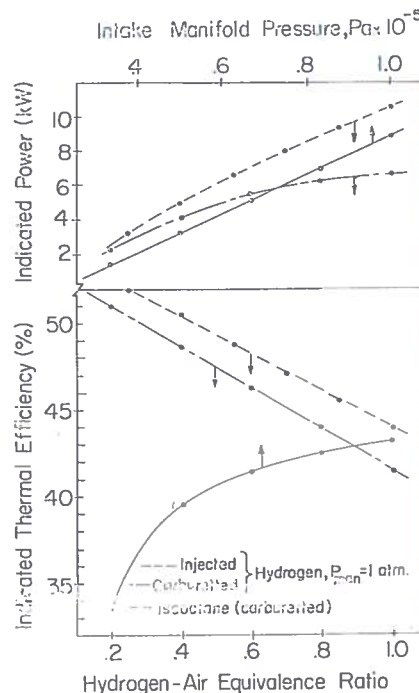


Figure 1 Comparison of hydrogen and isooctane performance, ideal fuel-air cycle analysis. The isooctane mixture is assumed to be throttled, the hydrogen unthrottled and either pre-mixed or injected directly into the cylinder. (Engine displacement 611 cm<sup>3</sup>, compression ratio 8).

reference isooctane case, the mixture is stoichiometric and the power varies with the intake manifold pressure. The throttling losses cause a substantial reduction in engine efficiency at low powers. For hydrogen, throttling losses are absent and the efficiency improves at low powers due to the higher specific heat ratio of the combustion products. Two hydrogen cases are shown; one assumes a premixed hydrogen air mixture, while the other assumes direct cylinder injection of the hydrogen fuel just prior to ignition. Both hydrogen cases give nearly the same efficiency, but direct injection gives 40% more power at  $\phi = 1$  than the premixed case. This is due to the reduced charge density caused by the low density fuel in the premixed case. That is, direct injection of hydrogen into the cylinder has a strong supercharging effect.

It should be noted that in this analysis the engine efficiency with isooctane is substantially lower than with hydrogen because the difference in the flammability limits of the two fuels requires throttling with isooctane but not with hydrogen. At full power where throttling is absent (manifold pressure =  $10^5$  Pa, equivalence ratio = 1.0), we obtain a comparison which depends on fuel properties only. Here, all three cases give nearly the same efficiency, and injected hydrogen gives 20% less power than isooctane.

### 3. ENGINE MODELING FOR NITRIC OXIDE EMISSIONS

Although an engine fueled with hydrogen would be free of any carbon containing emissions, nitric oxide (NO) would still be a potential exhaust emission product which would require control. In order to estimate the NO emissions from a hydrogen fueled engine, we have constructed a detailed model for the time varying thermodynamic properties of the high temperature combustion products and used these properties in the integration of the finite rate chemical kinetic equations governing NO formation. In the following, the model is briefly described and verified by comparison with experimental results.

#### Engine Combustion Model

Nitric oxide formation is a highly endothermic process which occurs in high temperature combustion products containing oxygen

and nitrogen. The formation rate is extremely temperature sensitive and also depends upon the stoichiometry. In combustion engine models then it is necessary to account for both the finite heat release rate and the burnt gas temperature gradient which are characteristics of the actual engine combustion process. We account for the burnt gas temperature gradient across the cylinder by assuming that the post-flame gases remain unmixed and dividing the burnt gas into a series of discrete adiabatic zones of equal pressure but different temperature. Such discrete zone models have been successfully applied to the computation of nitric oxide emissions from gasoline engines (18,19) and give temperature gradients in good agreement with experimental measurements (20).

The finite heat release rate may be specified in two ways. In the first method the cylinder pressure as a function of time is known from experiment, and the mass burning rate consistent with this function is computed. This approach is used by Lavoie, Heywood and Keck (21) and has the advantage that the combustion duration and engine power are as measured and the heat transfer is thus implicitly included. For this method, however, it is necessary to obtain an experimental pressure trace for each case or to use an empirical mass burning rate function with fixed combustion duration as has been done by Blumberg and Kummer (22).

For a hydrogen fueled engine, cylinder pressure traces were not readily available, and the wide variation in mixture stoichiometry seemed to rule out a model with fixed combustion duration. We therefore have used the second method of specifying the heat release rate where a semi-empirical turbulent flame speed is used to determine the combustion rate. Different approaches to specifying a turbulent flame speed in reciprocating engine combustion have been used by various workers (23-25). In general, for turbulent combustion in a closed vessel the effects of temperature and stoichiometry are accounted for through a laminar flame speed, and the turbulent flame speed is determined by multiplying this laminar speed by a factor which depends on the intensity of turbulence (26). For engine combustion the flame speed is observed to increase with engine speed (27), so the ratio of turbulent to laminar flame speed

must involve the engine speed. We have therefore used a semi-empirical turbulent flame speed of the form:

$$S_T = A \text{Re}^B S_L \quad 1)$$

In this expression A and B are empirically determined constants; Re is the Reynolds number based on the piston diameter, mean piston speed and burnt gas properties; and  $S_L$  is the laminar flame speed based on the Semenov theory (28). We have used  $B = 0.4$  after Delbourg (29) and Muzio (30). The Semenov laminar flame speed requires specification of an activation energy for an overall second order reaction between the fuel and oxidizer. The high temperature chain mechanism for hydrogen-oxygen combustion is reasonably well known and most of the chain propagation steps have activation energies near 20 Kcal/mole (31). We have therefore used 20 Kcal/mole for the flame speed activation energy.

Substitution for the temperature dependent transport and thermodynamic properties in  $S_L$  and Re enables  $S_T$  to be written as (32).

$$S_T = A' \left[ \frac{\text{NDLP}}{T_b^{1.67}} \right]^{0.4} \frac{R}{E_a} (T_b^{0.5} T_u^{1.25}) \frac{X_f F(\phi)}{\phi} \exp \left[ \frac{-E_a}{2RT_b} \right] \quad (2)$$

where:

N = engine speed (RPM)	$E_a$ = activation energy (cal/mole)
D = cylinder bore (cm)	$T_u$ = unburned gas temperature (K)
L = stroke (cm)	$X_f$ = mole fraction fuel
P = cylinder pressure (atm)	$\phi$ = equivalence ratio
$T_b$ = burnt gas temperature (K)	$F(\phi) = 1 - (1-\beta)/\phi \quad \phi > 1$
R = universal gas constant ( $1.987 \frac{\text{cal}}{\text{mole K}}$ )	$F(\phi) = 1 - \phi(1-\beta) \quad \phi \leq 1$
	$\beta = RT_b/E_a$

The constant A' was set equal to 5000 for best agreement with experimental data as discussed below.

In order to confirm the turbulent flame speed expression, we have compared our results with available experimental data. In most engine tests cylinder pressure measurements are not available and the spark advance for best torque is the only measured parameter which is indicative of flame speed — faster burning mixtures



requiring less spark advance for maximum power. Figure 2 shows the spark advance for best torque computed from our model and also shows available experimental data. The computations were carried out for the same engine conditions as reference (33) and reasonable agreement between calculation and this data is obtained for  $\phi \leq 0.6$ . For  $\phi \geq 0.7$ , heat transfer and engine knock limitations probably effect the experimentally determined spark advance, and the best torque spark advance from the adiabatic model exceeds the experimental value. Other available experimental data (34,35) for best torque timings for several other engines operating on hydrogen are also shown in Figure 2.

#### Nitric Oxide Formation Model

The chemical processes governing nitric oxide formation in high temperature combustion systems have received a great deal of attention and are summarized in a recent review (36). The post-flame reactions shown below, together with the assumption of steady state nitrogen atom concentration, are generally required for calculation of the NO formation rate in high pressure, high temperature systems (37,38).

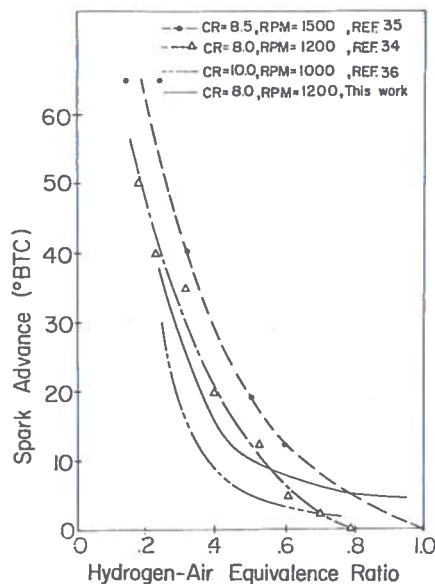
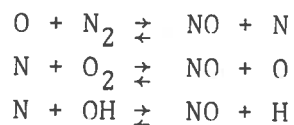


Figure 2. Maximum Power Spark Advance Versus Hydrogen-Air Equivalence Ratio (Same engine Conditions as in ref 33).

Although reactions involving  $N_2O$  have been found to be necessary for some systems under lean, low temperature conditions, our calculations for engine conditions indicate they are not important even in the leanest cases. Perhaps this is due to our assumption that at engine pressures oxygen atom equilibrium is rapidly attained in the post-flame gases, whereas other investigators (39) were studying atmospheric pressure stirred reactor systems with superequilibrium oxygen atom concentrations. The three reactions below are then sufficient for engine calculations. The rates for these reactions have been taken from evaluated rate data (40).



Given these reactions and the combustion model previously described, the evolution of the NO concentration is determined for each burnt gas zone under the assumption that all chemical species except NO follow their thermochemical equilibrium concentrations throughout the process. The NO concentration in each burnt gas zone is followed throughout the post-combustion portion of the Otto cycle, and the final emission level is determined by summing the contribution from each zone at exhaust valve opening. Further details of the model calculation are given in reference (32).

To verify the model predictions we have compared our computed results with experimental data of reference (33). The comparison is shown in Figure 3 where engine power and NO mole fractions are plotted as a function of equivalence ratio. The intake manifold pressure and spark timing for the model calculation were taken from the experimental data. The model overpredicts the engine power especially at the higher equivalence ratios due to the combined effects of heat transfer, intake flow losses and air humidity which are not included in the model calculations. Heat transfer losses typically reduce engine power by 10-15% (16,41). Computed dry air flows were about 5% greater than measured due to intake flow losses and the presence of water vapor ( $\sim 3\%$ ) in the air used in the experiments, and this accounts for a further 5% reduction in actual engine power.

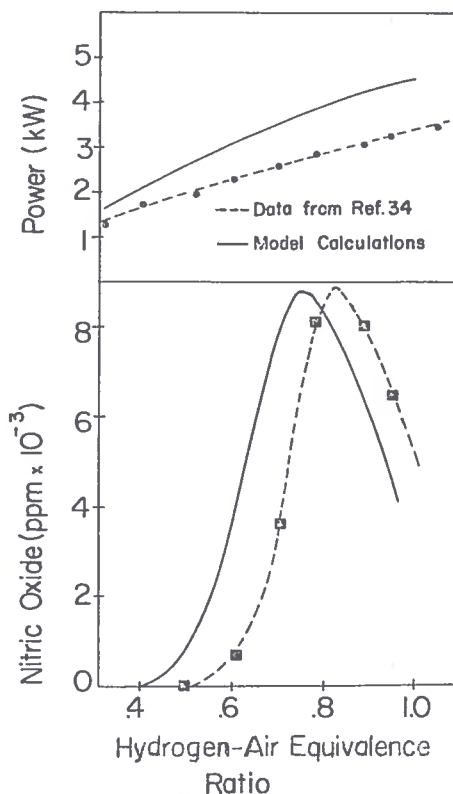


Figure 3. Power and NO Emissions with Adiabatic Model Compared with Experimental Measurements (Timing and manifold Pressure as in Ref 33, Compression Ratio 8, Displacement 611 cm<sup>3</sup>).

Although the shapes of the two NO curves in Figure 3 are similar, the model overpredicts the NO for  $\phi < 0.8$  and underpredicts NO for  $\phi > 0.8$ . These differences could be caused by a combination of heat transfer and flame speed effects. As explained in the following section, rate limited formation reactions govern NO in the very lean mixtures, while decomposition reactions govern NO in near stoichiometric mixtures. Lower temperatures in the leaner mixtures then result in less NO formation, but in the near stoichiometric mixtures lower temperatures limit NO decomposition during the expansion stroke and result in more exhaust NO. The differences between predicted and measured NO mole fractions shown in Figure 3 are thus qualitatively consistent with lower than predicted gas temperatures as would be caused by heat transfer.

It should also be noted that the NO predictions are very sensitive to the duration of combustion which is determined by the flame

speed model. Longer combustion durations result in lower burnt gas temperatures and this can effect the NO chemistry as described above. An example of the effect of combustion duration on NO emissions for  $\phi = 0.65$  is shown in Figure 4, and it is seen that the NO emissions are much more sensitive than other engine parameters to changes in combustion duration. Here again models which rely on experimental cylinder pressure information implicitly include the proper combustion duration.

In summary, although our model does not predict experimental results exactly, we feel the agreement is satisfactory for a model which does not require experimental cylinder pressure data. In the following section the application of the model to a wide range of engine conditions is illustrated.

#### 4. NITRIC OXIDE EMISSIONS FROM HYDROGEN ENGINES

On the basis of the above described model, nitric oxide emissions for hydrogen fueled reciprocating engines have been calculated for a wide variety of engine conditions. For most of these

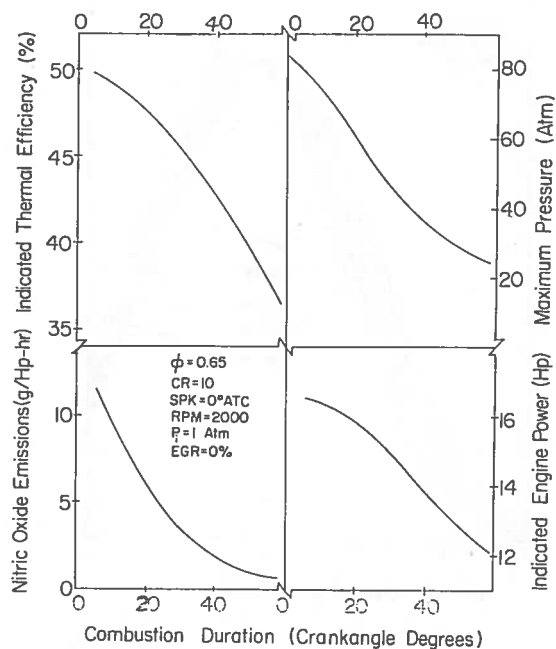


Figure 4. Effect of Combustion Duration on Engine Performance and Emissions

calculations we have assumed fuel injection directly into the cylinder, ignition at top center, an intake manifold pressure of one atmosphere, and 2000 RPM engine speed. The effects of speed, spark timing and manifold pressure on NO emissions from a hydrogen engine are given in reference (32).

Figure 5 shows the specific NO emissions computed for equivalence ratios from 0.5 to 1 and compression ratios from 6 to 14. Extremely low NO emissions are obtained for very lean mixtures due to the low combustion temperatures in this region. As with gasoline, NO emissions for hydrogen fuel reach a maximum to the lean side of stoichiometric and decrease with further increases in equivalence ratio. While we have not directly compared these NO levels with those obtained for gasoline under the same engine conditions, the NO values are generally in the same range as emissions for gasoline engines at wide open throttle (22). This is to be expected since the same chemical processes control the NO emissions in both cases and gas temperatures and stoichiometry are similar.

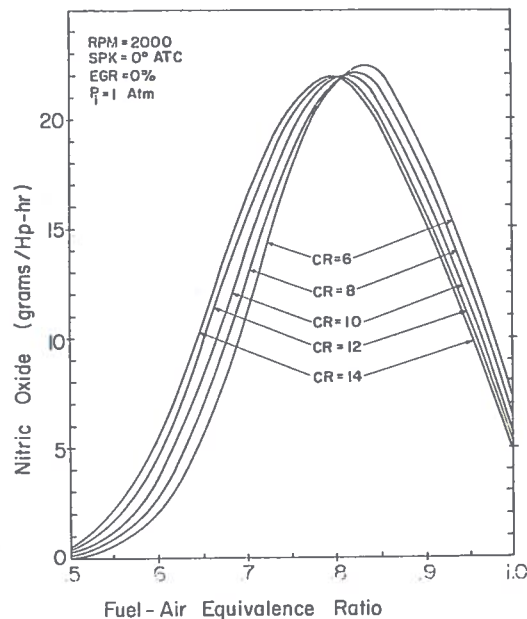


Figure 5. Computed NO<sub>x</sub> Emissions-Reciprocating Engine with Direct Injection of Hydrogen (Top center spark timing, one atmosphere manifold pressure).

It is interesting to note that the chemical processes controlling the net NO emissions are in different stages of evolution at different mixture stoichiometries. For equivalence ratios less than about 0.8 the NO is controlled by quenching of formation reactions during expansion, while for richer mixtures the NO emissions are primarily determined by the quenching of decomposition reactions during the expansion process. Figures 6 and 7 illustrate these effects. The Figures show the mole fractions of O, OH, H and NO and the gas temperature during the engine cycle for the first (0%), middle (50%) and last (100%) elements of charge to burn. The percentages given indicate the percent mass burned when that particular element burns. Figure 6 for  $\phi = 0.7$  shows that for this lean mixture the relatively high oxygen atom levels and moderate temperatures lead to NO mole fractions which are limited by thermal quenching of the NO formation reactions. Figure 7 for  $\phi = 1.0$  shows that in this stoichiometric mixture the high temperatures and resulting large free radical and atom concentrations greatly accelerate the NO reactions. The fast reactions, particularly the third reaction involving H and OH, allow the NO mole fraction to more closely follow chemical equilibrium, and substantial decomposition of NO is observed during the expansion stroke. This decomposition results in lower net NO emission for the richer mixture, and we have a situation where higher temperatures lead to lower NO emissions. Although NO decomposition is also seen in rich gasoline-air combustion products (22), the effect seems to be greatly enhanced with hydrogen fuel because of the increased significance of the third NO reaction due to the high concentrations of H and OH. In general then, the same chemical process control NO in both gasoline and hydrogen fueled engines, but the decomposition reactions become significant at leaner mixtures with hydrogen fuel because of higher combustion temperatures and different O, H and OH concentrations.

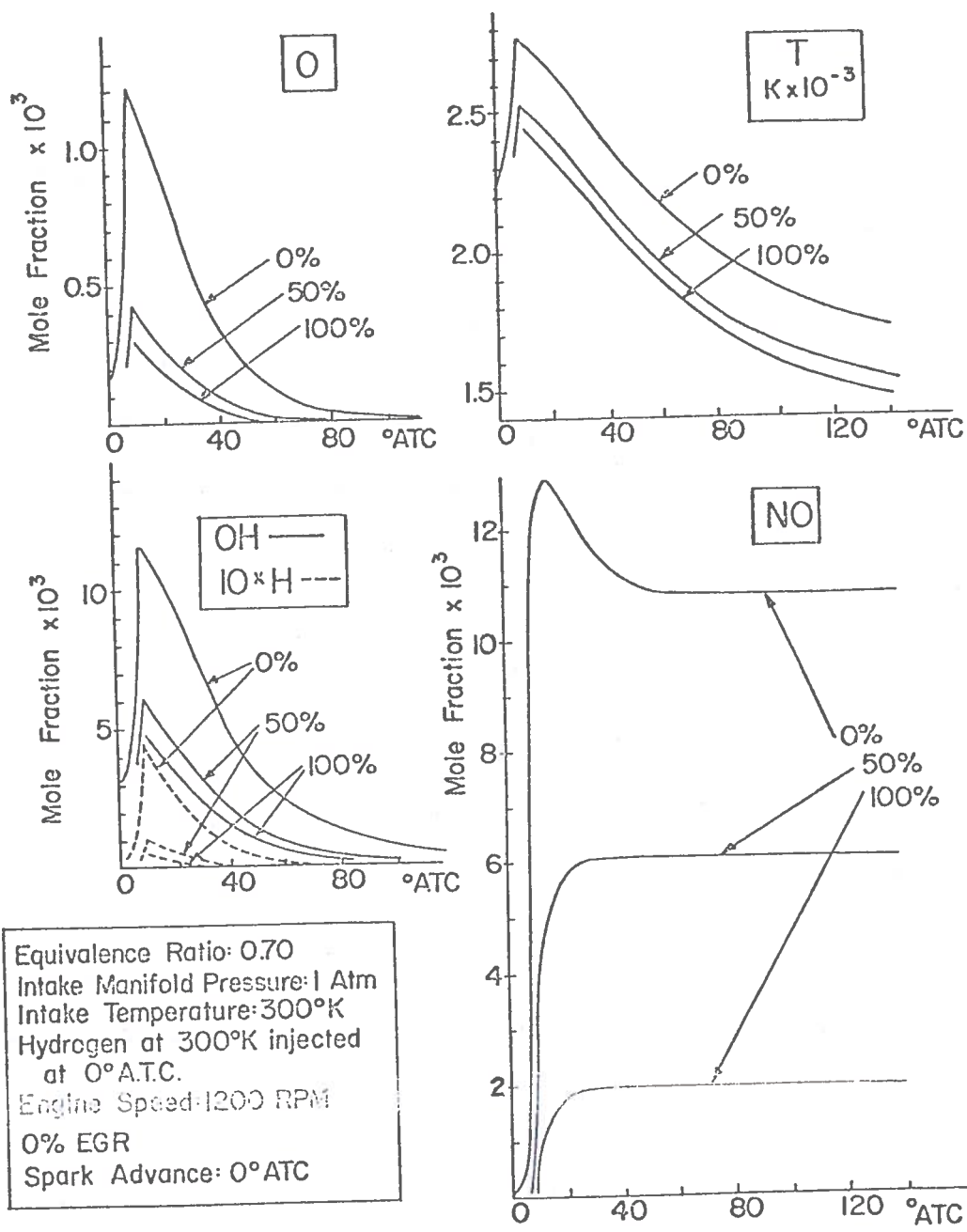


Figure 6 Composition and Temperature of Combustion Products During Engine Expansion Process, Lean Mixture. Mole Fractions of O, OH, H and NO and the Temperature are Shown for the First, Middle and Last Elements of Charge to Burn. NO Emissions are Determined by Quenching of Formation Reactions.

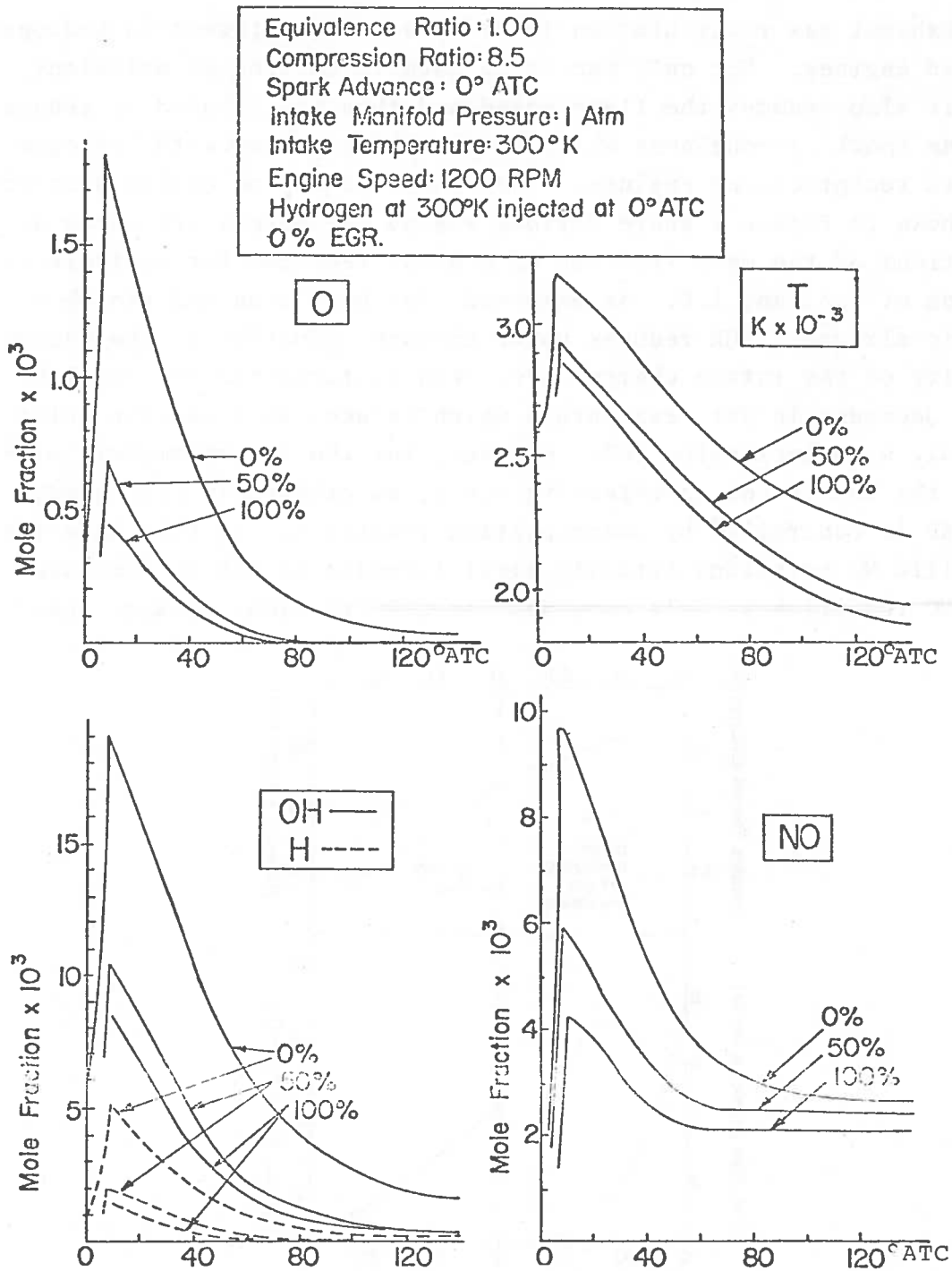


Figure 7 Composition and Temperature of Combustion Products During Engine Expansion Process, Stoichiometric Mixture. Mole Fractions of O, OH, H and NO and the Temperature are Shown for the First, Middle and Last Elements of Charge to Burn. NO Emissions are Determined by Quenching of Decomposition Reactions.



Exhaust gas recirculation (EGR) is also of interest in hydrogen fueled engines. Not only can it be used to control NO emissions, but it also reduces the flame speed and thus may be used to reduce engine knock or roughness which tend to be problems with hydrogen fueled reciprocating engines. The effect of EGR on engine operation is shown in Figure 8 where various engine parameters are shown as functions of the mass fraction of exhaust recycled for equivalence ratios of 0.65 and 1.0. As expected, for both lean and stoichiometric mixtures, EGR reduces power through reduction of the energy density of the intake charge. For lean mixtures the EGR results in a decrease in gas temperature which reduces NO formation quite rapidly with increasing EGR. However, for the stoichiometric mixture the EGR is not as effective since, as previously discussed, the NO is controlled by decomposition reactions. In this case the specific NO emissions actually first increase as EGR is increased and NO reduction is only obtained for EGR fractions greater than 0.2.

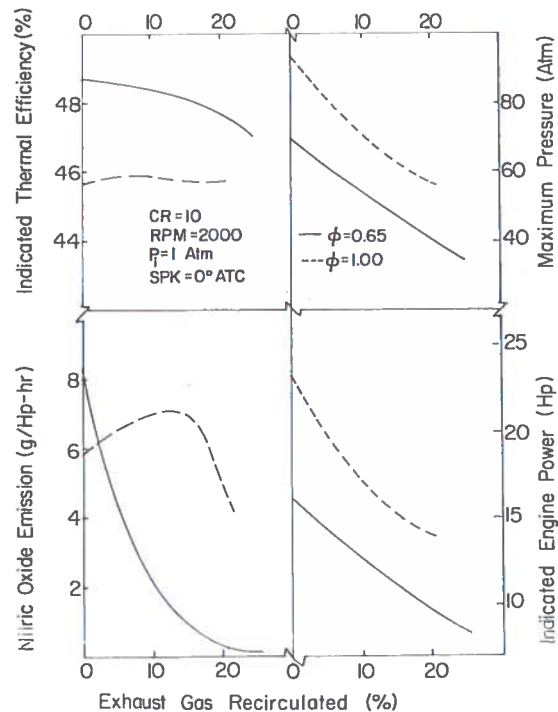


Figure 8 Effect of Exhaust Gas Recirculation on Engine Performance and Emissions, Hydrogen Fueled Engine with Direct Cylinder Fuel Injection at Two Equivalence Ratios. (% EGR is the Mass Fraction of Exhaust Recycled. Recycle Gas Temperature is Assumed to be the Mean of the Exhaust Gas and Intake Air Temperatures).

In considering NO emissions from hydrogen fueled vehicles consideration must be given to the emission level relative to Federal standards. At present the ultimate Federal standards for oxides of nitrogen ( $\text{NO}_x$ ) are specified at 0.4 g/mi average for a given driving cycle. In specific units, this translates to approximately 0.8 g/Hp-hr for a 3000 lb. vehicle (22). While it is difficult to quantitatively relate a driving cycle average emission to fixed operating point data, it is apparent that  $\text{NO}_x$  control could be obtained by mixture control in the case of a hydrogen engine with direct cylinder fuel injection. Figure 5 indicates that with a compression ratio of 8 and the equivalence ratio limited to about 0.55, it should be possible to meet this most stringent emission standard. Although this lean operation would limit engine power to about 55% of maximum power for that engine running on hydrogen, the power would nevertheless be about two-thirds of the maximum power available for that engine operating on gasoline. Also the hydrogen engine would be significantly more efficient than the gasoline engine by virtue of the unthrottled mode of operation.

If necessary, power output could be further increased by increasing the compression ratio of the engine. Engine knock and roughness usually associated with high compression ratio operation may not be a problem here because the very lean mixtures result in relatively slow flame speeds and lower unburned gas temperatures.

We have undertaken an experimental effort directed at examining hydrogen fueled engine performance and emissions with fuel injection directly into the cylinder under high compression ratio, lean mixture conditions. Preliminary results of this effort have been reported (42). This work is continuing and will attempt to define the design and operating parameters for a hydrogen fueled engine which is clean, highly efficient and produces adequate power.

## 5. CONCLUSIONS

In a future energy system based on hydrogen, reciprocating engines fueled with hydrogen may play a significant role in transportation power systems. Such powerplants can be highly efficient because they can be operated unthrottled using quality regulation

for power control. Nitric oxide emissions from hydrogen fueled engines are relatively high for near stoichiometric mixtures, but quite low for very lean mixtures. By using direct cylinder fuel injection and lean mixtures, hydrogen promises a highly efficient low emission engine of adequate power.

#### ACKNOWLEDGMENTS

This work was supported by the U.S. Department of Transportation, Office of University Research, under Contract No. DOT-OS-30113. Dr. Lawrence J. Muzio assisted in the development of the computer model.

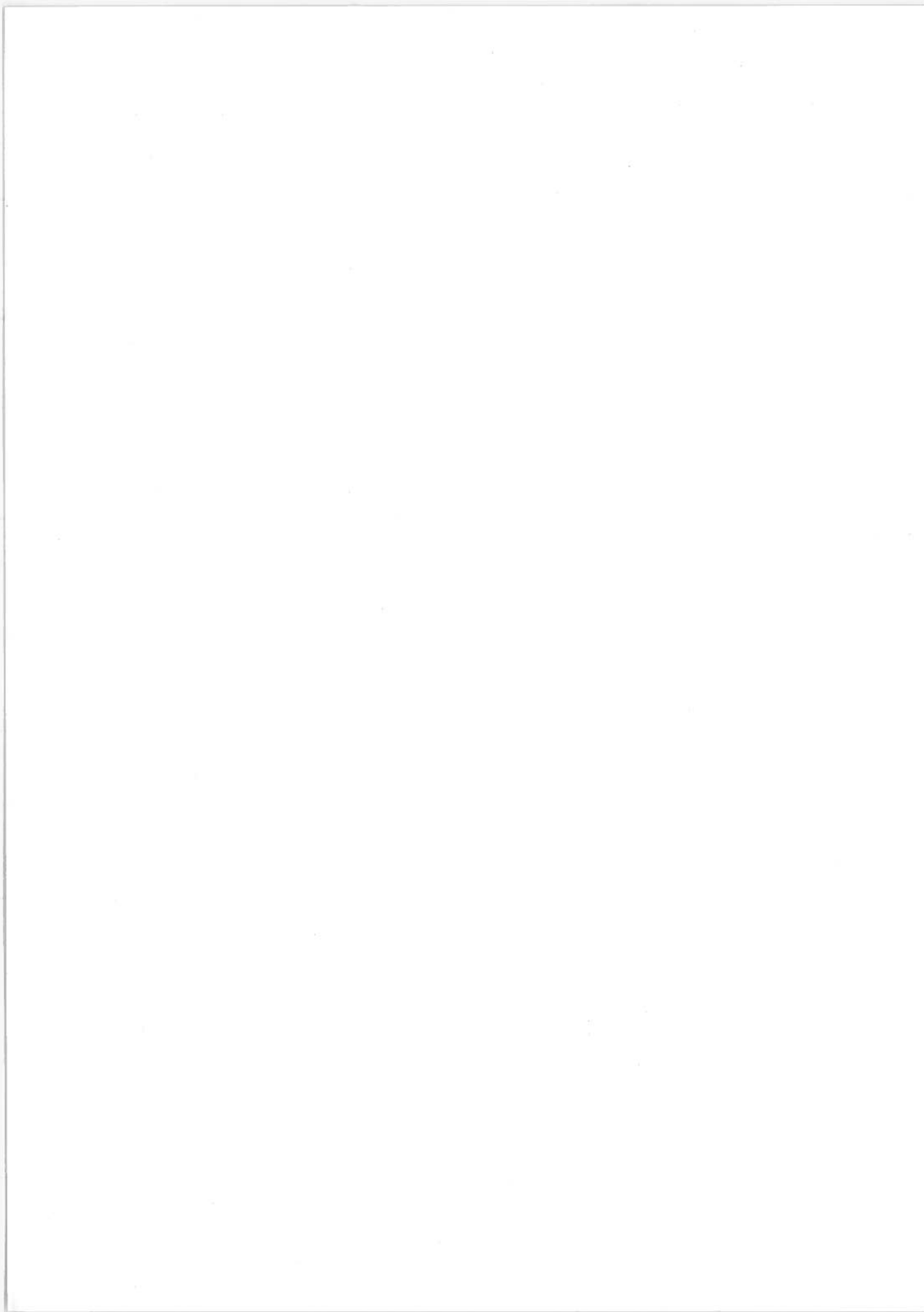
#### REFERENCES

- (1) Gregory, D. P., *Scientific American*, 228, No. 1, p. 13 (1973).
- (2) Gregory, D. P., Ng, D.Y.C., and Long, G.M., "The Electrochemistry of Cleaner Environments", J. O'M. Bockris, ed., Plenum Press, New York, New York, 1971, p. 226.
- (3) Winsche, W. E., Hoffman, K. C., and Salzano, F. J., *Science*, 180, 1325 (1972).
- (4) American Society of Mechanical Engineers, "9th Intersociety Energy Conversion Engineering Conference Proceedings", 1974, p. 394.
- (5) Linke, S., ed., "Cornell International Symposium and Workshop on the Hydrogen Economy, August 1973", to be published.
- (6) Veziroglu, T. N., ed., "The Hydrogen Economy Miami Energy (THEME) Conference Proceedings", The University of Miami, 1974.
- (7) Kant, F. H., et. al., "Feasibility Study of Alternative Fuels for Automotive Transportation", Report No. EPA-460/3-74-009a, Exxon Research and Engineering Co., Linden, New Jersey, June 1974.
- (8) McLean, W. J., "Alternative Fuels for Automobiles", submitted to National Academy of Sciences, Committee on Motor Vehicle Emissions, August 1974, to be published.
- (9) Synthetic Fuels Panel, Federal Council on Science and Technology, "Hydrogen and Other Synthetic Fuels", Report No. TID-26136, 1972.

- (10) "An Evaluation of Alternative Power Sources for Low Emission Automobiles", Report of the Panel on Alternative Power Systems to the Committee on Motor Vehicle Emissions, National Academy of Sciences, April 1973.
- (11) Richardson, R. W., "Automotive Engines for the 1980's", Eaton Corporation, 1973.
- (12) Austin, A. L., "A Survey of Hydrogen's Potential As a Vehicular Fuel", Report UCRL-51228, Lawrence Livermore Laboratory, June 1972.
- (13) Finegold, J. G., et. al., Paper No. 730507, Society of Automotive Engineers, Automotive Engineering Meeting, Detroit, May 1973.
- (14) Billings, R. E., "The Hydrogen Economy Miami Energy (THEME) Conference Proceedings", T. N. Veziroglu, ed., University of Miami, 1974, p. S8-51.
- (15) Swain, M. R., and Adt, R. R., 7th Intersociety Energy Conversion Conference Proceedings, September 1972.
- (16) Lichty, L. C., "Combustion Engine Processes", McGraw-Hill, New York, 1967.
- (17) Patterson, D. J., and Van Wylen, G., "Digital Calculations of Engine Cycles", E. S. Starkman, ed., Society of Automotive Engineers, New York, 1964, p. 82.
- (18) Caretto, L. S., Muzio, L. J., Sawyer, R. F., and Starkman, E. S., Combustion Science and Technology, 3, 53 (1971).
- (19) Komiyama, K., and Heywood, J. B., Paper No. 730475, Society of Automotive Engineers, Automobile Engineering Meeting, Detroit, May 1973.
- (20) Varde, K. S., and Lucas G. G., "Temperature History in the Combustion Chamber of a Spark Ignition Engine", presented at Society of Automotive Engineers, Toronto Meeting, 1974.
- (21) Lavoie, G. A., Heywood, J. B., and Keck, J. C., Combustion Science and Technology, 1, 316 (1970).
- (22) Blumberg, P., and Kummer, J. T., Combustion Science and Technology, 4, 73 (1971).
- (23) De Soete, G., "Advances in Automotive Engineering, Part IV, Combustion Processes in the Spark Ignition Engine", D. Hodgetts, ed., Pergamon Press, Oxford 1966, p. 35.
- (24) Phillips, R. A., and Orman, P. L., ibid., p. 93.
- (25) Lucas, G. G., and James, E. H., Paper No. 730053, Society of Automotive Engineers, Intl. Automotive Engineering Congress, Detroit, January 1973.

- (26) Andrews, G. E., Bradley, D., and Lwakabamka, S. B., "Measurement of Turbulent Burning Velocity for Large Turbulent Reynolds Numbers", Presented at XVth Symposium (Int'l) on Combustion, Tokyo, August 1974.
- (27) Arrigoni, V., Calvi, F., Cornetti, G. M., and Pozzi, U., Paper No. 730088, Society of Automotive Engineers, Int'l. Automotive Engineering Congress, Detroit, January 1973.
- (28) Dugger, G. L., Simon, D. M., and Gerstein, M., "Basic Considerations in the Combustion of Hydrocarbon Fuels with Air", NACA Report 1300, 1959, p. 148.
- (29) Delbourg, M. P., *Revue de L'Institute Francaise de Petrole*, 4, 530 (1949).
- (30) Muzio, L. J., "Spark Ignition Simulation and Prediction of Nitric Oxide Formation", April 1972, unpublished.
- (31) Stephenson, P. L., and Taylor, R. G., *Combustion and Flame*, 20, 231 (1973).
- (32) Fagelson, Jean-Jacques M. S. Thesis, Cornell University, November 1974.
- (33) Stebar, R. F., and Parks, F. B., Paper No. 740187, Society of Automotive Engineers, Automotive Engineering Congress, Detroit, 1974. Additional data provided by Dr. F. B. Parks, General Motors Research Laboratories.
- (34) Finegold, J. G., and Van Vorst, W. D., "The Hydrogen Economy Miami Energy (THEME) Conference Proceedings, T. N. Veziroglu, ed., University of Miami, 1974.
- (35) Oehmichen, M., "Wasserstoff als Motortreibmittelz", *Deutsche Kraftfahrtforschung Heft 68*, VDI-Verlag, Berlin, 1942.
- (36) Palmer, H. B., and Seery, D. J., *Ann. Rev. Phys. Chem.*, 24, 235 (1973).
- (37) Heywood, J. B., Mathews, S. M., and Owen, B., Paper No. 710011, Society of Automotive Engineering, Automotive Engineering Congress, Detroit, 1971.
- (38) Shahed, S. M., and Newhall, H. K., *Combustion and Flame*, 17, 131 (1971).
- (39) Malte, P. C., and Pratt, D. T., "The Role of Energy-Releasing Kinetics in NO<sub>x</sub> Formation: Fuel-Lean, Jet-Stirred CO-Air Combustion", Presented at XVth Symposium (Int'l.) on Combustion, Tokyo, August, 1974.
- (40) Baulch, D. L., Drysdale, D. D., Horne, D. G., and Lloyd, A. C., "Evaluated Kinetic Data for High Temperature Reactions, Vol. 2", Butterworths, London, 1973.

- (41) Taylor, C. F., and Taylor, E. S., "The Internal-Combustion Engine", 2nd. Edition, International Textbook, Scranton, 1961.
- (42) de Boer, P. C. T., McLean, W. J., Fagelson, J. J., and Homan, H. S., "9th Intersociety Energy Conversion Engineering Conference Proceedings" 1974, Paper No. 749056, p. 479.



HYDROGEN CAR DEVELOPMENT  
William D. Van Vorst  
University of California, Los Angeles  
Los Angeles, California

ABSTRACT

This paper reviews experimental investigations relative to hydrogen car development. A comparative study of the performance of a 1973 Chevrolet 350 cid., V-8 engine indicated thermal efficiencies of from 25 to 100% greater with hydrogen than with gasoline. The emission of nitrogen oxides was reduced approximately 90% when operating on hydrogen. With quality-governed, hydrogen operation, however, maximum power output is reduced by as much as 50%; with water injection, the figure might be 30%.

The kinetics and mechanism of magnesium alloy-hydride formation and dissociation were explored. The process was found to be diffusion controlled. Mg-10Al hydrides containing 7% hydrogen by weight were formed. This alloy did not show excessive fragmentation on cycling and would seem the only one potentially useful in transportation systems. Its temperature-pressure equilibrium condition is less than favorable, however.

A liquid hydrogen system was developed and installed in a 1973 Jeep. Details of the system are presented below. Basically it was found to be feasible and operating experience thus far is favorable.

## 1. INTRODUCTION

The hydrogen fueled engine was first demonstrated by Cecil in England ca. 1820<sup>1</sup>. It was a stationary engine and the advantages Cecil claimed for it were that its location was not restricted (as was the water wheel's) nor did it take a long time to reach full power after start up (as did the steam engine). About 100 years later, again in England and also in Germany, research was directed toward its use in engines for automobiles, submarines, and lighter-than-air aircraft. In 1933, Erren and Campbell<sup>2</sup> (Erren had extensive experience in Germany during the 20's) called attention to the solution hydrogen offered for two serious problems faced by England: the pollution of the atmosphere by the combustion of fossil fuels, and her dependence on foreign sources for petroleum. Forty years later, the same dilemmas confront much



larger sections of the world, and again the use of hydrogen offers hope for solution.

Realistic evaluation of such hope, however, requires the investigation of several factors. This report concerns those factors having to do with engine performance and fuel storage.

## 2. ENGINE PERFORMANCE WITH HYDROGEN

A 1973 Chevrolet V-8 350 cubic inch displacement (cid) engine was operated first on gasoline, with the required pollution control devices. These devices were then removed, appropriate modifications made and the tests repeated with hydrogen. Thermal efficiencies and nitrogen oxides emissions were determined as functions of power output at various engine speeds. Hydrogen operation was unthrottled, using a "quality governing" scheme - i.e. direct regulation of the hydrogen flow. Comparison of results indicates that thermal efficiency is significantly higher, and nitrogen oxides emissions dramatically lower with operation on hydrogen. Increases in efficiency of from 25 to 100% were noted, the greatest increase being obtained at lower power output. Nitrogen oxides emissions were reduced approximately 90% at the higher power loads - the severest condition. Figures 1 and 2 show the efficiency-power output relations obtained for engine speeds of 2000 and 3500 rpm. Figures 3 and 4 show the comparative production of total oxides of nitrogen. The dips in the curves for gasoline operation indicate the effectiveness of the pollution control devices. Unfortunately, at lower speeds (see Figure 1) this is accompanied by a corresponding drop in efficiency; this effect diminishes at higher speeds, however. The hydrogen curves of Figures 1 and 2 terminate "prematurely" due to the occurrence of pre-ignition and backfire, or more specifically "firing-back" through the intake system. No explicit correlations were developed, but maximum power with hydrogen was limited to roughly 50% that obtained with gasoline, as equivalence ratios\* were limited to under 60% by backfire. It

---

\*i.e. the ratio of the actual fuel-to-air ratio employed to the stoichiometric.

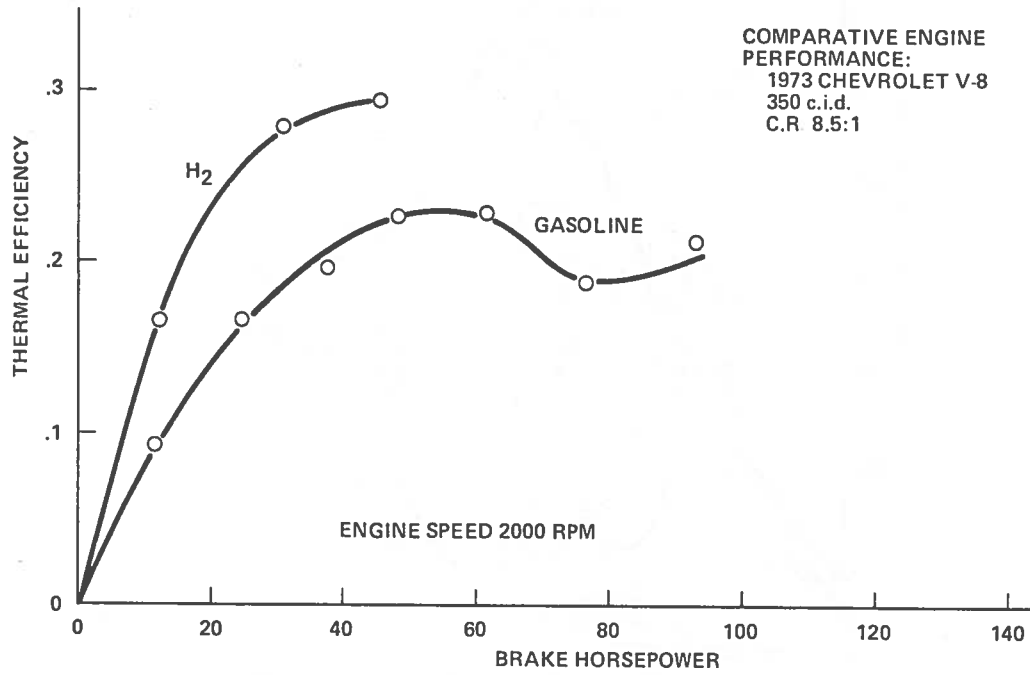


Figure 1. Thermal Efficiency Versus Power (2000 RPM)

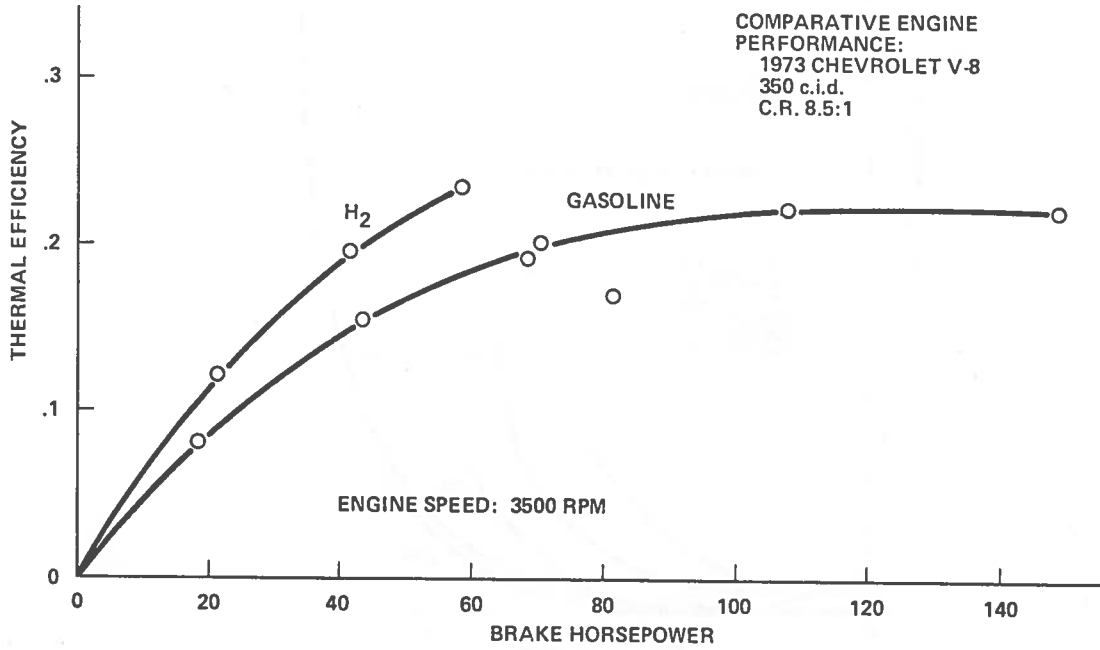


Figure 2. Thermal Efficiency Versus Power (3500 RPM)

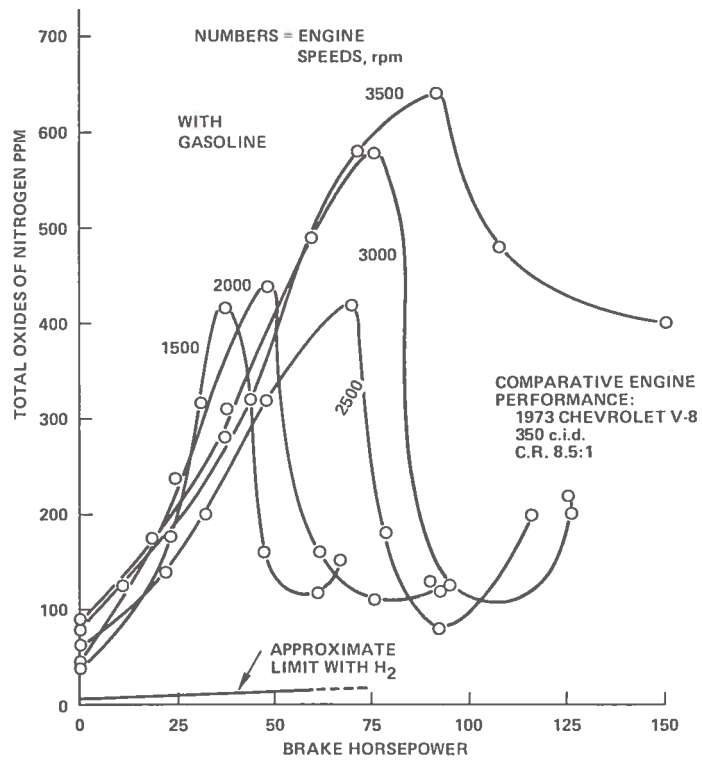


Figure 3. Oxides of Nitrogen Production with Gasoline

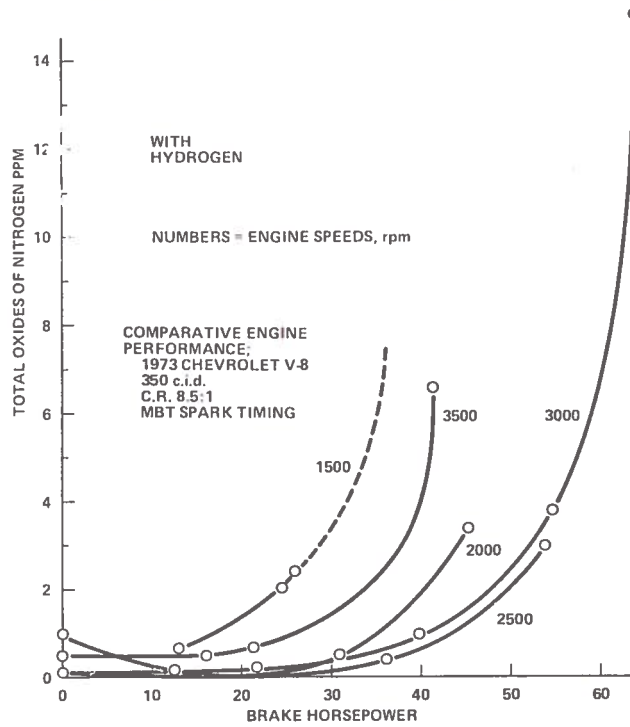


Figure 4. Oxides of Nitrogen Production with Hydrogen

must be noted however that this is with "quality-governing". With some form of charge dilution - exhaust gas recycle, or water induction, the power output should be raised to the neighborhood of 70% of that obtained with gasoline. It was found highly beneficial to narrow the spark plug gap significantly when using hydrogen. The engine performance characteristics obtained with (quality-governed) hydrogen were fed to the simulator of the University of Wisconsin project on "Increased Fuel Economy in Transportation Systems by Use of Energy Management." Results (assuming a 2000 lb. vehicle) indicated performance superior to that of a 60 horsepower Volkswagen with a top speed of 75 or 80 mph. Nitrogen oxides emissions were predicted to be 0.06 grams/mile, in contrast to the 1976-77 Federal standard of 0.4 grams/mile.

All in all, engine performance with hydrogen is basically satisfactory, and promises greater efficiency with a minimal contribution to air pollution.

### 3. HYDRIDE STORAGE OF HYDROGEN

The problem of containing hydrogen is generally well known. Despite its high heating value on a mass basis (over two-and-one-half times that of gasoline) its low density dictates a higher volume storage requirement. As an alternative to the use of liquid hydrogen, Reilly,<sup>3,4,5</sup> et al of the Brookhaven National Laboratories suggested the use of (reversible) hydrides (1968), and have explored the properties of a great number of intermetallic compounds. The appropriate hydride must have several properties: a fast rate of formation and dissociation over a favorable temperature-pressure equilibrium range with a low heat effect requirement; a high capacity for hydrogen; light weight; longevity with minimal fractionation and pulverization on continued cycling; and economic feasibility. The substance having an optimal mix of these properties continues to elude detection.

This work was directed toward a fundamental study of the kinetics of the hydride formation and dissociation phenomena, and concentrated on alloys rather than intermetallic compounds. In

particular, Mg-10Al\* and Mg-25Ni\* were investigated in detail. The formation and dissociation processes were found to be diffusion-controlled. Mg-10Al is the most promising for vehicular operation, having a hydrogen capacity over 7% by weight, and being highly resistant to fragmentation. Its heat requirement and temperature-pressure equilibrium range are less favorable, however, and some direct hydrogen combustion would be required to furnish hydrogen to the engine. In essence, this implies a penalty perhaps as high as 20 percent chargeable against fuel economy.

The findings of alloys, in contrast to intermetallic compounds, as possible suitable hydrogen storage systems is of considerable promise. Only two could be investigated thoroughly in the time available for this work, and while neither is entirely suitable much further study is warranted. The economy of production of gaseous hydrogen rather than liquid is such that the development of a hydride system of storage is of fundamental importance to the future "hydrogen economy".

#### 4. THE LIQUID HYDROGEN FUEL SYSTEM

While the hydride storage system offers considerable promise for the future, it must be acknowledged that those known at present are less than suitable for automotive applications. Iron-titanium on the one hand has acceptable thermodynamic equilibrium conditions and kinetics but would be prohibitively heavy. The magnesium-aluminum alloy discussed might be acceptable weight-wise, but could not be activated readily through use of exhaust gas heat - due both to the high temperature required and the magnitude of the energy requirement per se. Figure 5 gives exhaust gas temperatures obtained in this study; noting that the release temperature of magnesium-based hydrides seems to be about 300°C, exhaust gas energy for iron-titanium, but, again, it must be ruled out from weight considerations.

---

\*i.e. 10% aluminum and 25% nickel, by weight

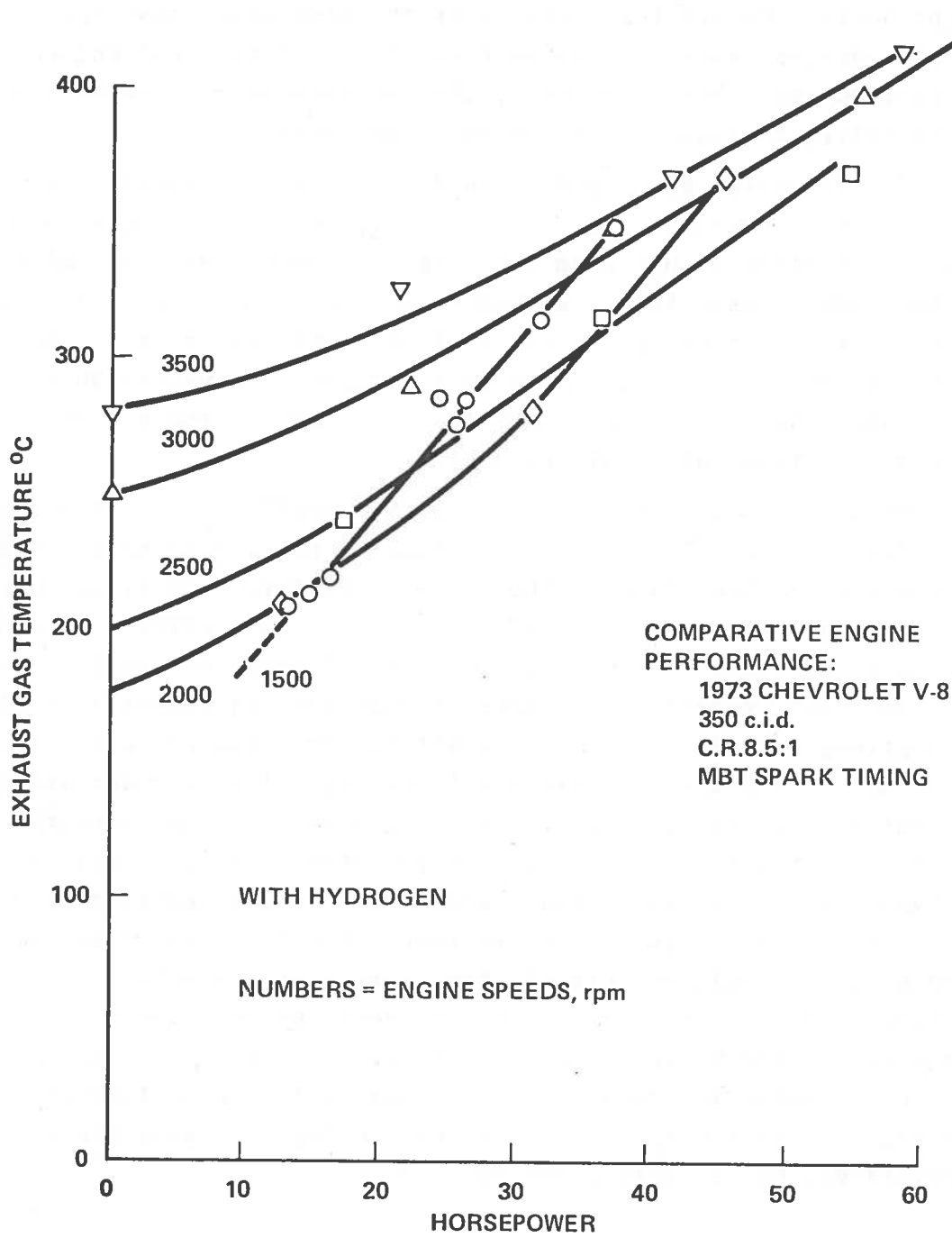


Figure 5. Exhaust Gas Temp. vs. Power Output at Various Engine Speeds

High pressure gaseous storage may also be ruled out on a weight basis. We are left, then with the conclusion that the liquid hydrogen system is the most feasible for the near future. In order to test this hypothesis, the development of a vehicle system operating on liquid hydrogen was undertaken.

In the system developed, liquid hydrogen was stored in a 50-gal. dewar\*; as required, a 12-watt heater in the tank generated pressure to force liquid from the tank to a vaporizer, from which hydrogen gas at essentially atmospheric temperature flowed to the engine. Cryogenic equipment was used up to the vaporizer. The system was vented at 35 psi through a catalytic converter so that water vapor was discharged rather than hydrogen. Figure 6 is a schematic representation of the system.

The vehicle employed was a 1973 AMC Jeep\*\* with a 232 c.i.d., 6 cylinder engine. The engine was modified to operate on hydrogen, using ordinary throttling of the fuel-air mixture. Water was used as the charge diluent, being injected via the carburetor and regular (gasoline) fuel system. Figure 7 is a diagram of the flow system. Although overall performance characteristics (specific fuel consumption, emission, etc.) could not be investigated in detail, it can be concluded that operation in general is highly satisfactory. Not surprisingly, several "second-generation" improvements are in order and could be easily incorporated. The top-works of the tank, through which liquid hydrogen enters and leaves must be better insulated to reduce heat leakage. The fuel system may be redesigned to permit occasional, temporary vapor takeoff to reduce pressure buildup in the tank - thereby reducing vent losses. The vaporizer, heated by engine cooling water, may be greatly reduced in size. Further instrumentation is desirable, in particular a fuel gage. This remains a challenging problem at liquid hydrogen temperatures, but certainly not insoluble.

---

\*donated by the Minnesota Valley Engineering Co.

\*\*made available by the U.S. Postal Service.

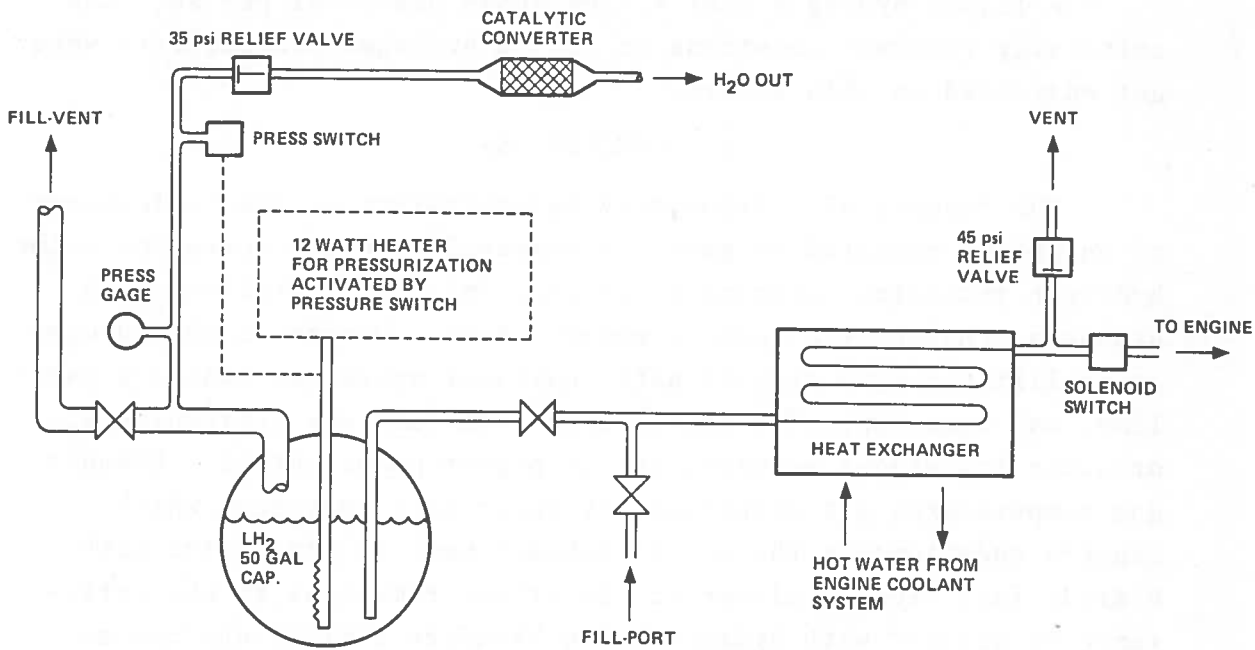


Figure 6. Liquid Hydrogen Fuel System

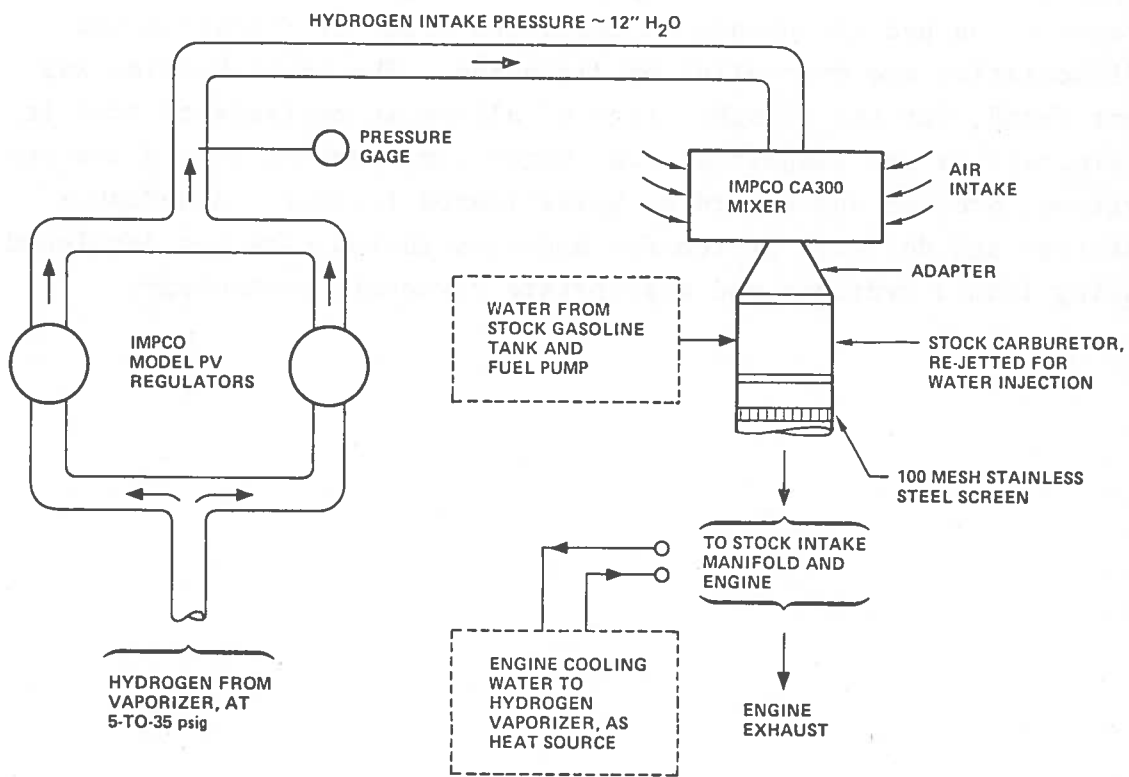


Figure 7. Flow of Hydrogen to Engine



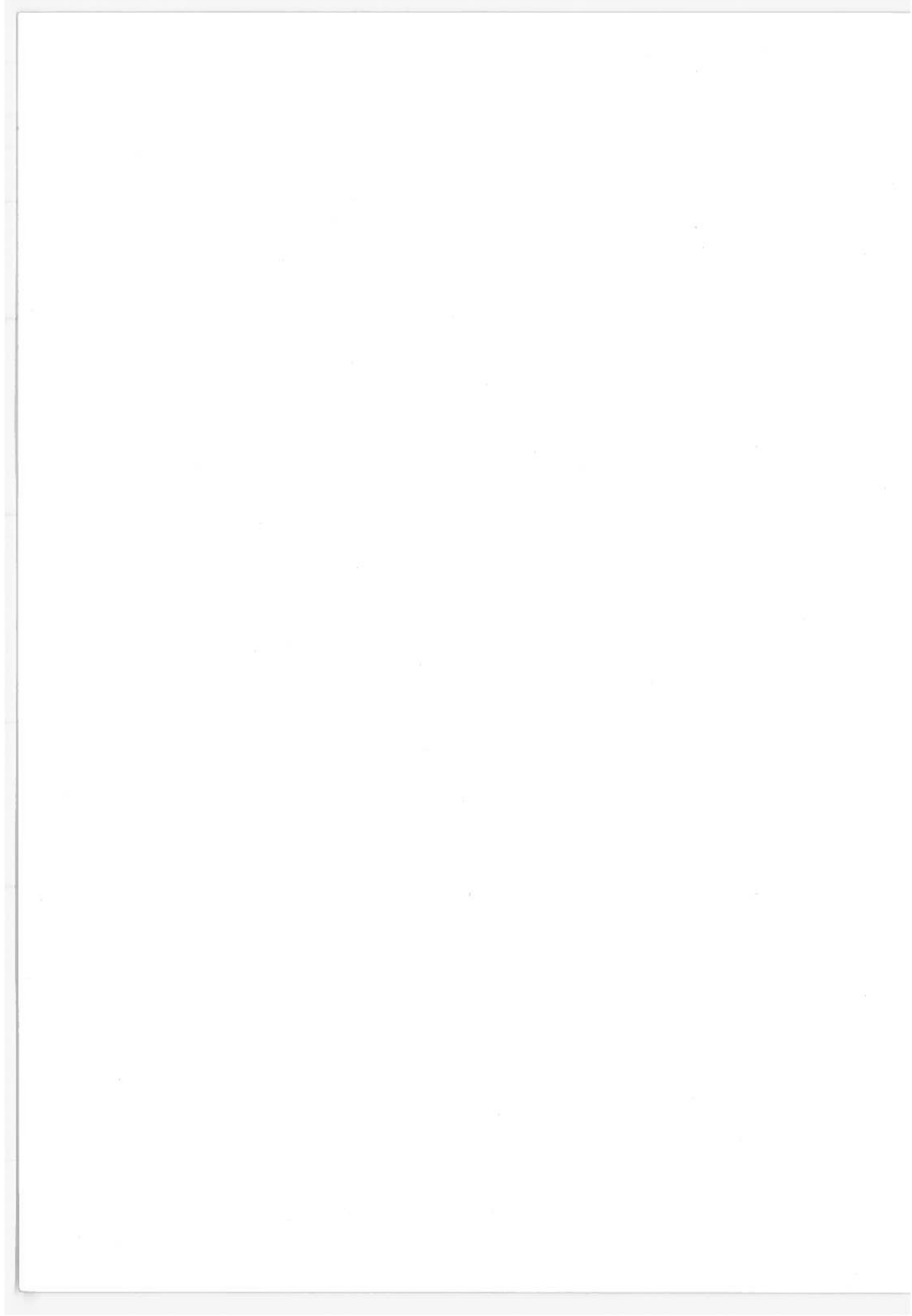
A liquid hydrogen fuel system seems practical per se. The critically relevant questions of liquid hydrogen availability were not addressed in this effort.

## 5. CONCLUSIONS

The results of a laboratory investigation of the performance of an engine operated on gasoline compared with its operation using hydrogen indicates superior efficiency and lower emissions with hydrogen, though at a reduced power output. Operation on hydrogen is facilitated by a significantly narrower spark gap than for gasoline, and some type of charge diluent (exhaust gas recirculation or water induction) is necessary at higher power output. Exhaust gas temperatures are significantly lower with hydrogen, which renders questionable the use of exhaust heat in connection with hydride fuel storage elements. Questions remain as to why efficiency is greater with hydrogen, how backfire limitations can be eliminated, and what specific variables need optimization if a hydrogen engine were to be especially designed. The fundamental research on hydride phenomena indicates rates of formation and dissociation are controlled by diffusion. The ideal hydride was not found, but the possibilities of alloys in contrast to true intermetallics was suggested; e.g. magnesium-aluminum alloys are not without promise and should be investigated further. A workable storage and delivery system for hydrogen-fueled cars was developed using liquid hydrogen and appropriate cryogenic technology.

## REFERENCES

1. W. Cecil, "On the Application of Hydrogen Gas to produce a moving Power in Machinery; with a Description of an Engine which is moved by the Pressure of the Atmosphere upon a Vacuum caused by Explosions of Hydrogen Gas and Atmospheric Air." Trans. of the Cambridge Philosophical Society. Vol. 1, (1822).
2. R. A. Erren and W. H. Campbell, "Hydrogen: A Commercial Fuel for Internal Combustion Engines and Other Purposes," J. Inst. Fuel, 6:277-290, (1933).
3. Reilly, J. J. and Wiswall, R. H., Jr., Inorganic Chem., 7 (1968) 2254.
4. C. H. Waide, J. J. Reilly, and R. H. Wiswall, Jr. "The Application of Metal Hydrides to Ground Transport," Proc. of the Hydrogen Economy Miami Energy (THEME) Conference, The University of Miami, Coral Gables, Fla, 1974.
5. G. Strickland, J. J. Reilly, and R. H. Wiswall, Jr. "An Engineering-Scale Energy Storage Reservoir of Iron-Titanium Hydrides," Proc. of the Hydrogen Economy Miami Energy (THEME) Conference, The University of Miami, Coral Gables, Fla. 1974.



AEEP  
CONTRACTORS COORDINATION MEETING  
ATTENDEES

A. Stuart Baldwin  
IIT Research Institute  
1825 K St., NW  
Washington, D.C. 20006

Charles Burton  
Arthur D. Little, Inc.  
Acorn Park  
Cambridge, MA 02140

N. Beachley  
Dept. of Mechanical Engineering  
University of Wisconsin  
Madison, WI 53706

Melvyn Cheslow  
The Urban Institute  
2100 M St., NW  
Washington, D.C. 20037

Darrell Beschen  
Federal Energy Administration  
12th and Pennsylvania Ave., NW  
Washington, D.C. 20460

Samuel K. Clark  
201 W. Engineering Building  
University of Michigan  
Ann Arbor, MI 48104

John Bishop  
Arthur D. Little, Inc.  
Acorn Park  
Cambridge, MA 02140

Carlos Coon, Jr.  
Southwest Research Institute  
850 Culebra Rd.  
San Antonio, TX 78284

Douglas Blake  
Scientific Energy Systems  
570 Pleasant St.  
Watertown, MA 02172

Henry Cotrill  
Jet Propulsion Laboratory  
California Institute of Technology  
4800 Oak Grove  
Pasadena, CA 91103

Thomas Bolan  
Hittman Associates, Inc.  
9190 Red Branch Rd.  
Columbia, MD 21045

R.E. Crosthwait  
Mobile Research and Development Corp.  
Research Department  
Paulsboro, NJ 08066

Dwight D. Bornemeier  
Michigan Energy & Resource  
Research Assoc.  
502 Executive Plaza  
Detroit, MI 48226

Norman Curry  
Cummins Engine Co.  
1000 Fifth St.  
Columbus, IN 47201

Connie Buckley  
Federal Energy Administration  
12th and Pennsylvania Ave., NW  
Washington, D.C. 20460

Alfred C.W. Daniels  
H.H. Aerospace Design Co., Inc.  
L.G. Hanscom Field  
Bedford, MA 01730

P.C.T. de Boer  
Grumman Hall  
Cornell University  
Ithaca, NY 14830

William J. Devereaux  
DOT/Office of the Assistant  
Secretary for Systems  
Development and Technology  
400 7th St., SW  
Washington, D.C. 20590

John Doohar  
Adelphi University  
Garden City  
Long Island, New York 11530

M.W. Dowdy  
Jet Propulsion Laboratory  
California Institute of Technology  
4800 Oak Grove  
Pasadena, CA 91103

Suniel Dutta  
Army Materials and Mechanics  
Research Center  
Watertown, MA 02172

Merrill Ebner  
Boston University  
207 Bay State Rd.  
Boston, MA 02215

J.F. Flagg  
Vice President-Director of Research  
Universal Oil Products  
10 UOP Plaza  
Des Plaines, IL 60016

Paul G. Foldes, Esq.  
Federal Trade Commission  
Washington, D.C. 20580

A.A. Frank  
Dept. of Mechanical Engineering  
University of Wisconsin  
Madison, WI 48042

W.S. Freas  
Milford Vehicle Emission Laboratory  
General Motors Proving Ground  
Milford, MI 48042

George Gazza  
Army Materials and Mechanics  
Research Center  
Watertown, MA 02172

Raymond E. Goodson  
Chief Scientist  
DOT/ Office of the Secretary  
for Systems Development  
and Technology  
400 7th St., SW  
Washington, D.C. 20590

William Hailey  
AVCO  
201 Lowell St.  
Wilmington, MA 01887

Harold M. Haskew  
Milford Vehicle Emission Laboratory  
General Motors Proving Ground  
Milford, MI 48042

F. Earl Heffner  
General Motors Corp.  
General Motors Technical Center  
Warren, MI 48090

Merrill G. Hinton  
The Aersospace Corp.  
2350 El Segundo Boulevard  
El Segundo, CA 90245

Daniel L. Hirsch  
DOT/National Highway Traffic Safety  
Administration  
400 7th St., SW  
Washington, D.C. 20590

Dr. Hoagland  
Scientific Energy Systems  
570 Pleasant St.  
Watertown, MA 02172

Allan Hoffman  
Senate Committee on Commerce  
Dirksen Senate Office Building  
Washington, D.C. 20510

William C. Holt  
Corporate Research Center  
Universal Oil Products  
10 UOP Plaza  
Des Plaines, IL 60016

Michael Horner  
Boston University  
207 Bay State Rd.  
Boston, MA 02215

Peter Huntley  
Orshansky Transmission Corp.  
18 Bellevue Rd.  
Belmont, MA 02178

Donald A. Hurter  
Arthur D. Little, Inc.  
Acorn Park  
Cambridge, MA 02140

Robert A. Husted  
DOT/Office of the Assistant  
Secretary for Systems  
Development and Technology  
400 7th St., SW  
Washington, D.C. 20590

Mont Hubbard  
Dept. of Mechanical Engineering  
University of California at Davis  
Davis, CA 95616

R.T. Johnson  
Mechanical and Aerospace Engin-  
eering Department  
University of Missouri-Rolla  
Rolla, MO 65401

Hans C. Joksch  
Center for Environment and Man, Inc.  
275 Windsor St.  
Hartford, CT 06119

R. Nathan Katz  
Army Materials & Mechanics  
Research Center  
Watertown, MA 02172

Frank L. Kinnear  
E.I. DuPont De Nemours & Company  
Wilmington, DE 19898

George E. Kochanek  
Borg-Warner Corporation  
R.C. Ingersoll Research Center  
Wolf and Algonquin Roads  
Des Plaines, IL 60018

Ronald Kopicki  
ICF, Inc.  
1828 L St. N.W.  
Washington, D.C. 20036

Robert L. Krick  
DOT/Office of the Assistant  
Secretary for Systems Development  
and Technology  
400 7th St. S.W.  
Washington, D.C. 20590

Michael Lauriente  
DOT/Office of the Assistant  
Secretary for Systems Development  
and Technology  
400 7th St. S.W.  
Washington, D.C. 20590

Eugene L. Lehr  
DOT/Office of Environmental Affairs  
400 7th St. S.W.  
Washington, D.C. 20590

L.H. Lindgren  
Rath & Strong, Inc.  
21 Worthen Rd.  
Lexington, MA 02172

R.L. Love  
Chrysler Corporation  
P.O. Box 1118  
Detroit, MI 48231

Stephen Luchter  
Environmental Protection Agency  
2929 Plymouth Rd.  
Ann Arbor, MI 48105

David Lee  
Arthur D. Little, Inc.  
Acorn Park  
Cambridge, MA 02140

Stuart W. Martens  
GM Environmental Activity Staff  
General Motors Technical Center  
Warren, MI 48090

A.E. Marshall  
Ford Motor Company  
Environmental Research Office  
The American Road  
Dearborn, MI 48121

William F. Marshall  
U.S. Bureau of Mines  
Bartlesville Energy Research Cntr.  
Bartlesville, OK 74003

Richard A. Matula  
Mechanical Engineering and Mech.  
Department  
Drexel University  
Philadelphia, PA 19104

Michael J. McDanold  
DOT/Federal Highway Admin.  
400 7th St. S.W.  
Washington, D.C. 20590

Gene Moulic  
AVCO  
Wilmington, MA 01880

William J. McLean  
Grumman Hall  
Cornell University  
Ithaca, NY 14830

C.E. Mc Inerney  
AiResearch Industrial Division  
3201 Lomita Blvd.  
Torrance, CA 90505

Gerald W. Meisenholder  
Jet Propulsion Laboratory  
California Institute of Technology  
4800 Oak Grove Drive  
Pasadena, CA 91103

Joseph Meltzer  
The Aerospace Corporation  
P.O. Box 92957  
Los Angeles, CA 90009

B.T. Morris  
Jet Propulsion Laboratory  
California Institute of Technology  
Pasadena, CA 91103

Paul A. Nelson  
Chemical Engineering Division  
Argonne National Laboratory  
9700 South Cass Avenue  
Argonne, IL 60439

Robert Nutter  
DOT/Office of the Assistant Sec.  
for Policy, Plans, and International  
Affairs  
400 7th St. S.W.  
Washington, D.C. 20590

Rod Nerrey  
ADL Consultant  
Acorn Park  
Cambridge, MA 02140

C. Orndorff  
Army Material & Mechanics  
Research Center  
Watertown, MA 02172

J. Henry Parker  
Rath & Strong Inc.  
21 Worthen Rd.  
Lexington, MA 02172

Ralph Pecora  
Texaco Research Center  
P.O. Box 509  
Beacon, NY

P.J. Philliou  
Scientific Energy Systems  
570 Pleasant St.  
Watertown, MA 02172

J.D. Powell  
Department of Aero & Astro.  
Stanford University  
Stanford, CA 94305

James A. Proodian  
Consultant  
Duxbury, MA 02332

Joe M. Rife  
Sloan Automotive Laboratory  
Massachusetts Institute of  
Technology  
Cambridge, MA 02139

Baldwin Robertson  
Fluid Meters Section, IBS  
National Bureau of Standards  
Washington, D.C. 20234

Julian G. Ryan  
Shell Development Company  
P.O. Box 262  
Wood River, IL 62095

C.F. Scheffey  
Director of Research  
DOT/Federal Highway Administration  
400 7th St. S.W.  
Washington, D.C. 20590

W.E. Schwieder  
Fuel Economy & Vehicle Noise  
Ford Motor Company  
The American Road  
Dearborn, MI 48121

Joseph Smith  
Department of Mechanical Engineering  
MIT  
Cambridge, MA 02139

G.W. Stanke  
Ethyl Corporation  
1600 W. 8 Mile Road  
Ferndale, MI 48220

Lew Steers  
NASA Flight Research Center  
Edwards, CA 93523

Richard Strombotne  
DOT/Office of the Assistant Sec.  
for Systems Development and Tech.  
400 7th St. S.W.  
Washington, D.C. 20590

William Swan  
Assistant Engineer, Advanced  
Car Systems  
Chrysler Corporation  
P.O. Box 1118  
Detroit, MI 48231

Rodney J. Tabaczynski  
Sloan Automotive Laboratory  
MIT  
Cambridge, MA 02139



Glenn D. Thompson  
U.S. Environmental Protection  
Agency  
2565 Plymouth Road  
Ann Arbor, MI 48105

George M. Thur  
Chief, Power Systems Development  
Branch  
Environmental Protection Agency  
2929 Plymouth Road  
Ann Arbor, MI 48105

Harry A. Toulmin  
Sun Oil Company  
Birmingham, MI 48011

Donald Trilling  
DOT/Office of the Assistant Sec.  
for Policy, Plans, and  
International Affairs  
400 7th St. S.W.  
Washington, D.C. 20590

P.D. Umholtz  
Stanford Research Institute  
353 Ranvenswood  
Palo Alto, CA

Earl E. VanLandingham  
NASA Code NE  
Washington, D.C. 20546

W. Van Vorst  
Engineering Systems Dept.  
School of Engineering and  
Science  
UCLA  
Los Angeles, CA 90024

Andrew Vasilakis  
Thermo Electron  
Waltham, MA

Jack Vernon  
Scientific Engineering Systems  
570 Pleasant St.  
Watertown, MA 02172

Charles Waide  
Brookhaven National Laboratory  
Upton, NY

Eugene Wallace  
International Harvester  
401 N. Michigan Avenue  
Chicago, IL 60611

Harry Weaver  
Motor Vehicle Manufacturers Assn.  
320 New Center Building  
Detroit, MI 48202

H.L. Welch  
Chrysler Corporation  
P.O. Box 1118  
Detroit, MI 48231

Sheila Widnal  
Director, Office of University  
Research, DOT  
400 7th St. S.W.  
Washington, D.C. 20590

R. Wilson  
Arthur D. Little, Inc  
Acorn Park  
Cambridge, MA 02140